STUDIES ON

DEHUMIDIFICATION POTENTIAL OF CLAY WITH ADDITIVES AND IMPREGNATED WITH CaCl₂ COMPOSITE DESICCANTS

Thesis

Submitted in partial fulfillment of the requirement for the degree of

DOCTOR OF PHILOSOPHY

by

HIREMATH CHANDRASHEKHARAYYA RACHAYYA

DEPARTMENT OF MECHANICAL ENGINEERING
NATIONAL INSTITUTE OF TECHNOLOGY KARNATAKA
SURATHKAL, MANGALORE - 575025
SEPTEMBER - 2019

DECLARATION

by the Ph.D. Research Scholar

I hereby declare that the Research Thesis entitled "STUDIES ON DEHUMIDIFICATION POTENTIAL OF CLAY WITH ADDITIVES AND IMPREGNATED WITH $CaCl_2$ COMPOSITE DESICCANTS" which is being submitted to the **National Institute of Technology Karnataka, Surathkal** in partial fulfillment of the requirements for the award of the Degree of **Doctor of Philosophy in Mechanical Engineering** is a bonafide report of the research work carried out by me. The material contained in this Research Thesis has not been submitted to any University or Institution for the award of any degree.

Register Number: **121186ME12P02**

Name of Research Scholar: **Hiremath Chandrashekharayya Rachayya**

Signature of the Research Scholar:

Department of Mechanical Engineering

Place: NITK, Surathkal, Mangalore.
Date: /   / 2019

CERTIFICATE

This is to certify that the Research Thesis entitled "STUDIES ON DEHUMIDIFICATION POTENTIAL OF CLAY WITH ADDITIVES AND IMPREGNATED WITH $CaCl_2$ COMPOSITE DESICCANTS" submitted by **Mr. HIREMATH CHANDRASHEKHARAYYA RACHAYYA** (Register Number **121186ME12P02**) as record of the research work carried out by him, is accepted as the Research Thesis submission in partial fulfillment of the requirements for the award of degree of **Doctor of Philosophy**.

(Dr. Ravikiran Kadoli)

Research Guide &Professor

Department of Mechanical Engineering

National Institute of Technology Karnataka,

Surathkal, India.

Chairman-DRPC

Department of Mechanical Engineering

National Institute of Technology Karnataka,

Surathkal-575025, India.

In dedication to the loving memory of my Father, my mother for making me be who I am, and my wife and daughter for supporting me all the way.

ACKNOWLEDGEMENT

ABSTRACT

The present work features the preparation and estimation of properties, dehumidification performance assessment and utilization of clay based composite desiccants. Transported clay suitable for pot making is used as desiccant carrier. Composite desiccant is formulated such that transported clay is heat treated (burnt clay) and impregnated with $CaCl_2$. To improve the performance of desiccant carrier, composite desiccants were synthesized using two additives namely saw dust and horse dung. Transported clay are moulded to near spherical shape and are subjected to shadow drying and later dried at higher temperature in a furnace. The heat treatment at 500°C reveals higher weight reduction and porosity. Heat treated desiccants are then characterized by scanning electron microscopy (SEM), Brunauer Emmet Teller (BET) and X-ray diffraction (XRD) techniques. The BET test reveals that clay samples subjected to 500°C posses higher pore volume and clay-horse dung particles exhibit higher surface area. Heat treated desiccants namely clay, clay with 20% saw dust and clay with 20% horse dung are impregnated with $CaCl_2$ solution of 50% concentration by soaking method. The SEM image and elements analysis indicated that the composite desiccant has porous surface and uniform distribution of $CaCl_2$ due to heating at 500°C. XRD pattern indicates the porous nature of burnt clay-additives composite desiccant. The decrease in height of diffraction peaks with $CaCl_2$ impregnation reveals the presence of $CaCl_2$. The variation of thermo - physical properties like thermal diffusivity, specific heat, density and thermal conductivity of burnt clay with and without impregnation of $CaCl_2$ and the effect of additives, namely, saw dust and horse dung at various percentages is investigated. Rapid transient measurement technique is used for the measurement of thermal diffusivity. Specific heat is determined by energy balance. The addition of saw dust and horse dung is seen to increase the specific heat of clay additives with $CaCl_2$ impregnated desiccants. The packed bed performance under the influence of inlet air humidity ratio, and temperature is presented experimentally. The heat of adsorption during the process is low and the bed operates at constant temperature, one dimensional PGC mass transfer model is adopted from conservation principle. The experimental results for reduction in moisture content are compared with theoretical results.

Adsorption - desorption experiments for moisture removal and addition from atmospheric air are conducted in vertical column in static and fluidized states. The desiccant beds are subjected to an initially set value of process air velocity, relative humidity, temperature and mass of bed. Moisture removal capacity, moisture addition capacity and heat content are the parameter indices adopted to measure the heat and mass transfer characteristics of vertical packed and fluidized bed comprising clay - additives - $CaCl_2$ composite desiccants. On comparing packed and fluidized beds, fluidization improves dehumidification performance and results in higher desorption rates. The results of the experimental study reveals that higher adsorption rates increases the water content of desiccant particles and found to enhance the cooling effectiveness coupled with dehumidification. Irrespective of the clay composite desiccant beds, higher enthalpy of process air exiting the composite desiccant beds is associated with higher adsorptivity.

A forced circulation laboratory model desiccant drying system operating in open loop was constructed and arranged. The green pea drying process is divided into two processes involving dehumidification by desiccant bed and grain drying by dehumidified process air. Moisture removal from the process air takes place by vertical packed composite desiccant bed. The grains were dried for process time of one hour. The experimental study reveals average heat content of air entering the dryer is 1.46, 2.46 and 2.38 kJ for burnt clay - $CaCl_2$, burnt clay - horse dung - $CaCl_2$ and burnt clay - sawdust - $CaCl_2$ beds of mass 700 g. The drying is quite sharp during initial process time of 500 s and from then onwards drying of green peas proceeds at constant rate. Finally the potential and perspective of fabricated desiccants in dehumidification and thermal enhancement is being outlined. The key contributions of the present research work highlights the development of low cost composite desiccants using naturally available materials like clay, horse dung and saw dust. These desiccants have potential application in agriculture, HVAC industry, and water extraction from atmospheric air.

Keywords: *Transported clay, Saw dust, Horse dung, Calcium chloride, Adsorption, Heat content, Composite desiccant dryer.*

CONTENTS

CHAPTER 3

PROPERTIES DETERMINATION OF CLAY WITH ADDITIVES AND IMPREGNATED WITH CaCl$_2$ COMPOSITE DESICCANT

vii

CHAPTER 5

CHAPTER 6

LIST OF FIGURES

xiv

xv

xvii

xviii

xx

LIST OF TABLES

NOMENCLATURE

a	specific surface area [m^2/m^3]
A_{sf}	total bed surface area [m^2]
A	cross sectional area of bed [m^2]
C_p	specific heat [J/kg K]
C_d	co-efficient of discharge
c_{1e}	moisture fraction of air [kg/kg of dry air]
c_{1s}	equilibrium layer moisture fraction of air [kg/kg of dry air]
d	diameter [m]
$\dot{d}$	drying rate [g/min]
D	diameter of desiccant bed [m]
E	voltage [mV]
g	acceleration due to gravity [m/s^2]
H	manometer head [m]
h_{χ}	convective mass transfer coefficient [m/s]
h	specific enthalpy of air [kJ/kg]
I	immersed weight of particle [g]
K	affinity constant
k	thermal conductivity [W/m K]
K_{ω}	gas side mass transfer coefficient [kg/ m^2 s]
L	length of the desiccant bed [m]
l	length of cylindrical rod [mm]

$\dot{m}$	mass flow rate [kg/s]
m	mass [kg]
M	moisture transferred or removed
p	perimeter of bed [m]
P	pressure [Pa]
Q	volume flow rate [m^3/s]
q	water content of desiccant [kg/kg dry desiccant]
R	gas constant [J/kg K]
r	radius [m]
S	humidity ratio of air [g/kg of dry air]
t	time [s]
T	temperature [°C]
T_{1e}	temperature of air across bed [°C]
U	fluidization velocity [m/s]
V	volume [m^3]
v	process air velocity [m/s]
W	weight [g]
Z	axial distance

Greek symbol

α	thermal diffusivity [m^2/s]
β	full width at half maximum [rad]
λ	wave length of X - ray [nm]
δ	small change
ε	porosity [%]
ζ	dry weight of particle

η	crystalline size [nm]
θ	bragg's angle
ι	thread weight [g]
μ	viscosity [kg/m s]
ξ	thickness of sample or pallet [m]
ρ	density [kg/m^3]
σ_1	cross sectional areas of pressure line[m^2]
σ_2	cross sectional areas orifice meter[m^2]
τ	concentration of $CaCl_2$
ϕ	desiccant pellet
Δ	uncertainty in the parameter
ψ	initial water content (g of water/kg of dry desiccant)

Subscripts

a	process air
act	actual
ads	adsorption
atm	atmospheric
b	bed
c	clay
$CaCl_2$	calcium chloride
cr	cylindrical rod
csd	clay or horse dung or saw dust
db	desiccant bed
dd	dry desiccant
des	desorption
e	exit, empty
f	final
gb	grain bed
H_2o	water
i	inlet, initial, intercept

out	outlet of the desiccant packed bed
o	initial value
sat	saturation
s	salt, sample, bed surface
total	total
v	vapor
w	water
wd	wet desiccant

Abbreviations

EDAX	energy dispersive X-ray analysis
GI	galvanized iron
MRC	moisture removal capacity
MAC	moisture addition capacity
PGC	pseudo gas side control
PVC	polyvinyl chloride
RH	relative humidity
Re	Reynolds number
SEM	scanning electron microscopy
SSR	solid side resistance
RMSE	root mean square error

CHAPTER 1

INTRODUCTION

1.1 INTRODUCTION

Heating, ventilation, and air conditioning (HVAC) systems in buildings are essential in hot and humid regions. Humidification and dehumidification of atmospheric air are essential for preserving agricultural, food, pharmaceutical products apart from human comfort. Research and development activity has garnered towards minimizing energy consumption and greenhouse gas emissions from the use of the materials and machines. The solar-assisted desiccant cooling system provides an efficient, cost-effective, and alternative hybrid air conditioning system. Apart from HVAC systems, the dehumidification potential of desiccant is utilized in the drying of agricultural products. Drying is an essential process in the agricultural sector that enables the preservation of food grains, cereals, and other agricultural products. The drawbacks of open sun drying led to controlled sun-drying systems. The incorporation of desiccant based systems with solar drying reduces the drying time and increases the efficiency of the systems. The humidification and dehumidification capacity of desiccant materials enables them to produce water from atmospheric air. Researchers have shown interest in tapping the water available in atmospheric air. Due to the importance of thermal comfort, drying and water production, researchers are proposing and investigating the use of hygroscopic materials to control temperature and humidity levels of process air. Hygroscopic materials can be employed because they function without the input of energy from an external agency.

1.2 BACKGROUND OF STUDY

In traditional air conditioning systems, control of temperature and humidity is a two-stage process. For accomplishing the dehumidification process, atmospheric air is cooled below its dew point and then heated to the desired temperature (Yao, 2010). Though conventional air conditioning system can efficiently handle the sensible load,

the treatment of latent load for hot and humid environments causes undesirable health issues and is an energy-intensive process. The dominant latent load in the traditional air conditioning system leads to higher energy consumption resulting in higher operation cost (Fazilati et al., 2017). One technology that can help to improve the dehumidification performance and eventually reduce the electricity consumption for hot, humid air conditioning systems is the use of desiccant dehumidification and cooling systems (Chiang et al., 2016 and Jain et al., 1995). The pre-conditioning of supply air using desiccants can improve the humidity and temperature in air conditioning systems, overall energy efficiency and is economically viable (La et al., 2010).

Food is a basic need for human beings after air and water. Increase in the world population demands the availability of more food. Drying increases food availability by reducing post-harvest losses. Drying of an agricultural product is an essential operation for more extended and safer storage (Kumar and Kalita, 2017). Open sun drying is the favored method, but the associated long time requirement and unfavorable weather restrict its application to many grain-growing regions of the world. There is no control over the drying rate; the crop may be over dried resulting in discoloration, loss of germination power and nutritional content. It is slow drying, and hence there can be deterioration of food due to fungi and bacteria. Heavy losses are reported because of occasional rains and unfavorable weather during post-harvest operations (Pranav et al., 2015).

The drawback of open sun drying led to the use of solar driers and exploring the new family of solar-based driers (Walid et al., 2014). Many researchers contributing to the drying of agricultural products have used direct mode, indirect mode, and mixed-mode solar dryers. Drying procedures that have been developed specify drying air temperature, initial and final moisture content and ambient air temperature with the objective of minimizing energy consumption (Billiris and Siebenmorgen, 2013). The concept of integrating silica gel desiccant tray unit with internal cooling for aeration of stored grains in the humid tropical climates has been demonstrated by simulation. The control of humidity and temperature of air entering the paddy silo by internal

cooling is feasible for practical application (Hung et al., 2009). Apart from silica gel the functioning of heat storage, phase change and clay desiccant materials with indirect solar dryers improves drying efficiency. Clay-based desiccants are employed in drying of agricultural products. The use of sodium and calcium bentonite clay reveals the preferable use of calcium-based bentonite at low moisture contents (Watts et al., 1985).

Water extraction from the atmospheric air has become a new trend. The literature reveals that the water content in atmospheric air is about 14000 km^3, whereas the freshwater in the earth is about 1200 km^3 (Hamed, 2002). This is the reason for the researchers to divert their concentration towards this field. Water can be extracted by adsorption/desorption process using desiccant materials. Calcium chloride based composite desiccant materials due to their excellent adsorption-desorption characteristics have applications in freshwater production from the atmosphere (Kumar and Yadav, 2017).

Desiccants are not only used for extracting water vapor from atmospheric air, but they can be used for removing toxic gases, for differentiating organic solvent from the solution. Due to the importance of the HVAC industry, aeration, drying, and water vapor extraction, researchers have studied the use of hygroscopic materials. The impact of hygroscopic materials depends on many factors; the amount and type of material, the physical and thermophysical properties, outdoor and indoor humidity levels, process air humidity, and temperature. Apart from desiccant material employed, the desiccant bed configuration is one of the prime components that impact the performance of desiccant based systems.

Several techniques to enhance the bed performance are discussed in the literature that includes the study on sorption process of silica gel desiccant in vertical, inclined, multilayered, rectangular, radial flow hollow cylindrical bed and annular bed configurations (Wang et al., 2009 and Zheng et al., 2014). Apart from changing the bed configurations, fluidizing a bed of solid desiccants brings adsorbent and adsorbate

3

in intimate contact, which enhances dehumidification-humidification of process air (Hamed, 2010).

Desiccant dehumidification-humidification systems use either liquid sorbent or solid desiccants. Another way to enhance the sorption performance is by composite desiccants produced by impregnating hygroscopic salts like chlorides, sulphates, bromides, glycols, and nitrates on to the porous host matrix. The porous materials employed are silica gel, alumina, and zeolite (Saha et al., 2009 and Tokarev et al., 2002). The use of these porous materials as desiccants is limited by higher regeneration temperature and release of heat of adsorption. To counteract the effect of adsorption heat during dehumidification, phase change materials are embedded into the desiccant bed. The embedded materials take up the heat released and thereby lower the process air temperature (Rady et al., 2009 and Ristic et al., 2012). Apart from commercially available porous materials, inert materials like clay, sepiolite, attapulgite, and bentonite can also be used (Chen et al., 2008). Clays being natural materials have attracted significant attention for sustainable material for the production of various industrial and agricultural products. They find application in the fields of ceramics, paper, paint, petroleum industry, process industries, catalysis, etc. (Konta., 1995).

Clay being nontoxic and naturally available is heat-treated and employed as carrier or host material for liquid hygroscopic salts. To control the liquefaction of calcium chloride salt and to enhance the low hygroscopic property of clay material and starch a new family of composite adsorbent of water vapor based on impregnating hygroscopic salt into the pores of host inert materials is being researched (Li et al., 2007).

1.3 SOIL, CLAY AND CLAY MINERALS

Soil is a three-phase system containing solid, liquid and gas. Solid particles mostly are made up of minerals with a wide range of sizes, shapes, and compositions. The liquid phase is water with a variety of dissolved salts, and the gaseous phase is mostly air (Kulkarni et al., 2016). The available soils are black cotton soil, silty soil, and fine

sand and coarse sand. The term clay refers to naturally occurring material composed primarily of fine-grained minerals, which is generally plastic at appropriate water contents and will harden when dried or fired. Although clay usually contains phyllosilicates, it may contain other materials that impart plasticity and harden when dried or fired. The minerals that are phyllosilicates which occurs in clay are the clay minerals. From the academic source there are four main groups of clays: kaolinite, smectite, illite, and chlorite. The classification of clay minerals is depicted in Fig.1.1. Minerals in which one tetrahedral sheet and one octahedral sheet form the crystal unit are known as 1:1 type minerals. The minerals in which one octahedral sheet is sandwiched between two tetrahedral sheets to form the crystal unit are known as 2:1 type minerals. 2:1:1 type minerals consist of two tetrahedral sheets and one shared and unshared octahedral sheet (Biswas and Mukharji, 1994).
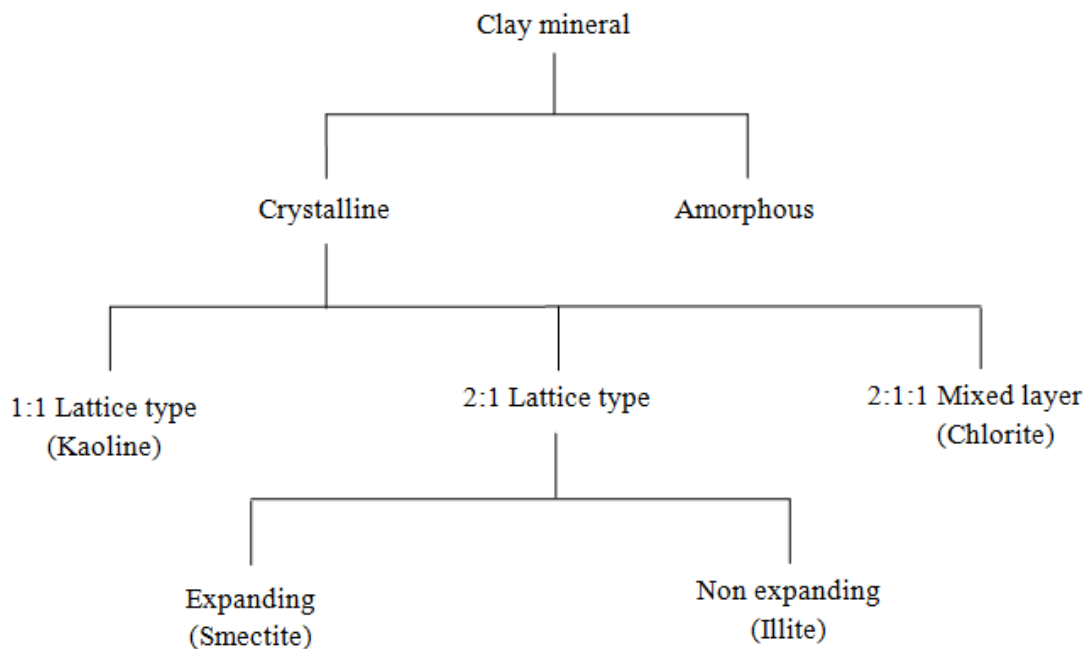
Fig. 1.1 Classification of clay minerals.

The clay minerals which are having significant adsorptive properties are attapulgite, montmorillonite, sepiolites, and bentonites. The property of retaining particle size and shape in the course of sorption and regeneration is essential for the use of a material

5

as a desiccant or adsorbent. Bentonite is an adsorbent primarily composed of montmorillonite. There are different types of bentonite, each named after respective dominant elements, such as potassium (K), sodium (Na), calcium (Ca) and aluminium (Al). For industrial purposes two main class of bentonite exist sodium and calcium bentonite. Calcium bentonite may be converted to sodium bentonite by a process known as ion exchange. Bentonite can be used as adsorbent due to its adsorption properties. Bentonite desiccants have been successfully used to protect pharmaceutical and medical types of equipment from moisture and extend shelf life. In fact in most common packaging environments, bentonite desiccants have higher adsorption capacity than silica gel desiccant

1.4 SOLID, LIQUID AND COMPOSITE DESICCANTS

The desiccants are of a hydrophilic and hydrophobic type. The hydrophilic solid adsorbents are clay, silica gel, activated alumina and zeolite whereas activated carbon is a hydrophobic solid desiccant. Apart from solid desiccants the liquid desiccants are specialized chemicals used for drying and purifying air or other gases. The hygroscopic salts available are calcium chloride, lithium chloride, lithium bromide, and glycols. The impregnation of hygroscopic salts onto the porous solid desiccants results in composite desiccants (Srivastava, 1998). Table 1.1 shows relative vapor pressure of $CaCl_2$ liquid desiccant and water vapor As temperature increases, the vapor pressure of $CaCl_2$ increases as compared to vapor pressure of water vapor. $CaCl_2$ has lower vapor pressure than water at the same temperature. Calcium chloride, also known as a common salt, which is a cheaper, non-toxic and readily available liquid desiccant. The dissolution of calcium carbonate or calcium oxide in hydrochloric acid produces calcium chloride. In solid form, calcium chloride is white in color, while in liquidated form, it is colorless. Its boiling point is as high as 1600 ºC. It is soluble both in inorganic solvents like water, as well as organic solvents like ethanol. It is hygroscopic in nature and absorbs moisture from air. If exposed to open air, it tends to become liquid. That is why; it is often called a deliquescent substance. It has a low melting point of 772ºC, which means it can be dissolved at a very low temperature

Table 1.1 Vapor pressure of $CaCl_2$ in comparison with water (Fotios, 1987).

Temperature (^{o}C)	Vapor pressure of $CaCl_2$ (mm Hg)	Vapor pressure of Water (mm Hg)
0	0	0
5	0	6.54
10	0	9.2
20	0	17.53
30	1.5	31.82
40	2.5	55.32
50	5	92.51
60	8	149.38
70	15	233.70
80	25	355.10
90	40	525.76
100	60	760

1.5 SIGNIFICANCE OF THE WORK

This research work primarily intends to study low-cost desiccants, naturally available and involves minimum processing time for preparing the desiccants. One such raw material for desiccants is clay. Most of the popular desiccants used in practice are silica gel, zeolite, and activated carbon. Researchers are developing many composite desiccants specifically impregnating liquid desiccants onto the solid desiccant. To improve the desiccant features of clay especially from the point of adsorption and desorption capability, additives like sawdust and horse dung which are available locally and in abundant were adopted. The local pot makers employ horse dung with clay which imparts strength and porosity to burnt pots. Sawdust is a byproduct of the wood industry is included as another additive. The technological burden in the preparation of the composite desiccant is minimal. However, the physics and mechanics of adsorption and desorption of these composite desiccants is of interest.

Keeping these points in mind this research has been taken up to explore the possibility of bringing into practice new composite desiccants

1.6 OUTLINE OF THE THESIS

The first chapter sets the background of the study citing the potential applications of desiccants in HVAC industry, drying, and water vapor extraction. Soil, clay and clay minerals of different forms are discussed. Apart from commercially available porous materials, inert clay minerals like clay, sepiolite, attapulgite, and bentonite are also highlighted. A list of solid, liquid, composite desiccants is presented. The physical and chemical properties of hygroscopic salt $CaCl_2$ are discussed. Finally the significance of the present research work is presented.

The second chapter reviews the literature pertaining to the determination of thermophysical properties of clay mineral and clay desiccants. The literature study on solid, liquid, composite, polymer and bio desiccants is presented. Particularly with emphasis on clay-based desiccants. The application of desiccant materials for drying of agricultural products, aeration and water production from atmospheric air is furnished. Citing the literature, the motivation is described, and finally the objectives of the research work are presented.

The third chapter details the procedure for the preparation of burnt clay and burnt clay -additives based $CaCl_2$ composite desiccants. Thermophysical properties of composite desiccants like porosity, thermal diffusivity, specific heat, density, and thermal conductivity are determined experimentally. The microstructure of clay composite desiccants is studied using SEM images, EDAX, and XRD techniques. The initial water content of heat-treated clay - $CaCl_2$, heat-treated clay - horse dung - $CaCl_2$ and heat-treated clay sawdust - $CaCl_2$ composite desiccants is calculated. Finally the chapter is summarized, and conclusions are listed.

The fourth chapter details the construction and arrangement of experimental set up to study the adsorption-desorption characteristics of composite desiccants. The performance of air heating unit and humidification unit are discussed. The

experimental procedure on packed and fluidized bed of clay composite desiccants is presented. The experimental parameters estimated are superficial velocity of air, bed porosity, bed specific heat, and saturation pressure and humidity ratio of process air. The measurement of experimental parameters and uncertainty of measured parameters is carried out. A summary of the chapter content is presented towards the end.

The experimental parameter indices to analyse the performance of clay composite desiccants in humidification and dehumidification processes are elaborated in chapter 5. The dehumidification experimental results for transient variation of process air humidity ratio and temperature are presented for clay composite desiccant vertical packed beds. The performances of vertical packed desiccant beds are compared by varying bed inlet air velocities and for differing bed masses. Adsorption and desorption experimental results for vertical packed and fluidized clay composite desiccant beds are discussed. An analysis of the mass transfer coefficient of the packed and fluidized bed is presented. Finally the chapter is summarized, and conclusions are listed based on experimental results.

In the sixth chapter, the theoretical modeling of vertical packed desiccant bed is described. The mass balance equations are written for water vapor conservation in gas and solid phases. The governing differential equations are solved for transient and spatial variation of process air humidity ratio by finite difference method. The auxiliary correlations with boundary and initial conditions employed to solve the governing equations are presented. The theoretical results are compared with experimental results of vertical packed clay composite desiccant beds. Finally the summary is poised with list of conclusions.

The seventh chapter consists of experimental study on potential application of clay composite desiccants in green pea drying. The detailed construction of experiential set up with two tray lab-scale dryer coupled with vertical packed desiccant bed is illustrated. The experimental results obtained are grouped for desiccant bed and grain dryer. The transient variation of moisture content, heat content, and enthalpy of process air entering the dryer are discussed and analyzed. The experimental results on

transient variation of moisture content, enthalpy of process air leaving the dryer are presented and analyzed. The results are compared for the identical bed mass and for the same surface area of the desiccant beds.

The eighth chapter outlines the key contributions and scope for future work. Summarizes the significance of low cost naturally available materials like clay, horse dung, and sawdust that are employed for the preparation of clay and clay additives composite desiccants. The dehumidification and humidification potential of clay composite desiccants can enable the development solar-assisted desiccant based systems for air conditioning, aeration and drying applications

CHAPTER 2

REVIEW OF LITERATURE

2.1 INTRODUCTION

In this chapter, a review on some of the past work on the characterization of clay materials, performance of desiccant materials, analysis, design, experiments, and applications of desiccant materials in the area of humidification and dehumidification technology is presented. The available literature is divided into three categories that include properties, performance, and application of clay-based and other desiccant materials.

2.2 PROPERTIES OF CAY MATERIAL

Middleton (1992) described the rapid transient method to determine the thermal diffusivity of rock samples found in western Australian sedimentary basins. The experimental work is based on the theory that employs a small rock sample with heat flux at the top surface with insulation on all other sides. The temperature measured at the bottom of samples is reduced by subtracting the initial ambient temperature and effectively making the measurements to initial zero temperature. The intercept measured from the time-temperature plot directly determines the thermal diffusivity. The thermal diffusivity is measured to the best accuracy of 3%. The results obtained are inconsistent with the results of other laboratory methods.

Fasunwon et al. (2008) experimentally determined the thermal properties of five rock samples found in Southwestern Nigeria. The rock samples tested are limestone, dolerite, marble, gneiss, and granite. The thermal properties estimated are thermal diffusivity (α) and thermal conductivity (k) of rock samples. A simple cost-effective transient measurement technique based on one-dimensional heat flow through the sample was adopted to determine thermal diffusivity. Specific heat of samples was measured by laboratory calorimetric experiment. Mass - volume measurement of samples gives density. Thermal conductivity was calculated using the

relation $k = \alpha \rho c$. Thermal conductivity values estimated for rock samples are in the range of 0.1 to 7 W/m K and are comparable with the literature data.

Adegoke et al. (2010) experimentally determined the variation of thermo physical properties of clay doped with heavy metals like lead, copper, nickel, cadmium, and zinc were doped into clay. Transient measurement technique was used to measure the thermal properties of clay-heavy metal particles. The temperature measurements at the top and bottom of clay samples were carried out to determine the thermal properties. The lowest thermal conductivity was found to be 9.58 W/m K, and the highest was found to be 10.50 W/m K. Thermal diffusivity ranged from 2.70×10^{-6} m^2/s to 3.48×10^{-6} m^2/s. Up to the limit of cation exchange, thermophysical properties increases with increase in concentration of heavy metals. With increase in temperature of clay and increase in concentration of heavy metal ions results in poor seed germination and stunted growth in crops.

Wang et al. (2010) investigated anisotropic thermal conductivity and permeability for disc compacted expanded natural graphite (DCENG) and plate compacted expanded natural graphite (PCENG) blocks. The steady-state thermal conductivity is investigated by using guard-hot plate method. The permeabilities of the samples were tested by using specially designed test rig. The measuring directions of thermal conductivity and permeability for DCENG and PCENG blocks are parallel and perpendicular to the direction of compression. For the density of 440 kg/m^3, the thermal conductivities of PEENG is 49% higher than that of DCENG. The gas permeability of PCENG is 3 times higher than that of DCENG. The current research on anisotropic thermal conductivity and gas permeability leads to the development of new materials with expanded graphite as a matrix.

Cmar et al. (2011) determined the applicability of sepiolite in desiccant production for humidity adsorption. The sepiolite clay mineral obtained from different regions of Turkey. Depending on the region of origin the mineral is designated as K, S and TTB type sepiolites. The two tests such as thermal treatment and $CaCl_2$ addition are employed to test the capacity of sepiolite based desiccants to control humidity at

different RH levels. The value of temperature for heat treatment is fixed from 100 to 550°C. The humidities employed are 20, 50 and 90% RH. The results of humidity uptake are compared with the Japanese and British standards that dictate the effective humidity uptake for sepiolite. All the samples have significant adsorption capacities at 300°C and yielded 14.7%, 12.8%, and 13.8% respectively for K,S and TTB sepiolites. At higher RH the adsorption capacities are in the order of TTB>K>S. The exposure of sepiolite samples at 20 and 90% RH showed the required value of adsorption capacities which are in line with Japanese and British standards. The addition of $CaCl_2$ enhances humidity uptake. The K - 5% $CaCl_2$ and TTB - 6% $CaCl_2$ desiccants reached the required adsorption capacities at 50% RH. TTB - $CaCl_2$ desiccant exhibits higher humidity uptake as compared to K - $CaCl_2$ and S - $CaCl_2$ desiccants.

Santurde et al. (2012) experimentally evaluated physical and mineralogical characteristics of clay with green sand (GS) and foundry sand (CS) in proportions of 0 - 50%. The samples are prepared on laboratory and industrial scale. The specimens were heat-treated in a temperature ranges of 850 - 1050°C to produce ceramic bricks. The addition of GS and CS to the ceramic matrix decreases the loss of ignition and water absorption. With higher heating temperature, the shrinkage and loss on ignition increases. The optimization study indicates to produce ceramic bricks with 35% of green sand and 25% of core sand so as to accomplish technological standards. The application of foundry sand as raw material for production of ceramic products is suggested based on the results of the physical and mineralogical evaluation.

Kulkarni et al. (2016) experimentally determined thermal properties of alluvial soil deposits on the bank of Krishna river located in Karad, Maharashtra state of India. The alluvial soil employed in making bricks is characterized by thermal conductivity and specific heat. The steady-state method with a one-dimensional approximation is used to determine thermal conductivity whereas transient heat conduction analysis through semi-infinite solid is adopted to determine the specific heat. The physical properties and sieve analysis data of soil are taken as input parameters to the six mathematical models available in the literature. The physical properties determined are bulk density, soil's solid density, and porosity. The sieve analysis classifies soil as

poorly graded sand with silt. Range of experimentally estimated value of thermal conductivity and specific heat are 0.24 W/m K to 0.35 W/m K and 674.7 to 1003.1 J/kg K respectively. Out of the six models, three mathematical models use bulk density, soil's solid density and porosity as input parameters. The model output values of thermal conductivities are in the range of 0.26 W/m K to 0.34 W/m K. The other three models use thermal conductivity of air as additional input parameter along with porosity of soil. The theoretical values of thermal conductivity obtained with these models are in the range of 0.24 W/m K to 0.29 W/m K.

Boukhemkhem and Rida (2017) experimentally investigated the adsorption of methylene blue from aqueous solution onto kaolin and modified kaolin clay mineral adsorbent. The modified kaolin was obtained by thermal treatment and acid treatment. The three adsorbents are characterized by microscopic and spectroscopic methods. Batch adsorption experiments are conducted for the removal of methylene blue by acid-modified kaolin with respect to initial concentration, residence time, pH and temperature. The theoretical study includes the application of pseudo-first-order and pseudo-second-order kinetic models for the adsorption of methylene blue by acid-treated kaolin. Langmuir and Freundlich isotherm models are employed to describe the isotherms of kaolin based adsorbents. The results of experimental study reveal higher adsorption capacity for acid-treated calcined kaolin as compared to raw kaolin and heat-treated kaolin. Higher surface area and cation exchange capacity result in higher adsorption capacity for modified kaolin. The pseudo-second-order kinetic model best explains the adsorption process with correlation coefficient higher than 0.99. The thermodynamic study reveals the spontaneous adsorption process which is endothermic in nature.

2.3 STUDIES ON CLAY AND OTHER DESICCANTS IMPREGNATED WITH CaCl$_2$

The literature cited below pertains to sorption behavior of a composite desiccant comprising clay, silica gel, sand, molecular sieve, and calcium chloride.

Close and Dunkle (1977) cited that adsorption as a method of storing energy in beds of adsorbent materials. They have shown that adsorbing materials can occupy a much smaller volume than non-adsorbing materials for the same quantity of energy stored. They showed that presently available materials are too expensive and need to develop new ones using hygroscopic salts and appropriate carrier materials.

Farayedhi and Gandhidasan (1995) reported that the use of silica gel and other solid desiccants requires relatively higher regeneration temperatures as compared to liquid desiccants. On the other hand, liquid adsorbents such as calcium chloride, lithium chloride, lithium bromide, and trimethylene glycols have high corrosive characteristics.

Kinsara et al. (1996) suggested the use of liquid desiccant to overcome the latent part of the air-conditioning cooling load. They proposed an energy-efficient system to reduce energy consumption in air-conditioning (A/C) system using $CaCl_2$ solution as a liquid desiccant. Two packed beds, a heat pump, air washers, and a cooling coil were the main features of the proposed system. The latent load of air-conditioning system was overcome by dehumidifying the air in a dehumidification packed bed using liquid $CaCl_2$ solution. The heat rejection from the condenser of the vapor-compression refrigeration machine was utilized for regeneration of liquid desiccant. A computer code was developed for performance study. They had compared performance of proposed system with conventional system. They concluded that the new system with $CaCl_2$ as a liquid desiccant could be used effectively to reduce electric energy consumption.

Thoruwa et al. (2000) developed three low cost, solar regenerative clay - $CaCl_2$ desiccant material. They analyzed moisture sorption and regeneration characteristics of new desiccant and compared those with commercial desiccants. Three clay mineral desiccants were analyzed. The composition of clay mineral desiccants are as follows: Type 1: 60% bentonite, 10% $CaCl_2$, 20% vermiculite and 10% cement; Type 2: 65% bentonite, 5% $CaCl_2$, 20% vermiculite and 10% cement; Type 3: 65% kaolinite, 10% $CaCl_2$, 20% vermiculite and 10% cement. The experimental cabinet was under

controlled environmental conditions of 85% (RH) and 25°C. The Bentonite - $CaCl_2$ (type 1) desiccant attained maximum moisture sorption of 45% dry weight basis (dwb) while type 2 and type 3 desiccants both showed average moisture sorption of 30% (dwb) after a state of equilibrium (120 h). The silica gel desiccant attained an average of 27% (dwb) and activated clay desiccant attained maximum moisture sorption of 27% (dwb) under the same environmental conditions. They concluded that the estimated cost of the fabricated desiccants was 0.11 times the cost of commercial silica gel desiccant.

Hamed (2000) analyzed the theoretical cycle for adsorption of water from air with subsequent regeneration. Properties of the desiccant ($CaCl_2$) were correlated in a simplified form. Heat and mass balance equations are developed for the operating cycle, and expression for cycle efficiency is introduced. The adsorption equilibrium relation of the desiccant $CaCl_2$ was correlated. The derived equation was a function of $CaCl_2$ concentration. The vapor pressure on the solution surface was found by knowledge of bed temperature and solution concentration. The theoretical analysis suggested that cycle efficiency, mass of stable solution and regeneration temperature are highly dependent on the concentration limits of the effective desiccant. Cycle efficiency greater than 90% can be obtained for different values of strong solution concentration, and the value decreases suddenly when the difference between strong and weak solution concentration is small. The regeneration temperature is highly dependent on the operating concentration of the desiccant

Hamed (2002) has investigated theoretically and also experimentally, the transient adsorption characteristics of a vertical packed porous bed with calcium chloride impregnated onto burnt clay as the desiccant. Their theoretical model incorporating gas side resistance describes the effect of independent parameters (time and vertical distance through the bed) on the adsorption process. He had also presented a simplified analytical solution for specific operating conditions. The isothermal adsorption of water vapor from atmospheric air using the clay - $CaCl_2$ bed was experimentally studied. Burnt clay pellets were impregnated with liquid calcium chloride solution to form the porous adsorbing surface. So grains of burned clay were

16

used as a desiccant carrier from the adsorption porous surface. The packed bed was prepared by arranging seven layers in a plastic cylindrical cover of 210 mm height. The average diameter of the burnt clay pellet was 9 mm. The grains were impregnated with calcium chloride solution with a concentration of 33.86%. Transient variation of exit air humidity ratio, mass of water adsorbed, desiccant concentration and vapor pressure on the bed surface are evaluated from experimental measurements. They found that the maximum change in the air humidity was about 0.5 g/kg of air at the starting of adsorption during small time period. The potential for moisture adsorption exponentially decreases with the increase in the dimensionless time. Good agreement between analytical solution of model and experimental results was obtained.

Aristov et al. (2002) presented a selective water sorbent (SWSs) for sorption air conditioning. These materials were composite and prepared by impregnating hygroscopic salt inside porous matrix with open pore. They have used two silica gel porous matrices and two salts to prepare four selective water sorbents (SWSs). One of the silica gel (KSK) was mesoporous with the average pore radius of 7.5 nm, while another microporous silica gel (KSM) had much smaller pores of just 1.8 nm radius. Silica gel porous matrices were filled with calcium chloride or lithium bromide aqueous solution of a fixed concentration. Salts concentration in the anhydrous samples was varied from 21.7 to 57.0 wt. %. They observed that the composites water sorbents had much higher moisture sorption capacity compared with pure silica gel at both low and high temperatures. Calcium chloride impregnated composite (SWS-1L) had sorbed as high as 0.75 g/g water at temperature of 28°C and pressure of 23.4 mbar compared to 0.1 g/g for pure silica gel. They found that despite high water uptake, composite could be regenerated at relatively low temperature. The mesoporous SWSs had indicated the mono-variant type of sorption equilibrium compared to di-variant sorption equilibrium for the pure silica gel.

Tokarev et al. (2002) prepared and studied new desiccant by confining $CaCl_2$ to mesoporous host matrix MCM-41 for the adsorption cooling/heating. The isobars, isosteres and isotherms of the water sorption were obtained for the composite, $CaCl_2$ confined in mesoporous of MCM-41, desiccant at the temperatures 293 - 423 K and

the vapour partial pressures 8.7 - 50.3 mbar. The water sorption was found to be a combination of the absorption and heterogeneous adsorption. The microstructure of MCM-41 contained monosized cylindrical mesopores. The sorption equilibrium in the system "water vapor CaCl$_2$-MCM-41" was studied by a TG method with use of a Rigaku Termoflex thermobalance. This new composite material was able to absorb up to 0.75 g of H$_2$O per gram of the dry sorbent. This high absorptivity assured the high values of the energy storage capacity (2.1 kJ/g). Most of the water sorbed could be removed at the relatively low temperature between 343 K and 393 K. So this material demonstrated two types of sorption behavior namely, water absorption and solid adsorption. This gave an opportunity to combine advantages of solid and liquid desiccants.

Hamed (2003) studied theoretically and experimentally the desorption characteristics of the packed bed containing granules of burned clay impregnated with calcium chloride as the effective desiccant. For this they defined theoretical model to describe the transient variation of air properties such as humidity, temperature as well as desiccant concentration. The interdependence of operating parameters of air and desiccant are correlated in theoretical model. Experimental studies on the transient variation of desiccant properties are reported. A low-grade heat source, solar energy, is used for desorption process. Study of adsorption/desorption characteristics shows that mass transfer rate is dependent on concentration gradient in the bed. For the specified operating conditions the desorption rate is higher as compared to adsorption, and consequently the effect of axial distance on concentration gradient is neglected. A plot of dimensionless concentration versus time shows good agreement between theoretical and experimental results.

Hamed (2003) investigated the natural absorption of water-vapor of the gaseous mixture on the horizontal surface of a sandy layer impregnated with calcium chloride liquid as the effective desiccant. Isothermal absorption is assumed in this analysis. He studied the effect of mixing ratio (sand/desiccant) on rate of adsorption and Grashoffs number on the mass transfer coefficient. The rate of absorption decreases with decrease in mixing ratio. It has been experimentally found that the mass transfer

coefficient rapidly decreases in the liquid zone due to decrease in void volume in the bed and the active mass transfer area.

Zhu et al. (2006) carried out an experimental study on composite silica gel supported $CaCl_2$ sorbent for low-grade thermal energy storage (TES). Sorption amount of up to 0.73 g water per gram composite sorbent was obtained at the temperature of 30°C and the relative vapor pressure of 0.8. This sorption capacity was very high compared to 0.15 g/g for the silica gel. The performance of composite sorbent was investigated in an open-type TES setup equipped with 40 kg composite sorbent particles. From comparison with other sensible heat storage (rock and water) and phase change (organic and inorganic) TES materials, they found that the composite sorbent, i.e. silica gel and $CaCl_2$ provided great potential as a TES system of small size and high storage density for low-grade heat storage. The properties of the water adsorbed on silica gel and composite sorbent were investigated by the weight method in a variable-temperature variable humidity apparatus. Silica gel took less time to reach 90% of the maximum adsorption capacity compared to composite. The composite sorbent can adsorb water vapor for a long time with high adsorption rate. The heat of sorption was found as a function of adsorbed water. The heat of sorption decreased slightly with the increase in amount of water adsorbed on the composite sorbet. TES setup equipped with 40 kg composite sorbent pellets shows a high specific TES capacity of approximately 1 kJ/g and storage efficiency of 0.78 at heat supply temperature of 30°C and relatively low charging temperature below 90°C.

Phate et al. (2007) numerically analysed the heat and mass transfer characteristics of cylindrical metal hydride bed for the sorption of hydrogen. The influence of L/D ratio and porosity on the flow of hydrogen within the bed is numerically simulated. The potential for driving the hydrogen within the bed is the concentration gradient. They concluded that the saturation time for the bed is more at higher porosity.

Daou et al. (2007) investigated the adsorption and refrigerating performances of a composite adsorbent (S40) and its host microporous silica gel matrix (S40). The mass ratio and the COP of the adsorption chiller system using composite adsorbent and

virgin adsorbent were compared. They concluded that with impregnation the ratio of specific cooling power was doubled and COP has been improved by 25%.

Ji et al. (2007) have presented experimental results on the water adsorption and desorption characteristics for a new highly efficient water selective composite adsorbent synthesized by MCM - 41 as host materials and calcium chloride as hygroscopic salt. They developed a new portable water production test unit. The experimental data demonstrate that the adsorption capacity of new composites is as high as 1.75 kg/kg of dry adsorbent, which is higher than composites synthesized by silica gel and calcium chloride. They also studied desorption characteristics of new composite desiccant, and they demonstrated that it could desorb 90% of the adsorbed water at about 80 ℃. The experimentally tested results have demonstrated the feasibility of the freshwater production with daily water productivity being more than 1.2 kg of freshwater per day per m^2 solar collector.

Tretiak et al. (2009) developed a desiccant consisting of clay and calcium chloride and tested using multiple sorptions and desorption cycles. The desiccant used in experiments was made of a 3:0.44 (by weight) mixture of commercial kaolin clay and vermiculite, respectively. Spherical pellets of 16.5 mm diameter were prepared. The final $CaCl_2$ content of the desiccant was found to be 18.5 % (db). Experiment setup was prepared for sorption and desorption test. Testing conditions were; inlet air temperatures from 23 to 36°C with corresponding relative humidities of 42 - 66% during sorption. Total time for sorption tests was 90 min, and superficial air velocities were maintained in the range of 0.17 to 0.85 m/s during experiment. Desorption was carried out at inlet air temperature from 50 to 57°C and superficial air velocities of approximately 0.3 to 0.6 m/s. A regression equation was determined for the mass of water sorbed by the clay - $CaCl_2$ desiccant with an R^2 value of 0.917. An equation for pressure drop through the desiccant was developed and compared to the existing theoretical models. They also found that due to repeated sorption experiments, the surface of the desiccant spheres began to break down, but the overall structure of the desiccant remained intact.

Saha et al. (2009) investigated the performance of two-bed adsorption chiller utilizing ksk-silica gel (average pore radius of 15 nm) impregnated with calcium chloride and water as adsorbate. They have modeled a single effect two-bed adsorption chiller. The model based on experimentally confirmed adsorption isotherm and kinetics data. Experimentally they compared cooling capacity and performances of adsorption chiller using RD silica gel with adsorption chiller using ksk-silica gel impregnated with $CaCl_2$ and water as adsorbent. From numerical simulation they found that cooling capacity increases up to 20% and COP up to 25% as compared to adsorption chiller utilizing silica gel - water pair. Optimum switching time of 30 sec is obtained for both cycles, and the cycle performance improves with increasing hot water temperature.

Yu et al. (2009) investigated the adsorption characteristics of a composite adsorbent comprising molecular sieve impregnated with $CaCl_2$ liquid desiccant. They studied the adsorption of PH_3 (Phosphine) adsorbate on molecular sieve impregnated with calcium chloride and virgin molecular sieve. $CaCl_2$ impregnation produces energetically heterogeneous surface. The isotherm data were collected experimentally by classical volumetric method. The isosteric heat of adsorption for gas phase adsorption was determined by applying Clausius Clayperon equation along with Freundlich isotherm to isotherm data at different temperatures. Freundlich equation gave better fit to the experimental isotherm data than Langmuir equation in the low-pressure range. The isosteric heat of adsorption indicated $CaCl_2$ modified molecular sieve had energetically heterogeneous surface. They confirmed that modified adsorbent has highest adsorption capacity than virgin adsorbent. Phosphine adsorption performance on $CaCl_2$ - molecular sieve involves heterogeneous surface. Nonlinear Freundlich isotherm equation was used instead of the monolayer Langmuir adsorption isotherm equation.

Ringvilakul and Kumar (2010) presented experimental results for the performance of counter flow dew point evaporative cooling system. The performance of the system was quantified in terms of temperature and humidity ratio of exit air and the system wet bulb and dew point effectiveness. The inlet conditions of the process air like

21

temperature, humidity ratio, and velocity are used to evaluate the system performance. The experimental setup consists of wet and dry channels separated by 0.5 mm thin-film cotton sheet coated evenly by polyurethane material. The parameters measured are dry bulb temperature, wet bulb temperature and velocity of air entering and leaving the dry channel. Similarly the temperatures and velocity of working air entering and leaving the wet channel are measured. Experiments are conducted under static and dynamic conditions. Static studies of the system performance indicate lower exit air temperatures at lower inlet air humidity ratio and temperatures. The slope of the outlet air temperature at constant humidity ratio is positively small and ranging from 0.15 to 0.17. For every 10°C rise of inlet air temperature, the exit air temperature increases by about 1.5 to 1.7°C. When inlet air humidity ratio decreased by 10 g/kg, the exit air temperature decreases by about 6.8°C for the same inlet air temperature. The results conclude that the system can supply outlet air temperature below 25°C when inlet humidity is below 11.2 g/kg. The experimental observations show higher wet bulb effectiveness at higher inlet air temperature and lower inlet air humidity ratio. The dew point effectiveness is high at higher inlet air temperature and at higher inlet air humidity ratio at constant inlet air temperature. The performance of the system under continuously varying conditions that is dynamic studies shows variation in wet-bulb effectiveness ranged from 101 to 104% and dew point effectiveness varied from 75 and 79%. The much lesser variation in dew point and wet bulb effectiveness under real-time ambient conditions depicts the potential of the system for air conditioning applications.

Lee et al. (2012) analyzed new polymer-based desiccant named super desiccant polymer (SDP) for sorption process. The super desiccant polymer was prepared by ion modification of polyacrylic acid sodium salt. Their primary purpose was to find sorption capacity and diffusivity of SDP. The uptake measurement method was used to find sorption capacity and diffusivity at temperature 30°C to 60°C and relative humidity from 5% to 70%. Four isotherms (30°C, 40°C, 50°C and 60°C) were obtained. The sorption capacity of SDP was similar to that of Lithium chloride- silica gel composite adsorbent at 0 to 50% RH. But it was three times higher than pure silica

gel and other types of silica gel. They had used modified Fick's diffusion model to describe a sorption behavior. Maximum sorption capacity was reached at relative humidity of 67%. Apparent diffusivity was in the range from 6.4×10^{-13} m^2/s to 5.9×10^{-11} m^2/s.

Chan et al. (2012) have investigated composite absorbents synthesized from zeolite 13X and CaCl$_2$ for application in solar adsorption cooling systems. The composite adsorbent was prepared by impregnating 41.5 mol% of CaCl$_2$ on the Ca ion-exchanged zeolite from a 40 wt% CaCl$_2$ solution condition. The water uptakes of the zeolite 13X/CaCl$_2$ composite adsorbents at different temperature were found by measuring the weight change using the thermogravimetric analyser. A cylindrical coordinate system was used for the numerical simulation. The equilibrium water uptake on the zeolite 13X was correlated theoretically by using the linear driving force model. The model correlations were solved with alternating direction implicit (ADI) finite difference method. There was a difference of 0.4 g/g in equilibrium water uptake recorded between 25 and 75°C at 870 Pa for the composite adsorbent. This was 41.9% of the zeolite 13X under the same environment.

Li et al. (2012) experimentally reported the adsorption capacity of sawdust - CaCl$_2$ composite desiccant for ammonia sorption in adsorption refrigeration applications. The effect of carbonization temperature and specific cooling power on sorption capacity and rate of adsorption is analyzed. The materials used for the preparation of composite adsorbent are sawdust, 50% CaCl$_2$ solution and amylum starch. About eight composite desiccants of circular-shaped 3 mm diameter are prepared by experimental procedure involving soaking, filtration, drying and finally carbonization at different temperatures ranging from 400°C to 800°C. The analysis of sorption capacity reveals increase in sorption capacity with increase in temperature and is higher for the composite carburized at 700°C. However above 800°C the sorption capacity decreases and the reduction is attributed to melting of CaCl$_2$ (782°C) which leads to the blocking of pores. More pores were induced in the composite adsorbent at higher temperature (above 800°C) but due to melting of CaCl$_2$ followed by blocking of pores results in lower sorption capacity. The results show 700°C as optimum

temperature for maximum sorption of NH_3 as high as 0.774 kg of NH_3/kg of composite adsorbent. The analysis of specific cooling power (SPC) with adsorption duration reveals 338 and 869 W/kg of SCP with cycle time varying from 5 to 20 minutes. The findings of the work argue effectiveness of carburized sawdust - $CaCl_2$ composite adsorbent for NH_3 adsorption refrigeration.

Zheng et al. (2014) prepared composite solid desiccant materials by impregnating salt solutions into different pore sized silica gel. They had used silica gel of three different pore sizes of 2-3 nm, 7-8 nm, and 9-10 nm. These silica gel were impregnated by LiCl, LiBr, and $CaCl_2$ for analysis. Isotherms were obtained for all composite desiccant. There was no hysteresis found in isotherm for composite desiccant prepared from 2-3 nm pore size silica gel. Isotherms for 7-8 nm and 9-10 nm pore size impregnated composite silica gel desiccant were Type IV isotherms with a hysteresis loop at higher relative pressure. The dynamic sorption quantities of composite samples on water were analyzed in a thermo-humidistat chamber under the test condition of 20°C and relative humidity of 0.7. Microporous silica gel (pore size 2-3 nm) was not good for host matrix due to less water uptake compared to pure silica gel. Water sorption capacity of composite desiccant prepared from 7-8 nm pore size and mesoporous silica gel was 2-3 times higher than pure silica gel. Composite desiccant prepared by impregnating $LiCl_2$ performed well compared to $CaCl_2$ and LiBr. All the isotherm data measured for several desiccants were fitted with Dubinin - Astakhov (D-A) equation based on the Polanyi theory.

Ramzy et al. (2014) modeled a desiccant packed beds of clay pellets impregnated with $CaCl_2$ (clay - $CaCl_2$) for air dehumidification. Three mathematical models were used for heat and moisture transfer for desiccant packed bed. These models were isothermal, adiabatic, and adiabatic diffusion. They used data of $CaCl_2$ vapor pressure chart from literature to produce the six-degree polynomial by the method of least square. The thermal conductivity of the clay - $CaCl_2$ pellets was assumed 1.8 W/m/K. Crank-Nicolson scheme was used to solve solid side diffusion equation, and explicit finite difference method was used to solve remaining equation. The diffusivity value of $5 \times 10^{-10}\,m^2$/s worked better compared to other two diffusivity values.

Chua (2015) carried out an experimental-analytical study on the heat and mass transfer of composite desiccants during air dehumidification. Three different composite desiccants were prepared by impregnating calcium chloride, lithium chloride, and polyvinyl alcohol (PVOH) on silica gel. Gas and solid-side resistance model (GSSR) was used to study the performance of the composite desiccants. The build-in UMFPACK solver in COMSOL was used for its robustness and accuracy. The effects of inlet air velocity, inlet air temperature, and humidity on moisture removal capacity, regeneration rates, and the pressure drops while dehumidification was part of the study. The moisture removal capacity of composite desiccants was almost two times as high as that of pure silica gel. Most of the operating conditions, Silica gel – $LiCl_2$ outperformed silica - $CaCl_2$ and silica gel - PVOH desiccants. From the regeneration experiment, it was observed that the silica gel - PVOH desiccant took less time for regeneration due to higher regeneration rate compared to other composite desiccants.

Rambhad et al. (2016) reviewed solid desiccant dehumidification and regeneration methods with emphasis on the use of solar energy. The concluded that the prospects of desiccant technology for thermal comfort applications likely to solve the problems faced by HVAC industries. Selection of correct desiccant materials, desiccant wheel geometry, desiccation, and regeneration are the parameters governing the satisfactory functioning of desiccant based systems.

Nciri et al. (2018) proposed a novel nomography tool for dimensioning of multi – packed bed dehumidifiers used in solar air conditioning. The methodology implemented compromises between the highest possible amount of heat and mass transfer and lowest possible pressure drop through the packed bed dehumidifier. The mathematical models governing the heat and mass transfer with variation of bed diameter, bed porosity, and bed height are presented. The nomography tool is integrated to simplify, speed up and expand all dimensioning possibilities of packed bed dehumidifier. The bed diameter, bed porosity, and bed height nomographs are constructed for applied examples. The bed diameter nomograph determines the bed diameter given the ventilation rate and number of beds. The bed porosity nomograph

gives bed porosity given the pellet diameter and bed diameter. The bed height monograph reveals bed height given bed porosity and pellet diameter. The nomographs presented also determines the appropriate ranges of ventilation rate, and number of beds given the bed diameter, the ranges of pellet diameter and bed diameter given the bed porosity and the range of bed porosity and pellet diameter given the bed height.

2.4 APPLICATION OF DESICCANT MATERIALS

Gad et al. (2001) have developed an integrated desiccant/solar collector for extraction of water from atmospheric air. They investigated theoretically and experimentally the system design characteristics, climate parameters, radiation intensity, and ambient temperature. For their study they used corrugated surface impregnated with calcium chloride solution as the adsorbent. The performance of a desiccant/collector system with a thick corrugated layer of blackened cloth to absorb water vapor at night from atmospheric air with subsequent regeneration during the day using solar energy. They found that solar operating system can produce 1.5 liters of fresh water per square meter per day. Cycle efficiency of more than 17% was recorded. The effect of ambient conditions on system performance was discussed. They suggested a design of slightly closed system to minimize vapor leak during regeneration.

Hodali and Bougard (2001) numerically simulated operational and physical parameters of silica gel adsorption unit integrated with solar collector and the dryer. Drying of apricots on the site of Marrakesh in Morocco is proposed. The mathematical model assumes adsorption due to a fixed bed adsorber comprising homogenous pellets of silica gel. The adsorbate is air and composed of ideal gases, water vapor, and dry air. The adsorption of water vapor by silica gel was described by a nonlinear adsorption isotherm. The dynamics of fixed bed adsorption is investigated by considering one surface and two intrapellet mass transfer resistances. The governing equations are derived by simultaneous mass and energy balances for dry air, water vapor, and adsorbent bed. The five nonlinear first-order differential equations include kinetics of adsorption, spatial and transient variation of concentration of dry air, water vapor, desiccant bed temperature and flowing air

temperature. The resulting sets of governing equations are written in matrix form and are solved by finite difference numerical technique. The heat of desorption supplied to the desiccant bed during day is rejected to the air during night adsorption. The bed exit air temperature is in the range of 20 to 31°C with respect to bed inlet air temperature ranging from 16 to 36°C. The numerical results reveal that sorption capacity of daily cycle of the unit depends on velocity of air, the desiccant properties, and unit dimensions. Further the dehumidification capacity of bed can be improved by employing a solar collector for regeneration and suitable air velocity. Due to the integration of desiccant bed with solar collector coupling efficiency of 86% is obtained for adsorbent - apricot ratio of 0.445. The optimum physical parameters found from numerical simulation are as follows. The length of collector, desiccant bed and dryer are 10, 1.5 and 1m respectively and the height and width for the three units are same and equal to 10 cm and 2 m respectively. During day and night the optimum velocity of drying air were 3 m/s and the optimum charging time is 7 p.m. Finally the integration of adsorbent unit with silica gel is economically justified, and the system can be employed for drying of different products.

Shanmugam and Natarajan (2006) experimentally and theoretically analyzed the forced convection desiccant integrated solar dryer for green peas drying under prevailing atmospheric conditions of Chennai, India. The desiccant bed is designed to contain solid desiccant comprising a mixture of 60% bentonite, 10% calcium chloride, 20% vermiculite, and 10% cement by weight. The desiccant is processed at 50°C for 24 h and dried at 200°C for 24 h in a vacuum furnace. The drying parameters such as drying rate, pick up efficiency, specific moisture extraction, moisture ratio, and mass shrinkage ratio is evaluated by theoretical correlations. Green peas drying experiments are conducted for airflow rates of 0.01, 0.02 and 0.03 kg/m^2 s. The experimental results show that solar dryer with desiccant unit is capable of drying products during off-sunshine hours and improve the quality of products dried. The products equilibrium moisture content was attained after operation time of 22, 18 and 14 h at 0.01, 0.02 and 0.03 kg/m^2 s, respectively. The drying of green peas with

desiccant unit produces more uniform drying in all the trays. Finally they found that the characteristics of the desiccant remain stable even after a year.

Nagaya et al. (2006) proposed and evaluated a low-temperature desiccant – based food drying system with controlled airflow and temperature. The food vegetables dried are cabbage, eggplant, carrot, butterbur, and spinach. The desiccant drying system employed consists of rotary silica gel desiccant dehumidifier and drying chamber. The drying chamber contains racks made of netting. The netting retains original shape and ensures temperature control and uniform drying conditions. The dry air output from the desiccant dehumidifier stage is heated to precisely 49°C by a 2 kW box heater. The constant temperature and humidity of 15% are maintained in the drying chamber to preserve color, vitamins, and texture of food items. The airflow is controlled by using fans mounted at top and bottom of the drying chamber. The moisture evaporation from the food products is accessed by placing a dish of water on top and bottom net racks. The experiments conducted without control of temperature and airflow rate demonstrates slow drying rates and uneven drying. The drying performed without temperature control and with air circulation reveals 5 times more water evaporated from the dishes without circulation. The water removed from the top and bottom dishes were uneven. The experiments with temperature and air circulation control show identical quantity of water removed from top and bottom dishes. The results for cabbage drying shows weight ratios of vegetables before drying and after drying (14 h) are similar to the weight ratios achieved by sun-drying (8 days). The colors of the dried vegetables are numerically evaluated using color channel values. The product dried by this method qualitatively reveals retainment of color and preservation of vitamin content as that of fresh vegetables. The drying system achieved 12 times higher drying speed than by sun-drying and 6 times higher than conventional desiccant based drying.

Hung et al. (2009) numerically simulated and analyzed heat and mass transfer in the integration of multi tray silica gel desiccant units with grain aeration systems. The simulation is conducted to predict the stored grain temperature and moisture content during aeration. The grain used in this work is paddy rice. The empirical desiccant

model predicts the condition of air leaving the desiccant unit. The theoretical silo or storage model in the form of differential equations is solved numerically. The simulation results predict the temperature and moisture content of paddy under various aeration conditions. The three conditions considered for the simulation are silo unit without desiccant trays, silo unit with desiccant trays but no internal cooling and silo unit with desiccant trays with internal cooling. The cooling water circulated removes the heat of adsorption. The dehumidified air enters the silo unit at lower temperatures. The results demonstrate the feasibility of integrating desiccant tray unit with internal cooling to control grain temperature and moisture content. The silo coupled with six desiccant trays with internal cooling results in moisture content of grain for safe storage close to its initial conditions. This ensures the grain moisture content is not excessively wet or dry under tropical climatic conditions. Finally the numerically simulated results could lead to the development of appropriate practical systems for keeping grains not too dry or wet.

Doymaz and Kocayigit (2011) investigated experimentally the effect of pretreatments and drying temperature on drying time and rehydration capacity of the green pea drying process. Experimentally the drying characteristics of three pretreated green pea samples with untreated control samples are compared. The pretreatment is carried out by blanching and by dipping the green pea in pretreatment solutions. Drying experiments are conducted in a cabinet type dryer with air at temperatures of 55, 60, 65 and 70°C. The air flows through the dryer horizontally at a constant velocity of 2 m/s. The four semi theoretical models namely Lewis, Henderson, and Pabis, logarithmic and Page models which are widely employed in biological and food materials are presented. The models employed describe the drying kinetics. Based on experimental drying conditions the effective moisture diffusivity and activation energy are estimated. The experimental results demonstrated that pretreatment reduces mass transfer resistance. Higher air temperatures of 70°C enhances drying rate and thereby reduces drying time. The estimation of moisture diffusivity and activation energy reveals the effect of pretreatment and air temperature. The range of values estimated is agreeable with values of literature. The theoretical study predicts

29

excellent fit for logarithmic and Page models. The study on rehydration capacities shows less shrinkage for pretreated green pea samples. Rehydration capacities of pre-treated green pea samples are higher than the untreated control samples.

Kumar and Yadav (2016) experimentally investigated the production of water from atmospheric air using saw wood - $CaCl_2$ composite desiccant in Indian humid climate. A solar-powered glass desiccant box type system is employed to regenerate the desiccant material. The system consists of fiber-reinforced plastic (FRP) container, glazing, wire mesh tray, water measuring cylinder, connecting pipes and composite desiccant material. Five types of desiccants are prepared using 1 kg of saw wood with $CaCl_2$ liquid desiccant having 20%, 30%, 40%, 50%, and 60% concentration. Adsorption of moisture by the desiccant exposed to atmosphere takes place during night, and subsequently the same desiccants are regenerated during day time. The adsorption rate in terms of quantity of water produced by the desiccants per unit time is analysed with respect to concentration of $CaCl_2$ and solar intensity. The maximum water collected by the saw wood - 60% $CaCl_2$ composite desiccant is 180 ml/kg/day. The quality of collected water is physically and chemically tested. The experimental results conclude that the water collection increases with increase in $CaCl_2$ concentration.

Many other works of literature on clay-based composite desiccants is illustrated in the form of table, and Table 2.1 highlights the clay-based composite desiccants. The underlying clay materials employed for the preparation of composite desiccant are calcium bentonite, sodium bentonite, sepiolite, kaoline, mined clay or attapulgite, mica, vermiculite, montmorillonite, and burnt clay. Apart from clay corn grit and starch, coconut coir and durian peels and mature coconut coir as desiccant are used to produce the desiccants.

Table 2.1 Summary of the literature on desiccant materials prepared from naturally available materials.

Sl. No.	Author and Year	Desiccant material	Description	Remark
1	Watts et al. (1985)	Calcium and sodium-based bentonite	Theoretically investigated the potential of bentonite, for moisture adsorption so as to report some experimental results for drying of corns.	Calcium based clay adsorbs more moisture than the sodium-based bentonite at low moisture contents and is preferable for grain drying applications.
2	Thoruwa et al. (1998)	Bentonite - $CaCl_2$	They proposed a device for grain storage. At night, a prototype device supplied dehumidified air, and it was regenerated by solar energy during the day. Experiments were performed for packed bed of bentonite $CaCl_2$ desiccant to produce dehumidified air. The desiccant was prepared from a mixture of bentonite, $CaCl_2$, vermiculite and cement in the ratio 6:1:2:1 by weight.	At night, during the dehumidification process, the humidity of air is reduced by 40%, and the temperature rise was 4°C. They found that more than 50% of the incident solar energy could be captured for use in the cyclic process.

3	Caturla et al. (1999)	Sepiolite clay	Performed experiment to study adsorption/ desorption of moisture by natural and heat-treated sepiolite clay. Sepiolite clay was heat-treated in the temperature ranges of 110 – 150°C. An experiment was performed for six different samples namely, natural sepiolite and 5 heat-treated sepiolites.	They found a change in volume of microporous after heating at above temperatures. Sorption isotherm changed from type II to type III when the heat treatment temperature was increased from 110°C to 500°C. Hysteresis was found for all the cases at relative humidity higher than 60%. From adsorption isotherms they concluded that the heat treatment of sepiolite degraded the adsorption capacity of normal sepiolite.
4	Thoruwa et al.(2000)	Bentonite with $CaCl_2$	Carried humidification – dehumidification experiments on packed bed comprising bentonite with $CaCl_2$ desiccant under simulated tropical conditions.	Based on their results they designed a prototype solar regenerative desiccant dehumidifying device employed for drying of cereal grains and crops. They concluded that the estimated cost of the fabricated desiccants was 1/9th the cost of commercial silica gel desiccant.
6	Beery and	Corn grit and	Reviewed the chemical and structural	The modification of surface properties of

	Ladisch (2001)	starch-based desiccant	properties of starch and corn grit on which the starch can be affixed. The starch-based adsorbents are hygroscopic for adsorption of water vapor.	starch results in adsorptive material with enhanced water sorption capacities compared to the corn grit. They concluded that the key parameters to increase the adsorptive capacity are porosity and surface area.
5	Hamed (2002)	Clay with $CaCl_2$	Experimentally studied the isothermal adsorption of water vapor from atmospheric air using burnt clay impregnated with calcium chloride desiccants.	The isothermal model for mass transfer is solved analytically for potential ratio and compared with experimental results
7	Ghosh and Bhattachar yya (2002)	Kaolin based desiccants	Adsorption experiments were performed for six different adsorbents namely, (1) Raw kaolin (2) Pure kaolin (3) Calcined raw kaolin (4) Calcined pure Kaolin (5) NaOH treated raw kaolin and (6) NaOH treated pure kaolin	NaOH treated kaolin showed maximum adsorption capacity. It adsorbed almost 100% methylene from a 12-ppm solution. Pure kaolin adsorbed more amount of methylene blue compared to raw kaolin. For both (raw and pure) kaolin, the adsorption capacity was reduced after calcination. Adsorption of methylene blue on kaolins was described by Freundlich and Langmuir equations.

| 8 | Khedari et al. (2004) | Agriculture wastes such as coconut coir and durian peels | Experimentally the performance of coconut coir and durian peel is compared with silica gel. The parameters compared are water uptake, adsorption rate, and exit air temperature. | For the same velocity of 4.2 m/s water adsorbed by coconut coir and durian, the peel was 30 g, 17 g H_2O per 100 g of dry desiccant. Silica gel adsorbed 5 g more than coconut coir desiccant. Lower values of an exit air temperature of coconut coir will reduce the cooling load in open cycle air conditioning systems Agriculture waste could be used as a desiccant instead of chemical desiccants such as silica gel. |
| 9 | Oliveira et al. (2003) | Bentonite clay-based magnetic adsorbent. | The adsorbents prepared are a pure iron oxide, clay - iron oxide (1:1), clay - iron oxide (1.5:1), clay - iron oxide (2:1). The adsorption isotherms for the adsorption of Ni^{2+}, Cu^{2+}, Cd^{2+} and Zn^{2+} from aqueous solutions on the clay - iron oxide (2:1) composite desiccant was studied. | The study reveals the magnetic adsorbents were having functional adsorption capacity for metal ion contaminants in water. The desiccant pellets excellent chemical stability in a wide range of water PH. The isotherm study reveals increased adsorption capacity for the composites as compared to bentonite |

				clay
10	Chamkhi et al. (2004)	Clay as a desiccant material	Studied the thermodynamic analysis of water sorption in clay. Desorption isotherm was obtained for three types of clay at three different temperature (40, 50, and 60°C) with the help of the static method.	Guggenheim Anderson de Boer (GAB) model was used to describe the sorption isotherm. Thermodynamic analysis like the heat of adsorption, net integral enthalpy and entropy were obtained at different moisture contents.
11	Li et al. (2007)	Mined clay (Attapulgite) and starch-based composite desiccant	A composite adsorbent of water vapor based on impregnating hygroscopic salt into the pores of host inert materials like-mined clay and starch is being researched	The novel superabsorbent composite having excellent water absorbency and water retention under load could be useful in agricultural and horticultural applications
12	Zhang and Wang (2007)	Superabsorbent composed of acrylamide with clays such as attapulgite, kaolinite, mica, vermiculite, and montmorillonite.	The reaction mechanism and thermal stability of polyacrylamide - clay super adsorbents were characterized by FTIR, XRD and TGA tests. The effect of clay type and content on equilibrium water absorptivity in aqua of these composites were investigated and compared.	The equilibrium water absorptivity decreases with increasing clay content resulting in a decreasing percentage of hydrophilic groups in polymeric network. The type of clay affects water absorbency and swelling of clay incorporated.

13	Rawangul et al. (2010)	Mature coconut coir as a desiccant	Experimentally investigated the use of mature coconut coir as a desiccant for moisture adsorption in engineering application. Moisture adsorption isotherms of dried coconut coir were determined by a static method.	The isotherms developed are of type V, which indicates porous material weak interaction. The study confirmed the feasibility of using coconut coir as desiccant.
14	Hiremath and Kadoli. (2013)	Burnt clay with $CaCl_2$	Experimentally and theoretically studied the transient heat and mass transfer characteristics of vertical packed burnt clay $CaCl_2$ composite desiccant.	Experimental results reveal the effect of bed mass and air velocity on dehumidification potential of clay - $CaCl_2$ composite desiccant. The deviation between the experimental and theoretical PGC model are due to the isotherm equilibrium relation.
15	Ramzy et al. (2014).	Burnt clay with $CaCl_2$	The theoretically studied the transient heat and mass transfer characteristics of vertical packed burnt clay $CaCl_2$ desiccant. The theoretical models namely are pseudo gas controlled and solid side resistance adiabatic models.	The model results are compared with the experimental results of the literature. Both adiabatic and adiabatic diffusion models provide acceptable predictions for the adsorption studies of clay - $CaCl_2$ desiccant beds.

2.5 MOTIVATION

The thrust is to develop low-cost desiccants for agricultural, industrial and commercial application is being revealed from the literature survey. The best features of solid and liquid desiccants can be explored by impregnating hygroscopic salts on to the pores of solid desiccants. The development of new desiccant based system opens new fields of research. The physics underlying these desiccant systems for sorption processes is adsorption and desorption. An excellent qualitative understanding and an accurate quantitative description of mass and heat transfer in these systems are necessary for modeling and evaluation of these systems. To gain insight into this subject it is first necessary to obtain experimental data for air and properties of bed which will result in model adaptation to be able to relate experimental data to the theoretical model. In this context our motto is to prepare low-cost adsorbents using locally available materials and to implement theoretical models.

2.6 OBJECTIVES OF THE PRESENT STUDY

The goal of this work is to provide theoretical and experimental analysis that qualitatively and quantitatively describes heat and mass transfer characteristics of desiccant bed comprising heat-treated clay - $CaCl_2$ liquid desiccant. In order to achieve these goals, the following objectives are set for the research work.

1. Experimental estimation of properties of transported soil (illite clay) with sawdust and horse dung additives based $CaCl_2$ composite desiccants. The study includes estimation of (a) Apparent porosity (b) Surface area (c) Pore volume (d) Initial water content (e) Thermal diffusivity (f) Specific heat (g) Density (h) Thermal conductivity and (i) Micro structural studies.

3. To investigate experimentally, the effect of desiccant bed inlet parameters like inlet air temperature, humidity, and velocity on heat and mass transfer characteristics of process air and desiccant bed comprising heat-treated clay - $CaCl_2$ and heat-treated clay - additives - $CaCl_2$ composite desiccants.

4. Experimental investigation on dehumidification performance of clay and clay-additives based fluidized composite desiccant bed with vertical packed desiccant bed.

5. To develop and numerically simulate the theoretical model of vertical packed desiccant bed to predict bed exit air humidity ratio in terms of process air moisture content. To compare present experimental results of vertical packed clay composite desiccant beds with theoretical model output.

6. To explore the application of fabricated clay and clay additives composite desiccants in aeration and drying of grains.

CHAPTER 3

PROPERTIES DETERMINATION OF CLAY WITH ADDITIVES AND IMPREGNATED WITH CaCl$_2$ COMPOSITE DESICCANT

3.1 INTRODUCTION

This chapter outlines the approach adopted to prepare the clay with additives and impregnating CaCl$_2$ composite desiccants. The size of the pellets, clay, and clay with additives, produced are of 10 mm size. The shapes of the pellets are nearly spherical, and these spherical clay and clay with additives after impregnation with CaCl$_2$ will be used to find adsorption and desorption characters in a vertical packed bed. Cylindrical shaped desiccant pellets are used for the fluidized bed experiments. These are prepared by injection method. The impregnation of CaCl$_2$ solution into heat-treated pellets is discussed. The thermal properties like thermal diffusivity, thermal conductivity, density, and specific heat are determined. The transient measurement technique is used to determine the thermal diffusivity of samples. The initial water content of desiccant pellets to be employed in theoretical study on heat and mass transfer characteristics of composite desiccant pellets is presented. Characterization of clay composite desiccants is by employing microscopic and spectroscopic experimental methods such as scanning electron microscopy (SEM), energy dispersive X-ray (EDAX) and X-ray diffraction (XRD) techniques.

3.2 PREPARATION OF DESICCANTS FOR PACKED BED

The raw materials used were transported soil, additives, and anhydrous CaCl$_2$ powder. In the present study the transported soil deposited on the banks of a lake is used as liquid desiccant carrier. The lake is located in Vijayapur district of Karnataka state, India. The transported soil is employed in making earthen pots, jars, and lamps by local pot makers. The soil in clinker form was collected from pot maker. The transported soil is then crushed and ground to obtain the powdered raw material. The

soil is tested for its constituents. Gravimetrically determined chemical composition of transported soil is compared with the composition of illite, montmorillonite, kaolinite and chlorite mineral clays. The principal mineral content of transported soil seems similar to illite clay mineral composition. The chemical composition of the transported soil and other clay minerals by weight percentage are presented in Table 3.1. SiO_2 and Al_2O_3 make up the significant portion of the composition.

Table 3.1 Clay mineral composition of transported soil and its composition with other clay minerals (Biswas and Mukharji, 1994).

Clay mineral	SiO_2	Al_2O_3	Fe_2O_3	MgO	CaO	K_2O	Na_2O
Transported soil (Present study)	51.2	26.4	12.5	3.8	2.1	0.92	0.45
Illite	50-56	18-31	2-5	1-4	0-2	4-7	0-1
Montmorillonite	42-46	0-28	0-30	0-25	0-3	0-0.5	0-3
Kaolinite	45-48	38-40	-	-	-	-	-
Chlorite	31-33	18-20	-	35-38	-	-	-

To improve the desiccant features of transported soil clay, especially from the point of adsorption and desorption capability, additives like sawdust and horse dung which are available locally and in abundant were used. The horse dung which is popularly used in making pots along with clay is employed as additive. Sawdust is a byproduct of sawmill is another additive considered for preparing clay-additives-$CaCl_2$ composite desiccants. The sawdust and horse dung additives are cleaned and processed for contaminations. A sieve is employed to obtain the fine form of horse dung and sawdust additives. The clay material is segregated into three parts. The first portion is without any additives. The second portion with 20 % horse dung and the third portion with 20 % sawdust by weight. The weight is measured by using digital balance having a range 0. 2 to 300 g and resolution of 0.01 g. The resulting clay and clay - additives are mixed with water and kneaded thoroughly to bring to a form similar to dough. The pasty clay (green clay) is then rolled manually on flat surface into cylindrical or rod-like form. The rolled clay is cut to required length. The following relation is used to

arrive at the length of the clay rod to be cut in order that specified size of sphere is achieved when cylindrical form of clay is formed into a sphere.

$$\frac{\pi}{4}d_{cr}^{2}l \text{ (volume of cylinder)} = \frac{\pi}{6}d_{\phi}^{3} \text{ (volume of sphere)} \qquad (3.1)$$

Where, d_{cr} is the diameter of cylindrical rod, d_{ϕ} is diameter of sphere, and l is the length of material to be cut. The length of clay rod should be 6 to 7 mm so that it can be transformed manually into a 10 mm size sphere. Fig. 3.1 (a) shows the photograph of clay rod being cut to required length and subsequently molded to prepare spherical shape.

(a)   (b)

(c)
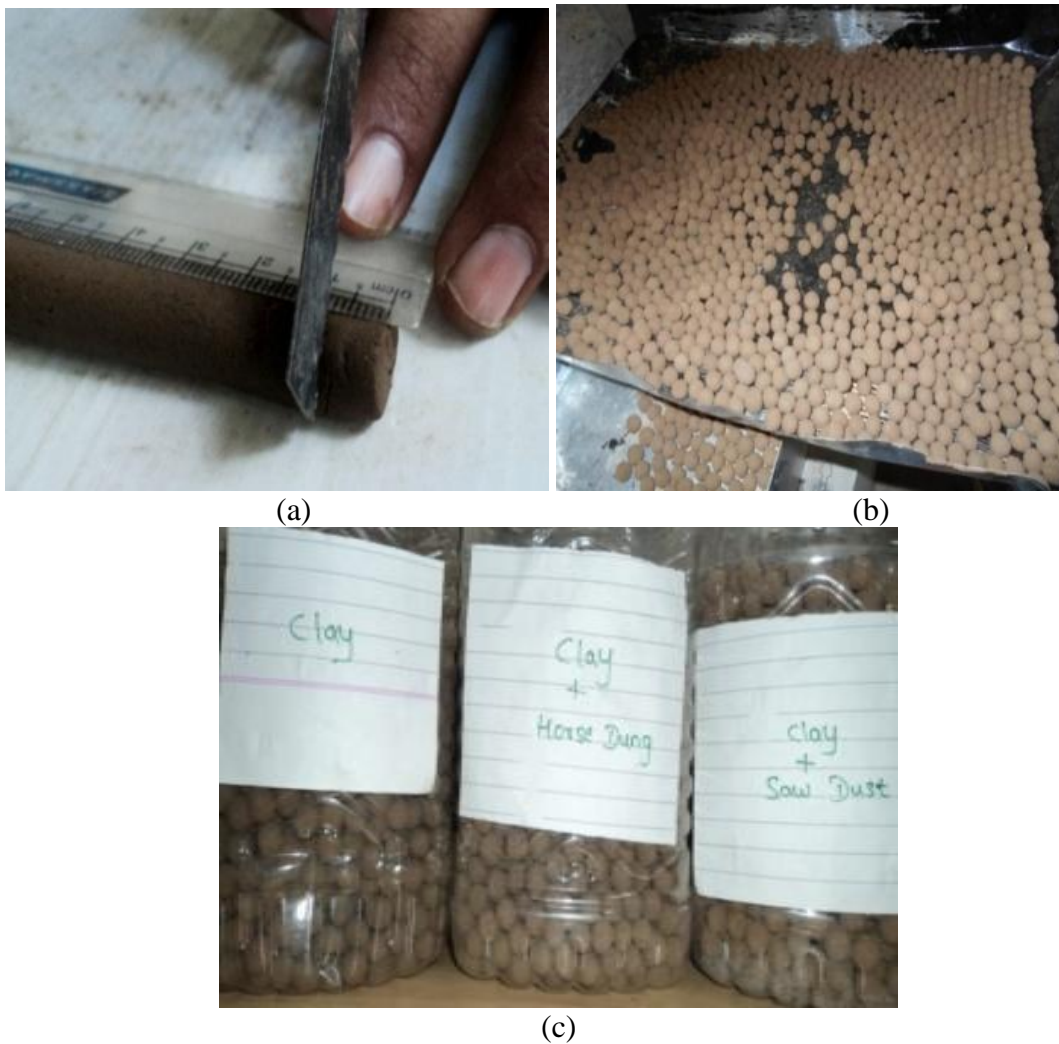
Fig.3.1 Photograph showing (a) clay rod being cut to the required length (b) clay pieces kept for drying (c) clay and clay - additives pellets.

41

As shown in Fig.3.2, a gauge is employed to check the correct diameter of the sphere formed. The diameter of the gauge is 10 mm. This enables us to separate the oversized and non-uniform pieces. The green pellets thus prepared are subjected to shadow drying in order to avoid the cracking of pellet that can likely occur when exposed to direct sunlight. To determine the drying temperature, samples of clay, clay-saw dust, and clay-horse dung pellets are placed in a 3.5 kW muffler furnace. Maximum temperature attained in the furnace is 1200°C. The pellets are heat treated for one hour at temperatures ranging from 100 to 800°C. After the desiccant pellets are heat-treated for about an hour, they are left to cool in the furnace. The heat treatment of pellets induces strength and porosity. The apparent porosity of heat-treated pellets before impregnation of hygroscopic salt is calculated according to the Archimedes principle.

3.2.1 Analysis of porosity of desiccants

The apparent porosity accounts the volume of open pores. Eq. (3.2) is used to calculate the apparent porosity of the heated pellets (Gupta, 2010).

$$\text{Apparent porosity } (\varepsilon_{dp}) = \frac{(S-\zeta) \times 100}{S-(I-\iota)} \tag{3.2}$$

Where ζ is dry weight, S is saturated weight, I is immersed weight of pellet and ι is the weight of thread. As shown in Fig. 3.3 (a), (b), (c) and (d), the weight of thread, dry weight, immersed weight, and saturated weight of pellets are recorded. Weight balance is used to measure the weights. For measuring saturated weight, the surfaces of the samples were slightly wiped off by wet cloth to remove surface adhered water, and weight of the sample is taken by suspending it in air. Figure 3.4 (a) and (b) shows the variation of weight reduction and change in apparent porosity with temperature. For all the three samples the maximum weight reduction and porosity values are recorded at 500°C. The apparent porosity values recorded at 500°C are 0.13, 0.23 and 0.26 for burnt clay, burnt clay-sawdust and burnt clay-horse dung pellets respectively.

(a)   Gauge   (b) Over size   (c) Under size   (d) Correct size

Fig.3.2. Copper gauge employed to check the shape and size of pellets.

43

(a) Thread weight measurement.   (b) Dry weight measurement

(c) Immersed weight measurement   (d) Saturated weight measurement

Fig.3.3. Photograph showing measurement of thread and pellet weights
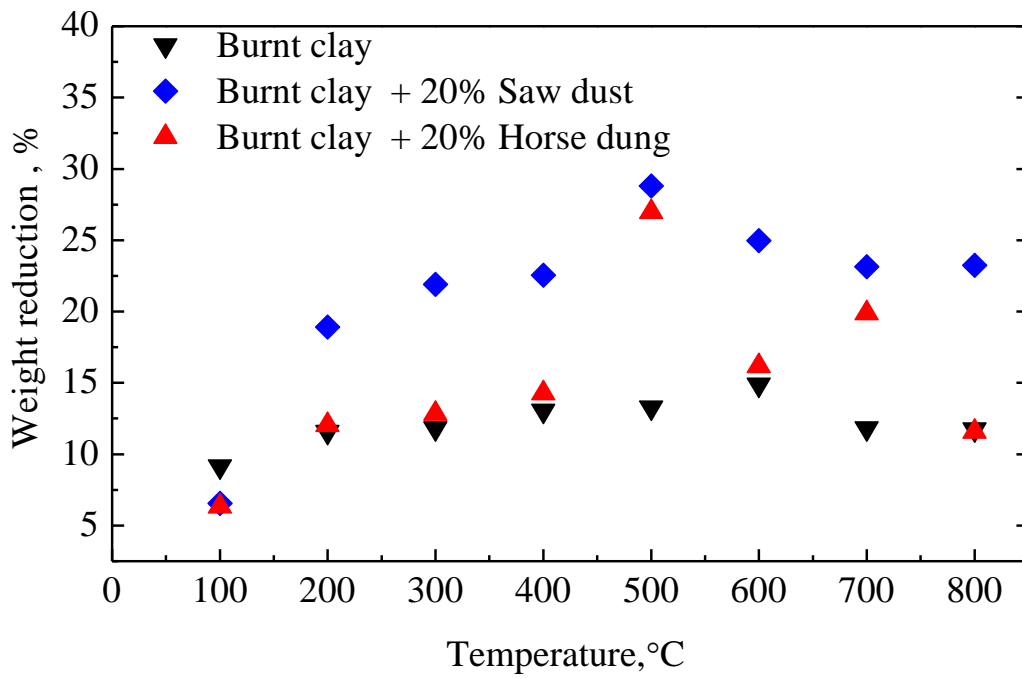
Fig.3.4 (a) Effect of temperature on weight reduction for heat-treated clay and heat-treated clay with additives.

44
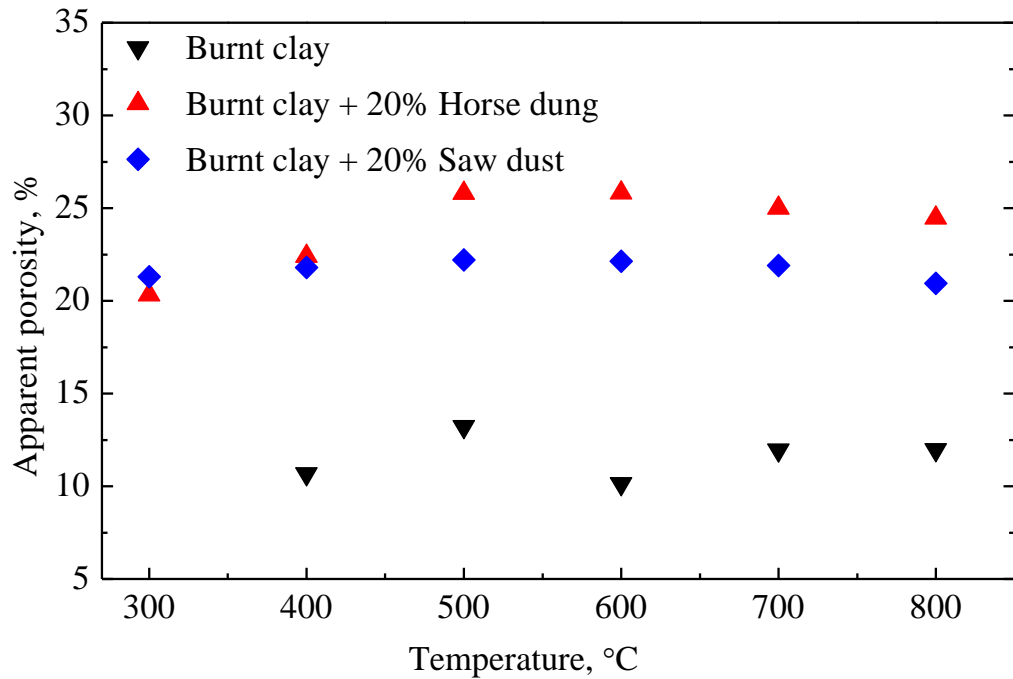
Fig.3.4 (b) Effect of temperature on apparent porosity for heat-treated clay and heat-treated clay with additives.

The information obtained above is supplemented by measuring other texture properties such as pore volume and surface area. The BET (Brunauer - Emmett - Teller) analysis of the samples measures pores volume and surface area. The system utilizes the principle of static volumetric technique to obtain nitrogen gas adsorption/desorption isotherms at regeneration temperature of 200°C. Figure 3.5(a) and (b) shows the variation of surface area and pore volume with temperature. The test reveals that with increase in temperature from 500°C to 800°C, the surface area decreases. The addition of 20% horse dung with clay results in higher values of surface area at 500°C. The surface area of burnt clay-sawdust samples is 59% less than the surface area of virgin burnt clay samples whereas the surface area of burnt clay samples is 28% less than the surface area of burnt clay horse dung samples. This indicates loss of number of pores especially smaller pores for burnt clay sawdust pellets. As shown in Fig. 3.5(b), pure clay has higher pore volume at 500°C. The pore volume of burnt clay increases by 62% and 36% as compared to clay sawdust and clay-horse dung pellets. The pore analysis of samples indicated loss of small pores for

45

burnt clay-sawdust samples. As a result, the internal surface area and pore volume of these samples is lower than burnt clay and clay-horse dung samples.
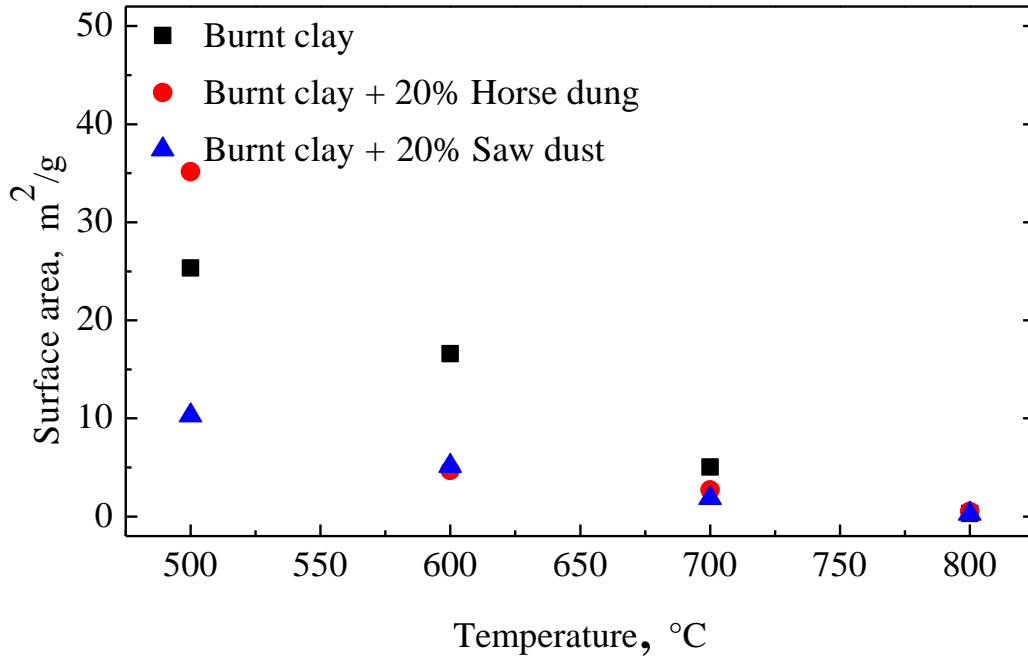
Fig.3.5 (a) Variation of surface area with temperature for heat-treated clay and heat-treated clay with additives.
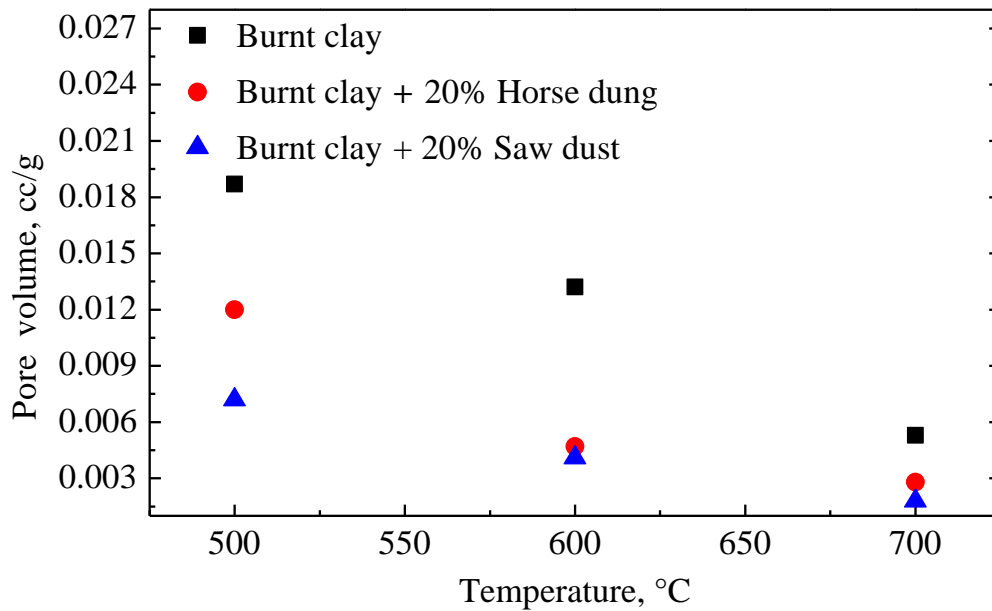
Fig.3.5 (b) Variation of pore volume with temperature for heat-treated clay and heat-treated clay with additives.

Based on the results of weight reduction, porosity, surface area and pore volume, the clay, and clay with additives pellets are heated to a temperature of 500°C. The number of clay and clay - 20% additives sample pellets produced are about 3000.

3.2.2 Preparations of desiccants for fluidized bed

To employ clay and clay with additives material in fluidization studies, 2 mm long and 2 mm diameter cylindrical-shaped samples are produced. A syringe is used to extrude the pasty clay and clay additives material. The extrusion procedure produces ¢2 mm × length 2 mm cylindrical-shaped clay and clay-additives pellets. The photograph of clay, clay-saw dust and clay-horse dung pellets produced by injection method are shown in Fig.3.6. The pellets produced are shadow dried and later stored in plastic box. At a later time, they are heat-treated at 500°C and after cooling the clay, and clay-additives samples are stored separately in plastic boxes. The pellets are then impregnated with $CaCl_2$ to form clay composite desiccants. The mass of clay and clay - additives desiccants for fluidized desiccant bed studies are 200 g and 300 g.

| (a) | (b) | (c) |
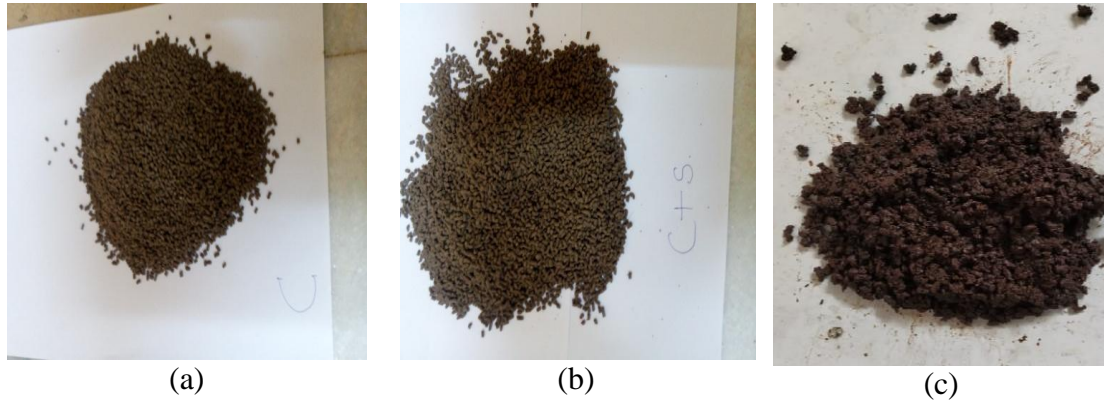
Fig.3.6 Photographs of (a) clay (b) clay - sawdust and (c) clay - horse dung pellets.

3.3 PREPARATION OF $CaCl_2$ SOLUTION AND IMPREGNATION ON TO CLAY

The heat-treated pellets are impregnated with $CaCl_2$ solution of 50% concentration. To ensure complete impregnation of $CaCl_2$ into the burnt clay and burnt clay additives spherical balls a soaking period of 24 hours is adopted. After impregnation the desiccants are sticky in nature. Hence the impregnated samples are again dried at 100°C and later on stored in airtight containers. The empirical correlation to calculate

the amount of salt required to prepare a solution of required concentration is given by Eq. (3.3) (Hamed, 2010).

$$\tau = \frac{m_s}{m_w + m_s} \tag{3.3}$$

Where m_s and m_w are the mass of salt and distilled water required to prepare a liquid desiccant solution of concentration τ. For a solution of 50% concentration, 1 kg of salt is added to 1 kg of distilled water. The burnt clay and clay - additives spherical balls are impregnated with calcium chloride solution with a concentration of 50 % by submersion of burnt pellets in the liquid solution for a period of more than 24 hours. Porous balls impregnated with $CaCl_2$ solution were strained to remove the excess liquid and avoid any dropping of liquid from the bed. After impregnation the overall weight of desiccants increased. After impregnation clay - additives desiccants shows higher gain in weight as compared to clay desiccants. The higher gain in weight indicates retention of more $CaCl_2$ salt onto the surface and in the pores of clay and clay additives composite desiccants. Higher mass of $CaCl_2$ salt is expected to result in increased dehumidification of process air. The increase in weight is as shown in Table 3.2.

3.4 MICROSTRUCTURE OF BURNT CLAY – ADDITIVES - $CaCl_2$ COMPOSITE DESICCANTS

The SEM micrographs show surface morphology of burnt clay-additives samples. This exercise was attempted in order to observe the changes that would occur when horse dung and sawdust were mixed with transported clay. Figure 3.7 shows the pictures taken using SEM at three different magnifications for burnt clay, burnt clay with horse dung and burnt clay with sawdust additives. The 5000X magnification of clay and clay additives samples shows clay platelets or grains of irregular shape and size. Even the large platelets of clay appear to be composed of smaller platelets or grains appearing in the form of valleys and peaks on the surface, which indicates the porous nature of the material. Overall the surface texture varies considerably. The surface appears mildly rough for clay with sawdust additives and much harsh for burnt clay.

Table 3. 2 Quantification of CaCl$_2$ impregnated into heat-treated clay and clay with additives desiccants.

Host material or desiccant carrier	Weight without impregnation (g)	Weight with impregnation (g)	The gain in weight (%)
Heat-treated clay (¢10 mm)	1.34 (Average weight of desiccant)	1.54 (Average weight of desiccant)	15.80
Heat-treated clay-20% horse dung (¢10 mm)	0.92 (Average weight of desiccant)	1.22 (Average weight of desiccant)	33.29
Heat-treated clay-20% saw dust (¢10 mm)	1.06 (Average weight of desiccant)	1.42 (Average weight of desiccant)	33.96
Heat-treated clay (¢10 mm)	900	957.03	6
Heat-treated clay with 20% horse dung (¢10 mm)	904.62	1007.3	11
Heat-treated clay with 20% saw dust (¢10 mm)	911.12	1053.37	15
Heat-treated clay (¢45 mm × length 15 mm)	69.66	75.49	9
Heat-treated clay with 20% horse dung (¢45 mm × length 15 mm)	37.38	46.33	24
Heat-treated clay with 20% saw dust (¢45 mm × length 15 mm)	34.44	49.41	41

In case of clay with horse dung additive, the surface is highly uneven with sharp ridges on the surface of grains. It may be noted that the addition of sawdust to clay and subsequent drying at higher temperature produces a surface that has an appearance as soft and smooth. In contrast, surface of the clay with horse dung additive is highly uneven with many ridges on the surface. Similar ridges are observed on the surface of burnt clay pellet. The average radius of surface pore is 6.4 μm, 8.5 μm and 6.1 μm for burnt clay, burnt clay-horse dung and burnt clay sawdust samples respectively. The average grain size is 3.35 μm along lengthwise and 2.93 μm along widthwise for burnt clay additives samples.

500X	2000X	5000X

Burnt clay

Burnt clay - Horse dung

Burnt clay - sawdust
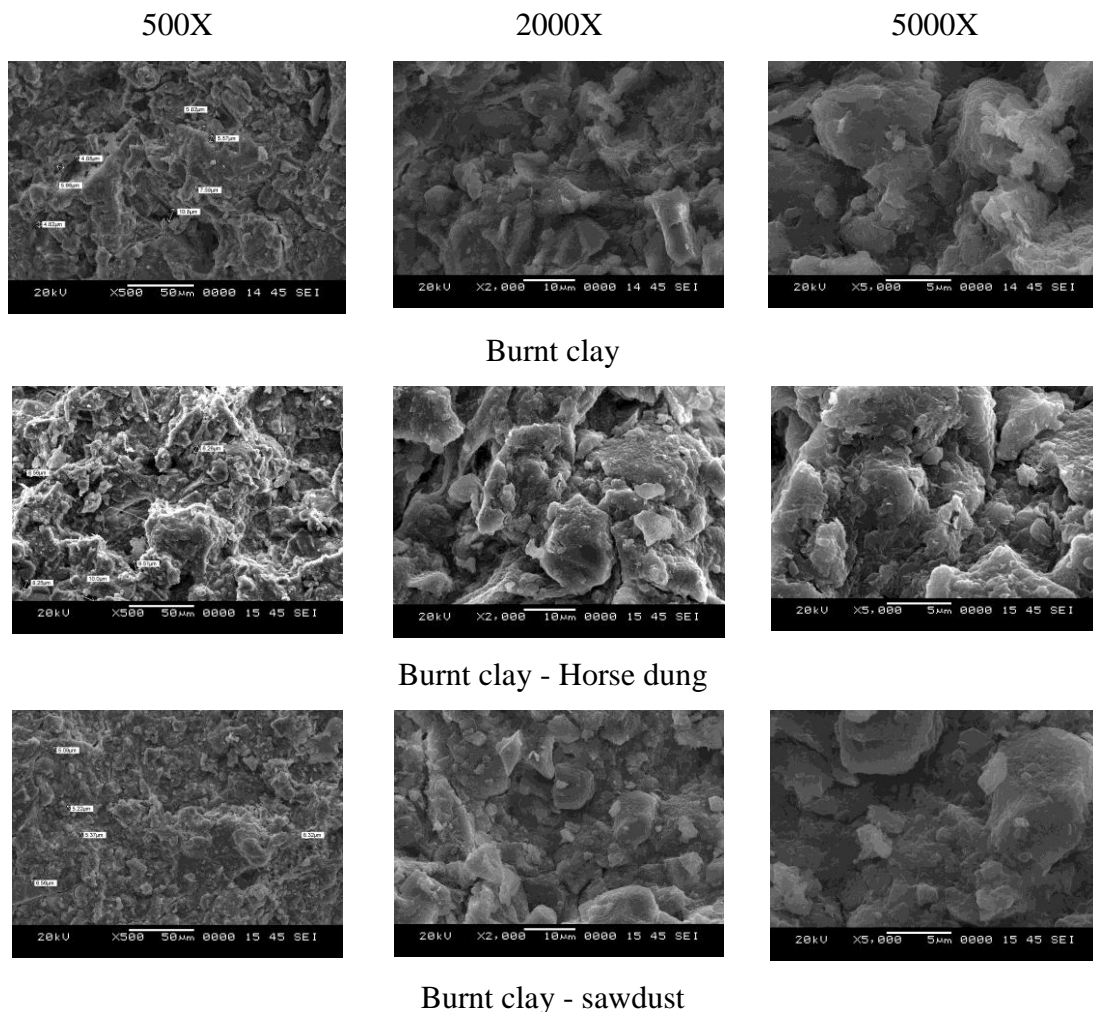
Fig.3.7 SEM micrographs of burnt clay and clay with additives sample without impregnation of $CaCl_2$ solution.

Fig.3.8 presents scanning electron microscopy images of uncut (2000X, 5000X) and the cut (10000X) surface of burnt clay additives $CaCl_2$ pellets. The images show the depth of impregnation and retention of $CaCl_2$ onto the pores and craters of burnt clay - additives grains. At 2000X magnification, burnt clay desiccants show scattering of impregnated $CaCl_2$ salt at localized sites. $CaCl_2$ impregnation appears as white spongy patches onto the clay grains. Similarly for burnt clay horse dung pellets, the white patches on clay grains indicate $CaCl_2$ presence. In case of burnt clay sawdust $CaCl_2$ samples the $CaCl_2$ salt is sparsely retained onto the pores and the craters. The average pore diameter is 2.02 μm, 2.38 μm and 1.58 μm for clay, horse dung, and sawdust additives composite desiccants respectively. The average sizes of grains measured are 2.79 μm and 2.97 μm along length and width wise respectively. The images under 5000X magnification also reveal the deposition of $CaCl_2$ salt onto the surface of clay and clay-additives pellets. The image shown under 10000X is the surface of cut section of the pellet. The desiccant pellet is cut into two halves. Accordingly the cut surface of the desiccant is examined. This image will reveal the internal surface morphology. On examination of the internal surface of the desiccant, it is found that the average pore diameters is 2.02 μm, grains of size, 4.93 μm and 4.24 μm along the lengthwise and widthwise are present. Lower values of pore diameter and larger crater surface area determine the depth and retention of $CaCl_2$ within clay and clay with additives.

Fig.3.9 (a, c, e) presents the energy dispersive spectrum (EDS) of burnt clay and burnt clay additives samples. The spectrum shows some differences in the distribution of additives. It seems that additives are concentrated in some areas. The dense white patches indicate the dispersion of sawdust in burnt clay. The distribution of sawdust is more significant than the distribution of horse dung in burnt clay. Fig.3.9 (b, d, f) presents the EDAX images showing peaks, and elemental composition of burnt clay, burnt clay horse dung, and burnt clay sawdust samples. The results of EDAX analysis are in agreement with the results of mineral analysis of raw clay shown in Table 3.1. The quantitative analysis of EDAX spectrum shows high content of Si and the presence of other alkali and alkaline elements like Carbon (C), Sodium (Na),

Magnesium (Mg), Aluminium (Al), Calcium (Ca) and Iron (Fe). The variations in intensities of Kα peaks corresponding to constituent elements are being observed. The SEM-based EDAX test had shown that burnt clay with horse dung and sawdust additives contain carbon and silicon as major elemental constituents with small amounts of Ca, Na, Al, Mg, and Fe. It is observed that with variation of drying temperature, the elemental analysis of burnt clay additives samples reveals decrease in composition of calcium as compared to sodium on atomic weight percentage. The calcium content decreases with increase in drying temperature for clay and clay-horse dung samples, whereas for clay sawdust samples calcium content increases with increase in drying temperature. For all other samples, with increase in temperature the sodium content increases.

| 2000X | 5000X | 10000X |

Burnt clay - $CaCl_2$

Burnt clay - horse dung - $CaCl_2$

Burnt clay - sawdust - $CaCl_2$
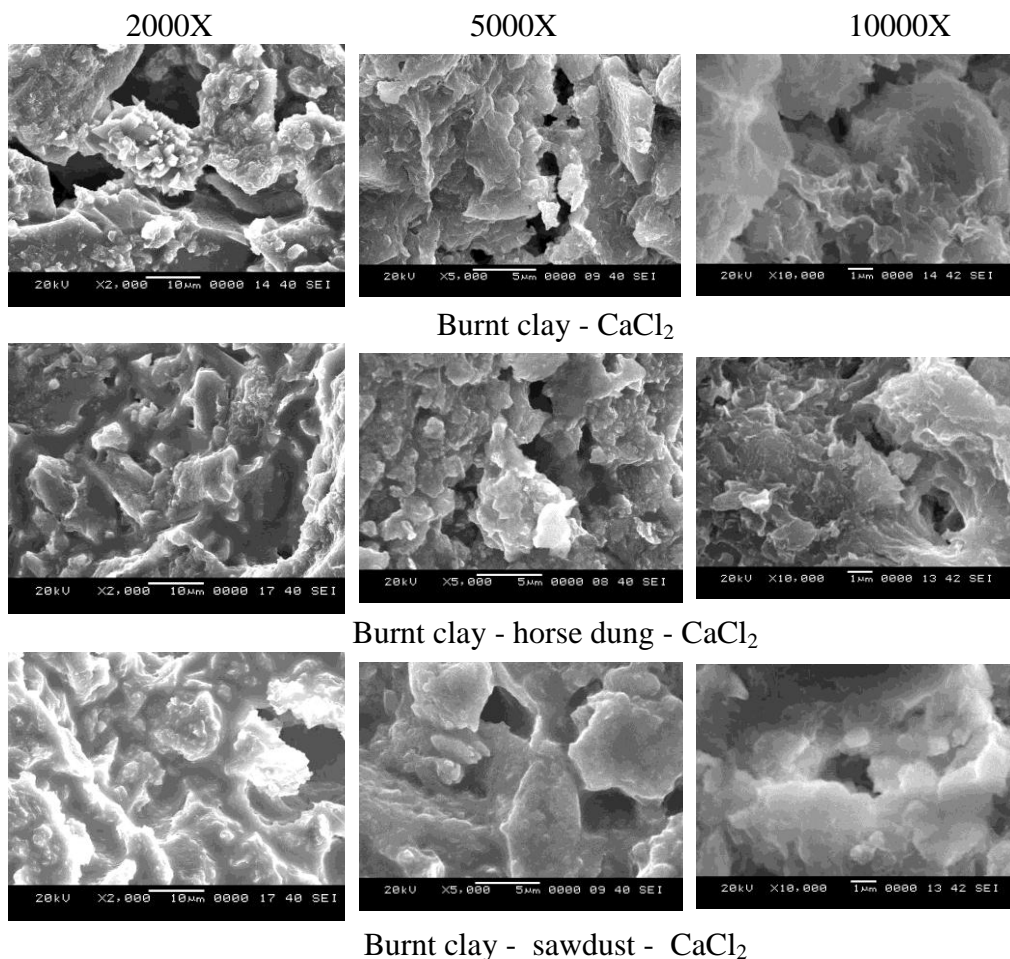
Fig.3.8 SEM micrographs of clay composite desiccants showing surfaces and cut sections.

52
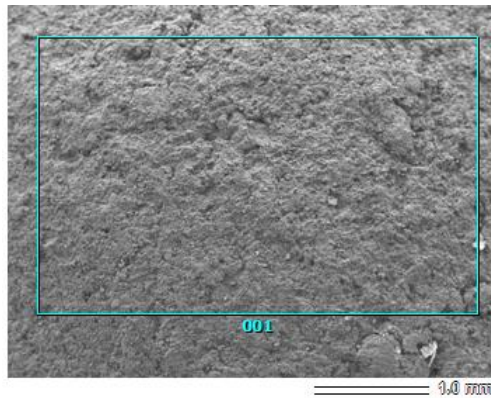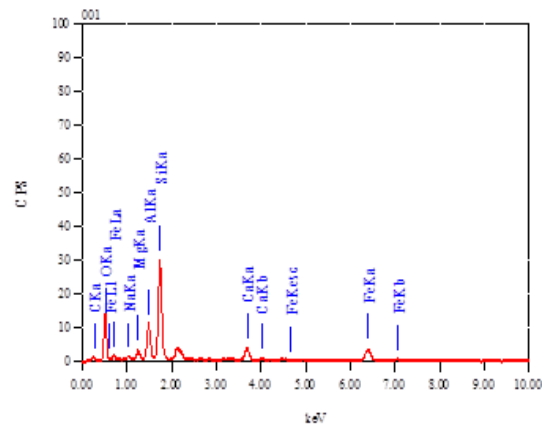
(a)   (b)
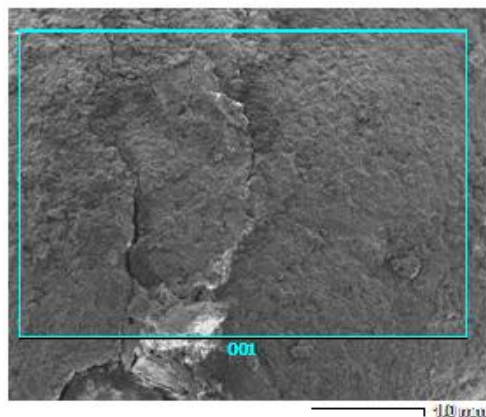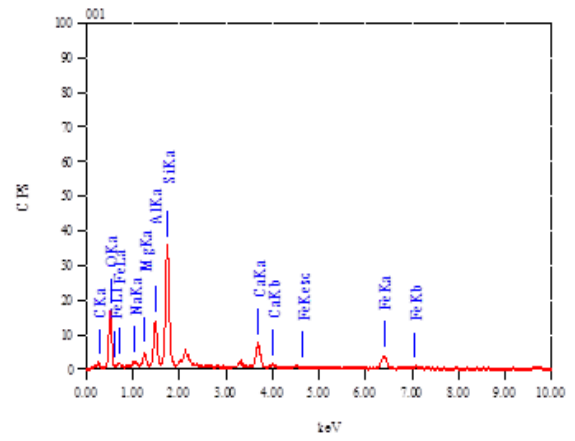
(c)   (d)
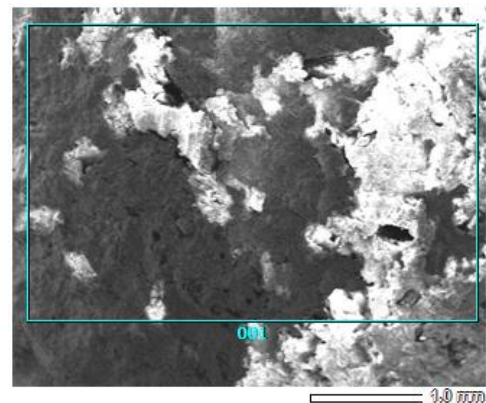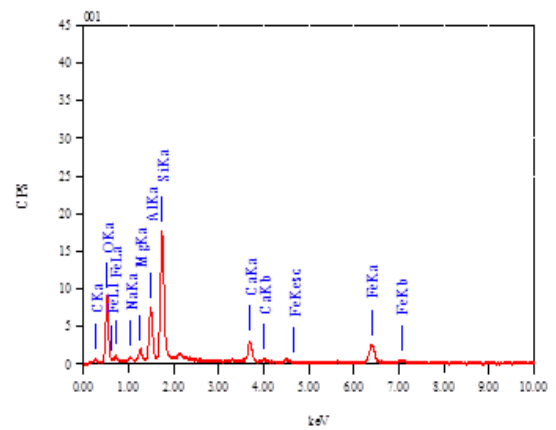
(e)   (f)

Fig.3. 9 EDAX images and spectrum of burnt clay (a, b) and burnt clay – additives as horse dung (c, d) and sawdust (e, f).

As shown in Fig.3.10 (a - e), a similar kind of X-ray diffraction pattern is observed for all the three samples with and without $CaCl_2$. The high intensity of diffraction peaks indicates good crystalline nature. The crystalline XRD pattern indicates the porous nature of burnt clay-additives composite desiccant. The decrease in the height of diffraction peaks with $CaCl_2$ impregnation reveals the presence of $CaCl_2$. The peaks for clay and clay additives samples with and without impregnation of $CaCl_2$ are not shifted and are at same basal spacing. The reflections corresponding to planes show the planes of presence of elemental oxides. The other smaller peaks correspond to other minerals present in clay additives and clay - additives - $CaCl_2$ samples. Debye-Scherrer's equation is used to calculate the average crystallite size of the clay and clay-additives based composite desiccants (Cullity, 1978).

$$\eta = \left(\frac{0.9\lambda}{\beta \cos\theta} \right) \tag{3.4}$$

In Eq. (3.4) η is crystalline size, λ (0.154 nm) is X-ray wavelength, β is full width at half maximum and θ is Bragg's angle. The maximum and minimum average crystallite sizes of minerals for burnt clay and burnt clay-additives samples with and without impregnation are presented in Table 3.3.

Table 3. 3 Quantification of average crystal sizes for heat-treated clay and clay with additives desiccants.

Sample Type	Average crystal size (maximum), nm	Average crystal size (minimum), nm
Burnt clay, Fig.3.10(a)	19.39 (K_2O)	1.46 (SiO_2)
Burnt clay - $CaCl_2$, Fig.3.10(b)	21.87 (SiO_2)	9.25 (K_2O)
Burnt clay - horse dung, Fig.3.1(c)	53.49 (K_2O)	12.71 (MgO)
Burnt clay - horse dung - $CaCl_2$, Fig.3.10(d)	42.75 (Fe_2O_3)	10.98 (N_2O)
Burnt clay - sawdust, Fig.3.10(e)	53.49 (K_2O)	12.71 (MgO)
Burnt clay - sawdust - $CaCl_2$, Fig.3.10(f)	14.03 (Na_2O)	9.45 (CaO)
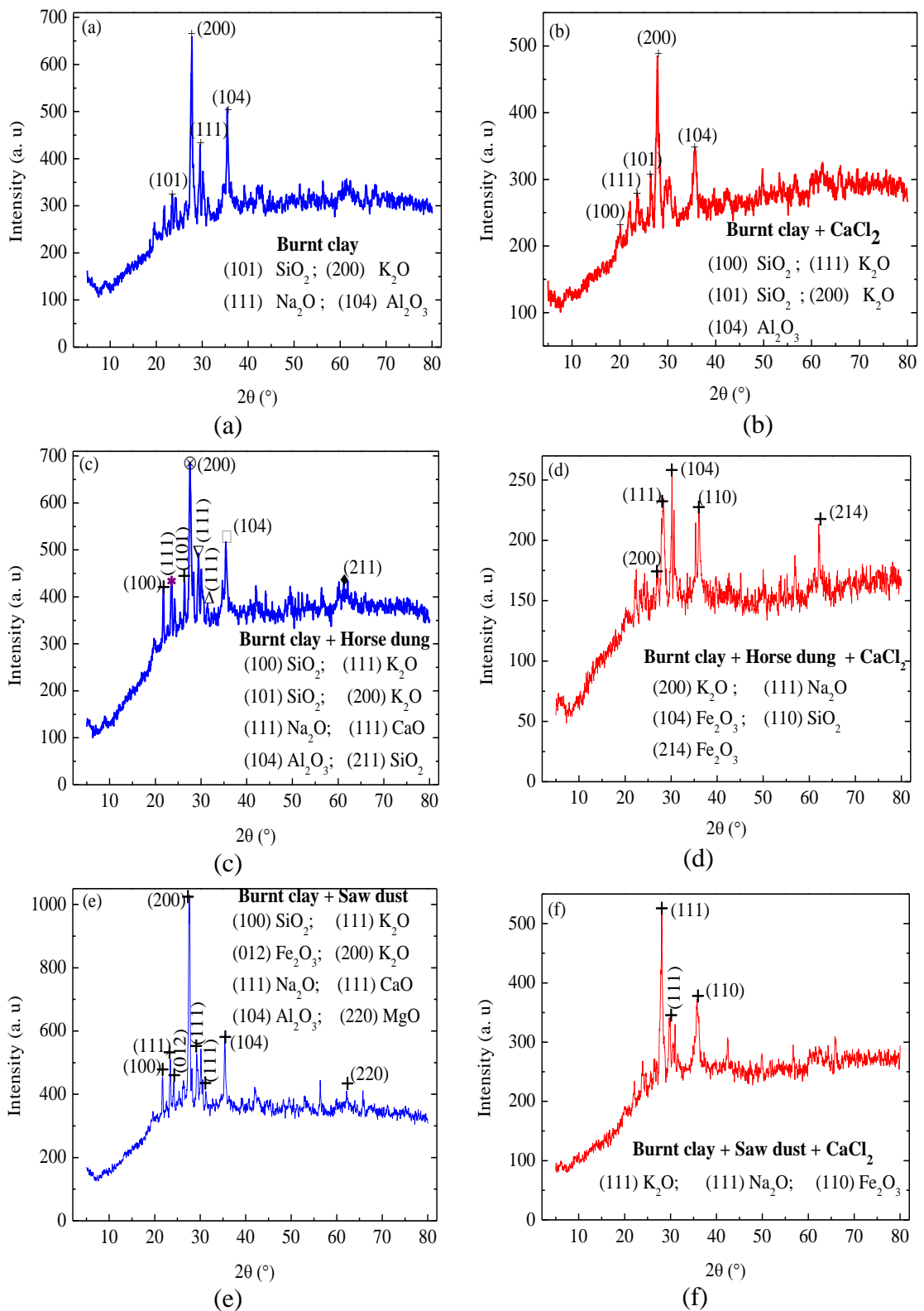
Fig.3.10 XRD spectrum of burnt clay and burnt clay - additives pellets.

3.5 DETERMINATION OF INITIAL WATER CONTENT

The water content of composite desiccant is estimated as follows. Five samples are picked from the lot and ensured that these are completely dried by subjecting them to hot environment in a furnace at 500°C. The duration of heating is about one hour. Each sample is weighed and averaged; thus, the dry weight of samples is determined. Five desiccant samples from the impregnated lot are chosen. The average wet weight of five samples is measured. By measuring the initial dry weight of clay and clay-additives samples before impregnation and final wet weight of composite desiccant after impregnation, the initial weight of water and weight of $CaCl_2$ is calculated on weight basis. For the solution of 'τ' concentration of $CaCl_2$, the initial water content of desiccants is estimated using the following equations.

$$\tau = \left(\frac{W_{CaCl_2}}{W_{CaCl_2} + W_{H_2O}} \right) \tag{3.4a}$$

Weight balance for desiccant pellets before and after impregnation is given by the following relation

$$W_{wd} - W_{dd} = W_{H_2o} + W_{CaCl_2} \tag{3.5}$$

Solving Eq. (3.4a) and Eq. (3.5) yields

$$W_{CaCl_2} = \left(\frac{W_{H_2O}}{\frac{1}{\tau} - 1} \right) \tag{3.7}$$

Substituting Eq. (3.6) in Eq. (3.5) results in Eq. (3.7).

$$W_{wd} - W_{dd} = W_{H_2o} + \left(\frac{W_{H_2O}}{\frac{1}{\tau} - 1} \right) \tag{3.7}$$

Eq. (3.7) gives the weight of water W_{H_2o}. The initial water content in grams of water vapor per kg of dry desiccant is given by

$$\psi = \frac{W_{H_2o}}{W_{dd} + W_{CaCl_2}} \qquad\qquad (3.8)$$

Table 3.4 presents the initial water content estimated for burnt clay - additives - CaCl$_2$ composite desiccants on a weight basis. For the solution of 50% concentration the initial water contents estimated for burnt clay- CaCl$_2$, burnt clay - sawdust - CaCl$_2$ and burnt clay - horse dung - CaCl$_2$ composite desiccants are in the order of 63.79, 86.04 and 93.44 g water / kg dry desiccant respectively. The initial water content data of clay - CaCl$_2$ and clay -additives - CaCl$_2$ composite is important in finding the isotherm behavior of desiccant materials. The initial water content of desiccant material is an essential input parameter in theoretical simulation of desiccant bed behavior in adsorption and desorption.

3.6 ESTIMATION OF THERMAL DIFFUSIVITY of CLAY AND CLAY ADDITIVES CaCl$_2$ DESICCANT MATERIAL

The thermal diffusivity is determined by using the rapid transient measurement technique (Midddleton, 1993). This method was adopted for the estimation of thermal diffusivity of rock samples. The method directly determines thermal diffusivity (α). Energy balance method is used for the estimation of specific heat (C_{p_ϕ}) and thermal conductivity (k) is calculated directly using Eq. (3.9). The theory is discussed for a one-dimensional single sample case.

$$k = \alpha \times \rho_\phi \times C_{p_\phi} \qquad\qquad (3.9)$$

Table 3.4 Initial water content values for burnt clay - additives - $CaCl_2$ composite desiccant.

Desiccant	Average dry weight (g)	Average wet weight (g)	Weight gain (g)	Weight of $CaCl_2$ = [0.5×weight gain] (g)	Weight of dry desiccant = [dry weight + weight of $CaCl_2$] (g)	Weight of water = [0.5×weight gain] (g)	Initial water content (g/kg)
Burnt Clay - $CaCl_2$	1.46	1.29	0.18	0.088	1.37	0.088	63.79
Burnt Clay - Saw dust - $CaCl_2$	0.76	0.89	0.14	0.071	0.83	0.071	86.03
Burnt clay - Horse dung - $CaCl_2$	0.68	0.83	0.141	0.071	0.076	0.0705	93.44

Physical model:

The physical model for the clay sample in the form of a circular disc is illustrated in Fig. 3.11.
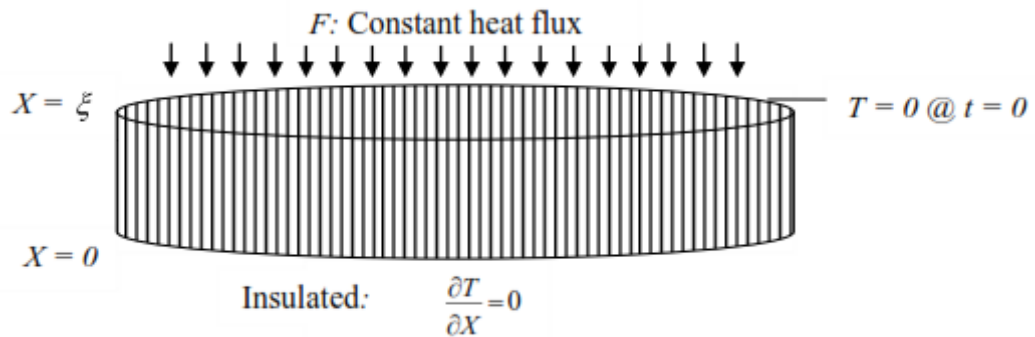
Fig.3.11 Diagram showing constant heat flux ' F ' at the top surface of clay pallet and the base is insulated.

The method of measurement proposed herein entails a constant heat flux at the top of an of clay disk, which is insulated at its base. Measurement of temperature at the base of the disk is recorded for various times after introduction of the constant heat flux at its top surface. The mathematical model is discussed for the one-dimensional (1-D) single clay disk case

Mathematical model:

The clay pellet is initially at zero temperature. At the surface where $Z = 0$ insulation is provided and has a constant heat flux introduced at the surface $Z = \xi$, at time $t = 0$. The temperature at a distance Z within the sample and at time t (after the introduction of the constant heat flux at $Z = \xi$ is given by Eq. (3.10)

$$\frac{\partial^2 T}{\partial Z^2} = \frac{1}{\alpha} \frac{\partial T}{\partial t} \tag{3.10}$$

Eq. (3.10) represents the governing equation to find the unsteady temperature at any cross-section of the clay sample. The associated boundary and initial conditions are as follows

59

Boundary Condition: $\dfrac{\partial T}{\partial Z}(Z=0,t)=0$ (3.11)

Boundary Condition: $F(Z=\xi,t)=\text{Constant heat flux}$ (3.12)

Initial Condition: $T(Z,t=0)=0\,°C$ (3.13)

The Eq. (3.10) is solved by applying the initial and boundary conditions. The solution is given in Carslaw and Jaeger (1959, P. 112) as

$$T(Z,t)=\frac{F\alpha t}{\xi K}+\frac{F\xi}{K}\left[\frac{3Z^2-\xi^2}{6\xi^2}-\frac{2}{\pi^2}\sum_{n=1}^{\infty}\frac{(-1)^n}{n^2}e^{\left[\frac{-\alpha n^2\pi^2 t}{\xi^2}\right]}\cos\frac{n\pi Z}{\xi}\right]$$ (3.14)

Where α is thermal diffusivity, k is thermal conductivity and ξ is the thickness of the clay sample. If measurement is made at the base of the slab $(Z=0)$, the expression for temperature becomes:

$$T(0,t)=\frac{F\alpha t}{\xi K}-\frac{F\xi}{6K}+\text{transient terms}$$ (3.15)

For times large relative to $\dfrac{\alpha\pi^2}{\xi^2}$ the transient terms are negligible, and the temperature versus time behavior becomes linear; the intercept t_i on the $T=0$ axis is:

$$t_i=\frac{\xi^2}{6\alpha}$$ (3.16)

The Eq. (3.16) can be used to find the thermal diffusivity directly from a series of temperature versus time measurements. In practice, the temperature is plotted against time, the intercept t_i is read from the resulting graph, and the thermal diffusivity is calculated using Eq. (3.16).

3.6.1 Experimental methodology

The methodology includes the sample preparation and fabrication of experimental set up for the diffusivity measurement. The transported soil containing illite clay mineral

is shared in four portions; one portion without additives; the second portion is mixed with 5%, 10%, 15% and 20% sawdust: third portion is mixed with 5%, 10%, 15% and 20% horse dung; fourth portion is mixed with 2.5%, 5%, 7.5% and 10% sawdust and 2.5%, 5%, 7.5% and 10% horse dung. Each part is molded to a thin disc of 20 mm thickness and 45 mm diameter and dried until there is no moisture content. The photographs of fabricated samples are shown in Fig.3.12. The samples are again divided into three groups; first group of samples are without heat treatment; second group is heat-treated to 500°C; third group of samples is with impregnation of heated samples with CaCl$_2$ solution of 50% concentration. The experimental set up for the measurement of thermal diffusivity is shown in Fig. 3.13.

(a)   (b)
(c)   (d)
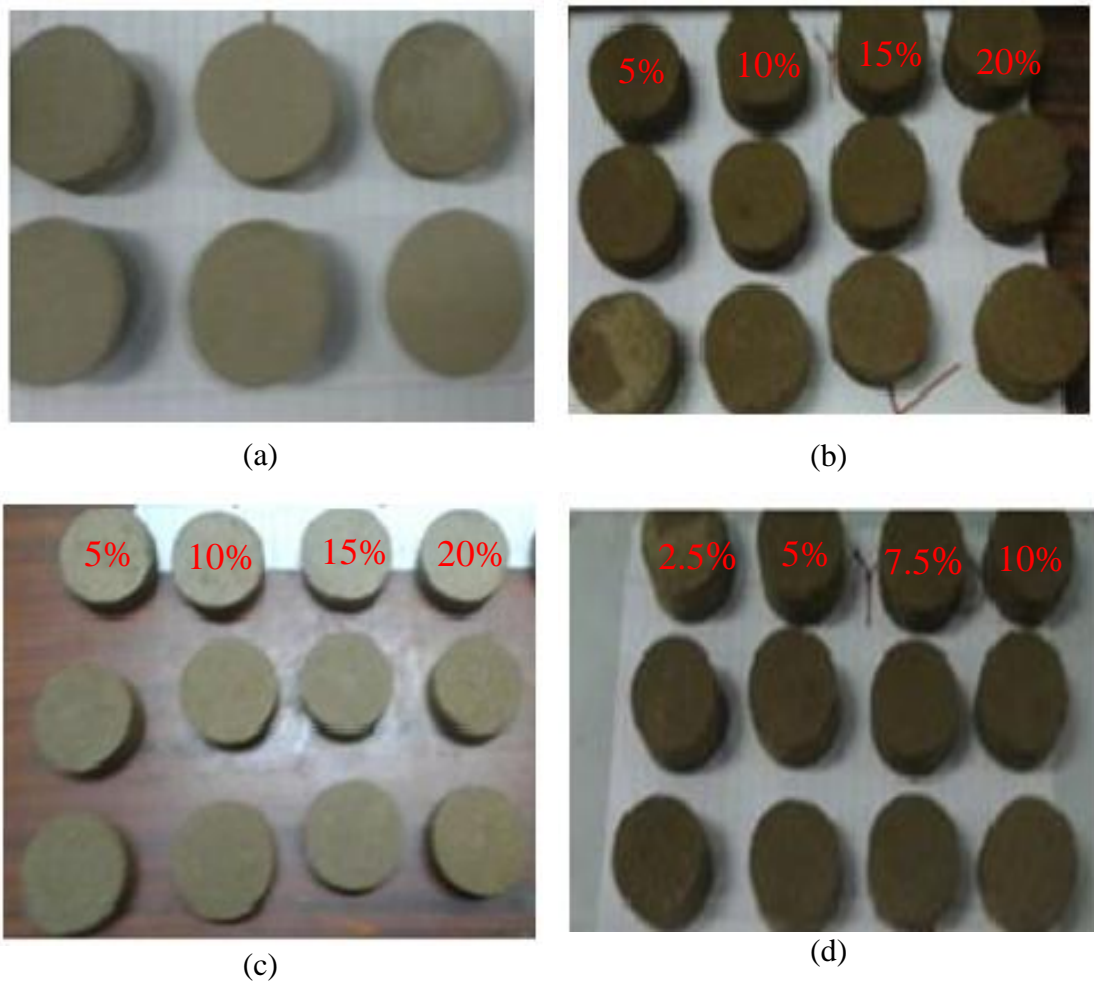
Fig.3.12 Photograph of clay and clay samples with additives (a) clay (b) clay mixed with sawdust (c) clay mixed with horse dung and (d) clay mixed with horse dung and sawdust.

61
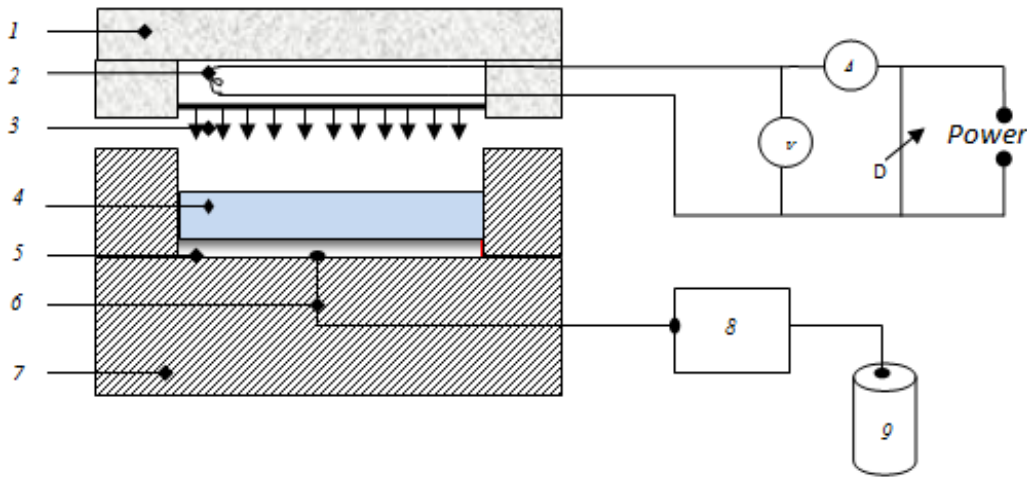
1. Heater holder   2. Heating coil with power supply   3. Heat flux   4. Clay sample

5. Copper foil   6. K- Type thermocouple   7. Sample holder with glass

wool insulation   8. Digital millivoltmeter   9. Cold junction or ice bath

Fig.3.13 Schematic of experimental set up for the measurement of thermal diffusivity of clay samples.
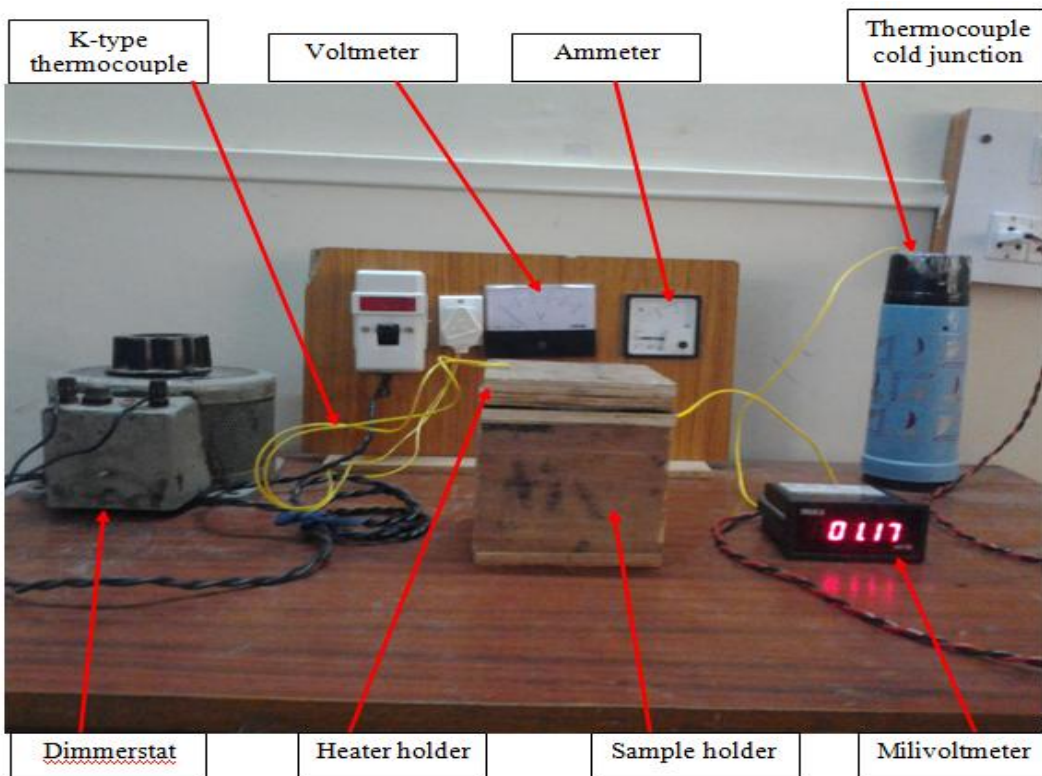
Fig.3.14 Photograph showing experimental set up for the measurement of thermal diffusivity of clay additives - $CaCl_2$ samples.

It comprises two wooden plates (1 and 7) of dimensions 120×120 mm and 9×120 mm stacked together to form a compact airtight box. The uppermost wooden plate has an embedded heating source (2), which can provide constant heat flux. The photograph of the thermal diffusivity measurement setup is shown in Fig.3.14. The experiment is carried out by rapidly exposing the top surface of clay sample that is insulated on all other surfaces to the heat source and measuring the temperature at the base of clay sample at an interval of 10 s up to 150 s after the introduction of heat flux. The measured initial time temperature at $Z = 0$ is subtracted from the subsequent time interval temperature and effectively making the measurements relative to zero initial temperature at $t = 0$. The temperature at the bottom of slab is plotted against time and the linear segment and intercept time t_i are then used to estimate the thermal diffusivity. The temperature versus time plots for the clay samples is shown in Fig .3.15. The plot results in a linear fit on the experimental data with co-efficient of determination $\left(R^2 \right)$ close to unity. The intercept t_i is read from the graph for temperature $T = 0$. Eq. (3.16) is used to calculate thermal diffusivity. The detailed estimation of thermal diffusivity with sample calculation is presented in appendix-I.
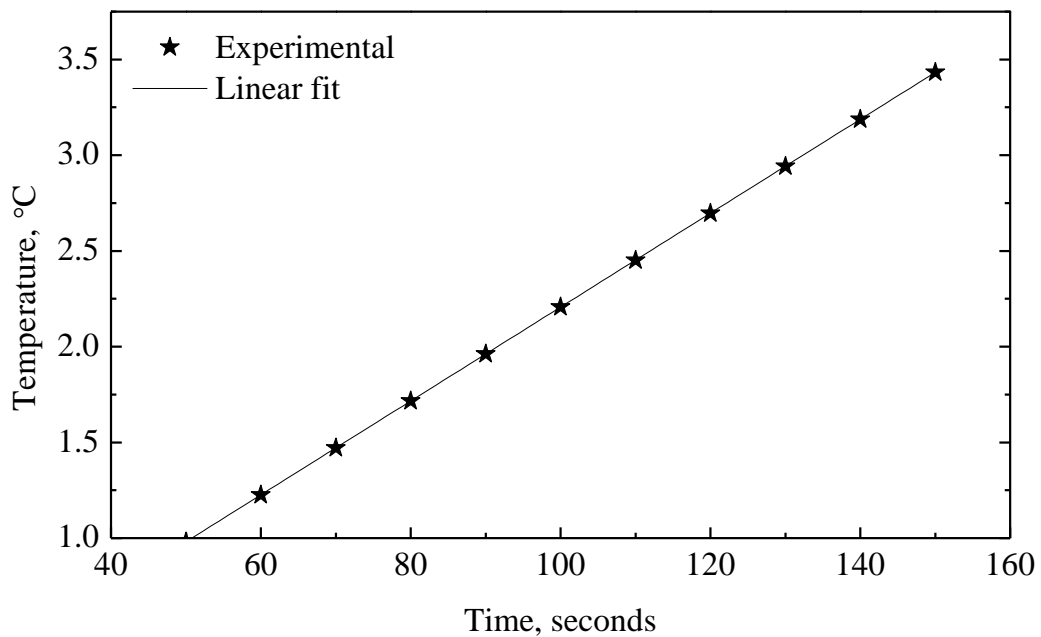
Fig.3.15 Graph of temperature versus time for pure unburnt clay composite desiccants.

The set up is calibrated for the measurement of thermal diffusivity of mild steel sample of the same dimensions as that of clay and clay with additives samples. The measured value is 7.35×10^{-6} m^2/s and agrees well with true values reported in data handbook (Kothandaraman, 2010). The thermal diffusivity is determined for two trails of experiments on every group of samples.

3.6.2 Estimation of specific heat of clay and clay-additives pellets with and without impregnation of CaCl$_2$

The specific heat of samples is determined by the energy balance between the clay samples and heated water. The photograph of experimental arrangement is shown in Fig.3.16. For pallets without impregnation are estimated using Eq. (3.17). The initial temperature (T_{ϕ_i}) of pellets before immersion in hot water is noted. The initial temperature (T_{w_i}) of water poured and sealed in the thermos flask is measured.

$$m_\phi C_{p_\phi} \left(T_{\phi_i} - T_{\phi_f} \right) = m_w C_{p_w} \left(T_{w_i} - T_{w_f} \right) \tag{3.17}$$

Measuring Jar   Thermos flask   Thermometer   Water heater
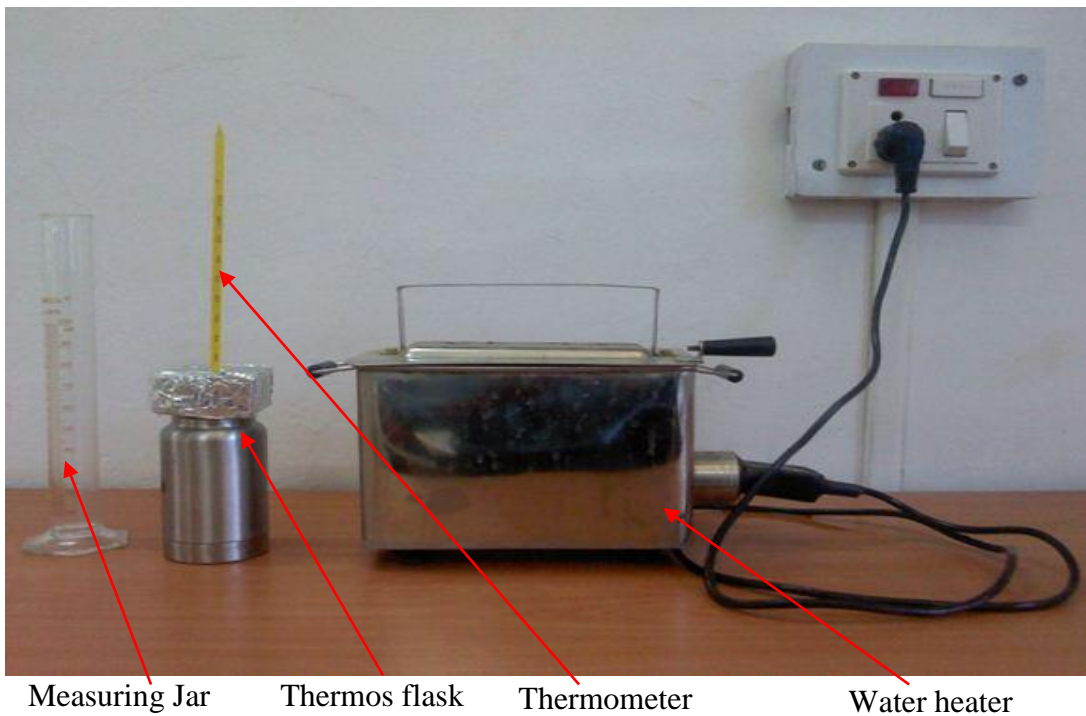
Fig.3.16 Photograph showing experimental set up for the measurement of specific heat of clay and clay additives samples.

The pellets are kept in hot water. Heat is transferred from hot water to clay pellets. Final temperatures of pellets (T_{ϕ_f}) and water (T_{w_f}) are measured. For $CaCl_2$ impregnated samples, specific heat is computed by using Eq. (3.18). The detailed sample calculation of specific heat is illustrated in appendix-I

$$C_{P_\phi} = \frac{\left(m_{CaCl_2} \times C_{P_{CaCl_2}}\right) + \left(m_c \times C_{P_c}\right)}{m_s} \qquad (3.18)$$

3.7 RESULTS AND DISCUSSION

Eq. (3.16) and (3.17) are used to calculate thermal diffusivity and specific heat. Density is calculated by mass volume ratio, and thermal conductivity is calculated by using Eq. (3.9). The results are grouped for un-burnt clay, burnt clay, burnt clay impregnated with $CaCl_2$ and with additives of sawdust and horse dung in different proportions.

3.7.1 Results for unburnt clay with and without impregnation of $CaCl_2$

Figures 3.17 and 3.18 represent the graphical representation of thermo physical properties for unburnt clay, burnt clay, and clay with impregnation of $CaCl_2$. The properties are calculated for the sample size of 45 mm diameter and 20 mm thickness. When clay samples are heat-treated the porosity of clay samples increases. As voids offer resistance to heat conduction the ability of material to conduct heat decreases. The void increases the ability of material to store heat. The thermal conductivity of the material decreases from 6.398 to 2.027 W/m K (see Fig. 3.18(b)). With heat treatment the ability of the material to store thermal energy decreases from 804.2 to 748 J/kg K and further with impregnation of $CaCl_2$ specific heat increases to 832.5 J/kg K (see Fig. 3.18 (a)). As the ability of material to store heat is more as compared to conduct heat relatively thermal diffusivity estimated for the samples, decreases from 3.33×10^{-6} to 1.025×10^{-6} m^2/s (see Fig. 3.17(a)).
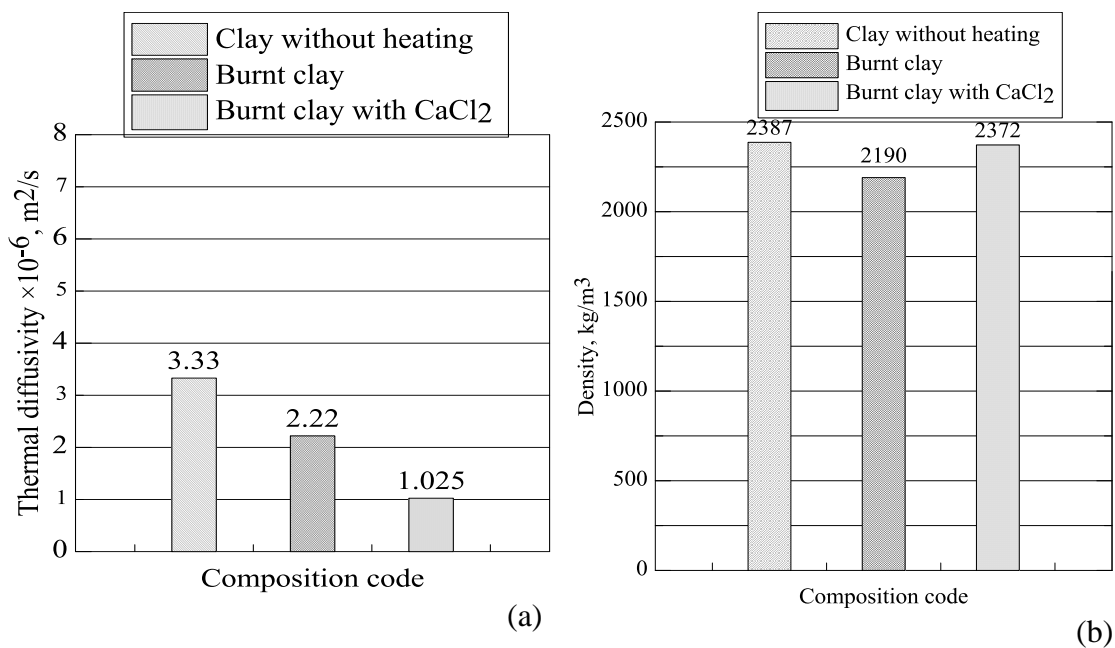
Fig.3.17 (a) Thermal diffusivity and (b) density for clay samples with and without impregnation of $CaCl_2$.
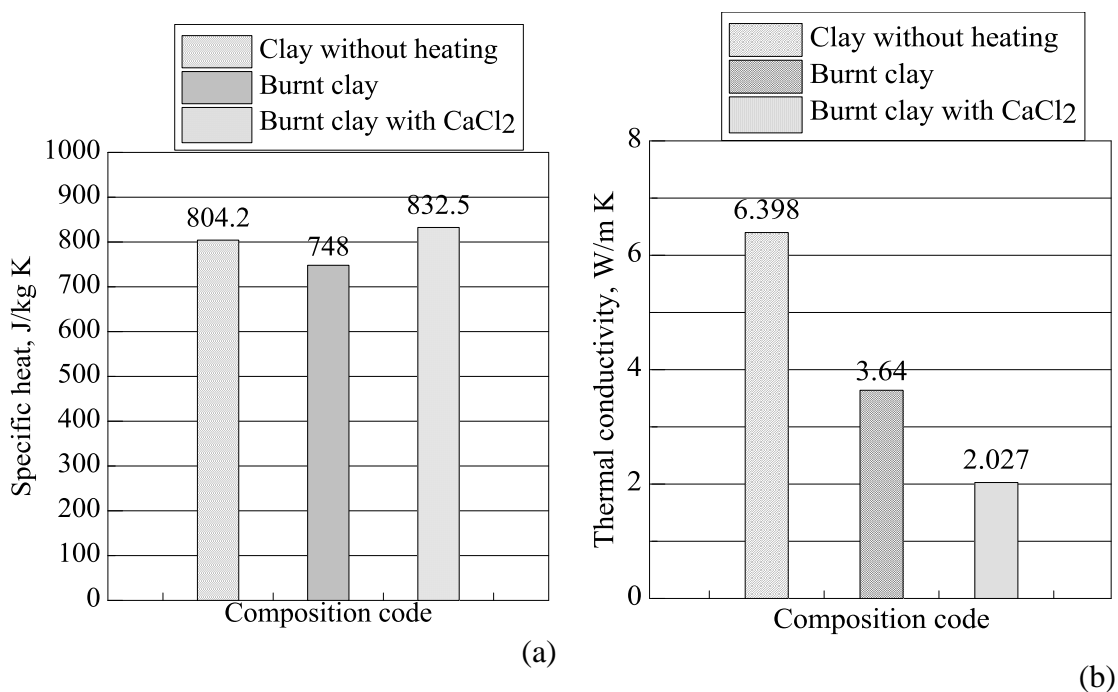
Fig.3.18 (a) Specific heat and (b) thermal conductivity for clay samples with and without impregnation of $CaCl_2$.

66

3.7.1 Results for pure clay with sawdust additive and with impregnation of CaCl₂

Fig. 3.19 and 3.20 show the graphical representation of thermo physical properties for clay with addition of sawdust, burnt clay with addition of sawdust and burnt clay with sawdust and impregnated with $CaCl_2$. The sawdust is added to clay in proportion of weight as of 5%, 10%, 15%, and 20%. The three sets of samples are clay - sawdust samples without heating, with heating and impregnated with $CaCl_2$. The properties are calculated for the sample size of 45 mm diameter and 20 mm thickness. Thermal diffusivity estimated for the clay - sawdust sample without heating, decreases from 3.75×10^{-6} to 9.38×10^{-7} m²/s for the sample composition of 5 to 20% sawdust additive. The binding of sawdust with clay reduces interior and exterior heat transport. Hence that results in lower values of thermal diffusivity. The ability of the material to conduct heat decreases from 8.8 to 1.4 W/m K, whereas the ability of the material to store thermal energy varies from 1283 to 1332.4 J/kg K. The density decreases from 1832 to 1332 kg/m³ for the same sample composition of 5 to 20% sawdust additive. Thermal diffusivity estimated for the clay - sawdust sample with heating, increases from 5.34×10^{-7} to 3.75×10^{-6} m²/s for the sample composition of 5 to 20% sawdust additive. The ability of the material to conduct heat increases from 0.69 to 4.54 W/m K, whereas ability of the material to store thermal energy increases from 762.9 to 1605 J/kg K, and the density decreases from 1693 to 754.5 kg/m³ for the same sample composition of 5 to 20% sawdust additive. The heat-treated samples containing progressive increase in sawdust additive from 5 to 20%, it is likely that higher carbon content is produced in samples The increased carbon content with heating results in higher thermal diffusivity, thermal conductivity and specific heat properties. Thermal diffusivity estimated for the burnt clay - sawdust sample with impregnation of $CaCl_2$, varies from 3.33×10^{-6} to 8.33×10^{-6} m²/s for the sample composition of 5 to 20% sawdust additive. The ability of the material to conduct heat decreases from 3.14 to 1.43 W/m K whereas the ability of the material to store thermal energy varies from 929.7 to 1461 J/kg K and the density varies between 1957 to 1114 kg/m³ for the same sample composition of 5 to 20% sawdust additive
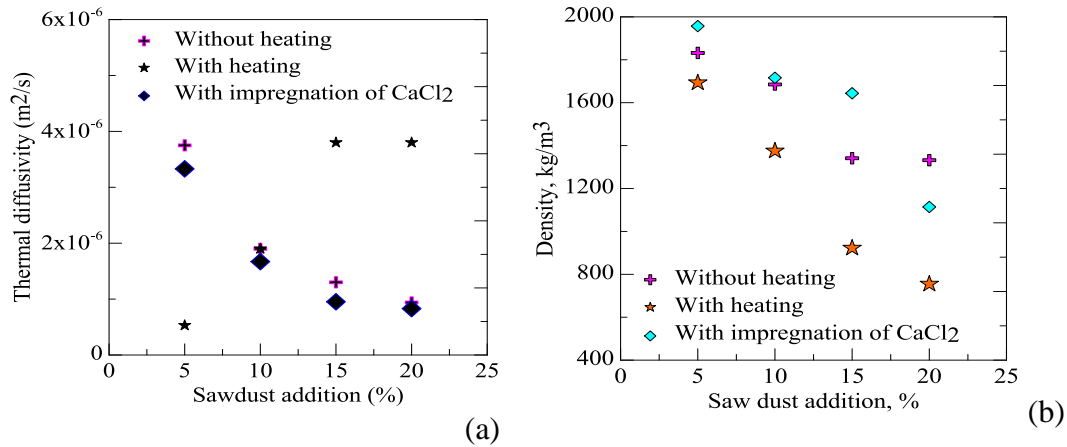
Fig.3. 19 (a) Thermal diffusivity and (b) density for clay - sawdust samples with and without impregnation of $CaCl_2$.
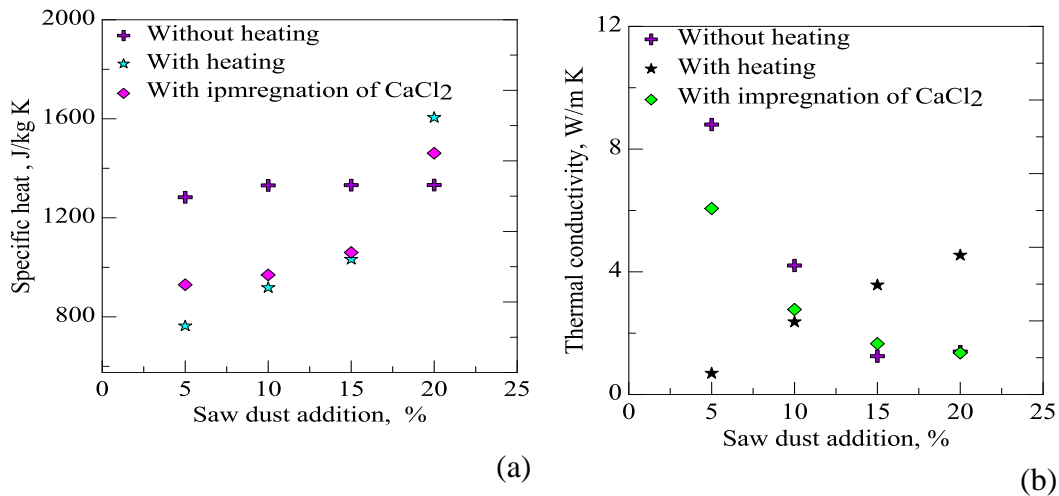
Fig. 3. 20 (a) Specific heat and (b) thermal conductivity for clay - sawdust samples with and without impregnation of $CaCl_2$.

3.7.2 Results for pure clay with horse dung additive and with impregnation of $CaCl_2$

The addition of horse dung yields the same trend of properties as that of sawdust additive. For samples without heating, with heating, with impregnation of $CaCl_2$ and with higher percentage of horse dung added to clay, higher will be the heat capacity, and lower will be the density of material. The horse dung added to clay samples or pellets in the proportions of 5%, 10%, 15%, and 20% .The properties are calculated for the sample size of 45 mm diameter and 20 mm thickness. Figs. 3.21(a) and (b),

68

3.22(a) and (b) shows the graphical representation of thermophysical properties like thermal diffusivity and density for pure clay - horse dung, burnt clay-horse dung and burnt clay - horse dung with impregnation of $CaCl_2$. Thermal diffusivity estimated for the clay-horse dung sample with no heat treatment decreases from 3.33×10^{-6} to 1.33×10^{-6} m^2/s for the sample composition of 5 to 20% horse dung additive. The ability of the material to conduct heat decreases from 7.81 to 2.68 W/m K, whereas the ability of the material to store thermal energy varies from 1198 to 1653 J/kg K, and the density decreases from 1831.75 to 1173.68 kg/m^3 for the same sample composition of 5 to 20% horse dung additive.

Thermal diffusivity estimated for the clay-horse dung samples with heating increases from 8.88×10^{-7} to 6.67×10^{-6} m^2/s for the sample composition of 5 to 20%. The ability of the material to conduct heat increases from 1.08 to 8.92 W/m K, whereas the ability of the material to store thermal energy varies from 718.05 to 1444.2 J/kg K, and density decreases from 1700 to 754 kg/m^3 for the same sample composition of 5 to 20% horse dung additive. Thermal diffusivity estimated for the burnt clay - horse dung sample with impregnation of $CaCl_2$, decreases from 1.21×10^{-6} to 8.33×10^{-7} m^2/s.
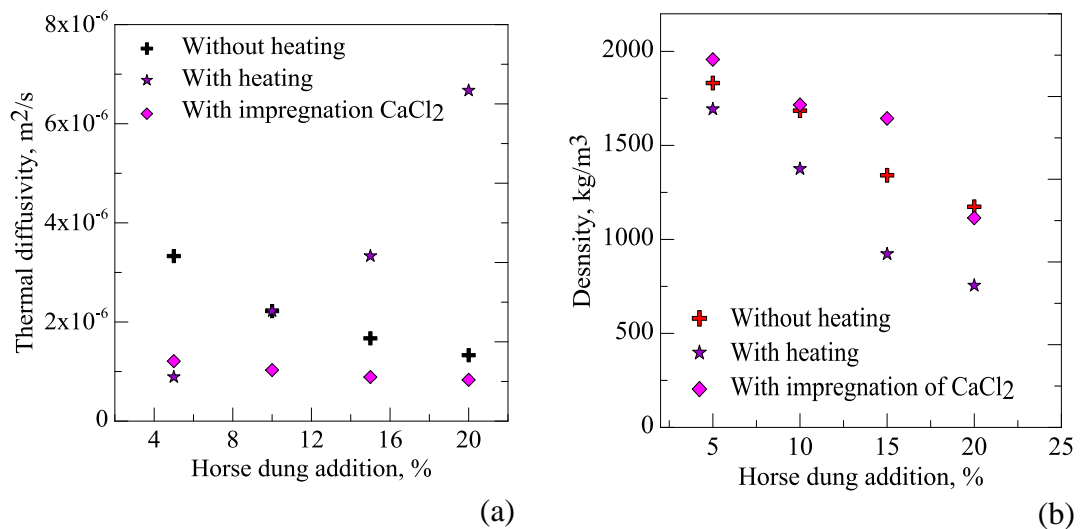
Fig.3.21 (a) Thermal diffusivity and (b) density for clay - horse dung samples with and without impregnation of $CaCl_2$.
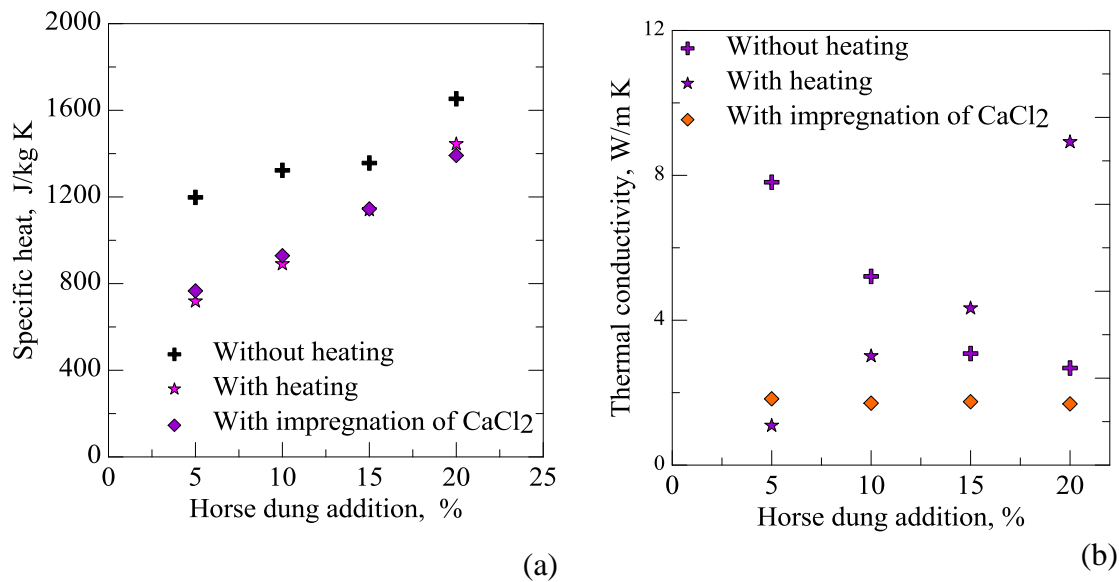
Fig.3.22 (a) Specific heat and (b) thermal conductivity for clay - horse dung samples with and without impregnation of $CaCl_2$.

The ability of the material to conduct heat decreases from 1.83 to 1.69 W/m K, whereas the ability of the material to store thermal energy increases from 766.39 to 1391.67 J/kg K and the density decreases from 1973 to 1457 kg/m^3, for the same sample composition of 5 to 20% horse dung additive.

3.7.3 Results for pure clay with horse dung-saw dust additive and with impregnation of CaCl$_2$

Figures 3.23 (a) and (b), 3.24 (a) and (b) shows the graphical representation of measured thermophysical properties for pure clay - horse dung - sawdust, burnt clay-horse dung - sawdust and burnt clay - horse dung - sawdust with impregnation of CaCl$_2$. The horse dung and sawdust are added to the unburnt, burnt and burnt impregnated samples or pellets in the proportions of 2.5%, 5%, 7.5%, and 10% . The properties are calculated for the sample size of 45 mm diameter and 20 mm thickness. Thermal diffusivity estimated for the clay - horse dung - sawdust sample without heating, decreases from 3.33×10^{-6} to 1.11×10^{-6} m^2/s for the sample composition of 2.5% to 10% horse dung - saw dust additives. The ability of the material to conduct heat decreases from 9.38 to 2.11 W/m K, whereas the ability of the material to store thermal energy decreases from 1339 to 1510 J/kg K.

70
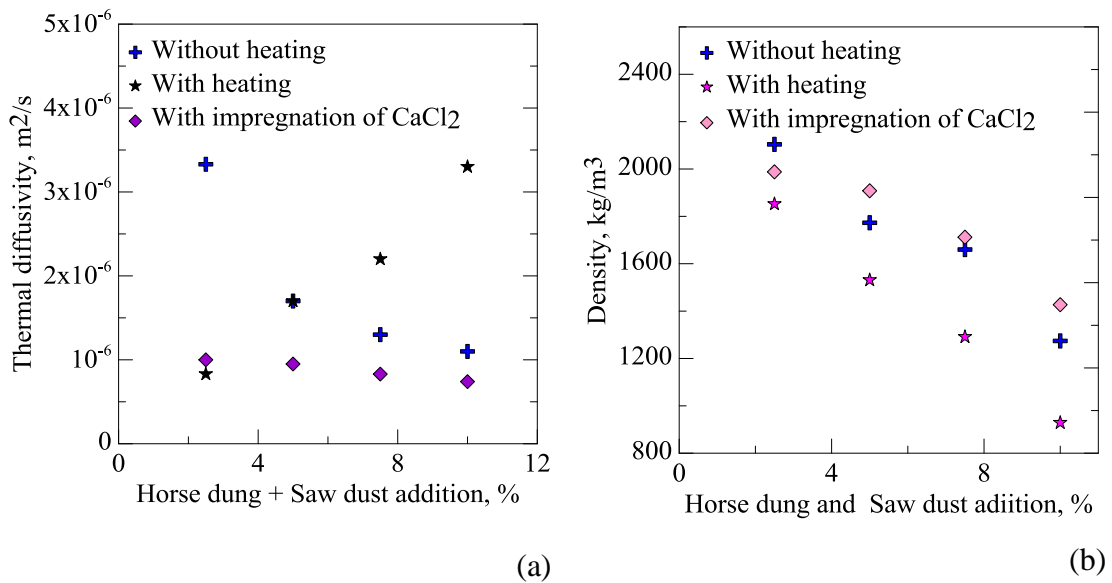
Fig.3.23 (a) Thermal diffusivity and (b) density for clay-horse dung-saw dust samples with and without impregnation of $CaCl_2$.
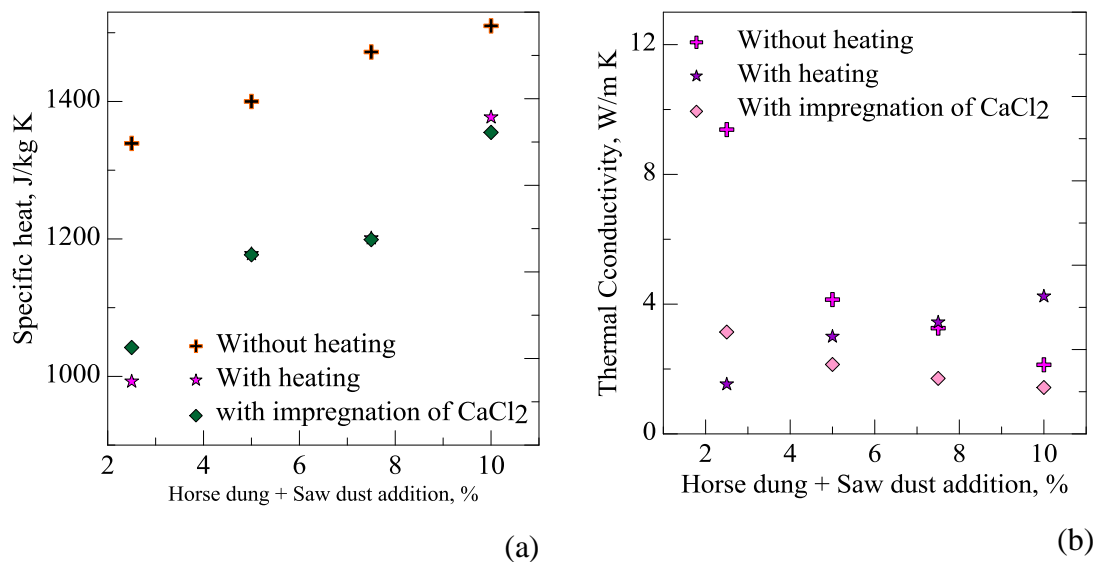
Fig.3.24 (a) Specific heat and (b) thermal conductivity for clay-horse dung-saw dust samples with and without impregnation of $CaCl_2$.

The density decreases from 2104 to 1274 kg/m^3 for the same sample composition of 2.5 to 10% horse dung - saw dust additives. Thermal diffusivity estimated for the clay - horse dung - sawdust sample with heating, increases from 8.33×10^{-7} to 3.33×10^{-6} m^2/s for the sample composition of 2.5 to 10%. The ability of the material to conduct heat increases from 1.53 to 4.24 W/m K, whereas the ability of the material to store

71

thermal energy decreases from 992.6 to 1377 J/kg K, and the density decreases from 1852 to 928 kg/m^3 for the same sample composition of 2.5 to 10% horse dung - saw dust additives. Thermal diffusivity estimated for the burnt clay - horse dung - sawdust sample with impregnation of CaCl$_2$, decreases from 1.02×10^{-6} to 7.41×10^{-7} m^2/s. The ability of the material to conduct heat decreases from 3.14 to 1.43 W/m K, whereas the ability of the material to store thermal energy decreases from 1042 to 1355 J/kg K, and the density decreases from 1988 to 1427 kg/m^3 for the same sample composition of 2.5 to 10% horse dung - saw dust additives.

3.8 SUMMARY

Gravimetric analysis for the chemical composition of transported soil has shown that SiO$_2$ and Al$_2$O$_3$ make up major portions of transported soil. Heat treatment temperature of desiccant is arrived at based on maximum weight reduction and porosity values at 500°C. The textural characteristics such as surface area and pore volume were determined by nitrogen sorption isotherms of BET. At temperature of 500°C the burnt clay CaCl$_2$ desiccant pellets exhibit more pore volume whereas burnt clay horse dung additives desiccant pellets show maximum surface area. Observations under SEM reveal surface morphology with coarse texture for burnt clay with sawdust and horse dung additives. The energy dispersive spectrum (EDAX) shows variation in intensities of Kα peaks of elements in all the three samples. XRD of heat-treated and impregnated samples reveal similar peak intensities of Si oxides. The transient measurement technique is used to measure the thermal diffusivity of pellets prepared. Specific heat is calculated by energy balance between water and clay, clay additives and impregnated CaCl$_2$ samples. The following conclusions are drawn from the work are

1. The heat treatment of clay additives pellets reveals a maximum reduction in weight at 500°C and correspondingly higher apparent porosity values are recorded at the same temperature of 500°C. The apparent porosity (volume of open pores) recorded at 500°C are 13%, 23%, and 26% for clay, clay - sawdust and clay - horse dung desiccants respectively.

72

2. BET analysis shows a higher surface area for 500°C heat treated burnt clay with 20% horse dung pellets, whereas bunt clay posses higher pore volume at 500°C.

3. SEM micrographs indicate the porous surface texture of burnt clay additives pellets and retention of $CaCl_2$ into the pores of burnt clay - additives - $CaCl_2$ composite desiccants.

4. The quantitative analysis of EDAX at 500°C reveals 7.13 %, 9.23 %, and 7.14 % by mass of carbon content with respect to burnt clay, burnt clay-horse dung and burnt clay- sawdust composite desiccants. The respective values of the calcium and sodium by weight are 4.31 %, 6.45 %, 5.06 % and 1.05 %, 1.02 % and 1.04 %.

5. XRD patterns show higher intensity diffractions indicating the crystalline structure of pellets. The average crystallite size for clay - additives pellets is from 53.49 - 1.46 nm. For synthesized clay-based composites desiccants is from 42.75 - 9.25 nm.

6. The initial water contents estimated for burnt clay- $CaCl_2$, burnt clay - sawdust - $CaCl_2$ and burnt clay - horse dung - $CaCl_2$ composite desiccants are in the order of 63.79, 86.04 and 94.44 g water / kg dry desiccant respectively.

7. The thermal diffusivity decreases by 33.33% and 69.69% for burnt clay and burnt clay - $CaCl_2$ as compared to unburnt clay. Heat treatment of clay decreases specific heat by 6.99%, and the impregnation of burnt clay with $CaCl_2$ increases specific heat by 11.29%.

8. The density decreases by about 8.25% for burnt clay as compared to unburnt clay. The impregnation of $CaCl_2$ increases density by 8.31% as compared to burnt clay. The heat treatment of clay decreases thermal conductivity by 43.11% as compared to un-burnt clay. The impregnation of $CaCl_2$ with heat-treated clay decreases thermal conductivity by 44.31%.

9. The addition of sawdust and horse dung additives in 5, 10, 15 and 20% by mass proportion with un-burnt clay increases the specific heat. Whereas higher percentage of additives sawdust and horse dung with un-burnt clay decreases thermal diffusivity, thermal conductivity, and density.

10. For the heat-treated clay with sawdust and horse dung additives in 5, 10, 15 and 20% by mass proportion increase the specific heat, thermal diffusivity, and thermal

conductivity. Whereas higher percentage of additives sawdust and horse dung with burnt clay decreases density.

11. $CaCl_2$ impregnation with burnt clay - sawdust and burnt clay - horse dung in 5, 10, 15 and 20% by weight increases specific heat. Whereas as for burnt clay - sawdust - $CaCl_2$ and burnt clay - horse dung - $CaCl_2$ in the same proportion of additives decreases thermal diffusivity, thermal conductivity, and specific heat.

12. For burnt clay - sawdust - $CaCl_2$ and burnt clay - horse dung - $CaCl_2$ desiccant material the density decreased by 53.03% and 38.58% as compared to burnt clay - $CaCl_2$ desiccant material. For burnt clay - sawdust - $CaCl_2$ and burnt clay - horse dung - $CaCl_2$ desiccant material, the specific heat increased by 75.49% and 67.17% as compared to burnt clay - $CaCl_2$ desiccant material. For burnt clay - sawdust - $CaCl_2$ and burnt clay - horse dung - $CaCl_2$ desiccant material the thermal conductivity decreased by 40.09% and 25.55% as compared to burnt clay - $CaCl_2$ desiccant material. For burnt clay - additives - $CaCl_2$ composite desiccant material thermal diffusivity decreased by 17.13% as compared to burnt clay - $CaCl_2$ composite desiccant material.

CHAPTER 4

EXPERIMENTAL SETUP TO INVESTIGATE ADSORPTION AND DESORPTION CHARACTERISTICS OF CLAY COMPOSITE DESICCANTS

4.1 INTRODUCTION

The main components of the desiccant sorption system are the adsorbent and the configuration of the bed. The set up is arranged to carry out process air humidification and dehumidification experiments when the desiccant bed is in static and fluidized configuration. The work involves designing and fabricating important units like air humidification and heating units. The air humidification and heating units are coupled to the main pressure line. The ball and gate valves are used to control and direct the flow of air through the experimental units and finally into the bed. The system of the packed bed of composite desiccant under step input of process air for humidification and dehumidification is implemented. Apart the dehumidification and humidification experiment of composite desiccant under fluidized state is carried out. The experimental results obtained from the physical system are helpful invalidating the results obtained from mathematical model.

4.2 EXPERIMENTAL SETUP

The schematic of the experimental setup is shown in Fig.4.1, are a single blow adsorption and desorption experimental test rig. The set up consists of air compressor with reservoir, pressure line, air heating unit, humidification unit, orifice meter, vertical column and measuring instruments kept at data measuring locations. Compressed air from the reciprocating air compressor is stored in a reservoir. Compressed air is drawn from the reservoir and is made to flow through the discharge pipeline (compressor line) made up of polyvinyl chloride (PVC). From discharge line

75

the air flows through the pressure line and then into the vertical column. The operating pressure of the compressed air line is approximately 0.2 to 3.4 bar gauge. The pressure line is a galvanized iron (GI) pipe and runs approximately up to 3500 mm. The diameter of pressure line is of 25 mm. Gate and ball valves are used to control the flow rate and direction of airflow through the pressure line and into the bed.
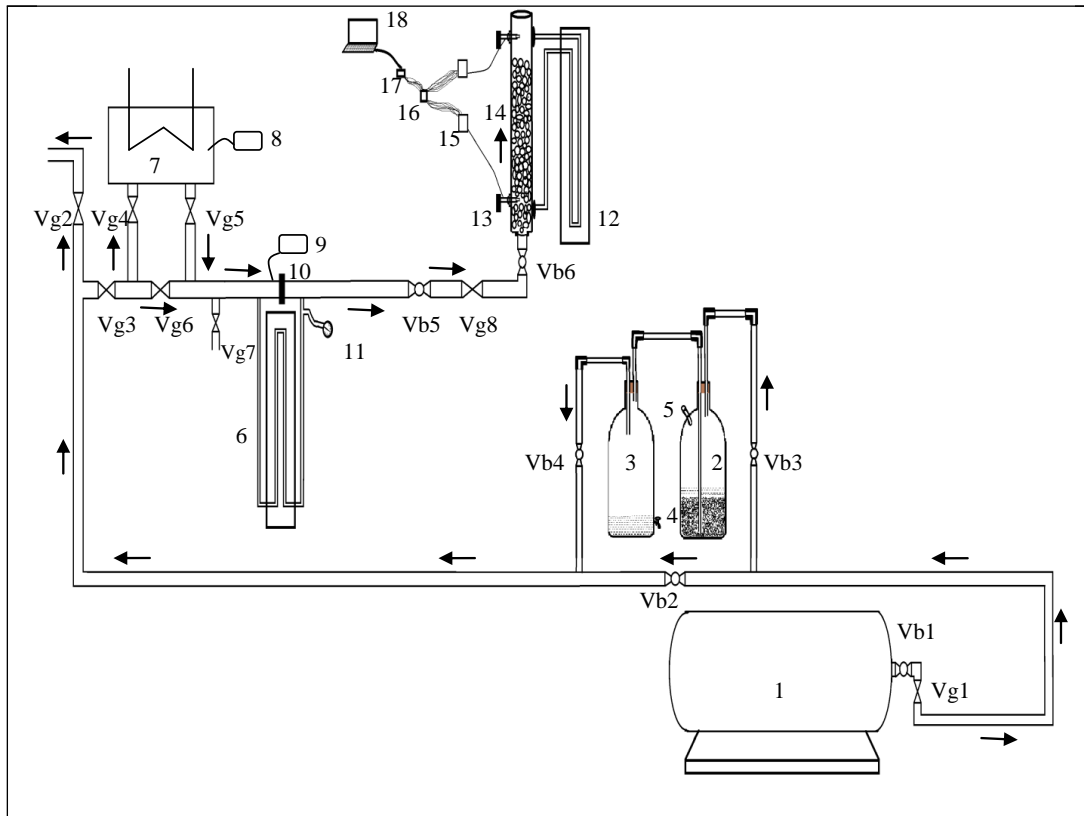
1. Air Compressor 2. Humidifier 3. Moisture damper 4,5.Waterline 6,12. U-tube manometer 7. Air heating unit 8,9. K- type thermocouples 10. Orifice meter 11. Pressure gauge 13,15. Hygrotransmitter 14. Desiccant column 16. 17. Arduino with voltage divider 18. computer : PR: Pressure line. CR: Compressor line ▷◯◁ : Ball valve (vb) ▷◁ : Gate valve (vg)

Fig. 4.1 Schematic layout of the experimental setup for testing of adsorption-desorption characteristics of composite desiccant.

The vertical bed is of a transparent acrylic tube having a height of 700 mm and a diameter of 50 mm to facilitate the observation of the desiccant pellets in fluidized state. The vertical column is provided with pressure taps and taps for locating the

76

hygrotransmitter. The main parameters measured are relative humidity, temperature and pressure drop of process air during adsorption and desorption experiments. The relative humidity (0 to 100 %) and temperature (-40 to 85ºC) at bed inlet and exit is measured using calibrated Hygroflex hygrotransmitter. The humidity transmitters at the bed inlet and exit are connected to computer through microcontroller interface. The transient values of humidity ratio and temperature of process air are written to excel file for every second during experimental work. Water filled U- tube manometer is connected across orifice meter. The diameter of the orifice is 10.12 mm; thickness of orifice plate is 3 mm. The chamfered sharpness of the orifice is 45º, and co-efficient of discharge (C_d) of the orifice plate is 0.68. In order to calculate the volume flow rate of air, the pressure drop across the orifice meter in terms of head of water is noted by using U-tube manometer. The gauge pressure of air in the process line is measured by using a pressure gauge having a range of 0 to 8 bars. Another water-filled U-tube manometer is employed to measure the pressure drop across the packed and fluidized beds. The calibration equation for the orifice meter with pressure line, air heating unit and humidification column are in the form of power-law fit and represented as

$$v = A \times (H_w)^B \tag{4.1}$$

Where H_w manometer deflection in meter of water column and v is superficial velocity in m/s. The values of constants A and B obtained by curve fitting and the range of velocities are shown in Table.4.1

Table 4.1 Range of velocities in humidification-dehumidification experimental runs.

Airflow line	A	B	Co-efficient of determination (R^2)	Velocity range (v m/s)
Orifice meter + Pressure line	3.411	0.333	0.980	0.5 – 2 m/s
Orifice meter + Air heating unit	3.035	0.288	0.997	0.5 – 2 m/s
Orifice meter + Humidification column	3.939	0.436	0.998	0.2 – 1.6 m/s

Fig. 4.2 shows the calibration curve for the process air velocity flowing through the main pressure line. The calibration curve yields a minimum velocity of 0.5 m/s and a maximum velocity of 2 m/s. Dehumidification or adsorption experiments at atmospheric pressure and temperature for vertical packed and fluidized clay and clay additives composite desiccant beds are conducted for the velocity of process air ranging from 0.5 m/s to 2m/s. Fig. 4.3 shows the calibration curve for the superficial velocity of process air flowing through the air heating unit. The minimum velocity and maximum velocities calculated are 0.5 m/s and 2 m/s. The regeneration of desorption experiments on clay and clay additives composite desiccant beds are carried at process air velocity ranging from 0.5 m/s and 2 m/s. The calibration curve for process air through the humidification column is shown in Fig.4.4. The maximum superficial velocity achieved is 1.6 m/s. The dehumidification experiments at set humidity of process air for clay and clay additives composite desiccants in packed and fluidized bed are conducted for the process air velocity ranging from 0.2 m/s to 1.6 m/s.
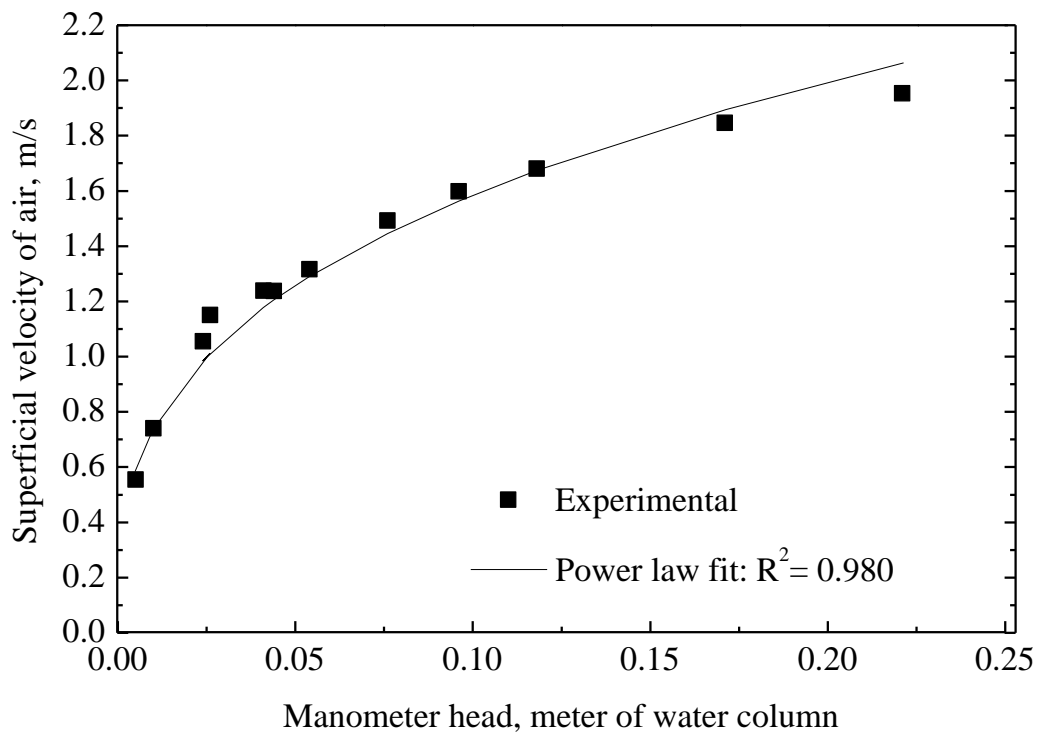
Fig.4.2 Calibration curve for process air velocity with orifice meter and main pressure line.

78
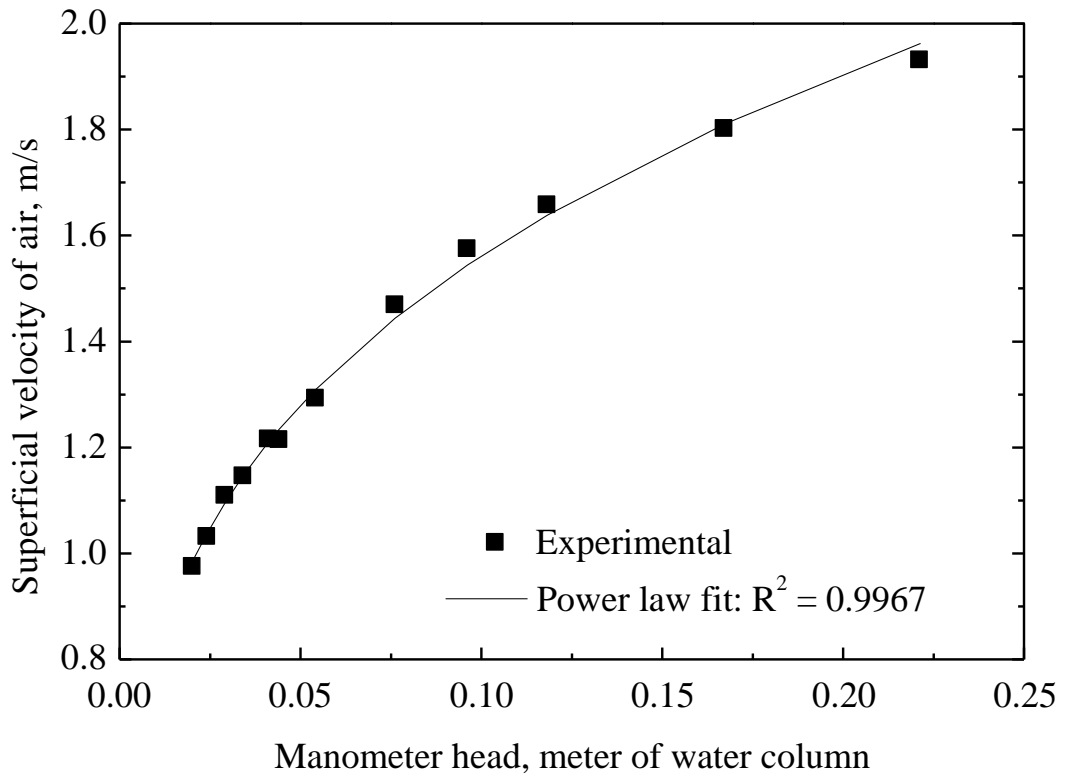
Fig. 4.3 Calibration curve process air velocity with orifice meter and air heating unit.
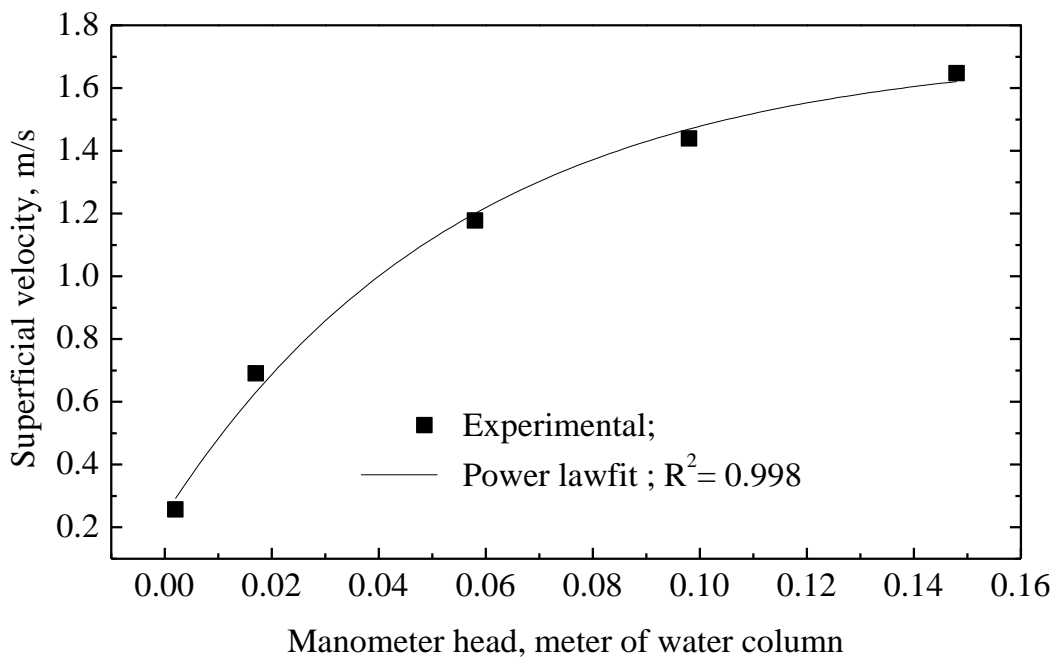
Fig. 4.4 Calibration curve for process air velocity with orifice meter and air humidification unit.

Fig 4.5 shows the variation of temperature with the change in emf of the circuit. A millivoltmeter having a range of 0 to 200 mV gives change in emf in terms of millivolts. A linear fit to experimental data enables measurement of temperature as function of change in emf. The pressure line air temperature and air heating unit temperatures are measured using K - Type thermocouples. A linear fit is obtained for the variation of emf with average temperature values from 30°C to 86°C. The calibration equation for the thermocouple is as follows,

$$T = (24.52 \times E) + 3.986 \tag{4.2}$$

Where emf E in mV and T is temperature in °C
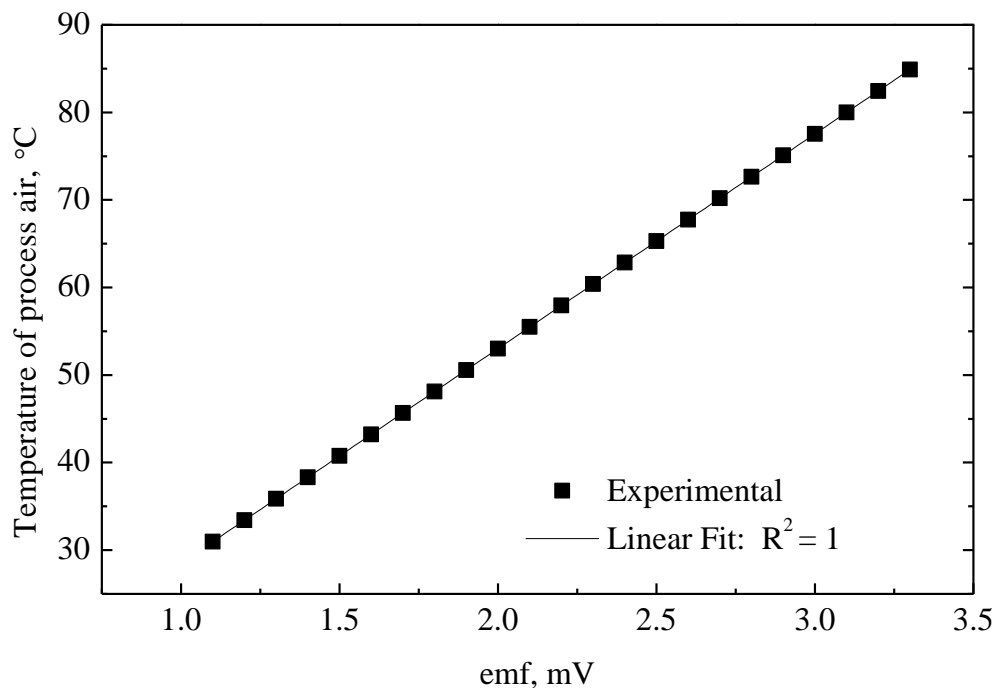
Fig. 4.5 Calibration curve for K-type thermocouple for temperature measurement.

Fig.4.6 shows the photograph of the test rig arranged to conduct experiments. Experiments for pressure drop across the desiccant bed and variation of exit air humidity ratio and temperature for step-change in inlet humidity ratio, temperature and velocity can be conducted. The results for bed pressure drop for clay composite desiccants without impregnation of $CaCl_2$ are discussed in appendix - II.

80

Fig. 4.6 Photograph of the experimental setup for adsorption-desorption experiments.

The details of the experimental unit are given in the following subsections

4.2.1 Reciprocating Compressor

The compressor is of reciprocating type driven by DC motor. The compressor line from the air reservoir to the main pressure line is of Polyvinylchloride (PVC) material. The compressor line diameter is 25.4 mm and length is 21.36 m. The compressor delivers air through compressor line (from valve Vb1 to Vg2) and then to the pressure line (from valve Vg3 to Vb6) of the experimental setup. The maximum volume flow rate available by the compressor is 0.0041 m^3/sec at 8 bar reservoir pressure. The maximum volume flow rate set in the pressure line at 0.3 bars is 0.0029 m^3/sec. The minimum volume flow rate set in the pressure line at 3.4 bars is 0.00024 m^3/sec. The specifications of the compressor are as shown in Table 4.2.

Table 4.2 Specifications of reciprocating air compressor.

Model and Make	TS03120HN; ELGI
Type	Reciprocating, Air-cooled, Splash lubricated
Displacement	18.16 m^3/hr.
Free air delivery @ 10bar	15 m^3/hr.
Working Pressure	12 bar
Number of cylinders	2
Volumetric efficiency	78%
Compressor speed	925 rpm
Air receiver capacity	220 Liters

4.2.2 Pressure Line

The pressure line is of 25 mm diameter of galvanized iron (GI) pipe and a length of 3500 mm. The pressure line is insulated with asbestos insulating material. This to reduce the heat loss from process air to atmosphere. The pressure regulator has a range of 0 to 10.5 bar is used to regulate pressure of the compressed air. Gate and ball valve are used to control the flow rate and direction of airflow through the pressure line and into the bed.

4.2.3 Air heating unit

During the adsorption process, the water content of desiccants increases. Removal of moisture from the desiccants enables dehumidification process. In this context heat energy is required for regeneration of the desiccants being saturated. Incandescent bulb based air heater housing copper coils are being fabricated and arranged. The air present in the heating unit surrounding the copper coil receives heat by radiation from the incandescent bulbs. The wattage of the six bulbs is 100 W each. The specifications of the materials used in making heating unit are shown in Table 4.3. The dimensions of the air heating unit and the arrangement of copper coil with bulbs are shown schematically in Fig.4.7. This unit is attached to the main pressure line. The

dimensions of the heating units are presented in the orthographic and isometric views. The photograph of the heating unit with incandescent bulbs is shown in Fig.4.8.

Table 4.3 Specification of materials used in fabricating air heating unit.

Material used	Ply-wood, GI sheets, Glass wool material, Copper coil, and Incandescent bulbs
Ply - wood box dimensions	$610 \times 450 \times 370$ mm
Coil used	The copper coil of 10 mm diameter and length 10 m
Number of turns of copper coil	6
Number of subs- turns of copper coil	3
Number of bulbs used	6 (Every 100 watts)

As represented in the photograph, inside surfaces of the heating box are covered with insulation material which minimizes the heat loss. A thin G I sheet of thickness 0.5 mm is cladded over the insulating material. The G I sheet is painted with highly reflective white paint. The copper coil is turned into six main turns. Each main turn consists of 3 sub turns. The six main turns are at a pitch of 150 mm longitudinally and vertically 150 mm apart. At each pitch of main turns six incandescent bulbs of each 100 W are fixed to the surface of the box. The total volume of the heating box is 99.9 $\times 106$ mm^3, whereas the volume occupied by the heating coil inside the box is 6.318 $\times$ 106 mm^3. It is known that a surface with black coating is having higher absorptivity of irradiation; the outer surface of the copper coil is painted with black paint. This enhances heat transfer rates to the process air flowing through copper coil. The air entrained in the box gets heated by natural convection and radiation due to incandescent bulbs. The hot air surrounding the copper coil through which process airflows. The process air is then heated due to hot air surrounding the copper tubes as well as irradiation heat from the incandescent bulb. K-type thermocouples (Chromel - Alumel) having a range of -250°C to 1260°C are used to measure the air temperature in heating unit, along process line, and at bed inlet.

Copper coil   Incandescent bulb

370

450

670

All dimensions are in mm
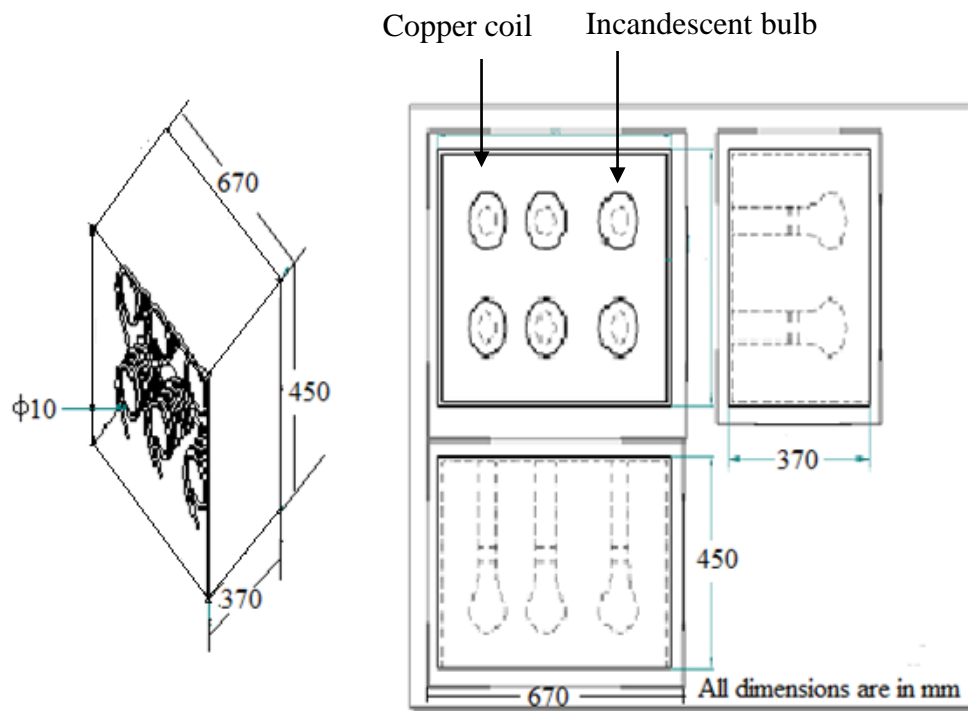
Fig. 4.7 Schematics of an air heating unit showing isometric and orthographic views.

(a)   (b)

Fig. 4.8 Photographs of air heating unit (a) bulbs in off condition (b) 100W bulbs in switched-on condition.

4.2.4 Performance of air heating unit

Experiments have been conducted to depict the variation of process air temperature along the pressure line for step-change in bed inlet air velocities. Experiments are conducted to determine the steady-state temperatures of process air. In order to know the effectiveness of heating unit, time variation of air temperature at different locations mainly in heating box, pressure line and at bed inlet is measured. Figure 4.9 shows the transient variation of air temperature at the inlet of bed.
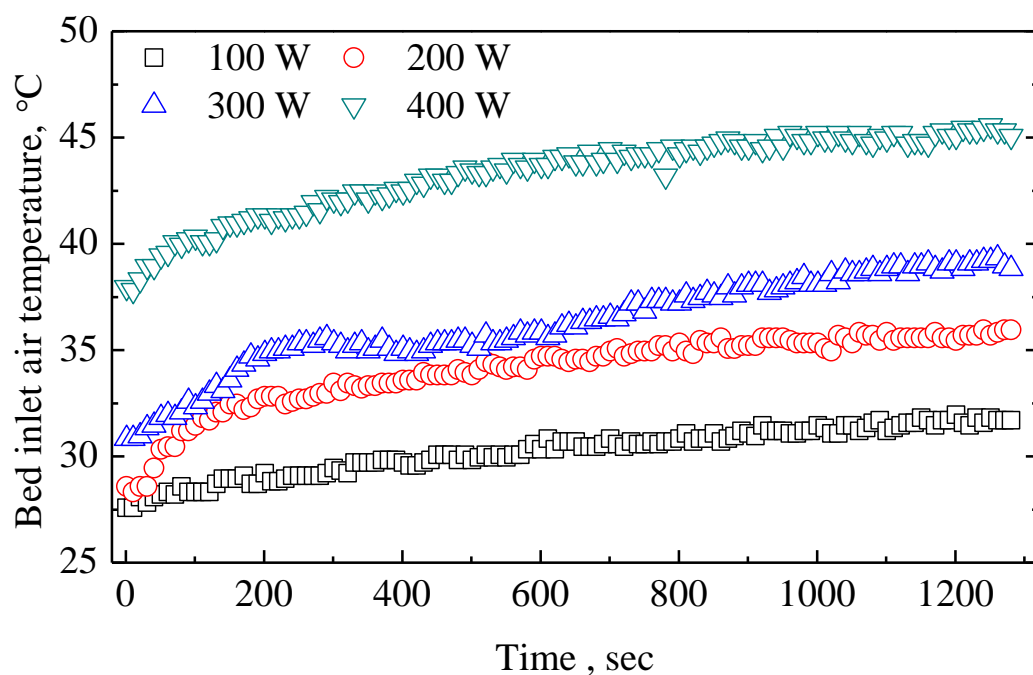
Fig.4.9 Transient variation of bed inlet air temperature with increase in heat input in steps of 100 W.

The irradiated heat is due to the burning of 100 to 400 W incandescent bulbs in steps of 100 W. The temperature values are recorded at a gauge pressure of 0.5 bar with air velocity of 1.5 m/sec. The ambient relative humidity and temperature recorded are 61% and 30°C. With increase in heat irradiated when incandescent bulbs of 100 W, 200 W, 300 W, and 400 W are kept on, the air contained in heating unit gets heated which in turn increases the temperature of process air flowing through the copper pipe. The steady-state values of bed inlet air temperature due to heat irradiated

from the glow of 100 W, 200 W, 300 W, and 400 W bulbs are 31.5°C, 35.5°C, 38.9°C and 45.1°C respectively.

Figure 4.10 shows the transient variation of bed inlet air temperature at 2 m/s, with the increase in heat irradiated due to burning of the incandescent bulbs from 600 to 3600 W in steps of 600 W. The duration of switching on the bulb is varied in steps. For the first duration (0-40 min) and for 600 W (one bulb), the air temperature increases to 42°C. For the next duration (45 to 85 min) and for 1200 W (two bulbs), the temperature attained by the air is 48°C. In the same manner the air temperature increases and finally the bed inlet air reaches 170°C when all the six incandescent bulbs are put on , and wattage is 3600 W.
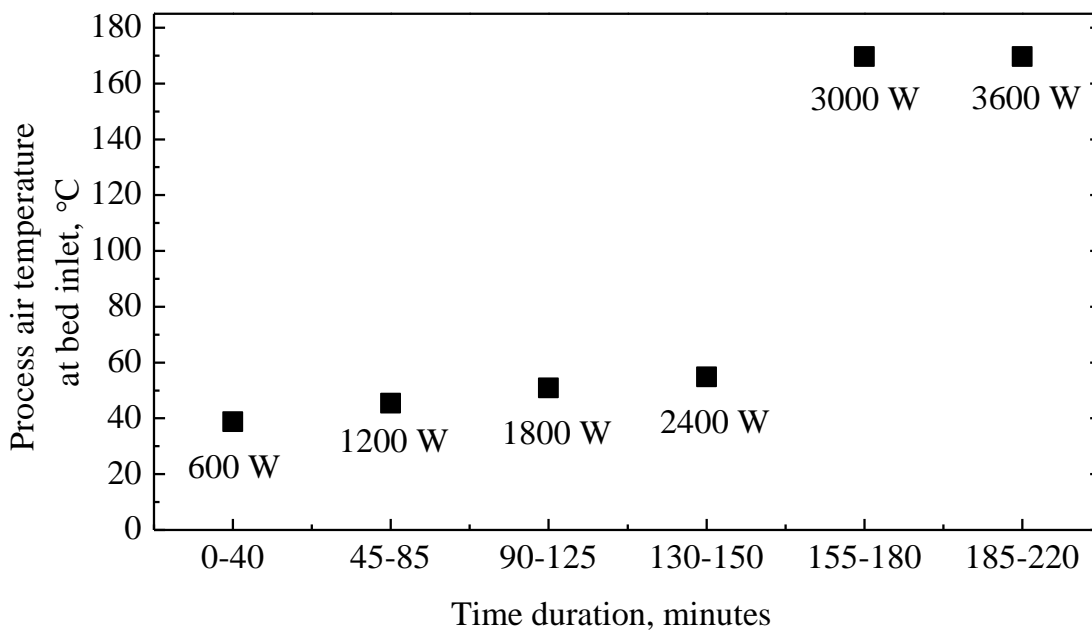
Fig. 4.10 Transient variation of bed inlet air temperature with increase in heat input in steps of 600 W.

Figure 4.11(a) shows the time variation of air temperatures at the bed inlet. For the bed inlet velocity of 1.5 m/s and heat input of 500 W, the bed inlet air temperature relatively increases as compared to atmospheric air temperature. At the end of 60 min, the bed inlet air temperature attains a steady-state at 52°C and increases by 40%. After reaching the steady-state, the process air is then let into the clay and clay additives composite desiccant beds.

86
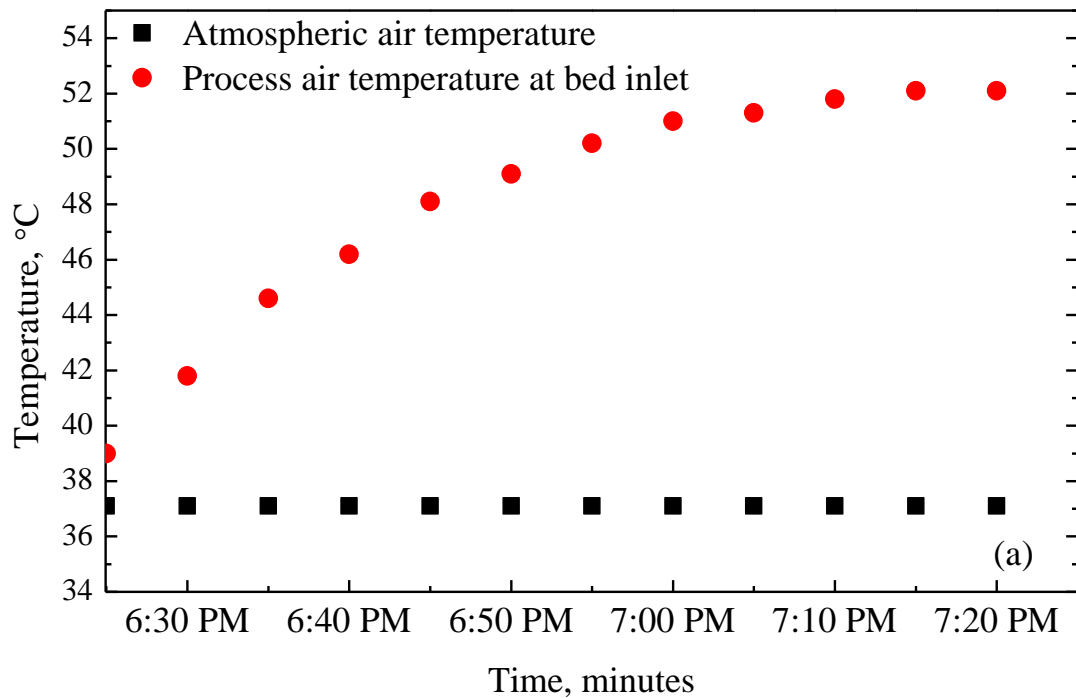
Fig.4.11(a) Transient variation of bed inlet air temperature with the velocity at 500W.

Figure 4.11(b) shows the variation of temperature of the air at the inlet to bed with wattage 3600 W for two hours of experiment. At velocities of 1, 1.5 and 2 m/s, steady-state of air temperature is at the 65 min of process time. From that time onwards the process air at bed inlet continues to operate at same temperature. At the end of 120 min, the temperature of air when compared to atmospheric air increases by 41°C. As shown in Fig.4.12 (a), with increase in velocity the heat transfer rate increases due to forced convection. It is evident from the results that irrespective of velocities, the process air attains the steady temperature at the end of 90 min of heating period. After the heating period of 90 min the air is let into the humidified bed at constant temperature and humidity. The hot process air takes moisture from the desiccant bed and leaves the bed at higher humidity levels than at the desiccant bed inlet. Higher the temperature of process air lower will be the time required for the regeneration of clay and clay additives composite desiccants.
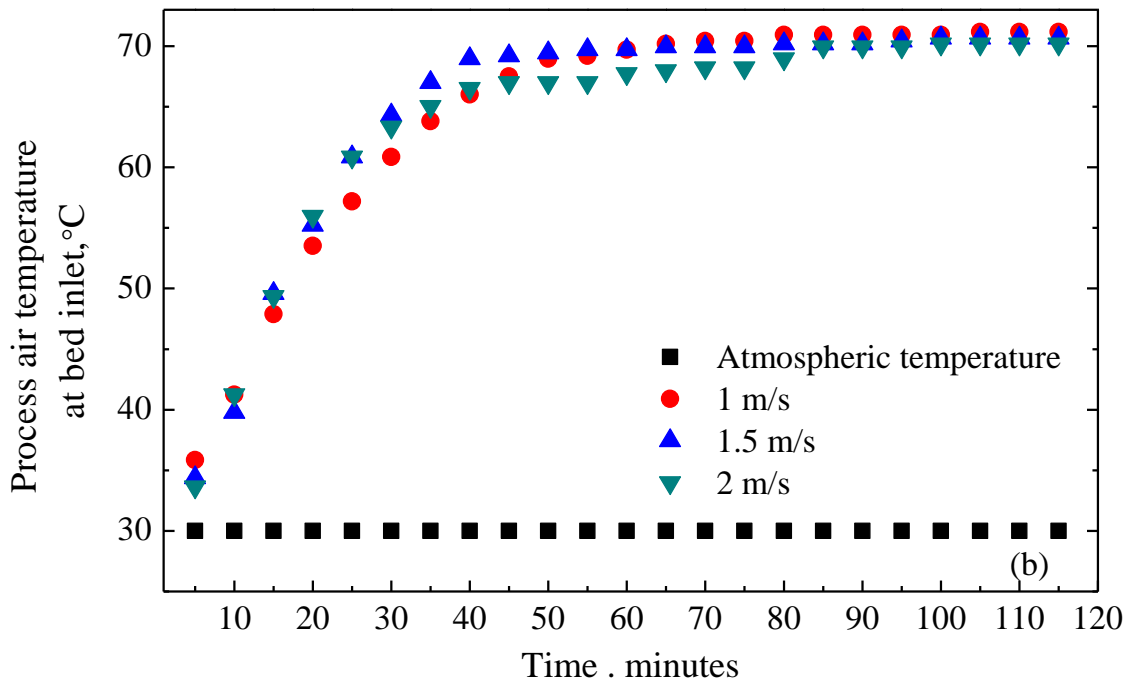
Fig.4.11(b) Transient variation of bed inlet air temperature with the velocity at 3600 W.
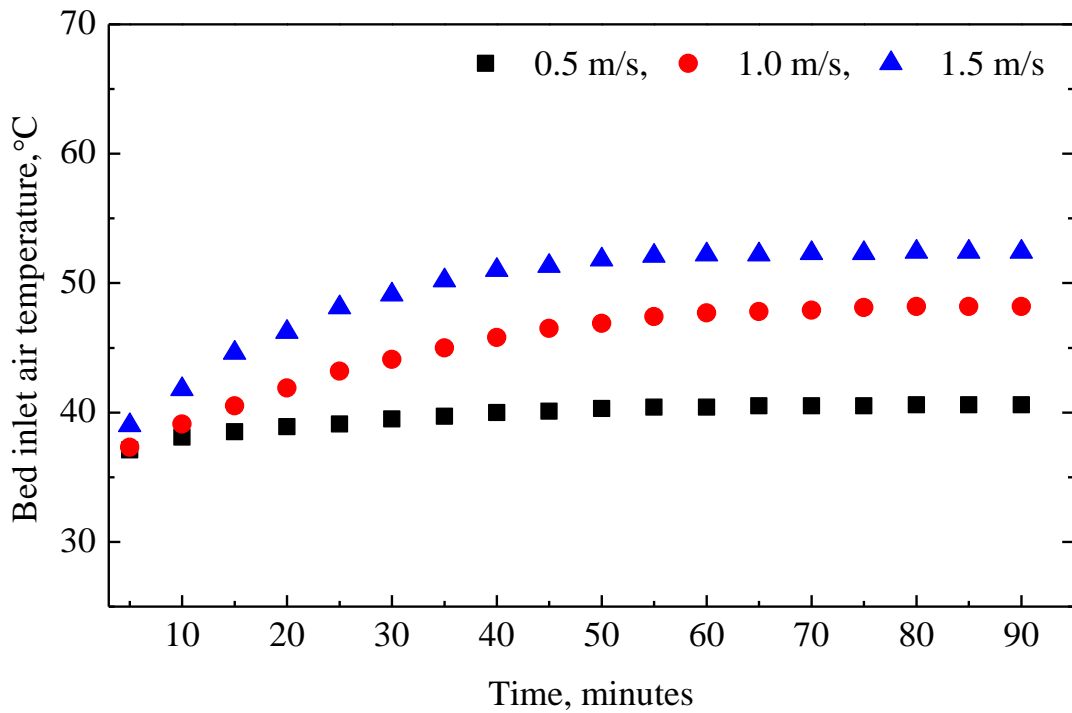
Fig.4.12 (a) Transient variation of process air temperature with the velocity at inlet of desiccant bed.

From Fig. 4.12 (b) shows the transient variation of process air velocity after 60 min of switching on the heating unit. This particular experiment reveals the capability to maintain steady-state in the humidity and temperature of air up to 1600 s at the bed inlet. Once the air attains the steady-state at the end of one hour, it continues to operate in the same state for the remaining duration of experiments. When the velocity of air at inlet to bed is 1.5 m/s and 2 m/s, the temperature of air is recorded as 55°C.
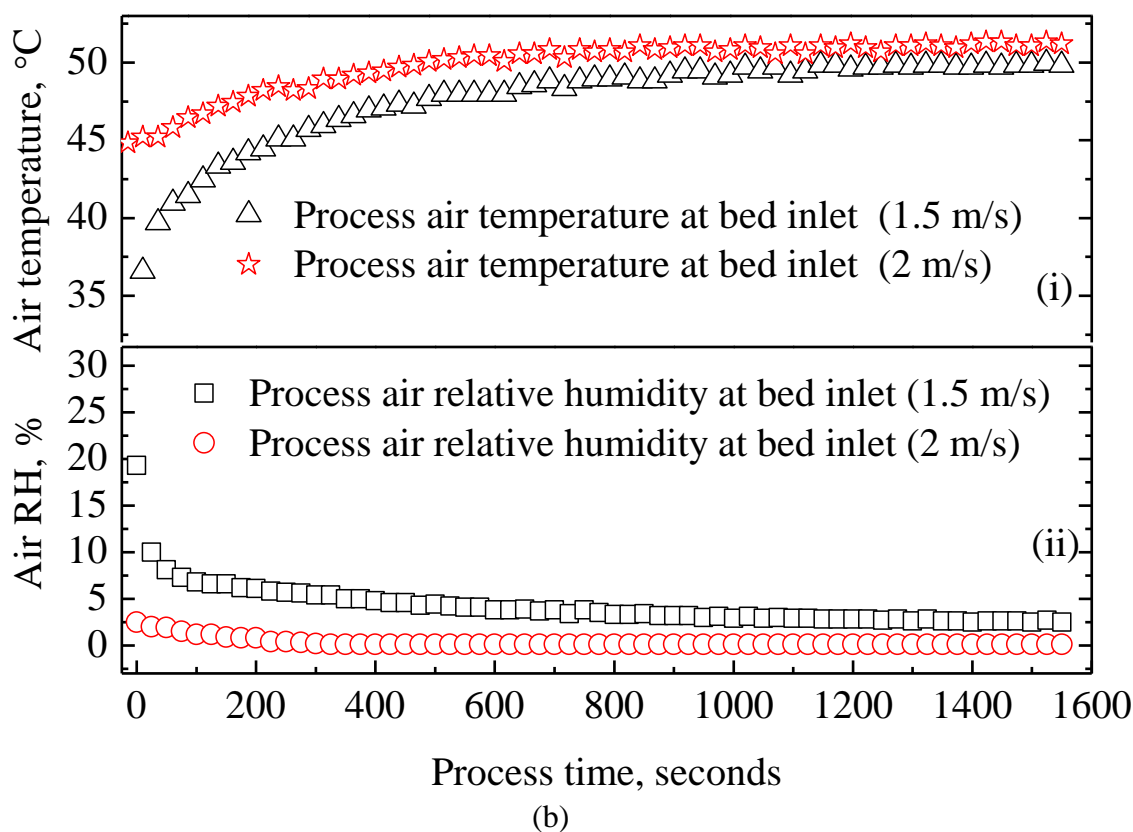
Fig.4.12 (b) Transient variation of process air (i) temperature and (ii) relative humidity with bed inlet process air velocity.

4.2.5 Specifications of vertical tube desiccant bed

The material of the vertical tube is acrylic (perspex) which facilitates the visualization of desiccant pellets in static and fluidized condition. The geometric description of the vertical tube is as follows: The length of the tube is 700 mm and 2 mm thick. The outside and inside diameters are 54 mm and 50 mm respectively. A flange securely connects the tube with the pressure line. A locking arrangement is provided for the

column to load and unload the desiccant pellets during experimentation. The vertical column is provided with pressure taps and taps for locating the hygro transmitter. The pressure tapings are 450 mm apart. The inlet and outlet humidity sensors are located at a distance of 450 mm apart. The desiccant bed temperature is measured axially along the column. A cylindrical plastic cap of 50 mm diameter is used to close the top end of the tube. The closing of the vertical tube ensures the protection of desiccants from atmospheric air. Before conducting the experiment, the cap is removed, and then the process air is let into the vertical packed desiccant bed. The photograph of the column used is shown in Fig. 4.13.
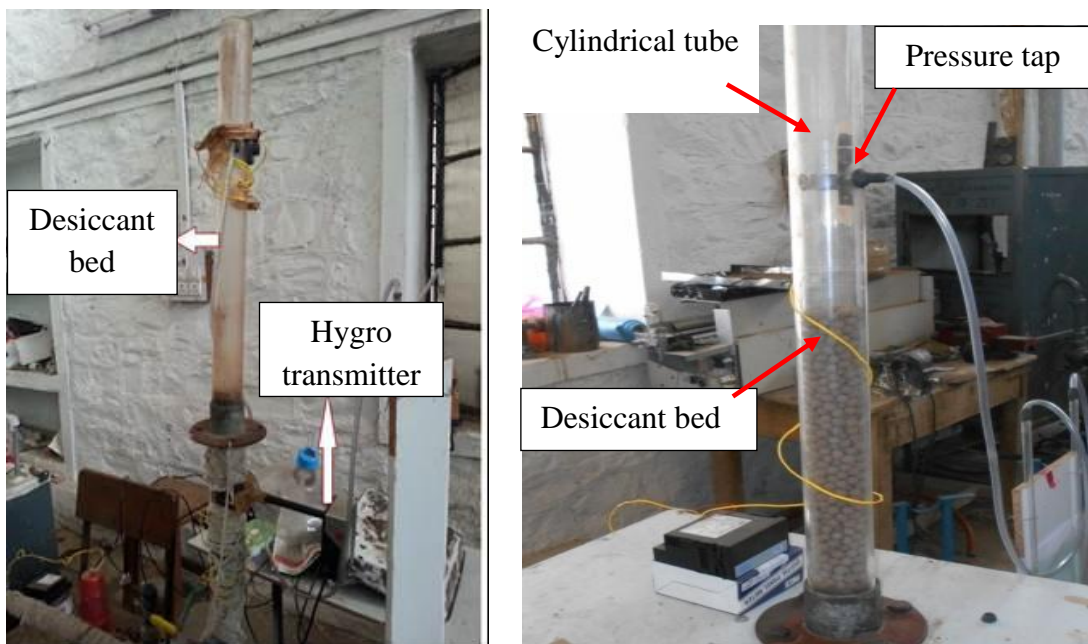
Fig. 4.13 Photographs of securely held vertical column acrylic tube for packed and fluidized bed experiments.

4.2.6 Arrangement of the air humidification unit

The schematic of air humidification unit is shown in Fig. 4.14. The unit comprises a humidifier for adding moisture (A) and a damper (B) for retaining the water pellets carried by moist air. For arranging the humidifier, twenty-liter capacity water can or container is used. About one-fourth portion of can is filled with pebbles. Initially the quantity of water in the humidification unit is sufficient to dip the pebbles. The mouth of the can or container is fitted with a stopper made of wood which houses the

90

openings for the dry air entry and exit for moist air. The photograph of humidification arrangement is shown in Fig.4.15. As compressed air enters the bottom portion, this causes bubbling of water pellets. The bubbling and higher contact time between air and water pellets increase wet bulb temperature of process air. The reduced difference between dry bulb and wet bulb temperatures ensures humidification at room temperature. The air leaving the humidification unit along with water droplets flows into the other twenty liters empty water can. As air expands into the damper, the water droplets condense out and are collected at the bottom of the tank. Then the humidified air then is directed into the compressor line. The humid air leaving the damper mixes with the dry air flowing through the main pressure line. By operating the ball valve Vb2 (See Fig.4.1) the mass flow rate of air in the pressure line is varied. This changes the humidity of air entering into the desiccant bed. The state of humidified air is measured at the bed inlet.
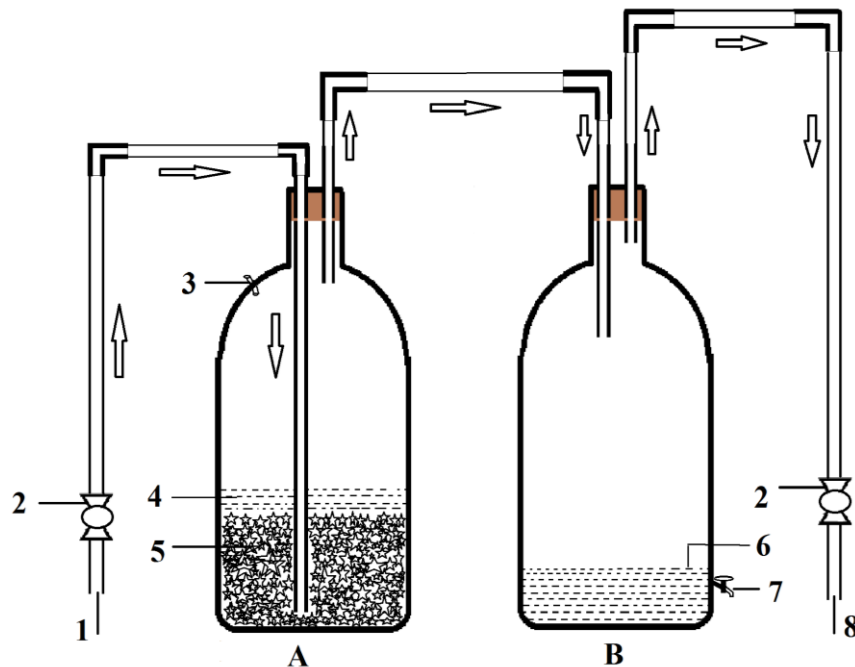
1.Air from compressed tank 2. A ball valve 3. Makeup water supply (Feedwater) 4. 5 Pebbles with water 6. Water collected 7. Tap for draining water 8. Humidified air

Fig. **4.14** Schematics air humidification unit with moisture damper**.**
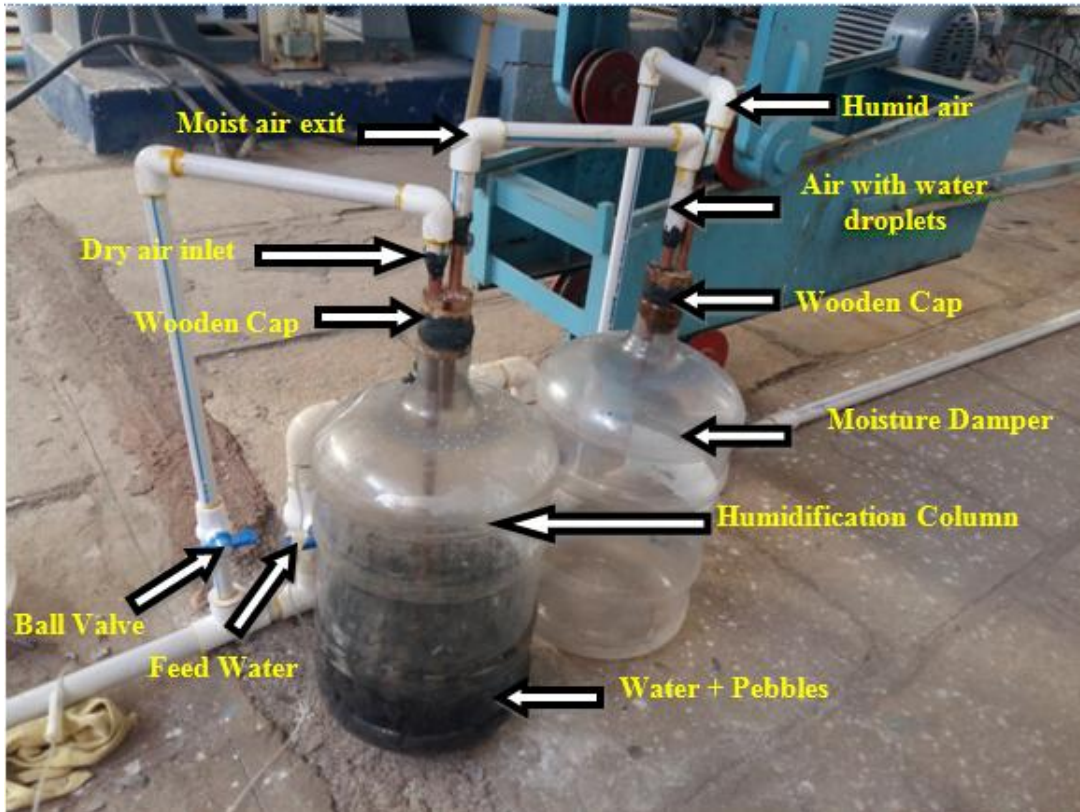
Fig. **4.15** Photographic view of air humidification column with moisture damper.

4.2.7 Performance of air humidifier

The time variation of humidity ratio of process air at bed inlet relative to atmospheric air is illustrated in Fig.4.16. The atmospheric humidity ratio is 3.69 g/kg, and the temperature is 15.1°C. As the air is let into the humidification column, the bubbling of water causes the change in humidity of air. At the end of process time of 90 min humidity attained by the air is 13% and the temperature is 37.9°C. The variation of process air humidity and temperature for one hour of experiment is shown in Fig. 4.17. The humidity of process air increases with increase in velocity. With increase in velocity of process air, intense mixing of water droplets with air results in humidified air. The average rise in humidity of air at the end of one hour of process is 43.38%. The average temperature of the air attained is 28.33°C. After attainment of steady-state, the process air is let into the bed at constant humidity and temperature.
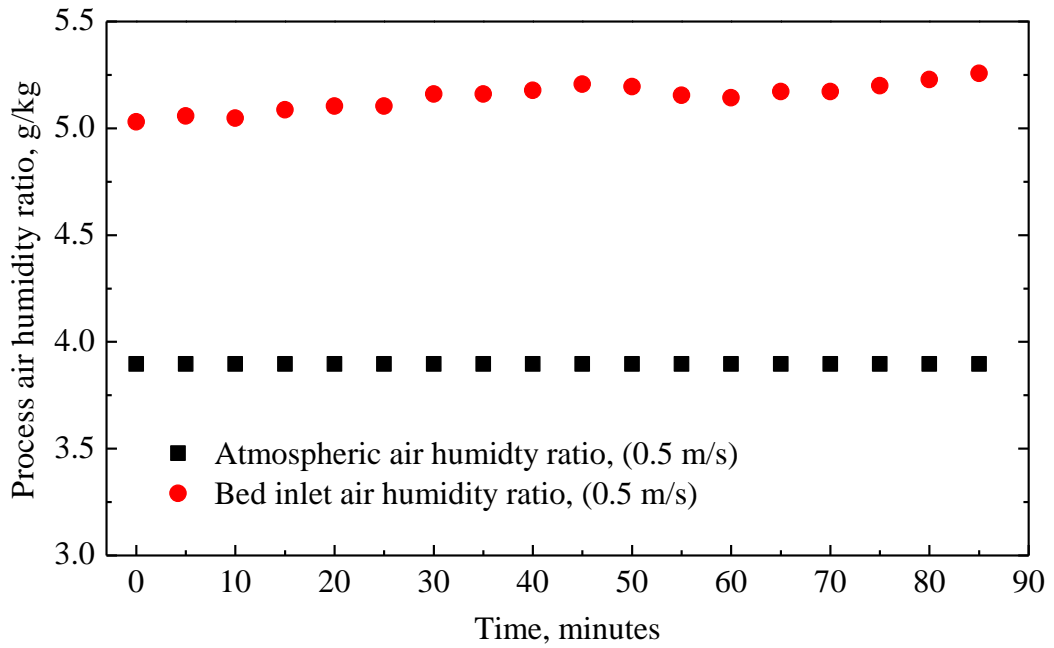
Fig.4.16 Performance of air humidification unit with bed inlet air velocity.
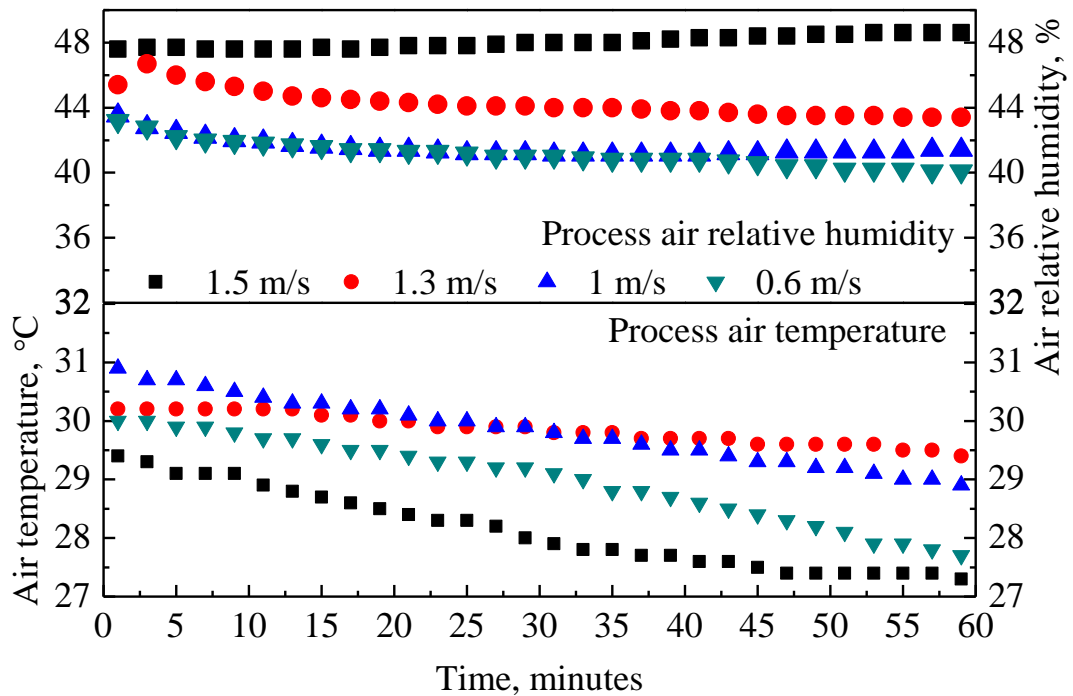
Fig.4.17 Performance of air humidification unit with variation in bed inlet air velocity.

4.3 EXPERIMENTAL PROCEDURE

The humidification and dehumidification experiments are conducted using clay - additives - $CaCl_2$ desiccant bed in static and fluidized configurations. The ball and gate valves are used to control the flow of process air. Experiments on adsorption process at atmospheric relative humidity are conducted by passing pressurized air through compressor line (from Vg1 to Vg3) and then to the pressure line (from valve Vg3 to Vg8) as can be seen from the experimental setup. Experiments at preset relative humidity are conducted by passing compressed air through the humidification column and then into the desiccant bed. Air preheating unit is fabricated and arranged to carry out desorption experiments. Experiments are conducted for step-change in inlet air velocity, temperature, and relative humidity. The valve positions for different sets of experiments are shown in Table 4.4. The valves are set into operation to conduct adsorption corresponding to a preset RH and RH corresponding to the atmospheric condition as well as desorption experiments. The experimental procedure is as follows:

1. Before starting the experiments, all pipeline connections, valve positions, power supply connections, data cable connections for sensors are checked to ensure proper working. The atmospheric relative humidity and temperature are noted.

2. The compressor and the air tank connections are checked for oil level and air leakages. Before starting the experiment, the ball valve Vb1 at the exit of the air tank is closed. After switching on the compressor, the valve position is correctly set, so that air pressure in the air reservoir is constant. During the experiments, the reservoir pressure is maintained between 5 to 8 bars.

3. The experiments to be conducted are grouped into three parts. The first set comprises adsorption experiments using packed bed under atmospheric humidity and temperature conditions. This set of experiments also involves adsorption at predetermined relative humidity and temperature. The second set of experiments are on desorption of packed bed of desiccant pellets at desired inlet air humidity and temperature. The third set of experiments includes adsorption-desorption studies on composite desiccant pellets in the fluidized bed configuration.

94

4. The hygro transmitter, microcontroller, the power and data cables as well as bed thermocouple connections are checked. The microcontroller code is launched in the laptop system and compiled. The ambient humidity and temperature are measured using the humidity sensor, and the values are saved to a file. The weight of clay and clay - additives - $CaCl_2$ desiccant before experimentation is recorded.

5. Now the compressor is switched on, the ball valve (Vb1) at the reservoir outlet is in the desired position. The air enters the compressor line made of PVC and then directed into the pressure line of galvanized iron (GI) pipe. Depending on whether air dehumidification or air humidification experiment, the process air is let into the air heating unit or into the pressure line.

6. Depending on whether the experimentation is for adsorption or desorption, the air is finally allowed to flow through the pressure line via air humidification unit or air heating unit.

7. The gate valve Vg7 is completely opened, and the air is allowed to flow freely to the atmosphere. The simultaneous operation of gate valves Vg7 and Vg8 enable to set the manometer deflection. After ensuring the constant head of water column in the manometer, corresponding pressure drop across orifice meter and process air temperatures are manually recorded. The superficial velocity is estimated, and the velocity at the inlet of empty bed is equal to the velocity at the exit of bed. A parallel vent (valve Vb6) is now opened, and process air is let flow to the atmosphere at pre-set velocity through the valve Vb6.

8. In the open position of valve Vb6, desiccants of known weight are poured into the vertical tube. The tube with desiccant pellets is securely held in the vertical position, and the open end of the tube is closed by a cap. The bed height is noted by using a steel scale. The humidity sensor used to measure the exit air humidity and temperature is fixed at the exit of the bed. The water levels in the two limbs of U - tube manometers, i.e. one across orifice meter and another along the bed are checked and ensured that the level of water columns in the manometer tubes is equal.

Table 4.4 Relative positions of valves for adsorption and regeneration processes.

Valves / Process	V_g1	V_g2	V_g3	V_g4	V_g5	V_g6	V_g7	V_g8	Vb1	Vb2	V_b3	V_b4	V_b5	V_b6
Adsorption (Atmospheric RH)	1	0	1	0	0	1	0	1	1	1	0	0	1	1
Humidification (Set RH)	1	0	1	0	0	1	0	1	1	0	1	1	1	1
Desorption	1	0	1	1	1	0	0	1	1	1	0	0	1	1
1 – Valve opened : 0 – valve closed Valve: V_g – Gate valve: V_b – Ball valve														

9. After fixing the tube with desiccants the cap is removed from bed exit, valve Vb6 is completely closed, and the process air is finally allowed to flow through the tube containing desiccant pellets. Simultaneously the microcontroller code is launched. The readings corresponding to relative humidity and temperature of process air at bed inlet and exit are displayed on the laptop monitor. The bed temperatures along bed length are manually recorded using an infrared thermometer.

10. The experiments are carried out till the end of process time. Towards the end of experimentation airflow to the bed, the section is cut off by simultaneously opening and closing of valves Vb6 and Vg8. The Arduino microcontroller code is stopped, and the transient values of relative humidity and temperature are written to a file and saved. After the experiment desiccants are taken out from the tube. The final bed mass is measured by using a digital weight balance.

11. The same procedure is followed for other sets of experiments on packed and fluidized composite desiccant beds in adsorption and desorption.

12. Care is taken to protect the desiccant pellets during the time of conducting experiments (loading, unloading, and measuring weight of desiccant mass). The desiccants are in airtight plastic covers.

4.4 ANALYSIS OF COMPOSITE DESICCANT BEDS IN FLUIDIZATION

The minimum superficial velocity required for fluidization is calculated using the Leva equation presented below as (Fungtammasan, 2001)

$$U = \frac{7.169 \times 10^{-4} d_\phi^{1.82} \left(\rho_\phi - \rho_a \right)^{0.94} \times g}{\rho_a^{0.006} \mu_a} \tag{4.3}$$

The minimum value of fluidization velocity estimated using Eq. (4.3) for burnt clay - additives - $CaCl_2$ desiccant pellets ranges from 1.2 to 1.5 m/s. Prior to the fluidization experiments, the tested minimum fluidization velocity for bed weights of 200 and 400 g is from about 1.2 to 1.7 m/s. An understanding of the principle of fluidization of desiccant pellets is required prior to the fluidized bed experiments. Figure 4.18 (a, b, c and d) illustrates the configuration of beds obtained by varying the process airflow

velocities. In the first configuration (Fig 4.18 (a)) the process air is passed through the porous bed of desiccant pellets supported on a fine mesh. The desiccant pellets are undisturbed at low velocity. Under such conditions, the porosity of the bed is same as that of packed bed. In the second stage (Fig. 4.18(b)) process air velocity is gradually increased above critical velocity of fluidization in which bed is suspended in air stream. The bed will have porosity slightly higher than packed bed. With further increase in velocity the upper bed pellets are moving towards a fluidized state. There are vigorous turbulence, rapid mixing, and the bed is in a state of bubbling fluidized bed. The bed porosity varies axially along the length of the bed. In the fourth stage (Fig.4.18 (d)) at higher velocity the pellets are blown out of the bed. Therefore to retain the pellets some amount needs to be recirculated to maintain a stable system called circulating fluidized bed. However in the present study the fluidization experiments are conducted up the stage of bed being bubbling fluidized bed.

(a) Fixed bed   (b) Fluidized bed   (c) Bubbling fluidized bed   (d) Circulating fluidized bed
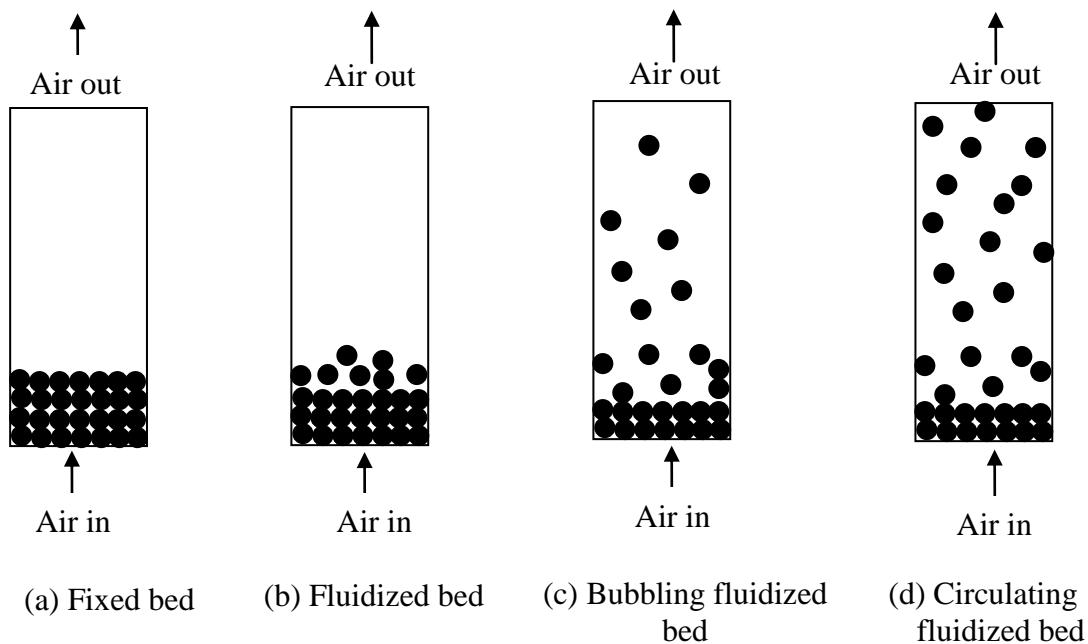
Fig. 4.18 Principle of fluidization showing stages of the fluidized bed.

Fig 4.19 (a, b, c and d) shows the photographic views of desiccants in a fluidized state. When the process air is introduced, initially the bed layers are slowly moved up. Within a short period of time, the bed is set in circulation, and the bed length changes

from L1 to L4 in variations of L2, L3 and so on. For the bed inlet velocity of 2 m/s, the initial static bed length (L1) before the onset of fluidization for clay, clay - horse dung and clay - sawdust composites desiccant bed of 300 g by weights are 14.5, 21 and 25 cm respectively in adsorption.

(a) Fixed bed

(b) Fluidized bed

(c) Bubbling fluidized bed

(d) Circulating fluidized bed
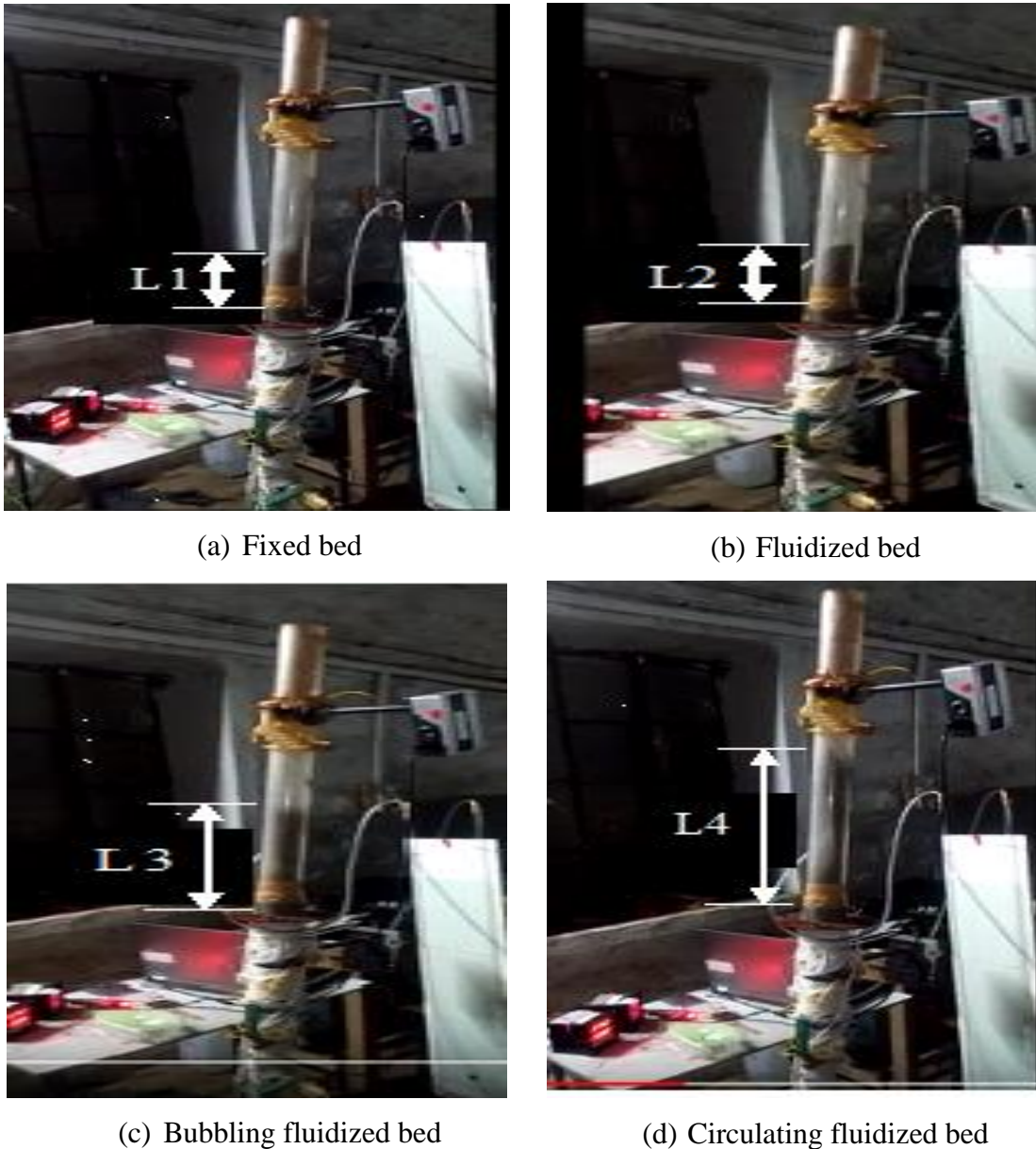
Fig. 4.19 Photographs of clay - $CaCl_2$ composite desiccant pellets in fluidisation.

It is seen that the bubbling of the pellets is more dominant at the upper portion than the pellets in the lower region of the bed. With time the clay composite desiccant

pellets within the bed move continuously. For the same bed inlet air velocity of 2 m/s and bed weights of 300 g, the maximum bed length (L4) attained by clay, clay - horse dung and clay - sawdust composite desiccant pellets are 24.3, 44 and 65 cm respectively in adsorption. For the bed inlet velocity of 1.5 m/s and bed mass of 200 g in desorption, the bed length changes from 10 to 16 cm for clay - $CaCl_2$, 12 to 21 cm for clay - horse dung - $CaCl_2$ and 14 to 24 cm for clay - sawdust - $CaCl_2$ composite desiccant pellets beds. As viewed in Fig.4.19, the fluidized bed can be divided into two zones. The upper portion moves upward in a fluidized manner, while the lower bed mass can be seen as packed bed in a quasi-static manner. For all the fluidized bed experimental runs the ratio of static bed length to maximum fluidized bed length calculated is less than unity in adsorption and desorption processes. The porosity of the composite desiccant bed varies along the length of bed.

4.5 EXPERIMENTAL PARAMETER ESTIMATION

The main parameters estimated are the superficial velocity of air, bed porosity, bed specific heat, and saturation pressure and humidity ratio of process air. The pressure drop across the orifice meter in terms of manometer deflection is used to calculate the volume flow rate of air through the pressure line.

$$Q_{act} = \frac{C_d \sigma_1 \sigma_2 \left(2gH_a\right)^{0.5}}{\left(\sigma_1{}^2 - \sigma_2{}^2\right)^{0.5}} \tag{4.4}$$

The density of process air is calculated by measuring pressure (P_a) and temperature (T_a) of air in pressure line using the following ideal gas equation,

$$\rho_a = \frac{P_a}{R_a T_a} \tag{4.5}$$

The mass flow rate of air is calculated as

$$\dot{m}_a = \rho_a \times Q_{act} \tag{4.6}$$

The process air velocity at bed inlet is estimated as

$$v_a = \frac{\dot{m}_a}{\left(\rho_a \times \frac{\pi}{4} d_\phi{}^2 \right)}$$

(4.7)

Cylindrical packed columns are the dominant type of columns and are used for sorption processes due to their high surface area ratios. The efficiency of fluid flow and transport processes through these beds is affected by their internal structure, which in turn depends on the geometrical make-up and arrangement of the packing material, as well as the ratio of the bed to desiccant pellet diameter. The specific macroscopic properties such as the voidage or packing density are widely accepted parameters used to define bed structure. The void fraction or bed porosity is the ratio of the volume of voids in bed to the total volume of bed (volume of voids and solids). The bed porosity is calculated by using the relation as given in Pesaran and Mills (1986).

$$\text{Bed porosity}(\varepsilon_b) = \left[1 - \frac{\rho_b}{\rho_\phi} \right]$$

(4.8)

The bed porosity calculated using Eq. (4.8) ranges from 0.45 to 0.57 for clay composite vertical static desiccant bed. Whereas for beds in fluidization, the estimated bed porosity values at the maximum height of the bed vary from 0.74 to 0.79. The bed porosities estimated for vertically packed heat treated clay and clay additives desiccant pellets without impregnation of $CaCl_2$ are graphically presented in the appendix - II (Fig.II.4).

4.6 DATA ACQUISITION (DAQ) SYSTEM

Data acquisition system (DAQ) is employed to record the transient values of relative humidity and temperature. DAQ is comprised of Arduino Uno microcontroller, voltage divider circuit, computer, and hygro-transmitters. The specifications of Arduino Uno microcontroller are shown in Table 4. Hygro transmitter provides an output voltage in the range of 0 to 10 volts for relative humidity and temperature,

whereas Arduino Uno working voltage range is from 0 to 5 volts. In order to match the voltage range of microcontroller with sensor voltage range it is required to process sensor voltage to its half value. The reduced output voltage from the voltage divider circuit is forwarded to microcontroller board. Fig.4.20 shows schematic of parallel resistance circuit constructed to achieve voltage reduction.

Table 4.5 Technical specifications of Arduino Uno microcontroller**.**

Instrument	Arduino Uno
Microcontroller Type	ATmega 329
Operating Voltage	5 V
DC current	40 mA
Clock Speed	16 MHz
Digital I/O Pins	14
Analog Input Pins	6
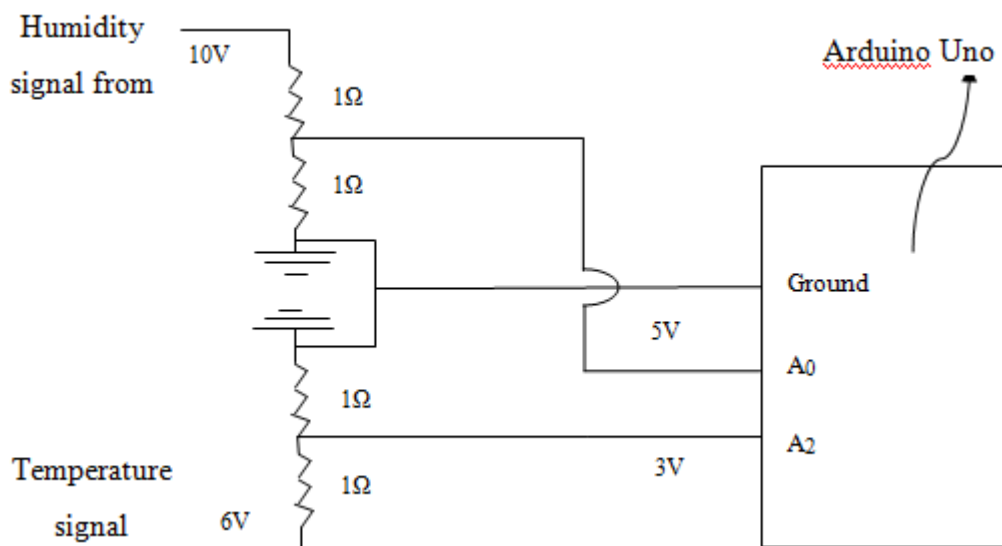
Fig. 4.20 Parallel resistance circuit to halve the hygro transmitter voltage signal.

The circuit is made of four resisters of 1Ω each. Two resistors are connected in parallel for temperature signal, and another two resistors are connected in parallel for

102

humidity signal. The values of temperature and humidity signal in terms of voltage output (0 - 10 V) from the sensors are stepped down to half of their voltage values (0 - 5 V). The microcontroller interfaced to computer reads voltage signals, and the values are written to a data file. The transient values of humidity and temperature at a sampling rate of 1 s are read and written by a microcontroller code embedded in the microcontroller.

Figure 4.21(a) and (b) shows the photographs of breadboards with 1Ω resistors. Arduino Uno is connected to the computer through a data cable. Arduino 1.6.7 software is used to read digital data from Arduino Uno. Once the Arduino Uno is connected to the computer, it gives information about voltage. To get the actual value of temperature and relative humidity corresponding to voltage, the relation between voltage and actual parameter is required. For this purpose the humidity probe is calibrated by manufacturer Jupiter electronics Mumbai. The calibration certificate provided by the company is shown in appendix - VI. The relative humidity and temperature at bed inlet and exit are measured using Hygroflex hygro transmitter. The humidity transmitter range for relative humidity measurement is from 0 to 100%, and the corresponding voltage output ranges from 0 to 10 volts.
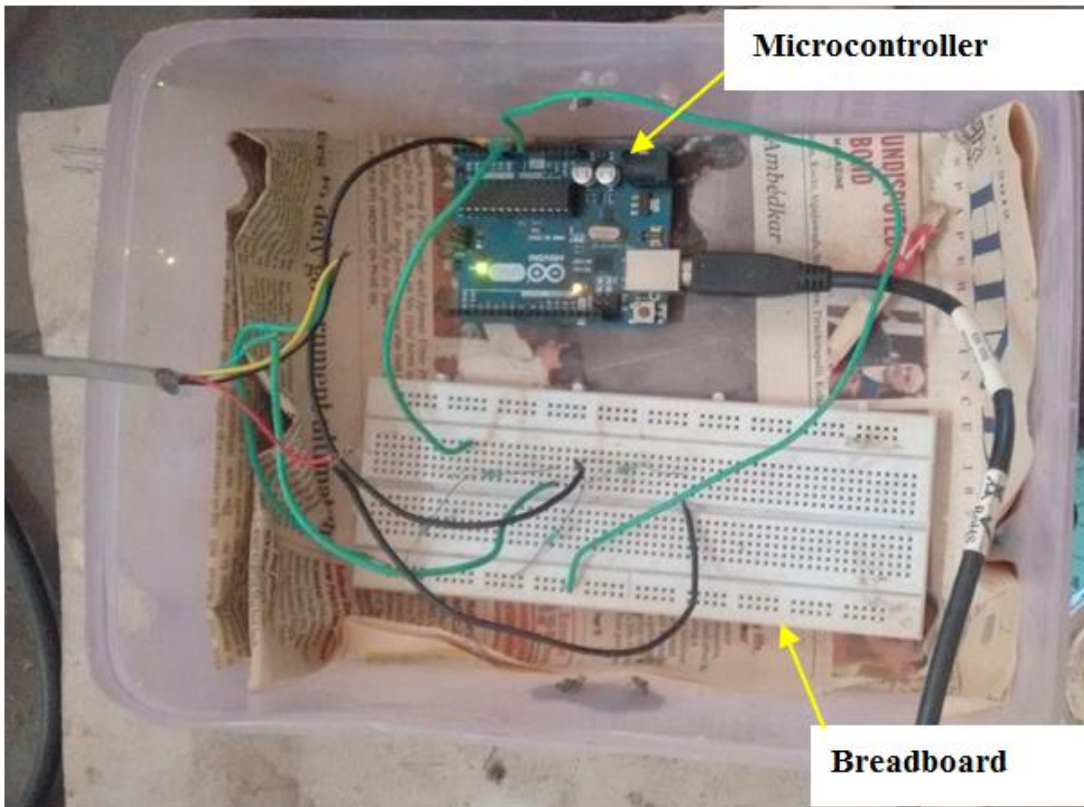
Fig. 4.21 (a) Photograph of bread board connected to Arduino microcontroller.
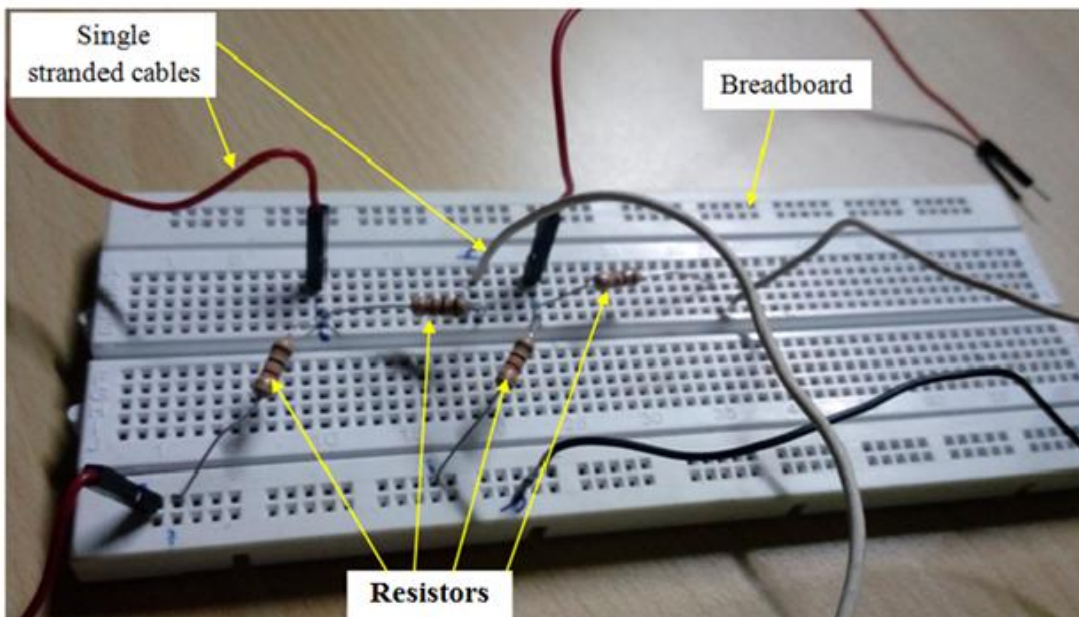
Fig. 4.21 (b) Photograph of breadboard with resistors connected in parallel.

Similarly, the temperature range is from -40 to 85°C, and the corresponding voltage output is from 0 to 10 volts. Subsequently the voltage outputs corresponding to relative humidity and temperature are written to excel file through Arduino Uno microcontroller interface code. Once the code is executed the voltage values to excel file for every second of process time. The voltage values written are corresponding to relative humidity and temperature of process air recorded by hygro transmitter at desiccant bed inlet, desiccant bed exit, and grain dryer exit.

The microcontroller operating voltage range is from 0 to 5 volts whereas for transmitter it is from 0 to 10 V. In order to get the input voltage from 0 to 5 V to microcontroller, a voltage step down circuit is designed and fabricated. The analog output in the form of voltage readings are displayed and converted to corresponding relative humidity and temperature as follows

$$\text{Relaive humidity (RH\%)} = 10 \ \times \ \text{Analog output} \tag{4.10}$$

$$\text{Temperature } (^\circ C) = (12.5 \times \text{Analog output}) - 40 \tag{4.11}$$

The saturation pressure, which is a function of air temperature, is calculated for every second of process air temperature values. The humidity ratio is a function of relative humidity and saturation pressure. The transient values of saturation pressure (P_{sat}) and humidity ratio (S) are evaluated as follows

$$P_{sat} = 610.78e^{\left(\frac{17.2694 \times T_a}{T_a + 238.3}\right)} \tag{4.12}$$

$$(S) = \frac{0.622 \times RH \times P_{sat}}{P_{total} - RH \times P_{sat}} \tag{4.13}$$

4.7 UNCERTAINTY ANALYSIS OF PARAMETERS

The uncertainties in the experimental measurement of parameters are calculated according to the procedure given by Kline, 1953. The parameters of interest measured are relative humidity, temperature, superficial velocity, and desiccant bed weight.

The humidity ratio (S) is a function of variables RH T_a and P_{total} is expressed as

$$S = \frac{0.622 P_v}{P_{total} - P_v} \tag{4.14}$$

The uncertainty calculation in the estimation of air humidity ratio S of process air is as shown:

$$\Delta S = \sqrt{\left(\frac{\partial S}{\partial P_v}\right)^2 \times \left(\Delta P_v\right)^2} \tag{4.15}$$

The vapor pressure P_v is a function of relative humidity and saturation pressure and is evaluated as:

$$P_v = RH \times P_{sat} \tag{4.16}$$

The uncertainty P_v is estimated as Eq. (4.17). The saturation pressure P_{sat} is computed as Eq. (4.18):

$$\Delta P_v = \sqrt{\left(\frac{\partial P_v}{\partial RH}\right)^2 \times \left(\Delta RH\right)^2 + \left(\frac{\partial P_v}{\partial P_{sat}}\right)^2 \times \left(\Delta P_{sat}\right)^2} \tag{4.17}$$

$$P_{sat} = 610.78 \times e^{\frac{17.2694 T_a}{(T_a + 273)}} \tag{4.18}$$

Uncertainty calculation in the estimation P_{sat} is as shown in Eq. (4.19): Hence the sampling uncertainty in estimation of S is as Eq. (4.20): The experimentally measured superficial velocity $\left(v\right)$ is a function of manometer displacement $\left(H_w\right)$ which resulted from curve fitting of measured superficial velocity as a function of manometer displacement (FIg.4.2). The superficial velocity is expressed as Eq. (4.21)

$$\Delta P_{sat} = \sqrt{\left(\frac{\partial P_{sat}}{\partial T_a}\right)^2 \times \left(\Delta T_a\right)^2} \tag{4.19}$$

$$v = 3.411 \times H_w{}^{0.333} \qquad (4.20)$$

The overall uncertainty in the estimation of superficial velocity (v) is given by

$$\Delta v = \sqrt{\left(\frac{\partial v}{\partial H_w}\right)^2 \times (\Delta H_w)^2} \qquad (4.21)$$

The uncertainty in the measurement of bed mass (m_b) of 300 g, is given by

$$\Delta m_b = \frac{0.01}{300} \times 100 = 0.0033\% \qquad (4.22)$$

The uncertainty in bed mass is expressed as

$$\Delta m_b = 300 \pm 0.0033\% \text{ g} \qquad (4.23)$$

The uncertainties calculated in measured parameters are listed in Table 4.6.

Table 4.6 Uncertainty values in the evaluated parameters.

Parameter	Uncertainty (%)			
	At bed inlet		At bed exit	
	Adsorption (clay-CaCl$_2$, 300 g, 2 m/s)	Desorption (clay-saw dust-CaCl$_2$, 300 g, 2 m/s)	Adsorption (clay-CaCl$_2$, 300 g, 2 m/s)	Desorption (clay-saw dust-CaCl$_2$, 300 g, 2 m/s)
Saturation pressure (P_{sat})	±0.8336	±0.6421	±7.7180	±2.6534
Vapor pressure (P_v)	±1.3019	±0.7749	±7.8021	±2.8685
Humidity ratio (S)	±1.3135	±0.7769	±7.8455	±2.8846
Superficial velocity (v)	±0.24 % @ $v = 1.74$ m/s			
Bed mass (m_b)	±0.0033% @ $m_b = 300$ g			

It can be noted that though the same devices are used for the measurement of air humidity and temperature at bed inlet and exit, but the uncertainty involved differs. This is because device uncertainty is fixed, but the uncertainty involved in the measured value is a function of other parameters which increases the propagation of uncertainty. The higher uncertainty values for humidity ratio in adsorption and desorption process are $\pm 8\%$. As humidity ratio is function of other parameters and this results in propagation of uncertainty.

4.8 SUMMARY

The experimental test rig arranged to conduct adsorption-desorption experiments on composite desiccant pellets in the packed bed configuration is extended to conduct similar experiments on fluidized bed. The air heating and humidification units fabricated are tested for performance in heating and humidifying the process air. The process parameters such as superficial velocity, bed porosity, bed specific heat, and humidity ratio are estimated experimentally. Data acquisition system comprising microcontroller, voltage divider circuit, and hygrotransmitter is explained. The calibration procedure adopted by the manufacturer is presented. Finally the uncertainties involved in experimental measurements are evaluated. The maximum average value of uncertainty estimated is $\pm 8\%$ for humidity ratio in adsorption and desorption. The following conclusions are drawn from the experimental work

1. The performance test on the air heating unit reveals maximum temperature attained by process air is 52°C at 1.5 m/s for 500 W heat input.

2. The average increase in humidity and temperature of process air at 1.5 m/s is 43.38% and 28.33°C.

3. The performance tests on air heater and humidification unit reveal that the process air attains steady-state values of humidity and temperature after 60 to 90 min of process time.

4. The higher uncertainties in desorption related to the measurement of humidity ratio of process air are due to propagation of errors encountered.

CHAPTER 5

EXPERIMENTAL RESULTS AND DISCUSSION

5.1 INTRODUCTION

To have insight into the heat and mass transfer performance characteristics of vertical packed burnt clay - additives - $CaCl_2$ composite desiccant beds, basic experiments are conducted. The transient values of exit air relative humidity and temperature are recorded with respect to inlet air relative humidity, temperature, velocity of process air and for different mass of bed. The performance indices defined are bed specific heat (C_{p_b}), moisture removal capacity (MRC_{ads}), moisture addition capacity (MAC_{des}) and mass transfer coefficient (h_χ). The experimental results for packed and fluidized beds are compared with respect to air humidity ratio, temperature and dew point effectiveness. The local mass transfer coefficient for the different adsorption and desorption tests are evaluated experimentally.

5.2 EXPERIMENTAL PERFORMANCE INDICES

The heat and mass transfer characteristics of the given desiccant bed are governed by the parameters like inlet air velocity, relative humidity, temperature, mass of the bed and porosity of the bed. The performance of the bed is evaluated using the following parameters:

$$C_{p_b} = \left[\frac{m_{CaCl_2}}{m_b} \times C_{p_{CaCl_2}} \right] + \left(\frac{m_{csd}}{m_b} \times C_{p_{csd}} \right) \tag{5.1}$$

$$MRC_{ads} = \frac{S_i - S_e}{S_i} \tag{5.2}$$

$$MAC_{des} = \frac{S_e - S_i}{S_e} \tag{5.3}$$

The bed specific heat (C_{p_b}) which influences the heat and mass transfer characteristics of desiccant bed is determined for composite desiccant beds. The difference in mass of desiccant before impregnation (m_{csd}) and after impregnation (m_b) gives the mass of CaCl$_2$ (m_{CaCl_2}) impregnated. By knowing the specific heat of CaCl$_2$ and clay composite pellets, gravimetrically the bed, specific heat values are estimated. The bed specific heat for burnt clay - CaCl$_2$, burnt clay–horse dung- CaCl$_2$ and burnt clay - sawdust - CaCl$_2$ composite desiccant beds are 2307.97, 4468.88 and 5036.41 J/kg K respectively. The dehumidification (MRC_{ads}) and humidification ability (MAC_{des}) are estimated using inlet and exit air humidity ratio. The analysis of mass transfer coefficient is investigated using the mass of bed, density of water vapor in air and at the surface of bed. The mass transfer coefficient for the convective mass transfer process is calculated in terms of vapor pressure density between the process air and the desiccant bed. The vapor pressures of air and bed are used to estimate vapor density difference. The mass transfer coefficient (h_χ) is a function of rate of mass transfer per unit area of bed ($\dot{m}_v$), density of water vapor in air (ρ_{v_i}) and density of water vapor at solid surface (ρ_{v_s}). The density of water vapor in air and at bed surface is evaluated as a function of vapor pressures (p_{v_i} and p_{v_s}) at process air temperature and bed surface temperature. The mass transfer coefficient (h_χ) is estimated using Eq. (5.4) to (5.8)

$$h_\chi = \frac{(\dot{m}_v)}{\left(\rho_{v_i} - \rho_{v_s}\right)} \tag{5.4}$$

$$\dot{m}_v = \frac{\Delta m}{A \Delta t} \tag{5.5}$$

$$\rho_{v_i} = \frac{p_{v_i}}{R T_{a_i}} \tag{5.6}$$

$$\rho_{v_s} = \frac{p_{v_s}}{R T_s} \tag{5.7}$$

The values of vapor pressure (p_{v_i} and p_{v_s}) are estimated using the data extracted from Calcium chloride data handbook - 2003 of Dow chemical company. A four-degree polynomial relating the vapor pressure (p_v) and CaCl$_2$ concentration (τ) is obtained. The polynomial is of the form:

$$p_v = a_0 + a_1\tau + a_2\tau^2 + a_3\tau^3 + a_4\tau^4 \tag{5.8}$$

For the CaCl$_2$ concentration of $\tau = 0$ to 50% and for the temperatures of 20 and 40°C, the constants (a_0 and a_4) are furnished in Table 5.1.

Table. 5. 1. Regression constants for vapor pressure (mm of Hg) v/s temperature (°C) chart.

Regression Constants \ Temperature	20°C	40°C
a_0	17.86085149	53.0389912
a_1	-0.1534159594	0.03443817921
a_2	0.0006167150232	-0.0352294261
a_3	-0.0001772467701	0.0003926850743
a_4	$2.283595335 \times 10^{-6}$	$-4.475770425 \times 10^{-7}$

5.3. ANALYSIS OF DEHUMIDIFICATION EXPERIMENTAL RESULTS FOR BURNT CLAY COMPOSITE DESICCANTS

The transient variation of exit air humidity ratio and temperature in comparison to inlet air humidity ratio and the temperature is presented in Fig.5.1 and Fig.5.2. During these two experimental runs the desiccant is used for the first time. The process air with relative humidity of 80 to 90% is introduced into the desiccant bed of burnt clay - CaCl$_2$. The humidity level of process air reduces to 46% towards the end of process. It can be seen that the outlet, inlet air humidity ratio and temperature with adsorption time have similar trend. For example, the exit air humidity ratio firstly decreases and

then increases with time and later on decreases steadily with time. During the initial period, that is, from 0 to 80 s, the ratio of outlet to inlet air humidity ratio is less than one and adsorption process has occurred. Consequently during this period, the vapor pressure on the desiccant surface is less than the vapor pressure of process air at the inlet. Because of this the mass transfer direction will be from air to desiccant surface. At 1 m/s the maximum reduction in moisture occurs when the processing time is below 100 s, whereas at 2 m/s minimum value of exit air humidity ratio is observed at process time slightly more than 100 s. In between 100 s to 400 s there is a transition from unsteady state to steady-state. From 400 s onwards the capability of the bed to adsorb moisture is very minimal.

As presented graphically in Fig.5.1 and 5.2, the region I can be split into two periods. The period from 0 to 100 s owing to higher desiccating power of bed maximum dip in exit air humidity ratio is seen. From 100 to 500 s the transition from higher desiccation to minimal desiccation occurs. Region II commences from 500 s onwards the bed behavior seems to be monotonous, and change in exit air humidity ratio steadies and may near the inlet humidity condition. During initial stages of operation irrespective of superficial velocity the water vapor or moisture content of process air transferred to the bed. The transferred vapor gets condensed into the pores and capillaries of desiccant pellets. The condensation results in the release of heat and that in turn increases the surrounding air temperature. With progress in time the bed water content increases and the exit air temperature decreases and would attain temperature near to that of inlet air temperature. At 1 m/s the maximum rise in exit air temperature with respect to inlet air temperature is 4°C at process time of 630 s. At the end of two hours of process time the temperature difference between inlet air temperature and exit air temperature is 2°C. The increase in bed water content is about 11.58 g with respect to initial bed weight of 400 g. At 2 m/s the rise in exit air temperature with respect to inlet air temperature is 6°C at about process time of 550 s. At the end of two hours of process the exit air temperature is 1.6°C higher than inlet air temperature. The bed weight increases from 400 g to 416.8 g.
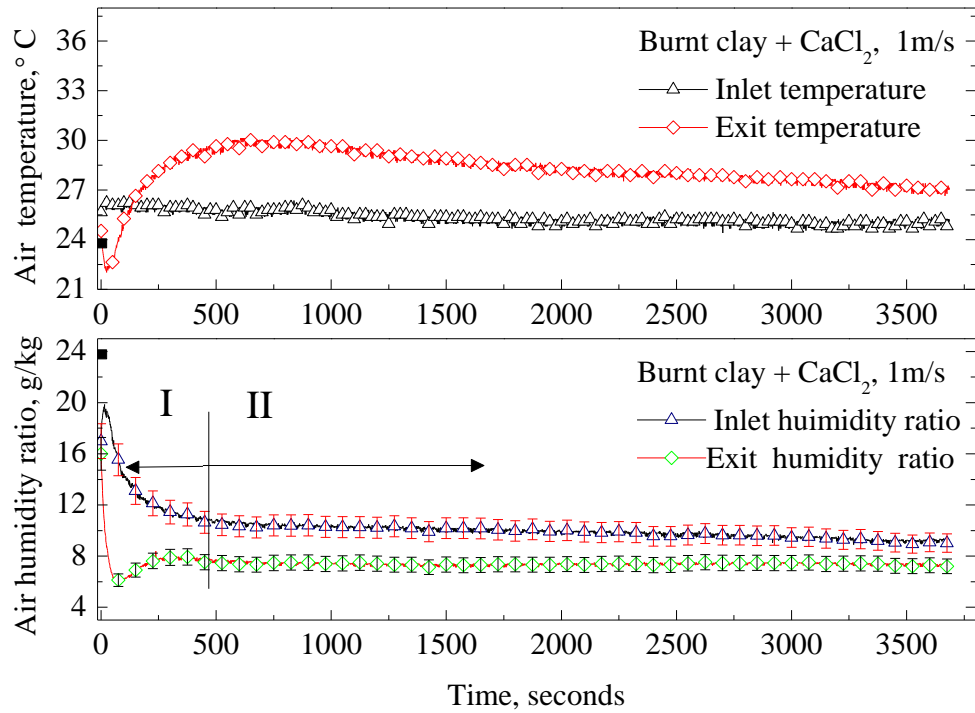
Fig. 5.1 Experimental time variation of exit air temperatures and humidity ratio for burnt clay with CaCl₂ impregnated packed vertical bed (1 m/s).
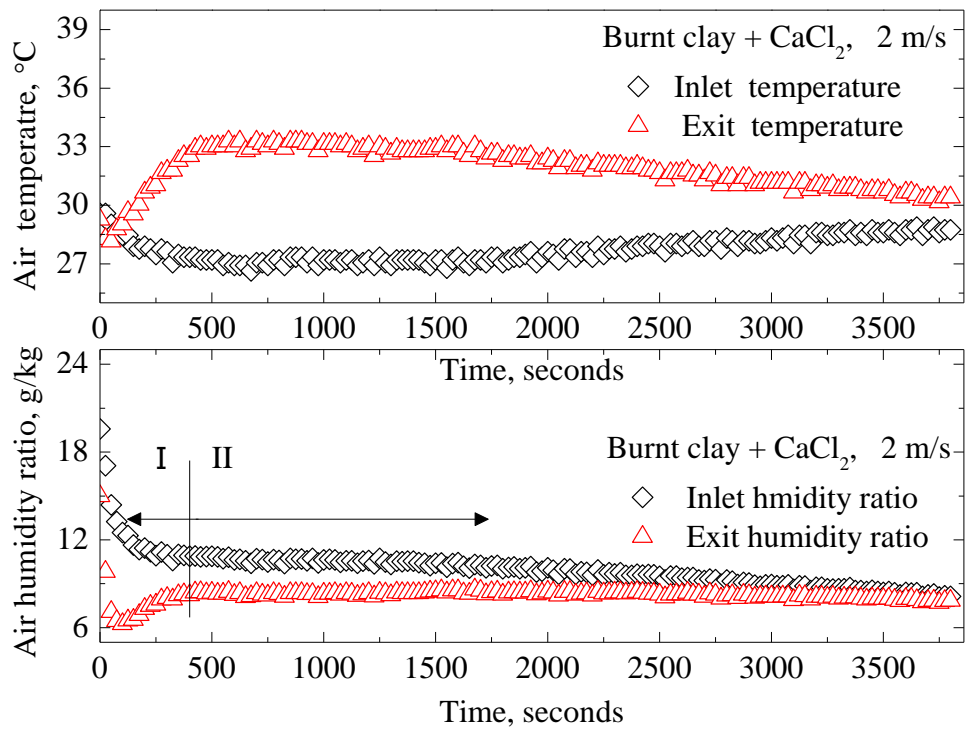
Fig. 5.2 Experimental time variation of exit air temperatures and humidity ratio for burnt clay with CaCl₂ impregnated packed vertical bed (2 m/s).

The experiments are conducted depend on outdoor conditions of the lab. The inlet air humidity ratio and temperature of air let into the bed vary as time progresses. In order to assess the heat and mass transfer performance during the dehumidification process, moisture removal from the process air is expressed as percentage of moisture reduction. As a result the evaluation of the dehumidification process for different variables like, inlet air velocity, and weight of the bed can be discussed irrespective or independent of the laboratory conditions. The reduction in moisture content of air is evaluated in percentage moisture reduction by the Eq. (5.2).

As shown in Fig.5.3 and Fig.5.4, the absolute humidity and temperature of air at bed inlet and exit are presented graphically in terms of the percentage change in moisture at every interval of time. During initial period of adsorption the moisture removal for 1 m/s increases from 8 to 61% and then decreases to a value of 28%. The decrease is due to variation in bed temperature, bed water content and $CaCl_2$ concentration during the process. During initial stages of process the bed is dry, and moisture uptake increases. The vapor pressure is low on the bed surface which results in transfer of moisture from air to desiccant surface. With progress in time the bed water content increases and bed temperature drops. Due to this vapor pressure on desiccant surface increases and moisture transfer potential from air to bed decreases. With progress in time the bed gets saturated and operates at constant temperature. With advancement in time the moisture removal rate tends to become steady, and ultimately it decreases the bed moisture uptake capacity. At 2 m/s the reduction in moisture content of air increases from 20 to 52% and then onwards decreases to a value of 18%. Irrespective of the velocity of airflow through the bed, the maximum reduction occurs at process time which is below 500 s. From then onwards adsorption process continues to proceed till the saturation of desiccant bed. The velocity of process air through the bed is varied from 0.5 m/s to 2 m/s in steps of 0.5 m/s. The dynamics of the process is observed for the full process time and for the initial period of 500 s.
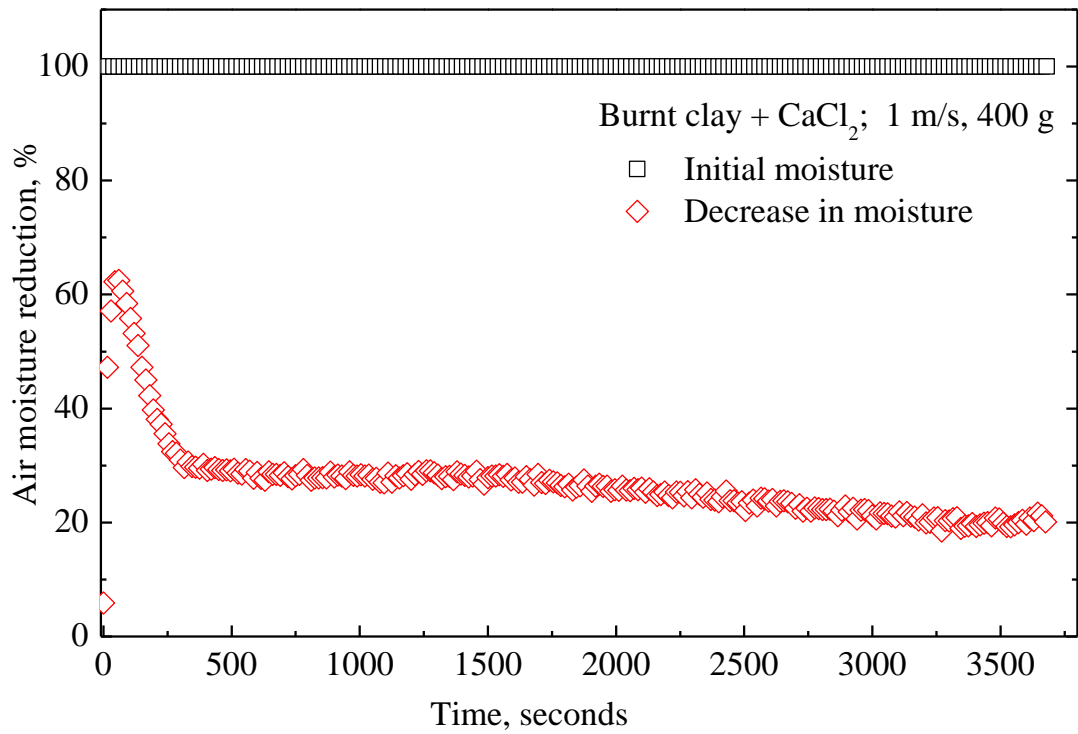
Fig.5.3 Experimental time variation of exit air moisture content relative to inlet air moisture content for vertical packed burnt clay $CaCl_2$ bed.
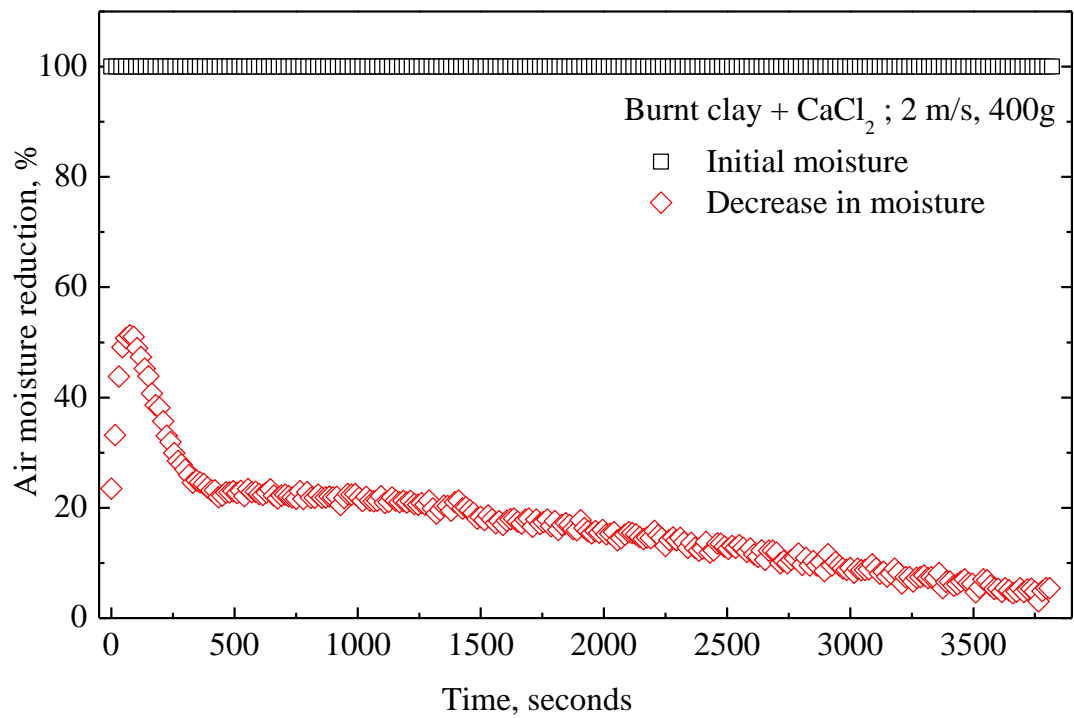
Fig.5.4 Experimental time variation of exit air moisture content relative to inlet air moisture content for vertical packed burnt clay $CaCl_2$ bed.

Figs.5.5 and 5.6 illustrates the adsorption behavior of burnt clay - $CaCl_2$ bed for the different velocity of process air. At lower velocity that is less than 1m/s, the bed is active enough to take moisture. The bed moisture uptake capacity increases gradually up to 300 s. From then onwards moisture uptake capacity decreases significantly (i e minute change from one time step to next time step) with progress in time. At velocities higher than 1 m/s, the beds are hyperactive within an initial time span of 150 s. From then onwards moisture transfer rate decreases sharply at 200 s. Between 200 and 400 s there is a gradual decrease in moisture uptake capacity. For the remaining period moisture removal capacity decreases and the desiccant beds continue to adsorb till saturation. The increase in bed water content with respect to an initial bed weight of 400 g is 7.09 g,11.58 g,14.34 g and 16.89 g at 0.5 m/s, 1 m/s, 1.5 m/s and 2 m/s respectively.
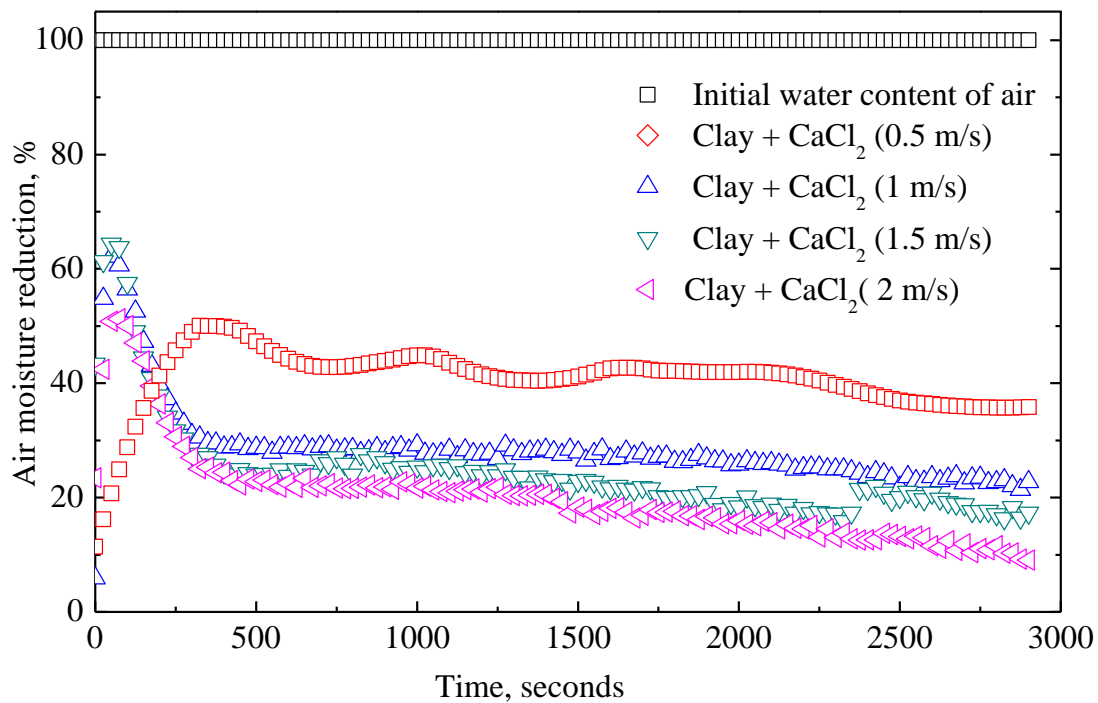
Fig.5. 5 Transient variation of process air moisture reduction at different velocities for burnt clay with $CaCl_2$ impregnated packed vertical bed.

116
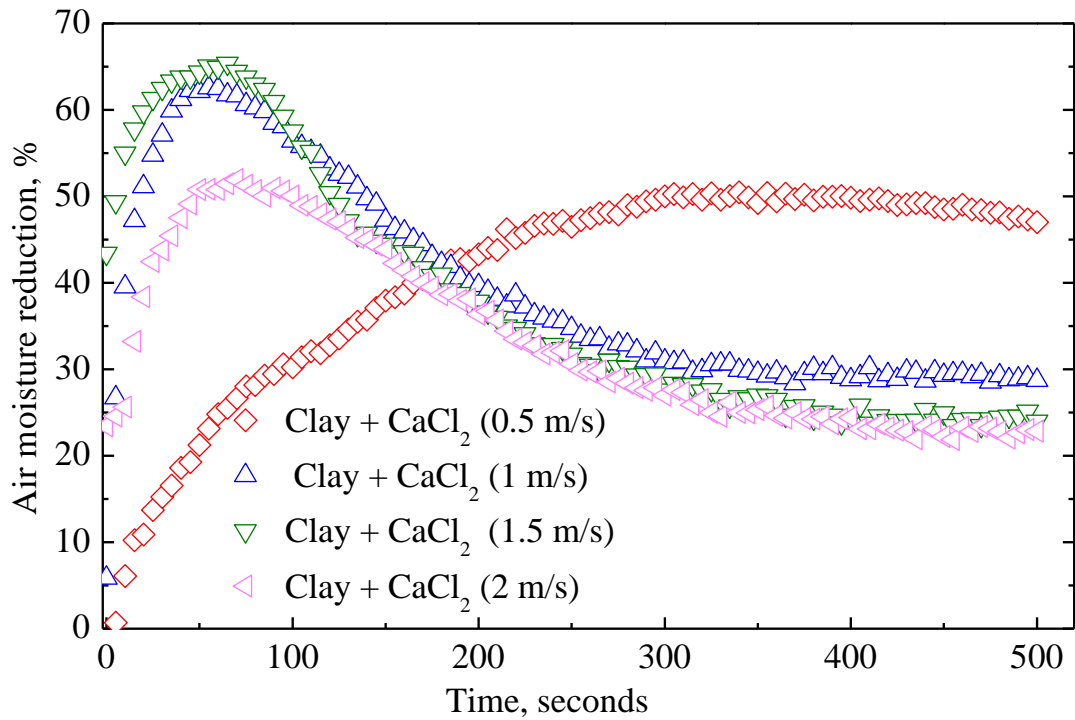
Fig. 5.6 Transient variation of process air moisture reduction at different velocities for burnt clay with $CaCl_2$ impregnated packed vertical bed and details during 0 - 500 s.

Fig. 5.7 and 5.8 show the influence of mass of bed on transient variation of change in moisture content of air for bed weights of 250, 500 and 750 g. The process air velocity to the bed was maintained at 0.5 m/s and 1 m/s. The composite desiccants used during these experiments had already undergone adsorption process. The inlet air humidity level was of the order of 18 to 25%. It is seen that increasing bed height increases the moisture removal rate. However the amount of moisture adsorbed by the bed is greatly influenced by the velocity of the process air. When the velocity of the air across the bed 0.5 m/s the amount of moisture adsorbed is considerably large when compared to the bed operated at process air velocity of 1m/s. The increase in residence time for process air, in turn, increases moisture removal rate. With increase in bed mass from 250 g to 750 g the desiccant bed height increases.

117
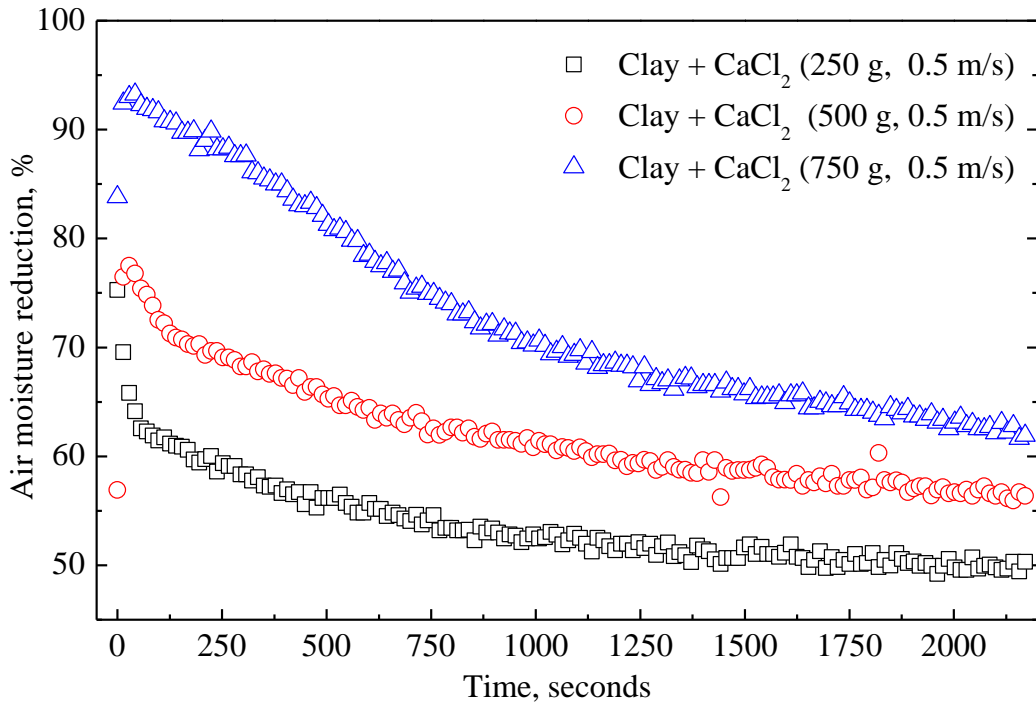
Fig. 5.7 Effect of the mass of desiccant on the moisture reduction in process air when the velocity of process air is 0.5 m/s.
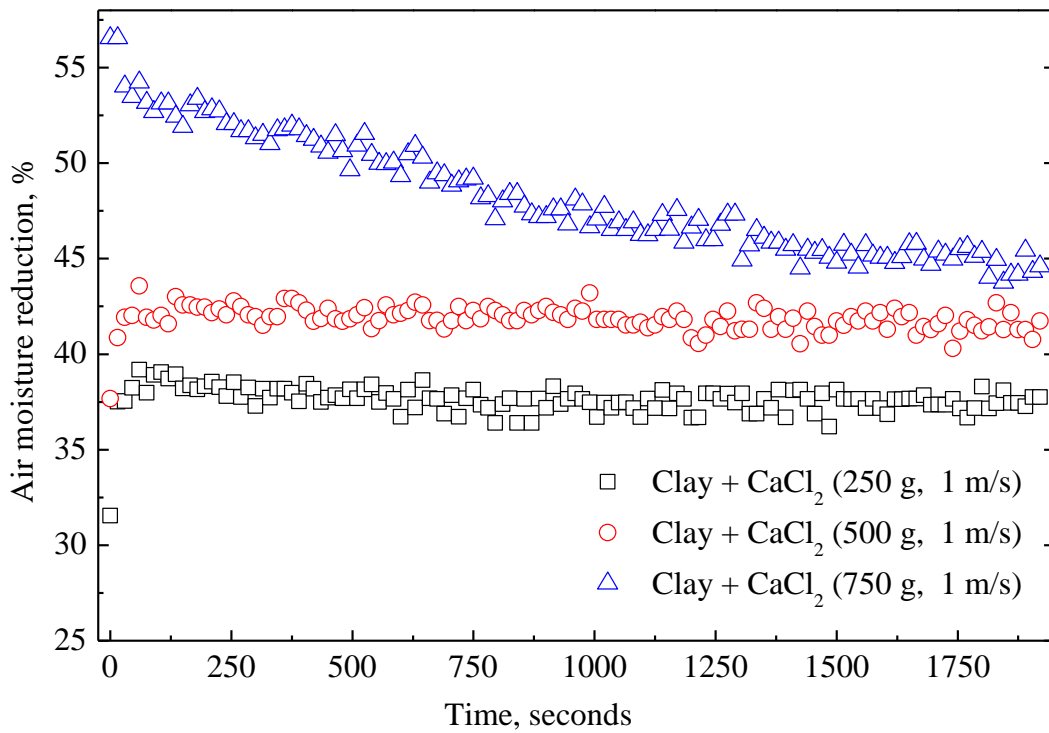
Fig. 5.8 Effect of the mass of desiccant on the moisture reduction in process air when velocity of process air is 1 m/s.

Due to this interfacial area available for mass and heat transfer is more. There is a rapid initial transfer of moisture from the air to the desiccant. With progress in time the composite desiccant beds with higher bed masses continue to operate in adsorption mode. At the end of process time the bed of lower mass saturates early as compared to higher bed masses.

5.4 ANALYSIS OF DEHUMIDIFICATION EXPERIMENTAL RESULTS FOR BURNT CLAY - HORSE DUNG - CaCl₂ DESICCANT BED

Fig.5.9 (a) and (b) shows the transient variation of change in the moisture content of air for burnt clay horse dung additives $CaCl_2$ composite desiccant beds. The various experimental parameters are similar to that described for burnt clay $CaCl_2$ desiccant beds. However, when the velocity of process air at inlet of bed is 0.5 m/s, 250 s of adsorption the bed with 750 g is more active compared to the beds of 500 g and 250 g. Beyond 250 s the desiccant beds of 750 g and 500 g have more or less the same adsorption capacity.
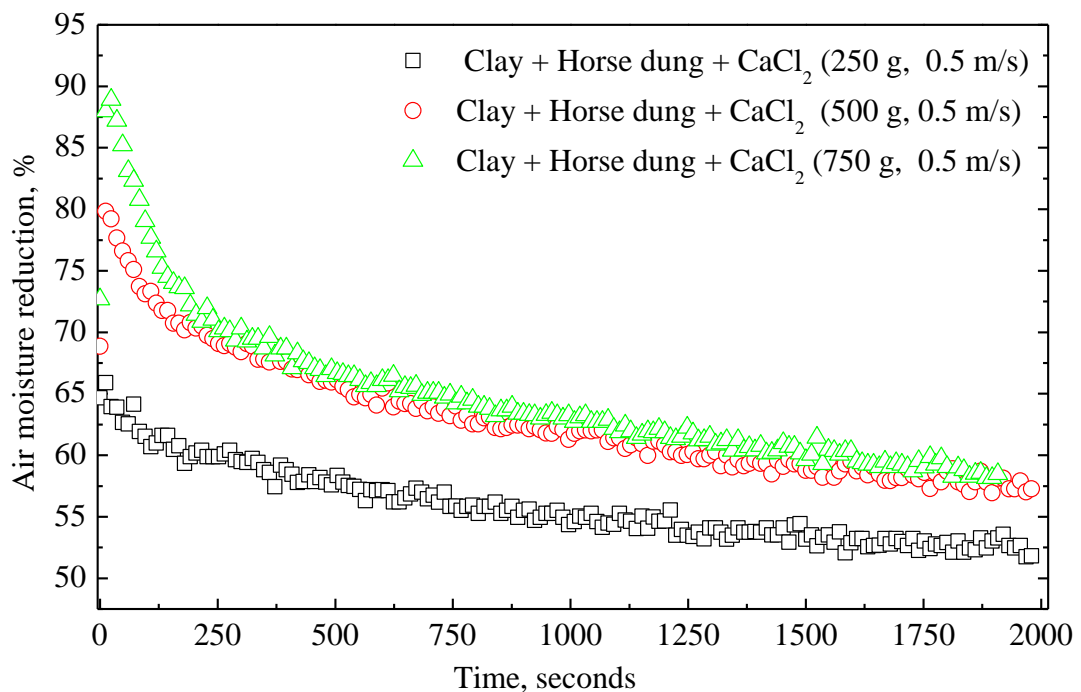
Fig. 5.9 (a) Transient variation of reduction in moisture content for clay - horse dung- CaCl₂ bed at 0.5 m/s.

119
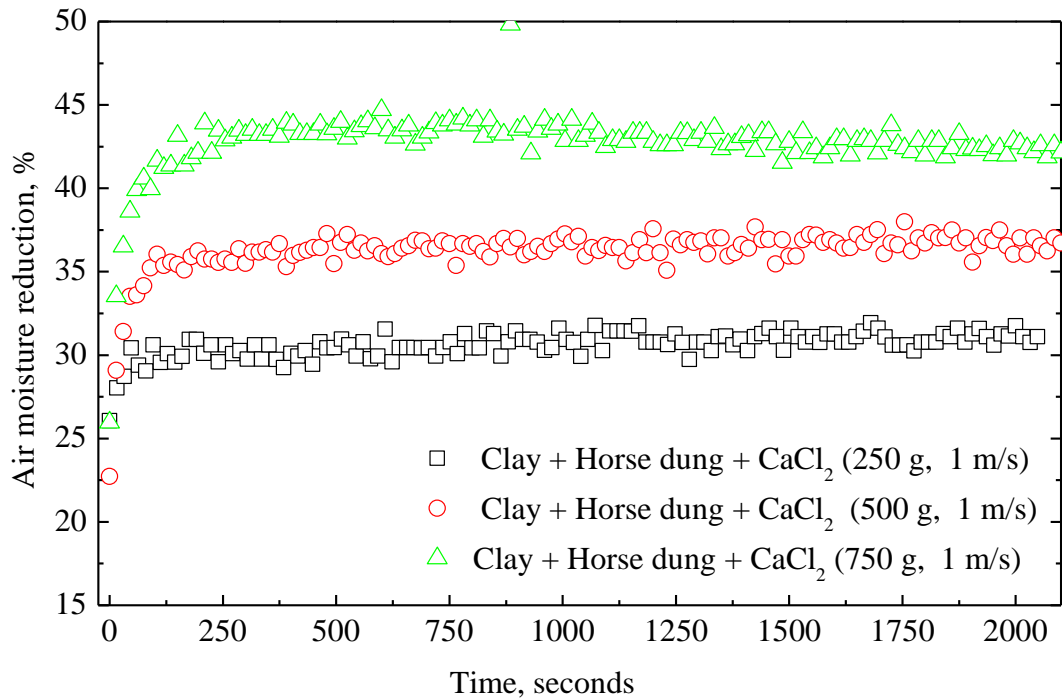
Fig. 5.9 (b) Transient variation of reduction in moisture content for clay - horse dung- CaCl$_2$ bed at 1 m/s.

Overall the characteristics of adsorption curves are similar to the adsorption characteristics of burnt clay CaCl$_2$ desiccant beds. At the lower velocity of 0.5 m/s and for the clay-horse dung desiccant bed masses of 250 g, 500 g and 750 g the exit air behavior for moisture reduction proceeds in falling rate period (downward slope). With the end of process time the capability of beds to adsorb reaches to its minimum value. At 1 m/s the trend for process air moisture reduction is heading in upward slope manner. With progress in time (above 250 s) the trend for moisture reduction scales in a steady-state manner.

5.5 ANALYSIS OF DEHUMIDIFICATION EXPERIMENTAL RESULTS FOR BURNT CLAY - SAW DUST - CaCl$_2$ DESICCANT BED

Fig.5.10 (a) and (b) shows the transient behavior of the burnt clay - sawdust - CaCl$_2$ desiccant bed. As shown Fig.5.10 (a), the desiccant bed of 500 g weight shows considerable increase in dehumidification of process air as compared to 250 and 750 g beds.

120
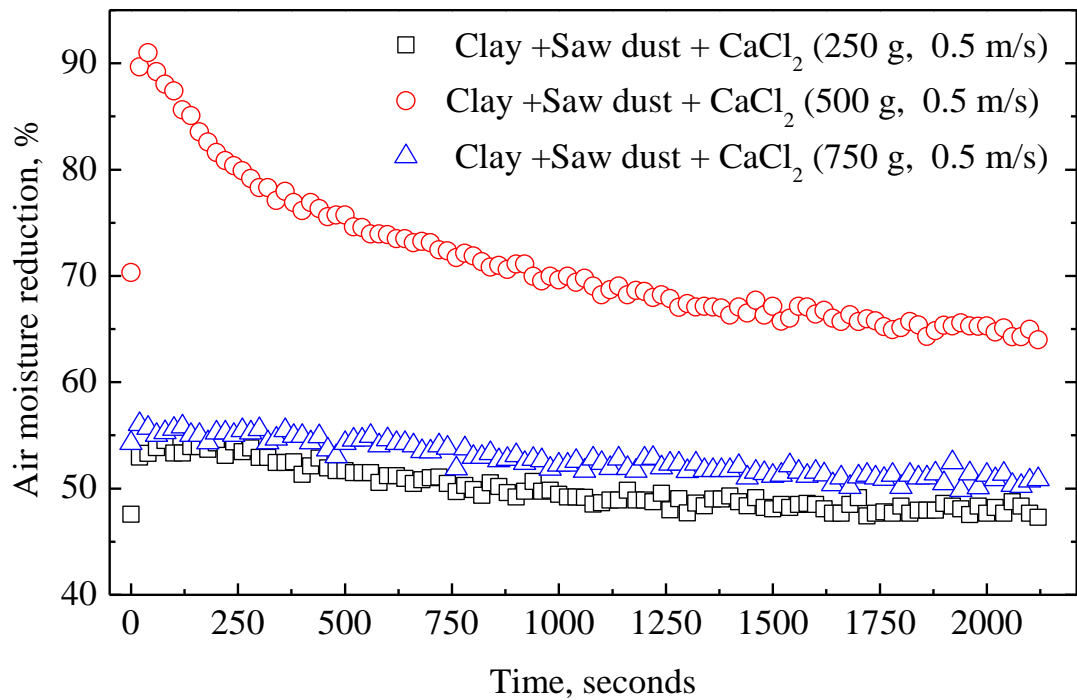
Fig. 5.10 (a) Transient variation of reduction in moisture content for clay - sawdust - $CaCl_2$ bed at 0.5 m/s.
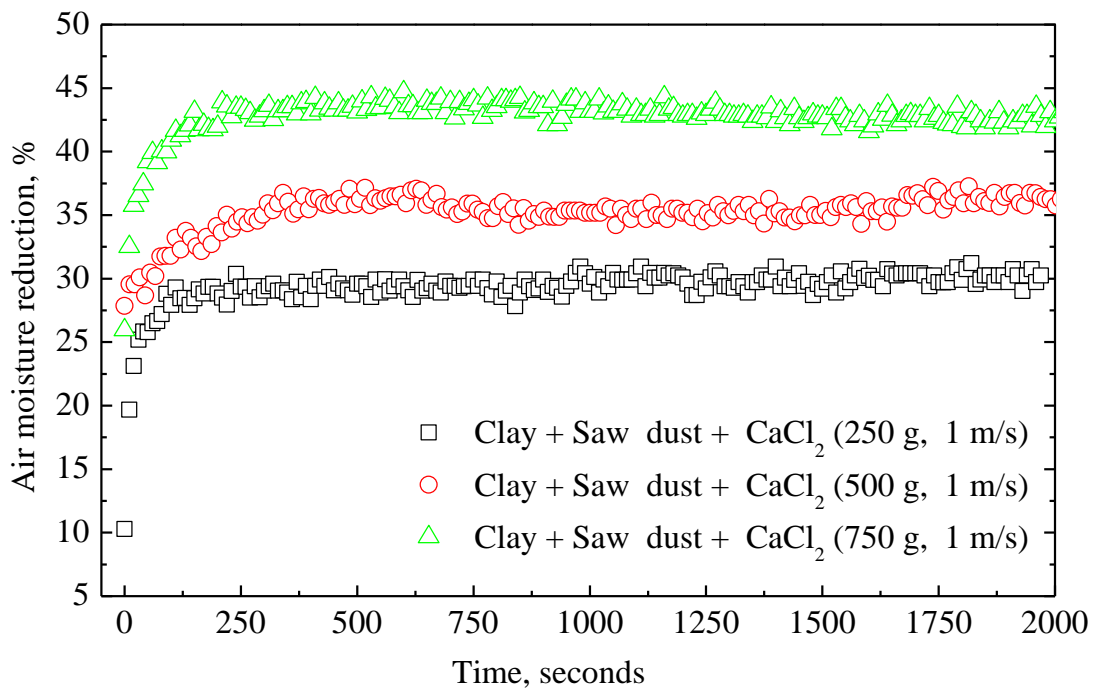
Fig. 5.10 (b) Transient variation of reduction in moisture content for clay - sawdust - $CaCl_2$ bed at 1 m/s.

121

This is contrasted when compared to burnt clay - $CaCl_2$ and burnt clay - horse dung - $CaCl_2$ beds. Apart from the beds of 250 g and 750 g have same capacity of moisture adsorption. Fig. 5.10 (b) shows that with increase in mass of bed, increases the surface area increases which in turn maximizes the moisture removal capacity. When the velocity of process air through the bed is lower, the absorptivity of bed is high as compared to bed through which velocity of air is high.

5.6 ANALYSIS OF DEHUMIDIFICATION EXPERIMENTAL RESULTS FOR BURNT CLAY - ADDITIVES - $CaCl_2$ DESICCANT BED

Effect of additives like sawdust and horse dung to the transported clay for dehumidification potentiality is examined. Fig.5.11 presents the adsorptive behavior of nearly new clay additives composite desiccant beds subjected to higher humidity levels.
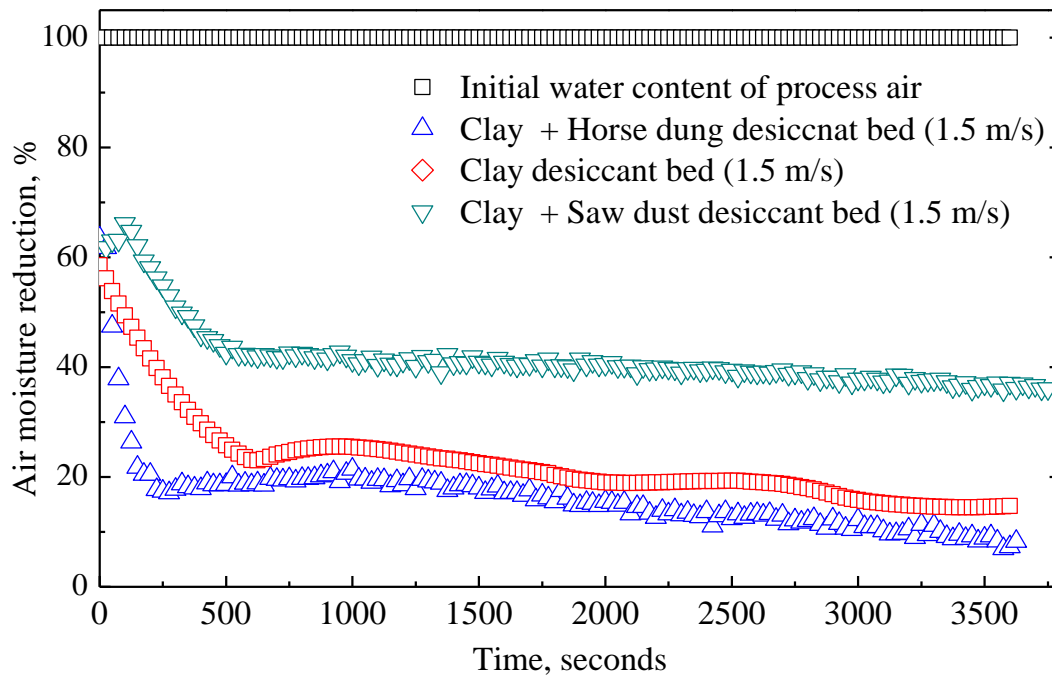
Fig. 5.11 Transient variation of moisture reduction from process air in composite desiccant packed vertical clay and clay - additives composite desiccant beds.

Fig.5.12 presents the details of the transients of during the initial stages, 0 to 250 s, of the adsorption process. It is clear that the adsorption process is highly dependent on the composition of the desiccant pellet. The beds are more or less equally active to

take moisture from process air during initial time period of 0 to 250 s. The increase in bed water content with respect to initial bed weight of 400 g are 13.72 g, 14.34 g and 15.12 g for clay, clay horse dung and clay sawdust additives composite desiccant beds.
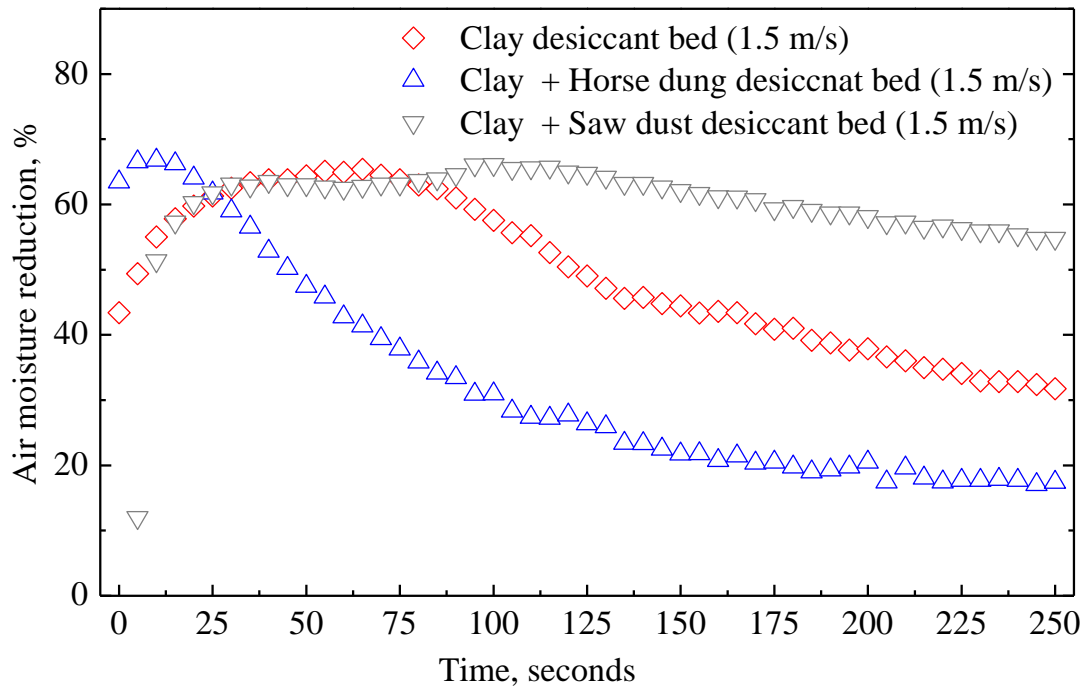
Fig. 5.12 Transient variation of moisture reduction from process air in composite desiccant packed vertical clay and clay - additives composite desiccant beds.

In these experimental runs, three bed with mass of desiccant as 250, 500 and 750 g are considered. The velocities of inlet air to the bed are 0.5 m/s and 1 m/s. The desiccant samples introduced into the vertical column are those who have been already subjected to few numbers of adsorption process and subsequently regenerated. Experiments are conducted at the process air humidity ranging from 18 to 25%. From the Fig.5.13 (a), (c) and (e) that for low velocity of 0.5m/s each of the composite desiccant perform differently depending on the mass of the bed. For example the performance of 750 g mass of burnt clay $CaCl_2$ is much better compared to burnt clay horse dung $CaCl_2$ and burnt clay sawdust $CaCl_2$ composite desiccant beds. However at higher velocity as presented in Fig.5.13 (b), (d) and (f), moisture reduction from the process air is better for burnt clay $CaCl_2$ bed. The beds operating at lower velocity of

0.5 m/s shows higher moisture reduction than beds operating at 1 m/s. As cooling effect predominates at higher velocities the vapor pressure difference between the air surrounding the desiccant and desiccant surface decreases significantly. Because of this the bed moisture intake capacity is low at higher velocities. Higher pore volume and moderate surface area for burnt clay desiccant and the retention of $CaCl_2$ into pores results in higher dehumidification rates as compared to other two desiccant beds. At drying temperature of 500°C the addition of horse dung to transported clay increases the surface area with moderate pore volume. The clay - $CaCl_2$ with horse dung additive shows similar bed behavior as that of clay - $CaCl_2$ desiccant bed. The addition of sawdust neither increases the pore volume nor the surface area. The burnt clay-saw dust with $CaCl_2$ also results in dehumidification of process air.

However, experimental runs of clay - $CaCl_2$ bed reveal higher dehumidification capacity at every interval of time. This is evident from the fact that the visual examination of clay - $CaCl_2$ desiccant pellets shows deteriorated surface as shown in Fig .5.14, which is exposed to flow of process air. The surface deterioration and descaling are due to increased number of cycles of use. However the photograph (Fig.5.15) of burnt clay - horse dung - $CaCl_2$ composite desiccant pellets retained their size and shape as compared to other two desiccant pellets. Figure 5.16 reveals that with increased use the surface of clay - sawdust - $CaCl_2$ desiccant pellets surface gets powdered as compared to clay - horse dung - $CaCl_2$ desiccant

124
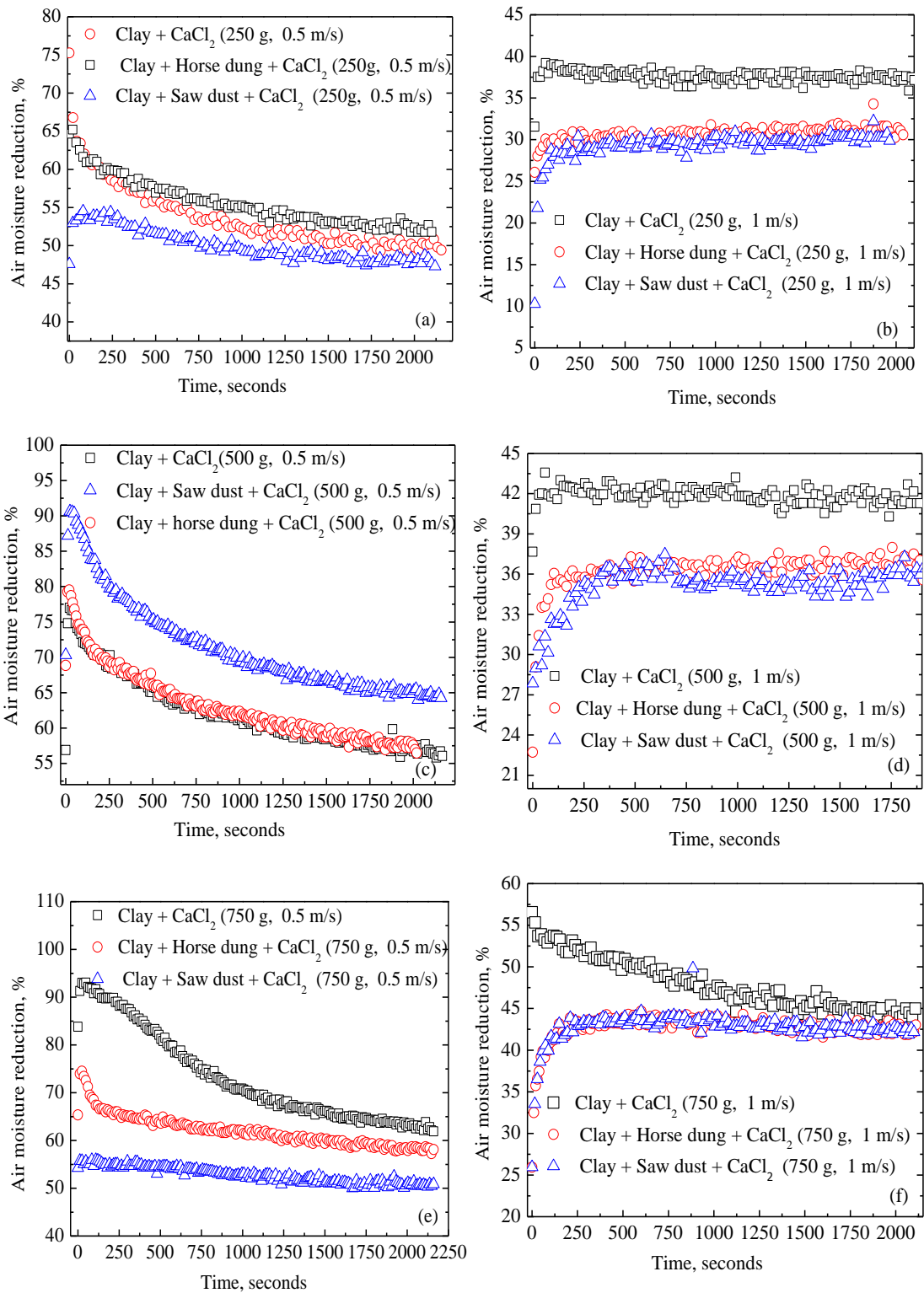
Fig. 5.13 Effect of the velocity of process air on air moisture reduction for burnt clay -additives - CaCl$_2$ composite desiccant beds.

Fig.5. 14 Photograph showing the size and shapes retained by desiccants with increased use for burnt clay - CaCl$_2$.
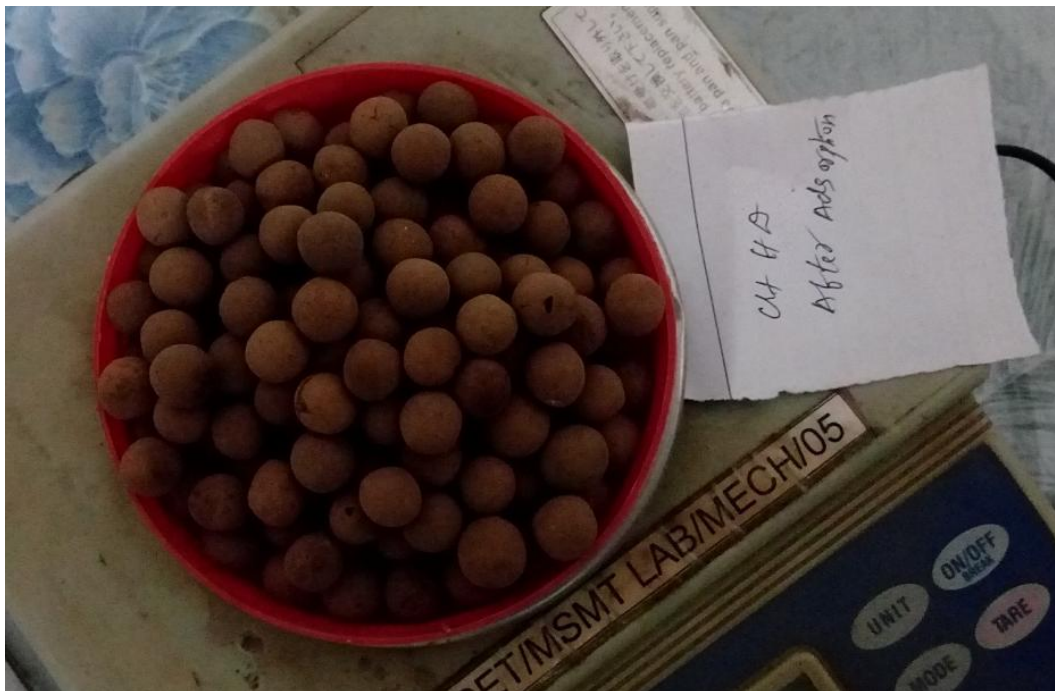
Fig.5.15 Photograph showing the size and shapes retained by desiccants with increased use for burnt clay - horse dung - CaCl$_2$.

Fig. 5.16 Photograph showing the size and shapes retained by desiccants with increased use for burnt clay - sawdust - CaCl₂.

5.7 COMPARISON OF VERTICAL PACKED AND FLUIDIZED BED OF BURNT CLAY - ADDITIVES - CaCl₂ DESICCANTS IN ADSORPTION

The test results of the packed bed and fluidized bed systems in adsorption are presented in Table 5.2. The effect of inlet air velocity to the bed, humidity ratio, temperature, and mass of bed on exit air humidity ratio and temperature are shown in Figs. 5.17 to 5.21.

Table 5.2 Experimental observations for packed and fluidized beds in the adsorption process.

Run	Composite desiccant bed	Process	Mass of bed (g)	Velocity (m/s)	Pressure drop (kPa)	Water content	Atmospheric humidity ratio and temperature	
1	Clay – $CaCl_2$ (packed)	Ads	300	2	0.35	2.18% (increase)	9.83 g/kg	24.5°C
1a	Clay – $CaCl_2$ (fluidized)	Ads	300	2	1.09	3.40% (increase)		
2	Clay - horse dung - $CaCl_2$ (packed)	Ads	200	1.5	0.39	2.6% (increase)	9.55 g/kg	25°C
2a	Clay - horse dung - $CaCl_2$ (fluidized)	Ads	200	1.5	0.64	4.00% (increase)		
3	Clay - horse dung - $CaCl_2$ (packed)	Ads	300	2	0.32	2.4% (increase)	10.92 g/kg	21.3°C
3a	Clay – horse dung - $CaCl_2$ (fluidized)	Ads	300	2	0.94	2.93% (increase)		
4	Clay - saw dust - $CaCl_2$ (packed)	Ads	200	1.5	0.13	2.42 % (increase)	10.76 g/kg	21.0°C
4a	Clay - saw dust - $CaCl_2$ (fluidized)	Ads	200	1.5	0.64	4.46% (increase)		
5	Clay - saw dust – $CaCl_2$ (packed)	Ads	300	2	0.30	1.98% (increase)	9.74 g/kg	24.8°C
5a	Clay - saw dust - $CaCl_2$ (fluidized)	Ads	300	2	1.12	2.22% (increase)		

The experimental time variation of exit air humidity ratio and temperature through a packed and fluidized bed of burnt clay - $CaCl_2$ desiccant pellets are shown in Fig 5.17 (a) and (b). In case of fluidized bed the amount of air passing through the bed per unit time increases. Due to fluidization the surface area available for transfer of moisture is more and hence results in increased moisture removal capacity of the bed. At the end of 7000 s, both packed and fluidized beds are capable of water vapor adsorption. This is evident from the larger difference between the inlet and exit air humidity ratios. The rise in temperature of air is marginally higher in case of fluidized bed.

In case of the packed bed, the heat generated due to adsorption gets stored in the desiccant pellets whereas in fluidized bed the adsorption heat is easily transferred to the process air. The heat of adsorption increases the temperature of bed and exit air temperature. For the same cross-sectional area of the bed, the force required to maintain the pellets in the fluidized state is higher as compared to bed in static condition. Hence higher pressure drop is necessary to overcome the higher gravity forces in fluidization.

Experimental results for the composite desiccant bed of clay-horse dung - $CaCl_2$ in packed and fluidized states are shown in Figs.5.18 (a, b) and 5.19 (a, b). The results for exit air humidity ratio and temperature shows similar trends as that of burnt clay - $CaCl_2$ composite desiccant beds.

It can be observed that the instantaneous rise in temperature of the exit air during the initial stage of the process is less for the bed of horse dung composite desiccant. This is due to the addition of horse dung namely, 20% by weight, which increases the thermal capacity of bed. For the same mass of bed and velocity of air, the maximum decrease in bed exit air temperature with respect to inlet air temperature is about 18% as compared to 14% in case of burnt clay - $CaCl_2$ desiccant bed. However, the maximum moisture removal rate in case of burnt clay-horse dung - $CaCl_2$ is 45% as compared to 47% while using clay - $CaCl_2$ desiccant beds. Comparison of packed and fluidized beds for exit air humidity ratio reveals that shortly after the process, the exit air moisture content drops to a minimum and then increases toward the inlet air humidity ratio.

Fig. 5.17 (a) Transient variation of exit air humidity ratio corresponding to run 1 and run 1a.

Fig. 5.17 (b) Transient variation of exit air temperature corresponding to run 1 and run 1a.

Fig. 5.18 (a) Transient variation of bed exit air humidity ratio corresponding to run 2 and run 2a.

Fig. 5.18 (b) Transient variation of bed exit air temperature corresponding to run 2 and run 2a.

131

Fig. 5.19 (a) Transient variation of exit air humidity ratio corresponding to run 3 and run 3a.

Fig. 5.19 (b) Transient variation of exit air temperature corresponding to run 3 and run 3a.

132

With progress in time, the transfer of moisture from air to the bed decreases and adsorption rate is almost constant. However even after the processing time of 3000 s and 6000 s the moisture adsorbing capacity of the bed progresses at very slow rate as compared to the initial stages of process.

The plots of temperatures indicate temperature rise in the fluidized bed is much higher as compared to packed bed. The inclusion of horse dung additive to clay increases the heat capacity of the bed. As a result the exit air temperature is lower with respect to inlet air temperature. The transient variation of exit air humidity ratio and temperature for burnt clay - sawdust - $CaCl_2$ packed and fluidized beds are depicted in Figs. 5.20 (a) and (b), Figs 5.21 (a) and (b). Similar trends for moisture reduction and temperature are observed as that of runs corresponding to clay - $CaCl_2$ and clay - horse dung - $CaCl_2$ beds. In test run4 the maximum reduction in moisture occurs at process time below 500s. However in other test run5, the maximum reduction in moisture content occurs when process time is above 500 s. The maximum difference between inlet and exit air humidity ratio is observed for beds of 300 g desiccant pellets. At the end of process time of 4000 and 3000 s the exit air humidity ratio values tend towards the inlet air humidity ratio. Results reveal that even after the end of process time, the beds are capable of taking moisture at lower adsorption rates. The presence of sawdust additive in the composite desiccant causes gradual increase in exit air temperature with respect to inlet air temperature.

Fig. 5.20 (a) Transient variation of exit air humidity ratio corresponding to run 4 and run 4a.

Fig. 5.13 (b) Transient variation of exit air temperature corresponding to run 4 and run 4a.

Fig.5.21 (a) Transient variation of exit air humidity ratio corresponding to run 5 and run 5a.

Fig.5.21 (b) Transient variation of exit air temperature corresponding to run 5 and run 5a.

135

The maximum rise in exit air temperature in packed and fluidized beds is lower than the inlet air temperature. For the same mass of bed, the velocity of air being unchanged, the reduction in moisture content for clay with 20% sawdust and impregnated with $CaCl_2$ in fluidized condition is 45% as compared to 48% and 47% in burnt clay and burnt clay horse dung composite desiccant beds respectively. Due to higher thermal capacity of packed bed the exit air temperature is lower compared to the temperature of air exiting the fluidized beds. The addition of sawdust with clay induces marked temperature difference between bed inlet and exit air. For the same mass of bed and air velocity at inlet for fluidized bed, the maximum decrease in bed exit air temperature with respect to inlet air temperature is about 18% as compared to 15% and 21% in burnt clay - $CaCl_2$ and burnt clay - horse dung - $CaCl_2$ composite desiccant bed.

5.8 COMPARISON OF VERTICAL PACKED AND FLUIDIZED BED OF BURNT CLAY - ADDITIVES - $CaCl_2$ DESICCANTS IN DESORPTION.

Table 5.3 lists the parameters for different runs of experiments in desorption. The temperature of the air used for regeneration has a range of 48 to 55°C. Figs.5.22 to 5.28 compares the desorption process of all the three types of clay additives based composite desiccant pellets in packed and fluidized modes of process. Fluidized bed composed of clay impregnated $CaCl_2$ desiccant pellets show higher absorptivity and higher exit air temperatures as compared to packed bed of similar pellets, refer to Fig.5.22 (a) and (b).The fluidized bed rapidly transfers moisture to air. In between the time period of 500 to 750 s, the fluidized bed behavior changes from adsorption to desorption behavior and continues to operate until the end of process time.

136

Table 5.3 Experimental observations for packed and fluidized beds in the desorption process.

Run	Composite desiccant bed	Process	Mass of bed (g)	Velocity (m/s)	Pressure drop (kPa)	Water content	Ambient humidity ratio and temperature	
6	Clay –CaCl$_2$ (packed)	Des	200	1.5	0.09	1.9% (decrease)	9.39 g/kg	27°C
6a	Clay -CaCl$_2$ (fluidized)	Des	200	1.5	0.37	2.9% (decrease)		
7	Clay - Saw dust -CaCl$_2$ (packed)	Des	200	1.5	0.21	1.2% (decrease)	9.41g/kg	26.7°C
7a	Clay - Saw dust -CaCl$_2$ (fluidized)	Des	200	1.5	0.37	2.9% (decrease)		
8	Clay - Saw dust -CaCl$_2$ (packed)	Des	300	2	0.40	1.5% (decrease)	9.48 g/kg	28°C
8a	Clay - Saw dust -CaCl$_2$ (fluidized)	Des	300	2	1.05	1.8% (decrease)		
9	Clay -Horse dung- CaCl$_2$ (packed)	Des	200	1.5	0.09	0.5% (decrease)	10.09g/kg	24.8°C
9a	Clay -Horse dung- CaCl$_2$ (fluidized)	Des	200	1.5	0.40	1.0% (decrease)		
10	Clay -Horse dung- CaCl$_2$ (packed)	Des	300	1.5	0.11	1.3% (decrease)	12.25g/kg	29°C
10a	Clay -Horse dung- CaCl$_2$ (fluidized)	Des	300	1.5	0.51	2.0% (decrease)		
11	Clay -Horse dung- CaCl$_2$ (packed)	Des	300	2	0.38	1.8% (decrease)	9.79 g/kg	29°C
11a	Clay -Horse dung- CaCl$_2$ (fluidized)	Des	300	2	1.82	2.9% (decrease)		
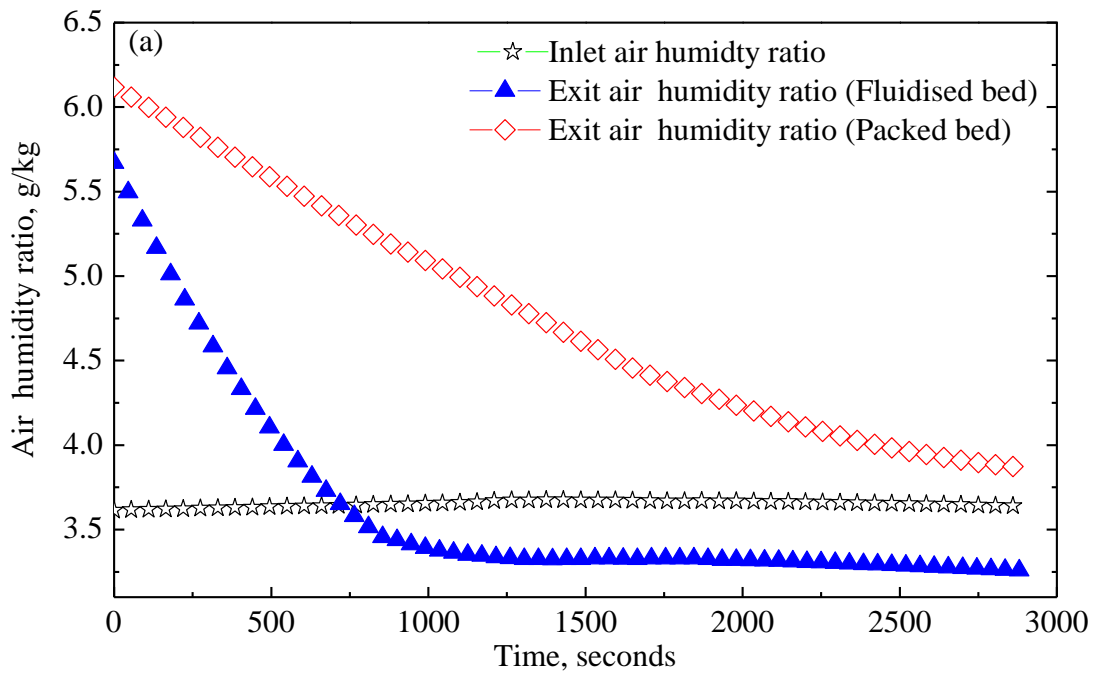
Fig. 5.22 (a) Transient variation of exit air humidity ratio corresponding to run 6 and run 6a.
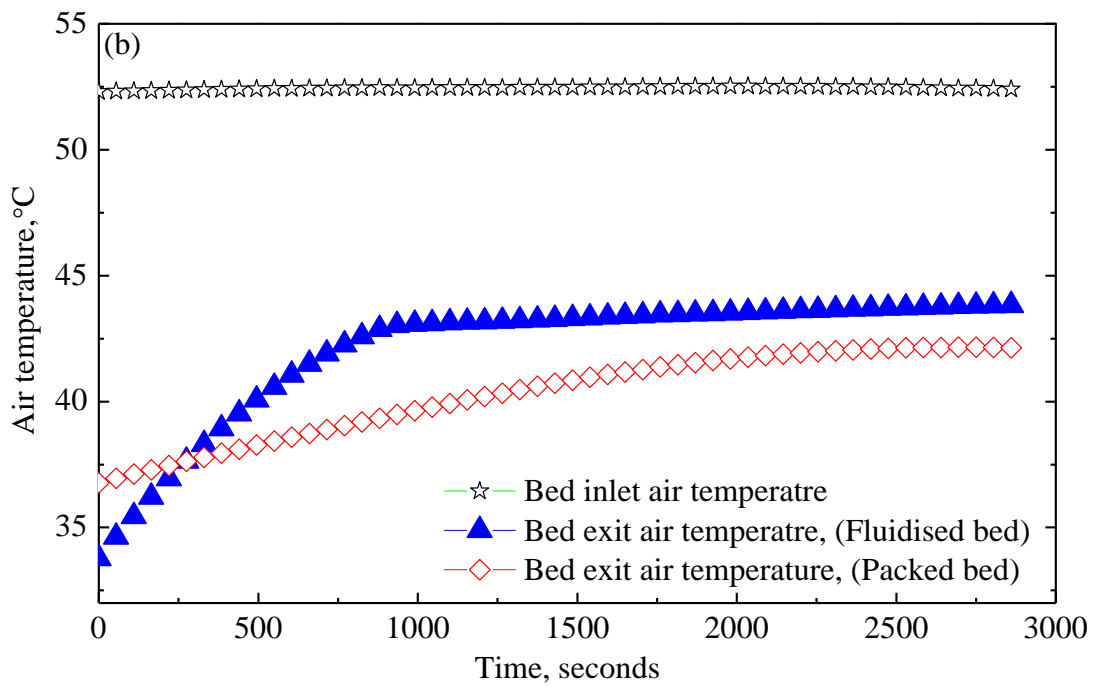
Fig. 5.22 (b) Transient variation of exit air temperature corresponding to run 6 and run 6a.

138

Up to 750 s, the exit air humidity ratio in case of fluidized bed is higher than inlet air humidity ratio, and beyond 750 s the exit air humidity ratio continues to decrease and is below inlet air humidity ratio. The process air temperature leaving the bed remains constant till the end of process. It seems that after 750 s, the bed takes moisture from the air at constant temperature. Compared to moving bed, packed bed steadily desorbs its water content. At the end of process the difference between inlet air humidity ratio and exit air humidity ratio seems to increase. As the desiccant pellets in fluidized state are dried at a faster rate, the exit air temperature increases up to 750 s, and after that the process air temperature attains steady-state, see Fig.5.22 (b). At the end of process the rise in exit air temperature for both static and fluidized beds are well below the bed inlet air temperature. This reveals the requirement of lower temperature regeneration air than the supplied one during the experiment.

The dynamics of the clay-saw dust composite desiccant bed to desorb water is presented in Fig 5.23 (a) and (b). The transient variation of exit air humidity ratio and temperatures for packed and fluidized clay - sawdust - $CaCl_2$ beds in desorption reveals similar trends. For the bed inlet air temperature of 49.3°C and humidity ratio of 3.56 g/kg, fluidized and packed beds continue to operate in the desorption mode. At the end of process the exit air humidity ratio nears the inlet air humidity ratio; however the rise in exit air temperature is lower than the bed inlet air temperature. At the end of process, the mass of packed bed decreases from 200 g to 197.85 g, and fluidized bed mass decreases to 194.3 g. Consider the time variation of exit air humidity ratio and temperatures for burnt clay - sawdust - $CaCl_2$ pellets packed and fluidized beds in desorption as shown in Fig.5.24 and 5.25. For the bed inlet air temperature of 51.93°C and humidity ratio of 3.63 g/kg, fluidized bed shows higher desorption rate and higher exit air temperatures as compared to packed bed. Before the processing time of 500 s, the fluidized bed pellets are completely dried, and from 500 s onwards the bed operates in adsorption mode. However the packed bed completely dried at about 1000 s. The temperature profiles demonstrate that it is possible to use lower temperature regeneration air as compared to present 51.3°C. The mass of the packed bed decreases from 300 g to 297.6 g and mass of fluidized bed decreases to 295.6 g at the end of the process
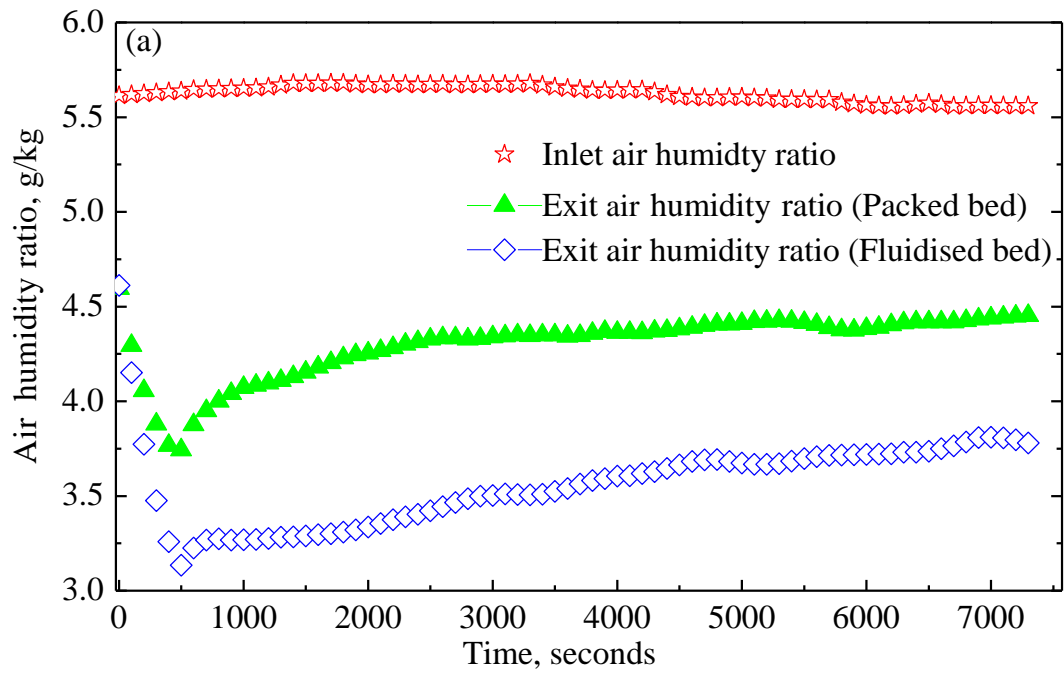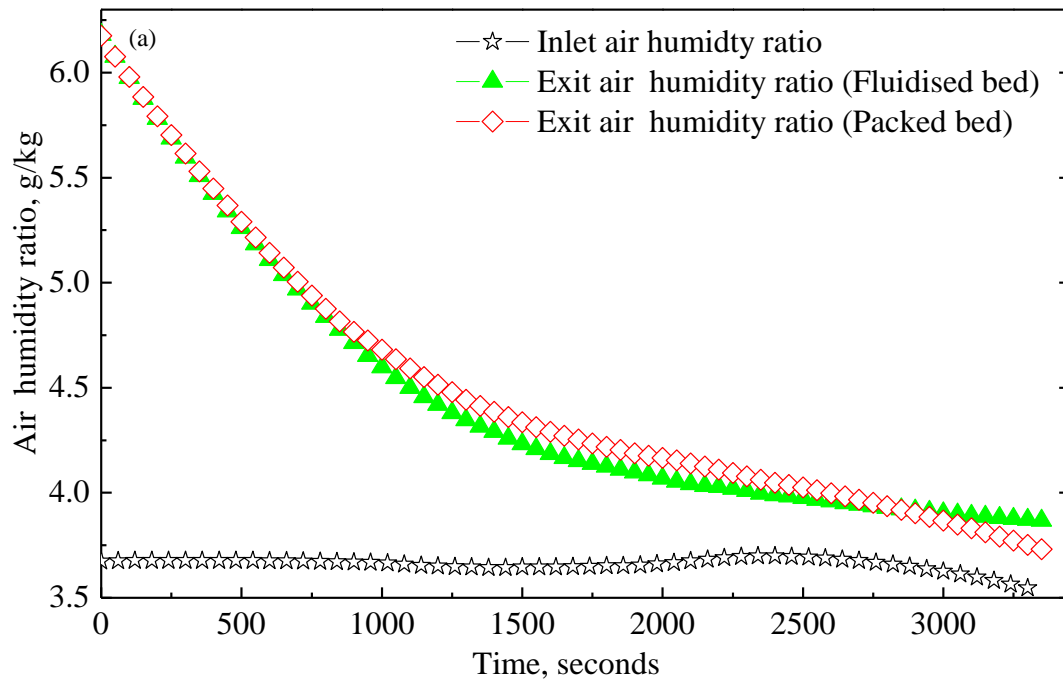
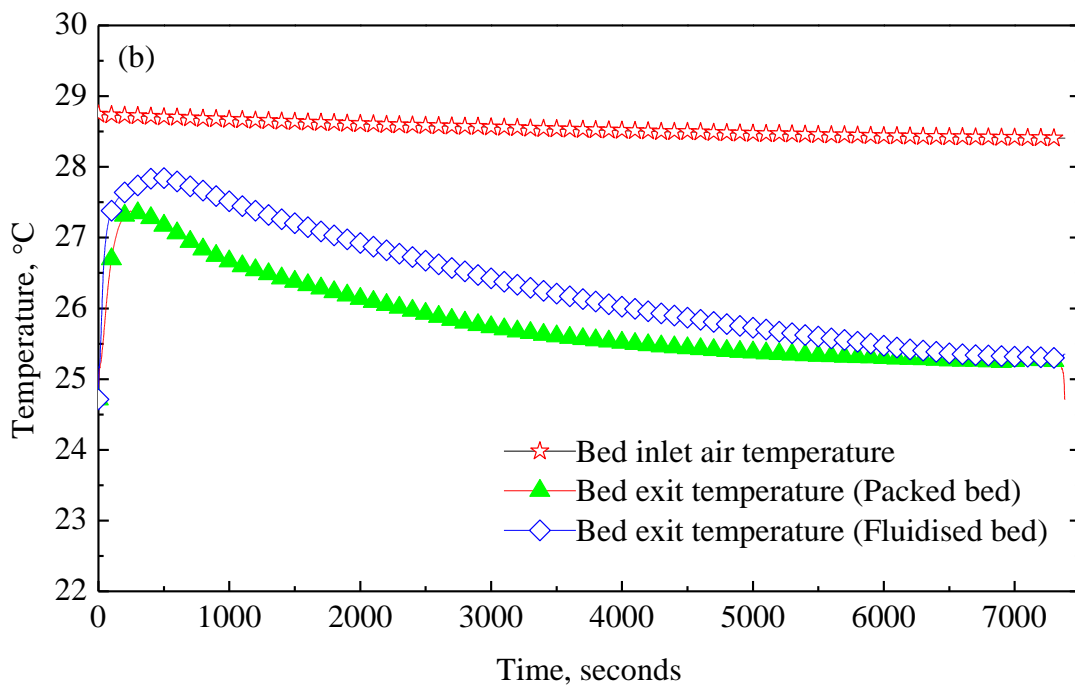**Fig. 5.23 (a)** Transient variation of exit air humidity ratio corresponding to run 7 and run 7a.
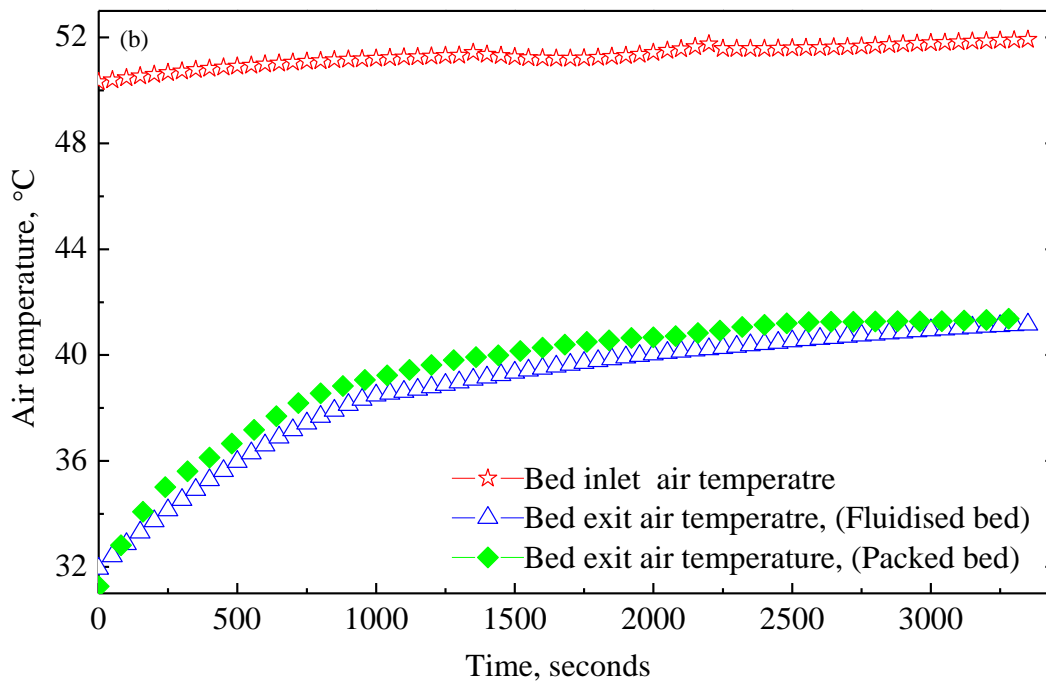
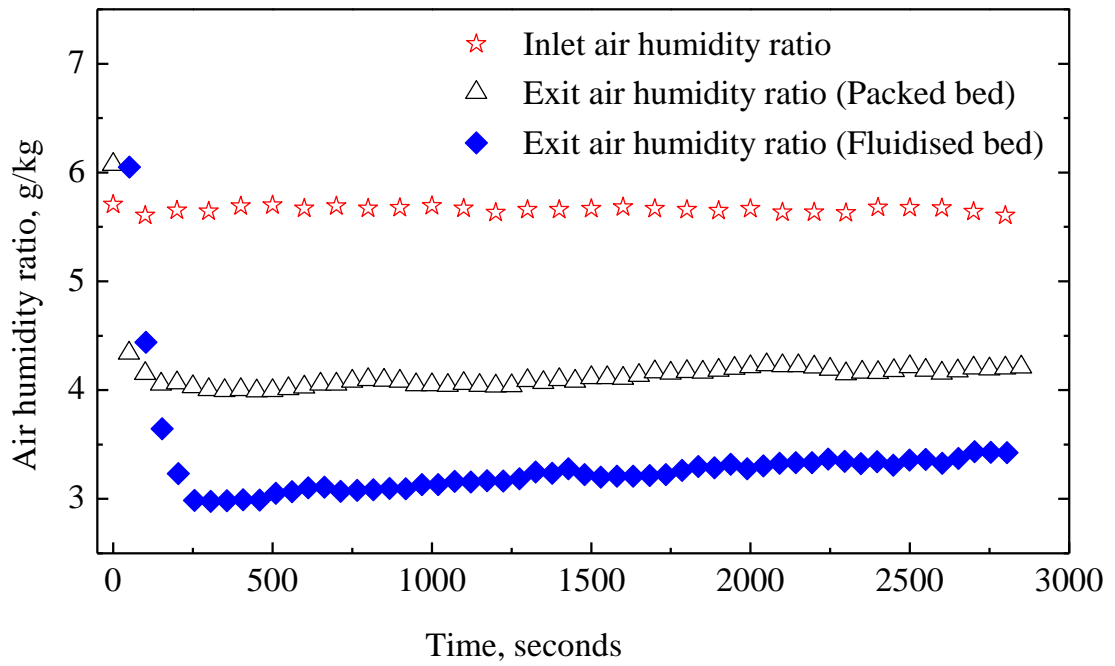**Fig. 5.23 (b)** Transient variation of exit air temperature corresponding to run 7 and run 7a.
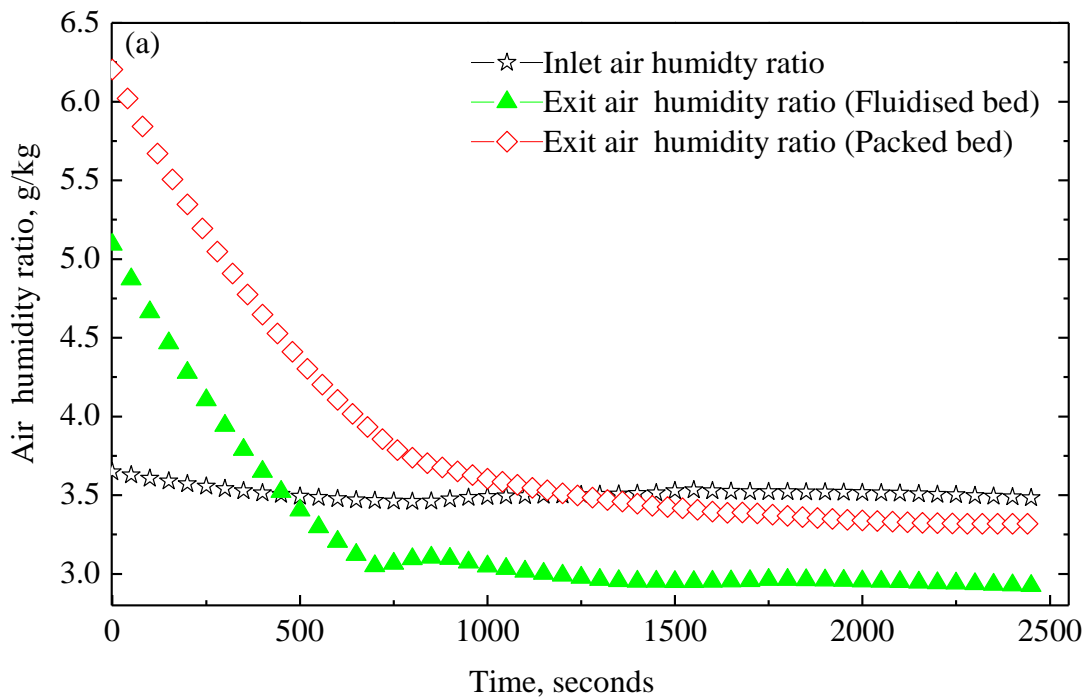
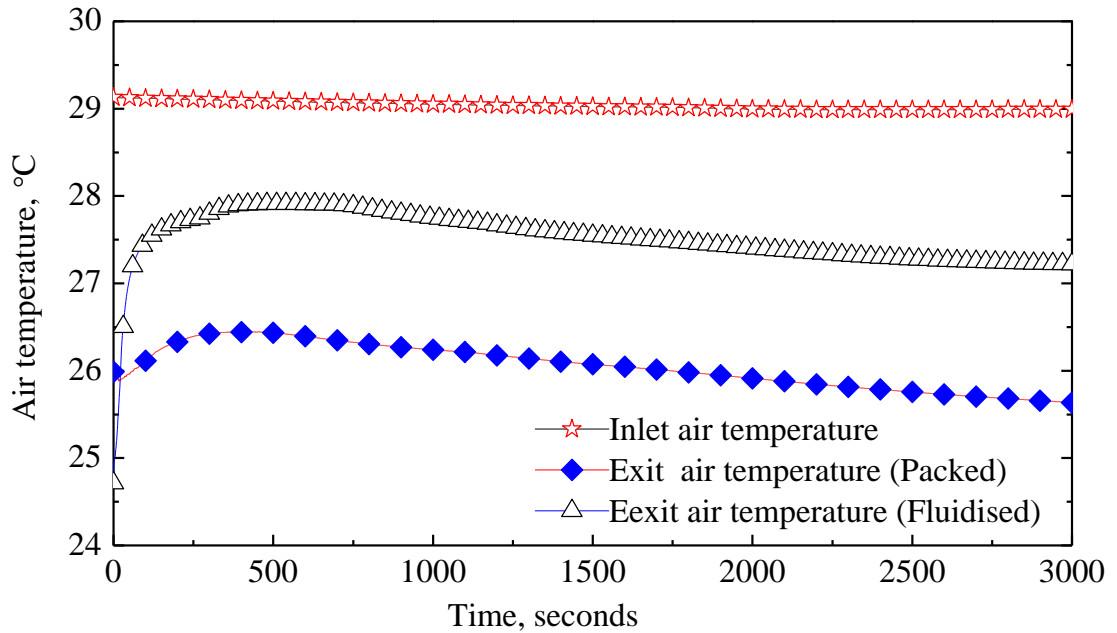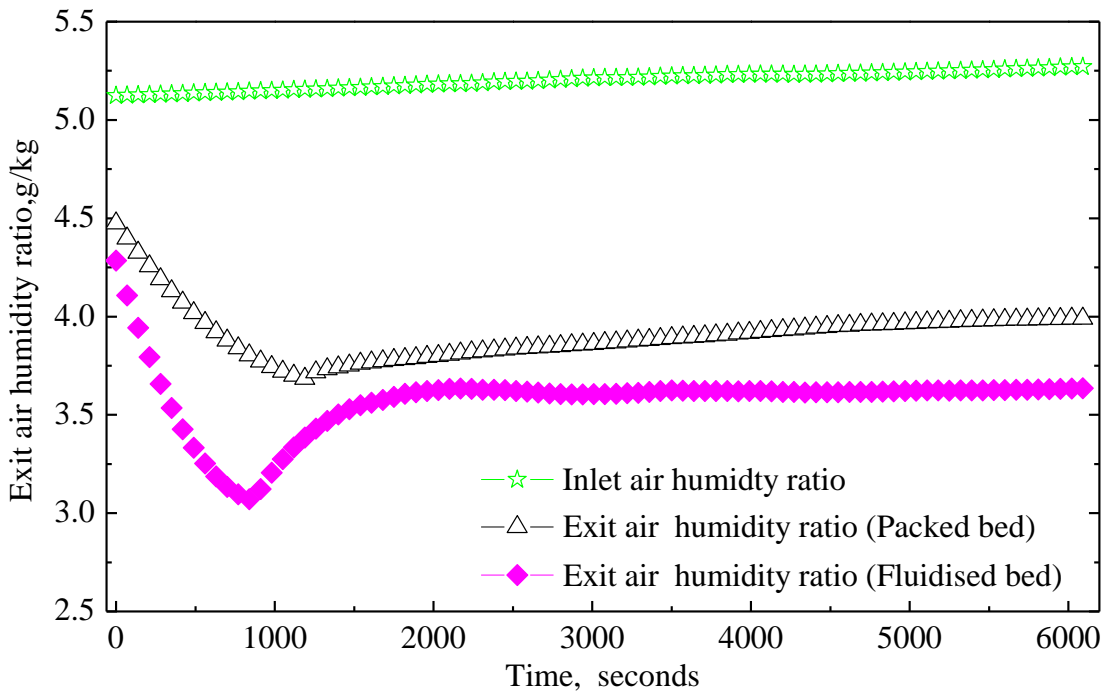**Fig. 5.24** Transient variation of exit air humidity ratio corresponding to run 8 and run 8a.
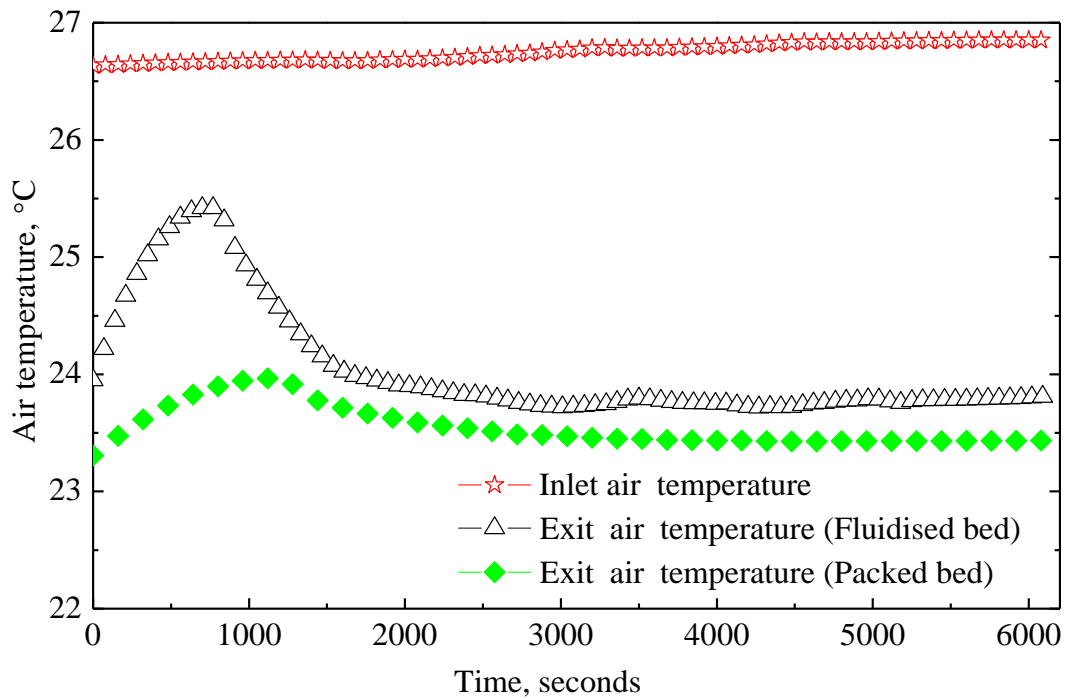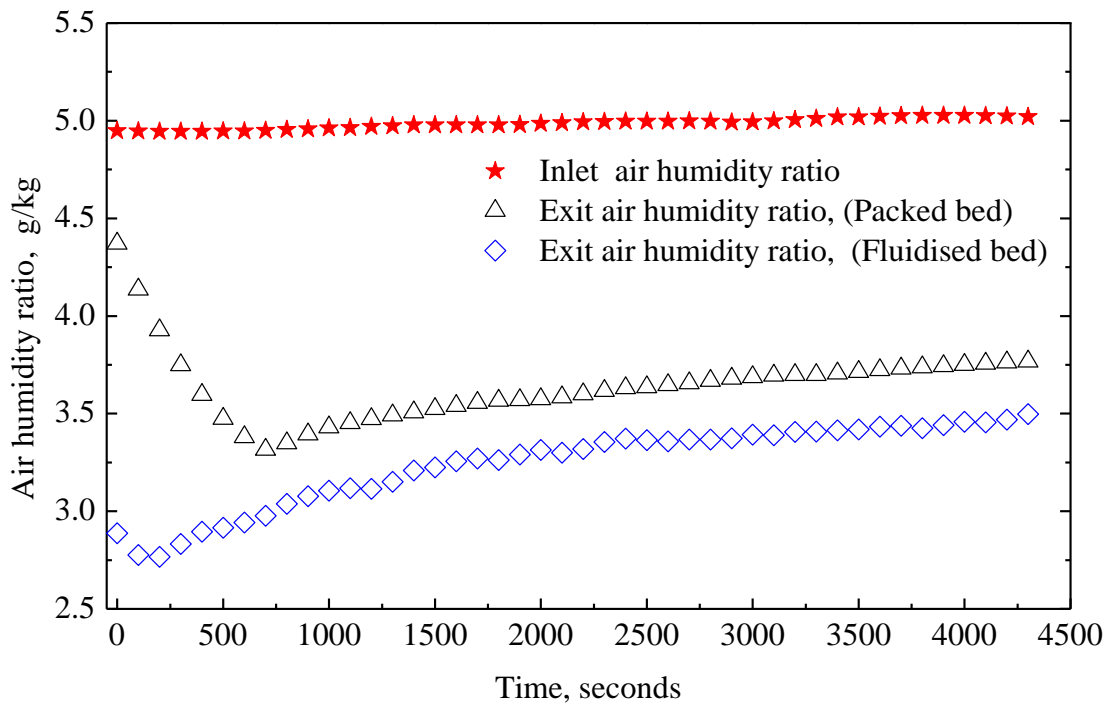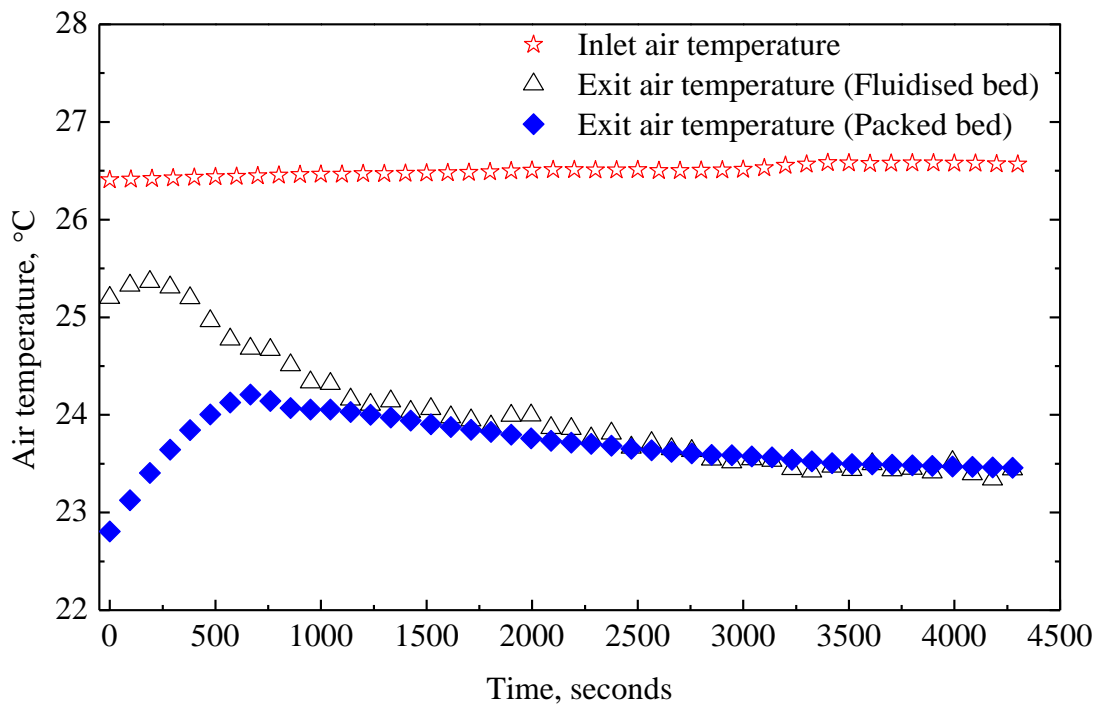

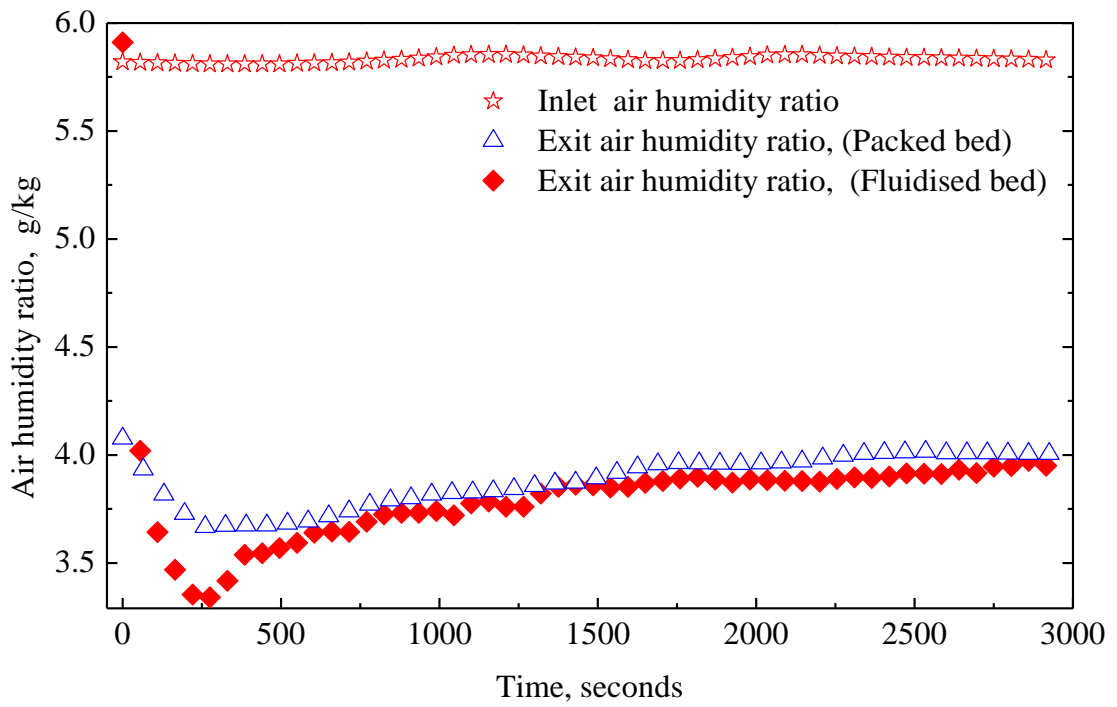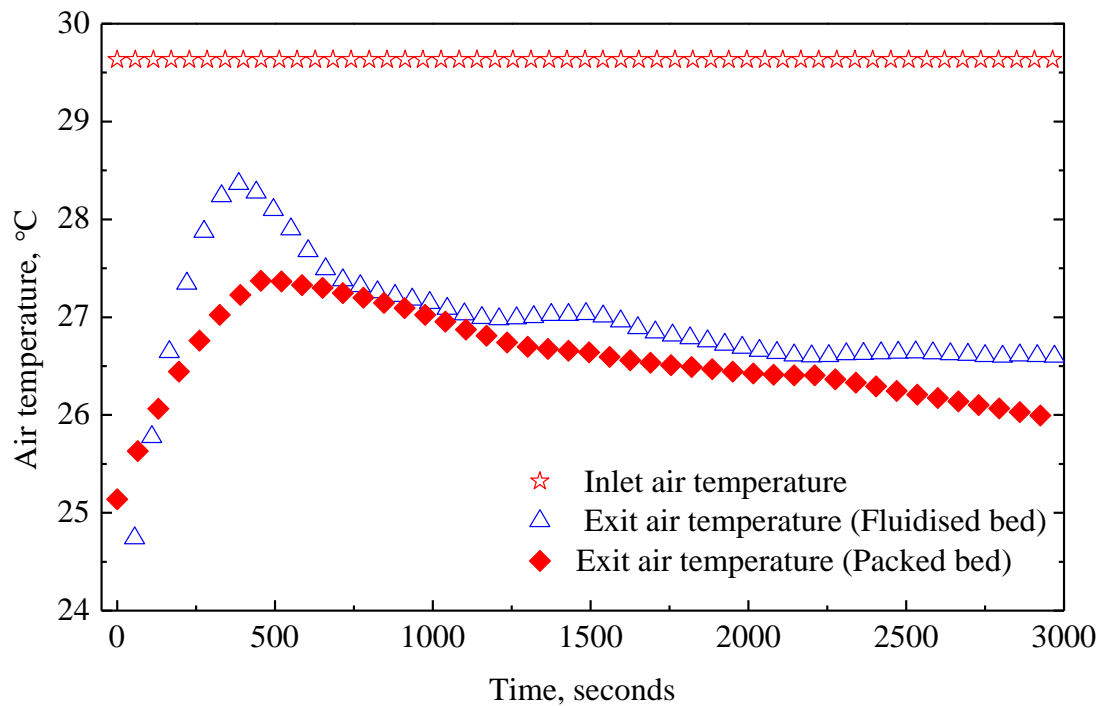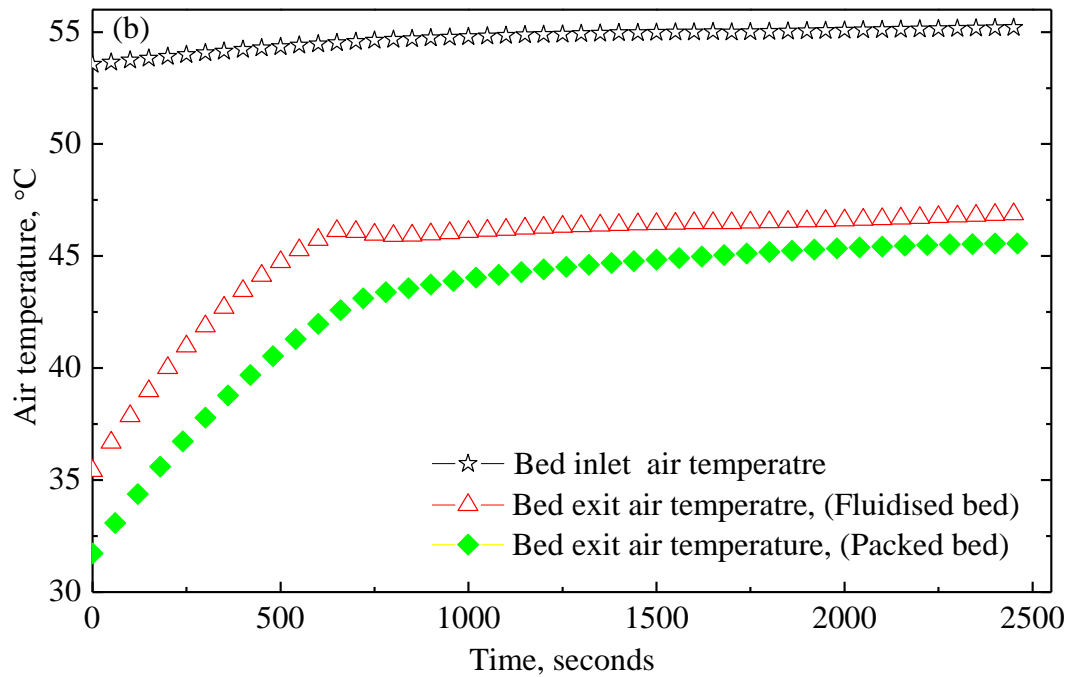**Fig.5.25** Transient variation of exit air temperature corresponding to run 8 and run 8a.

141

Figs.5.26, 5.27 and 5.28 depicts the comparison of time variation of exit humidity ratio and temperatures for burnt clay - horse dung - $CaCl_2$ pellets packed and fluidized beds in the desorption process. As shown in Fig.5.26 (a) and (b) for the bed inlet air humidity ratio of 3.53 g/kg and temperature of 48.74°C, the packed as well as fluidized beds are dried completely within 1500s and from that time onwards it seems to take moisture from the regeneration air. The average steady-state temperature difference between inlet and exit air is about 6°C.

An illustration of the transient variation of exit air humidity ratio and temperature for burnt clay - horse dung - $CaCl_2$ pellets in packed and fluidized beds during desorption process is shown in Fig.5.27 (a) and (b). For the bed inlet air humidity ratio of 3.89 g/kg and temperature of 50.65°C, the mass of bed decreases from 300 g to 296 g for packed bed and for fluidized bed decreases to 294 g. During initial period of operation the vapor pressure on the bed surface is at higher value than the vapor pressure of process air. Because of this the transport of moisture is from bed to air. Before the attainment of process time of 1000 s, the ratio of exit to inlet air humidity ratio is greater than one. Beyond 1000 s and up to the end of 5000 s, the ratio of exit to inlet air humidity ratio is less than one. The humidity ratio of air exiting the bed reaches the inlet air humidity ratio and drops to its minimum value at about 1000 s. The packed bed lags behind the fluidized bed in reaching inlet air moisture content. From this time period onwards the exit air moisture content starts to drop below the inlet air moisture content. At the same time the increase in exit air temperature becomes steady, and the bed starts to take moisture that is isotheral adsorption prevails. At the end of process time the rise in exit air temperature reaches steady state, and because of cooling effect produced by bed, the exit air humidity ratio drops below inlet air humidity ratio.

Desorption studies of the packed and fluidized bed corresponding to test run 11 and 11a are shown in Fig.5.28 (a) and (b). The bed inlet air velocity and initial mass of bed are 2 m/s and 300 g respectively.

142
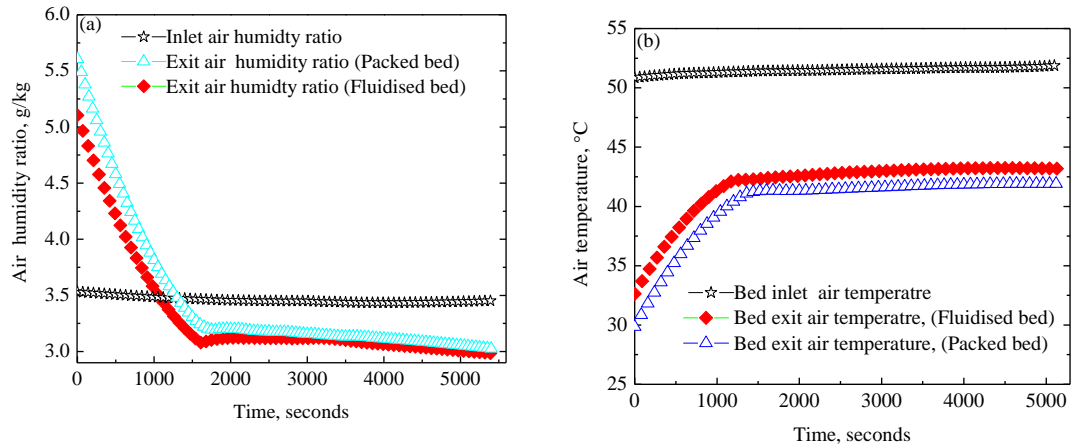
Fig. 5.26 Transient variation of exit air (a) humidity ratio and (b) temperature corresponding to run 9 and run 9a.
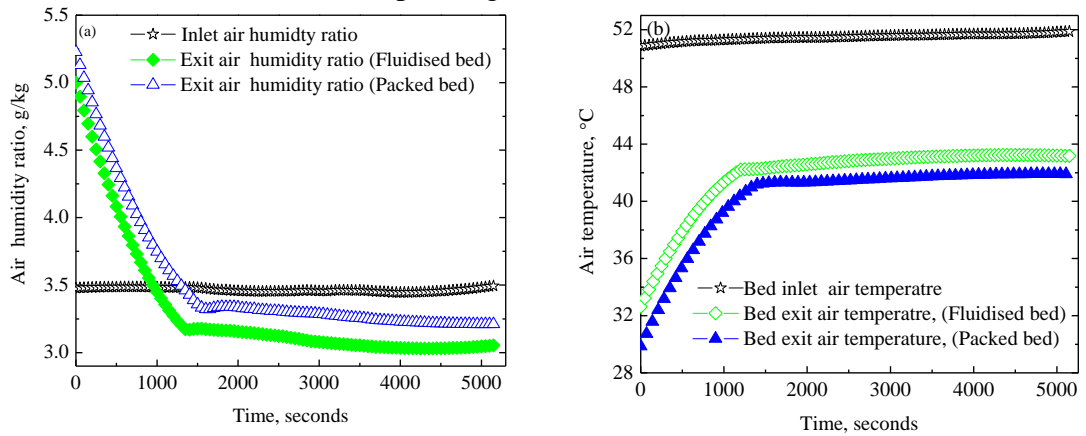
Fig. 5.27 Transient variation of exit air (a) humidity ratio and (b) temperature corresponding to run 10 and run 10a.
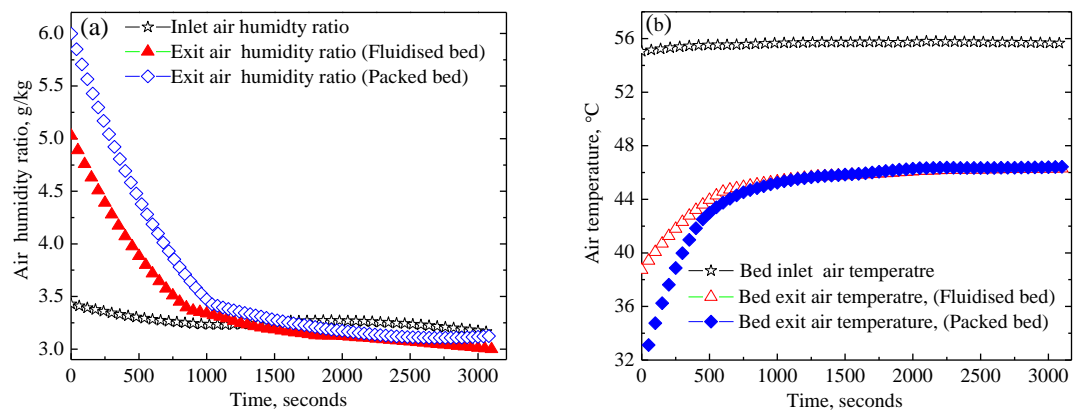
Fig. 5.28 Transient variation of exit air (a) humidity ratio and (b) temperature corresponding to run 11 and run 11a.

For the bed inlet air humidity ratio of 3.64 g/kg and temperature of 55.14°C, the fluidized bed takes less time for desorption as compared to the packed bed. The equilibrium of moisture content between bed inlet and exit air for both packed and fluidized beds is attained at about 1000 s. Because of higher thermal mass of packed bed exit air takes slightly more time in reaching inlet air humidity ratio. As shown in Fig.5.28 (b), during the early stage of the process, the temperature of the air exiting the fluidized bed is greater than the air exiting the packed bed. However after 750 s the difference between inlet and exit air temperatures for packed and fluidized beds remains steady. At the end of process, mass of packed bed decreases to 294.6 g and the mass of bed corresponding to fluidized state decreases to 291.38 g

5.9 COMPARISON OF VERTICAL PACKED AND FLUIDIZED BED OF BURNT CLAY - ADDITIVES - CaCl$_2$

Moisture removal capacity in adsorption process evaluated using Eq. (5.2) is presented in Fig.5.29 (a) and (b) for a packed and fluidized bed. The adsorption capability is being compared using all the three composite desiccants. The inlet velocity of the process air to the bed is 2 m/s, and the mass of bed is 300 g. For all the three packed and fluidized bed the whole process is categorized into three zones. The process dynamics for the fixed time can be divided into three zones namely, fast dynamics, medium dynamics, and slow dynamics. In the first region, which is from 0 to 550 s, the removal of moisture from the process air by the packed and fluidized beds is too rapid. The peak value of moisture removal is attained at about 500 s. In medium dynamics region that is from about 550 to 2500 s, the uptake by the clay composite desiccant beds is steadily progressing.
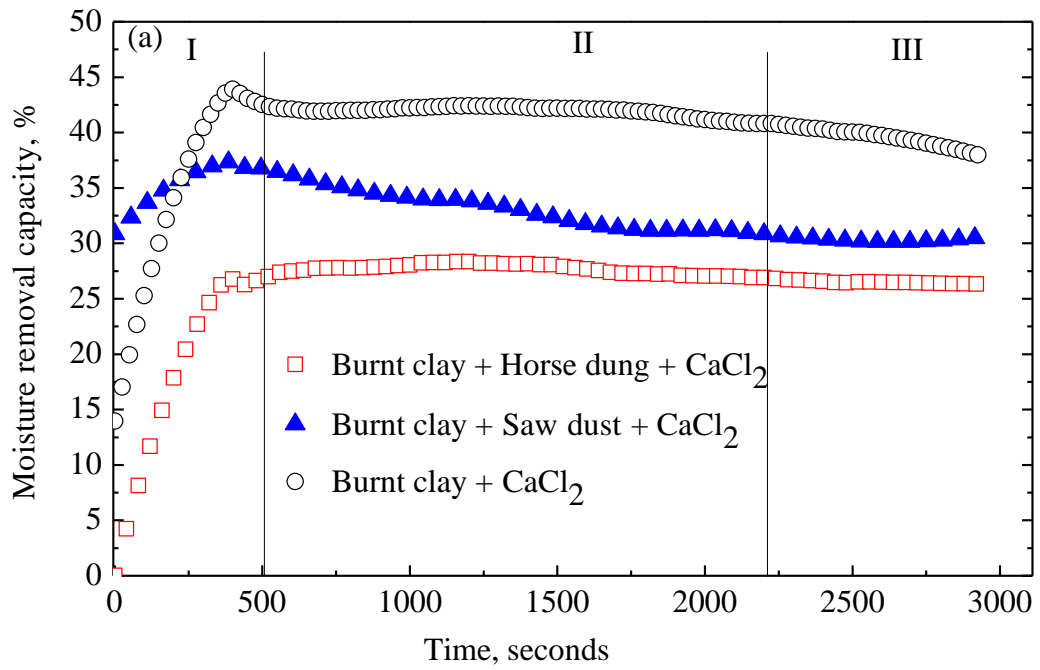
Fig. 5.29 (a) Comparisons of vertical packed clay - additives - CaCl$_2$ beds in adsorption.
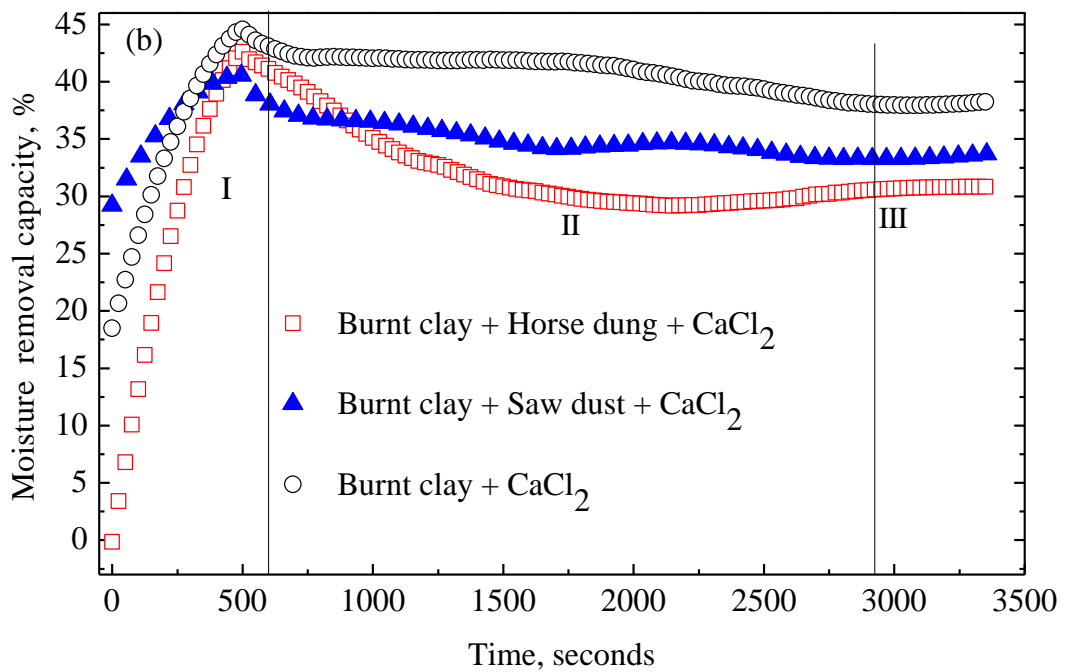
Fig. 5.29 (b) Comparisons of fluidized clay - additives - CaCl$_2$ beds in adsorption.
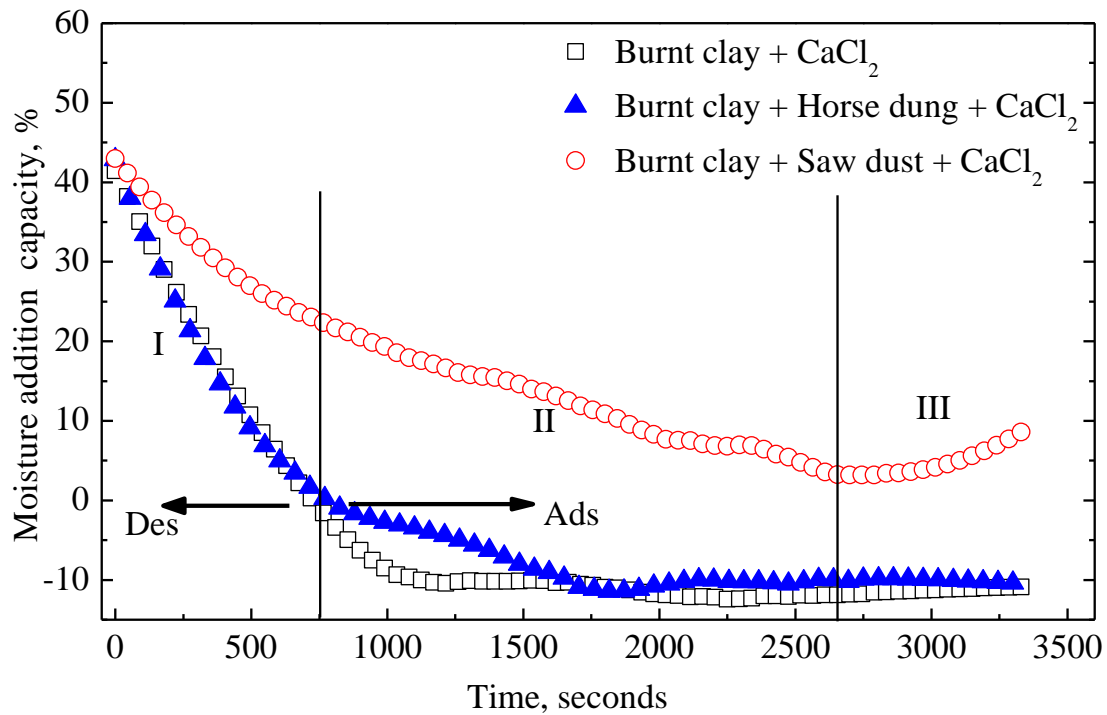
Fig .5.30 Comparisons of packed clay - additives - CaCl$_2$ composite desiccant packed beds in desorption.
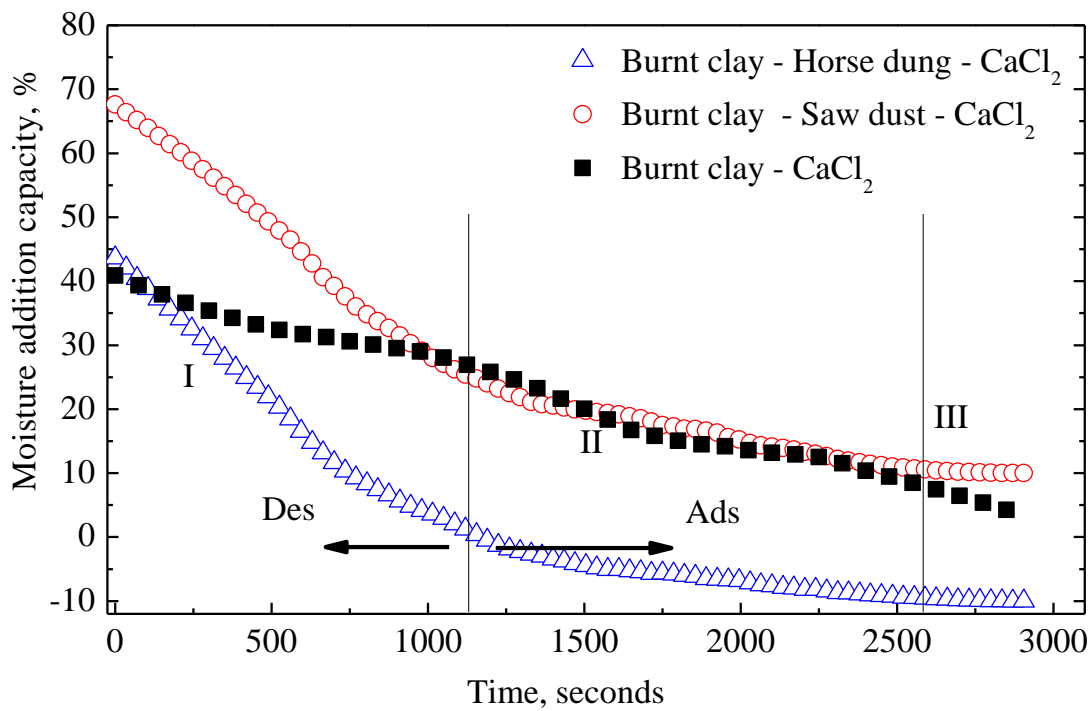
Fig .5.31 Comparisons of fluidized clay - additives - CaCl$_2$ composite desiccant fluidized beds in desorption.

146

In the medium dynamics region, clear demarcation of adsorption process can be identified. Burnt clay - $CaCl_2$ composite desiccants in a state of packed and fluidized bed the absorptivity is high when compared to clay - sawdust - $CaCl_2$ and clay - horse dung - $CaCl_2$ composite desiccant beds. This is attributed to the fact that the addition of sawdust and horse dung additives increases the thermal inertia of the bed. The increase in thermal inertia lowers the dehumidification capacity of the clay-additives composite desiccant bed. In the third region, due to increase in bed water content the moisture removal capacity of beds decreases as compared to adsorptive power in second region. Moisture addition capacity in desorption process is evaluated using Eq. (5.3). For the bed inlet velocity of 1.5 m/s and mass of bed as 200 g, the whole desorption process can be divided into three zones into packed and fluidized beds as shown in Fig.5.30 and 5.31.

The bed inlet air temperature is 52°C, and relative humidity is 5.3%. Owing to higher dryness of beds, the rate of desorption is rapid in the first fast dynamic zone. Comparing the humidification capacity of the beds in packed bed mode of operation it seems that burnt clay - $CaCl_2$ and burnt clay-horse dung - $CaCl_2$ composite desiccant beds are completely dried before the end of 750 s. After this process time the composite desiccant beds operate in adsorption mode. However burnt clay-sawdust - $CaCl_2$ desiccant bed continues to desorb until 3400 s. The desorption process for all the three beds in fluidization progresses up to 1250 s. At this instant of time, burnt clay-horse dung - $CaCl_2$ bed is dried completely as compared to other two desiccant columns. From this time onwards the bunt clay-$CaCl_2$ and burnt clay-sawdust - $CaCl_2$ composite beds operate in desorption mode whereas burnt clay-horse dung - $CaCl_2$ bed continues to operate in adsorption mode.

5.10 ANALYSIS OF MASS TRANSFER COEFFICIENT

The mass transfer potential in terms of mass transfer coefficient for the convective mass transfer process is calculated by using the Eq. (5.4) to (5.8). The mass transfer coefficient in terms of transverse velocity for different runs in adsorption and desorption is presented in Figs 5.32 to 5.34. It can be seen that mass transfer coefficient reaches its peak value during initial stages of adsorption process. With

increase in process time the mass transfer coefficient decreases and reaches minimum value. The change in mass transfer coefficient during process is greater in fluidized beds as compared to packed beds. During desorption higher values of mass transfer coefficient are noted in fluidized beds. The change in mass transfer coefficient during adsorption and desorption processes can be attributed to change in heat and mass transfer characteristics of packed and fluidized beds.
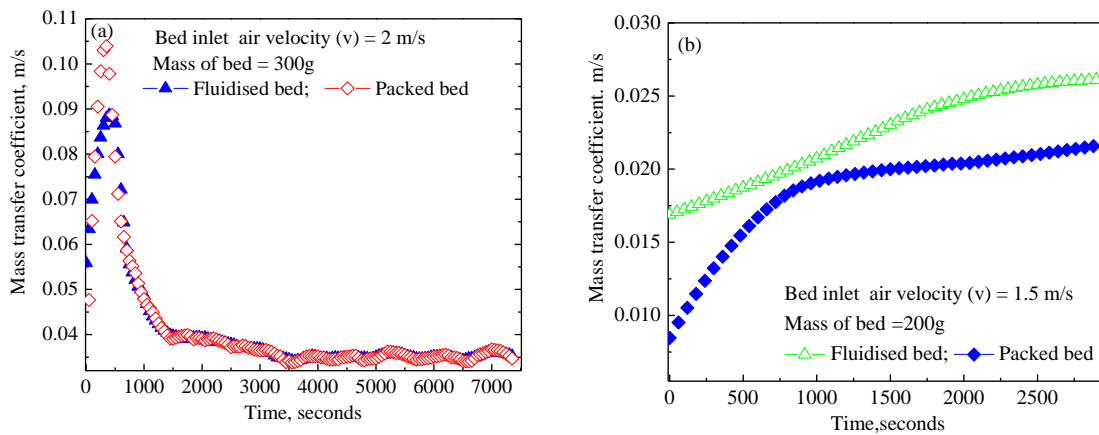
Fig. 5.32 Transient variation of mass transfer coefficient for burnt clay - CaCl$_2$ desiccant pellets beds in (a) adsorption and (b) desorption.
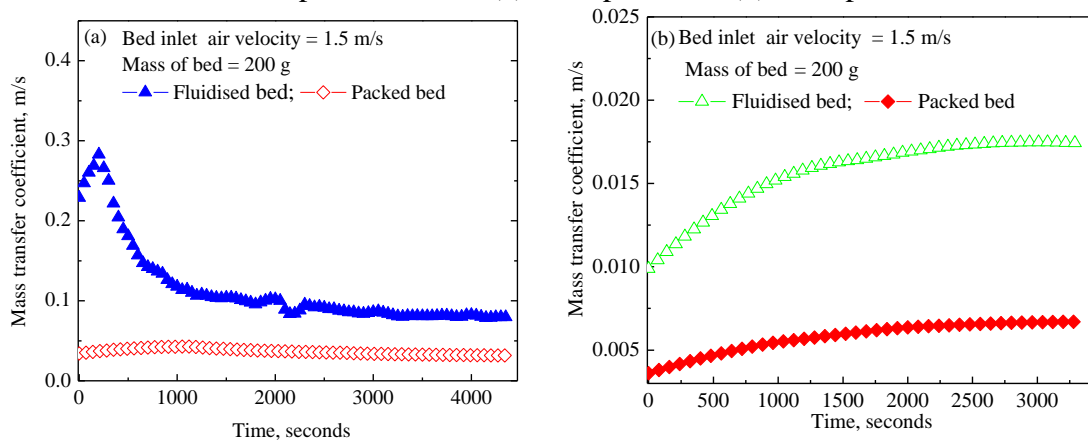
Fig. 5.33 Transient variation of mass transfer coefficient for burnt clay - sawdust - CaCl$_2$ desiccant pellets beds in (a) adsorption and (b) desorption.
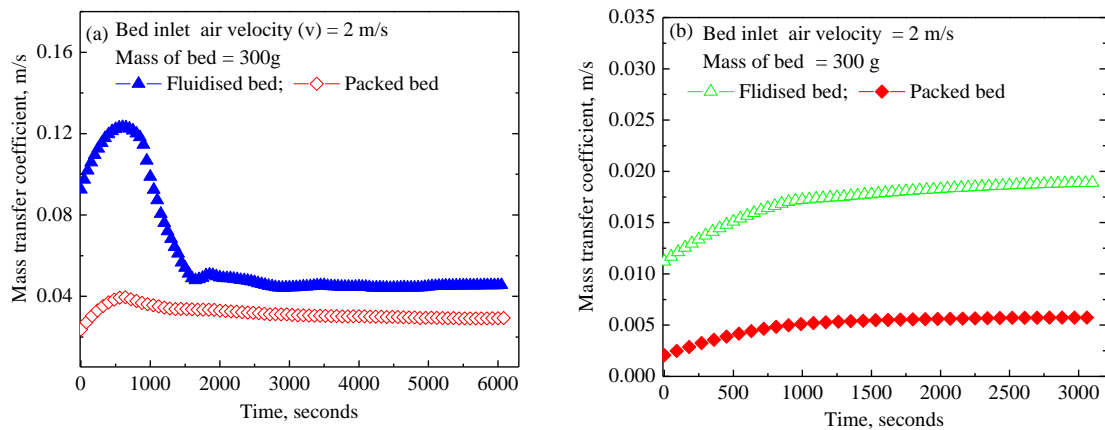
Fig. 5.34 Transient variation of mass transfer coefficient for burnt clay - horse dung - CaCl$_2$ desiccant pellets beds in (a) adsorption and (b) desorption.

5.11 ANALYSIS OF WATER UPTAKE CAPACITY OF BURNT CLAY COMPOSITE DESICCANTS

From the analysis of dehumidification potential of vertical packed burnt clay composite desiccants, it is revealed that moisture uptake capacity of clay composite desiccants in packed bed mode operation seems to be non-uniform. Within the processing time, all the desiccant pellets may not be active to take moisture. In order to access the dehumidification potential of composite desiccants, solitary burnt clay - CaCl$_2$, burnt clay - sawdust - CaCl$_2$ and burnt clay-horse dung - CaCl$_2$ desiccants pellet is exposed to different humidity conditions at constant temperature. The water content of desiccants is a function of surrounding equilibrium layer moisture content and temperature. The experiments are conducted by keeping the desiccant pellet in a temperature-controlled humidity chamber. The water uptake is calculated by initial mass of desiccant and the mass of the desiccant at a particular time period during adsorption. Fig. 5.35 (a) to (d) depicts the time variation of water uptake by desiccants at 45°C and exposed to humidity conditions of 24%, 34%, 42%, and 52%. For the process air relative humidity of 24% and 34%, the trends for water uptake by desiccants are alike and proceeds coincidentally with each other. The qualitative behavior of coincidence spans beyond 50 min. From that onwards the water content monotonously increases for clay-additives based desiccants whereas for clay-based desiccant tending towards saturation.

149
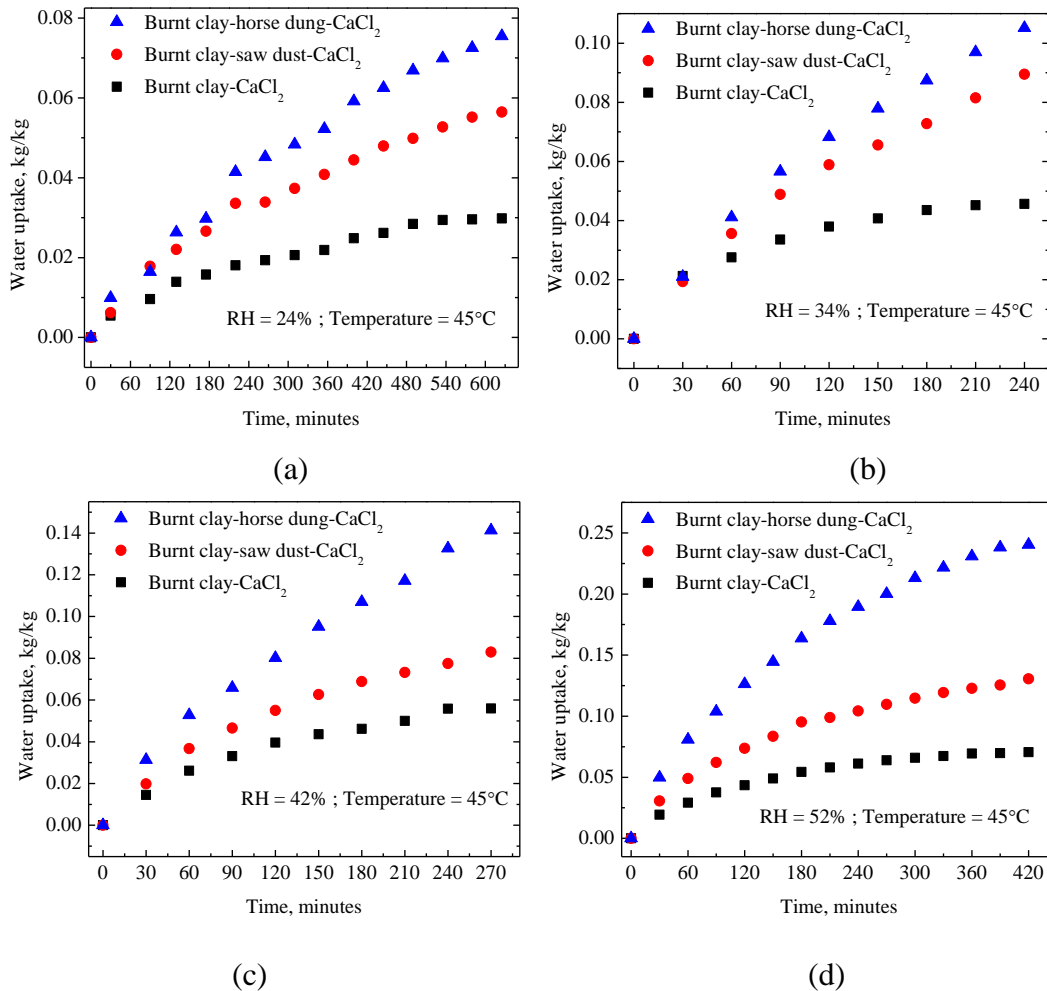
Fig. 5.35 Transient variation of moisture uptake capacity for burnt clay - additives - CaCl₂ desiccants in adsorption.

For the relative humidity of 42% and 52%, the water content of composite desiccants increases nearly in equal proportion. Below the processing time of 50 min, the concentration of moisture shared by the desiccants seems to be nearly the same. Beyond that time span the water content of composite desiccants is scaled up till near to the saturation. From the results it seems that the water content of burnt clay - $CaCl_2$ composite desiccant attains equilibrium with the water content of layer surrounding the desiccant pellet. As compared to clay additives desiccants attainment of equilibrium condition is at quicker rates for burnt clay - $CaCl_2$ desiccant. As compared to clay composite desiccant the moisture uptake is higher for clay-additives based composite desiccants. The photographs of clay and clay additives composite desiccants presented in appendix - III shows the potential of fabricated composite

desiccants in moisture adsorption. Fig.5.36 depicts water content of clay and clay additives composite desiccants with different humidity conditions of process air such as 24%, 34%, 42%, and 52%. The corresponding adsorption times are 670, 240, 270 and 420 minutes respectively. From the results it is observed that at higher relative humidity, higher will be the water content of clay and clay-additives based composite desiccants. Irrespective of process air humidity and process time burnt clay - horse dung - $CaCl_2$ composite desiccant exhibit higher water content followed by burnt clay - sawdust - $CaCl_2$ and burnt clay - $CaCl_2$ composite desiccant.
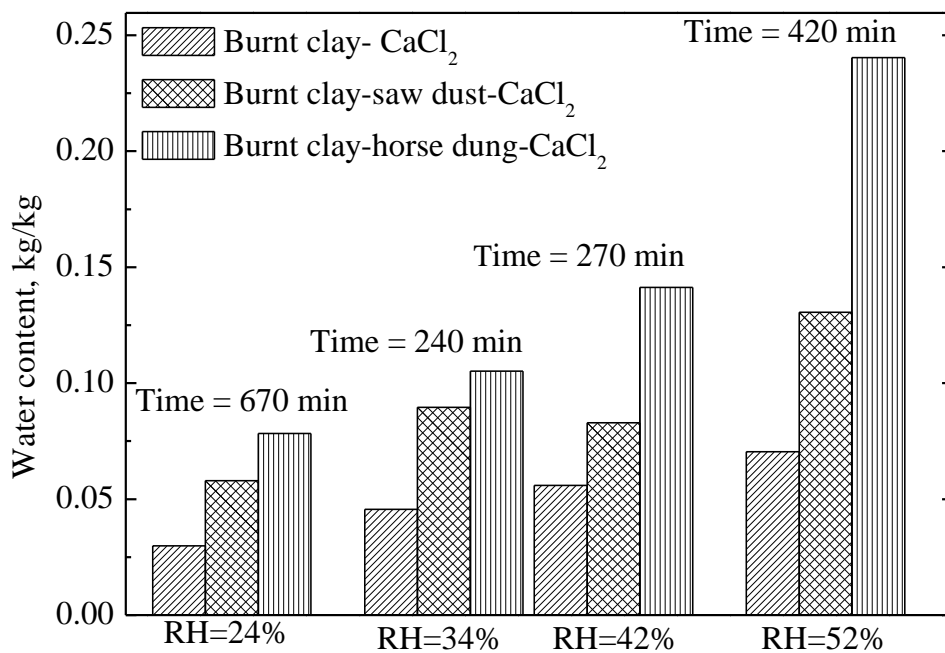
Fig. 5.36 Water content of variation burnt clay - additives - $CaCl_2$ desiccants in adsorption.

5.12 SUMMARY

Experimental parameters measured are evaluated in terms of moisture addition capacity, moisture removal capacity, dew point effectiveness, and mass transfer coefficient. The vapor pressure which is a function of bed temperature and $CaCl_2$ concentration is correlated using the curve fitted data of vapor pressure - $CaCl_2$ concentration chart. The dehumidification potential of burnt clay additives $CaCl_2$ composite desiccant bed is being discussed with variation of process air velocity and bed mass. Experimentally the heat and mass transfer characteristics of vertical packed

and fluidized bed of burnt clay - additives composite desiccant pellets are compared in adsorption-desorption processes. Based on the experimental results the following conclusions are presented:

1. Test results show that dehumidification performance decreases with increasing air mass fluxes. This is because of high air velocities lead to reduced residence time in the dehumidifier and result in limited mass transfer rates between moist air and to the desiccant surface.

2. At higher humidity of process air, the heat liberated during the adsorption process going to decrease the moisture removal rate of clay additives based composite desiccants. Whereas for process air with lower humidity, the sensible heat transferred to the bed from process air will decrease the mass transfer potential towards the bed.

3. For the same set of operating conditions, the average adsorption rate for clay – $CaCl_2$ packed bed is 40% as compared to 32% and 26% in clay-saw dust and clay-horse dung $CaCl_2$ packed beds.

4. For the same set of operating conditions, the average desorption rate for clay – $CaCl_2$ packed bed is 39% as compared to 35% and 31% in clay-saw dust and clay-horse dung $CaCl_2$ packed beds.

5. Fluidization improves dehumidification performance. Compared to packed beds, fluidization results in higher desorption rates.

6. During desorption, the pressure drop through fluidized clay-$CaCl_2$ and clay-additives - $CaCl_2$ composite desiccant beds is lower than the respective static composite desiccant beds. Whereas during adsorption, higher values of pressure drop are noted in fluidized beds as compared to packed beds.

7. As compared to vertical packed desiccant beds, the mass transfer potential is more in vertical fluidized beds.

8. For the identical humidity and for the same process time burnt clay-horse dung-$CaCl_2$ composite desiccant shows higher absorptivity and higher water content followed by burnt clay-saw dust - $CaCl_2$ and burnt clay - $CaCl_2$ composite desiccant.

152

CHAPTER 6

MATHEMATICAL MODEL OF A VERTICAL PACKED DESICCANT BED

6.1 INTRODUCTION

The process air and properties of bed affect the behavior of desiccant bed in humidification and dehumidification processes. The heat of adsorption and isotherm property of desiccant material essential for the coupled heat and mass transfer analysis of humidification and dehumidification processes. The mathematical models governing heat and mass transfer characteristics available in the literature are pseudo gas controlled (PGC) isothermal, pseudo gas controlled (PGC) adiabatic and solid side resistance (SSR) adiabatic diffusion models. The PGC isothermal model (Hamed, 2001) assumes bed operation under isothermal condition. The mass transfer process in a vertically packed desiccant bed containing burnt clay - additives - $CaCl_2$ composite desiccant is modeled by a set of two governing differential equations. Both equations are coupled by isotherm equation involving affinity constant. The adiabatic and diffusion model for vertically packed silica gel bed is presented by Pesaran and Mills-1986. The adiabatic model considers gas side resistance with heat of adsorption. The model equations depict the spatial and transient variation of air and bed behavior with respect to humidity ratio, water content, and temperature. The adiabatic diffusion model considers solid side resistance with heat of adsorption. The radial variation of water accumulation in silica gel desiccant is considered to estimate average water content of bed. The model equations are coupled by isotherm property relating equilibrium relative humidity and bed water content at constant temperature. The isotherm is the desiccant material property that determines saturation capacity of desiccant materials. The experimental results for step-change in inlet air humidity, temperature and velocity are compared with the theoretical results. The present work employs isothermal mathematical model. The governing equations are numerically solved and compared with the experimental results for burnt clay - $CaCl_2$ desiccants.

153

6.2 THEORETICAL ANALYSIS OF DESICCANT PACKED BED

The physical system is shown in Fig.6.1 (a). The bed is of cylindrical shape and fixed vertically. The bed containing spherical desiccant pellets is defined in the domain [0 - L] and [0 - D] m. Process air with a velocity (v) m/s is allowed to pass through the bed at temperature (T_{1e}) °C; the moisture fraction of inlet air is (c_{1e}) kg/kg of dry air. For one dimensional analysis, the airflow is assumed to be in axial z direction. The control volume in the direction of flow is shown in Fig.6.1 (b). The solid line represents the solid phase, and the dotted line represents gas phase.
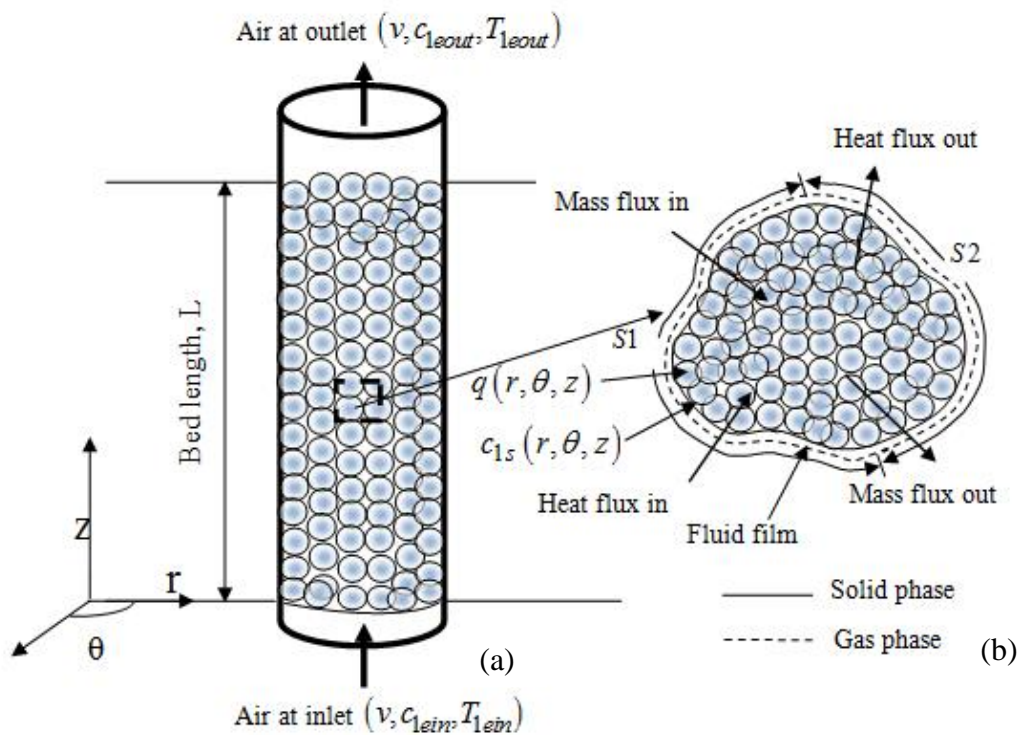
Fig. 6.1 Physical system (a) packed desiccant bed, (b) arbitrary control volume.

As shown in Fig.6.2, consider an arbitrary region of fixed V bounded by surface S. Let ds be the elemental area of the surface. Let ρ be the density of desiccant material. $\hat{n}$ be the unit normal to the surface. $S1$ and $S2$ are the control surfaces, across which net influx and outflux of mass are represented. $\left(\left(\rho c_{1e}\right)v\right)_{in}$ and $\left(\left(\rho c_{1e}\right)v\right)_{out}$ are the mass fluxes of species, water vapor entering and leaving the

154

control volume in gas phase. $((\rho q)v)_{in}$ and $((\rho q)v)_{out}$ are the mass fluxes of water entering and leaving the control volume in solid phase in the flow direction.
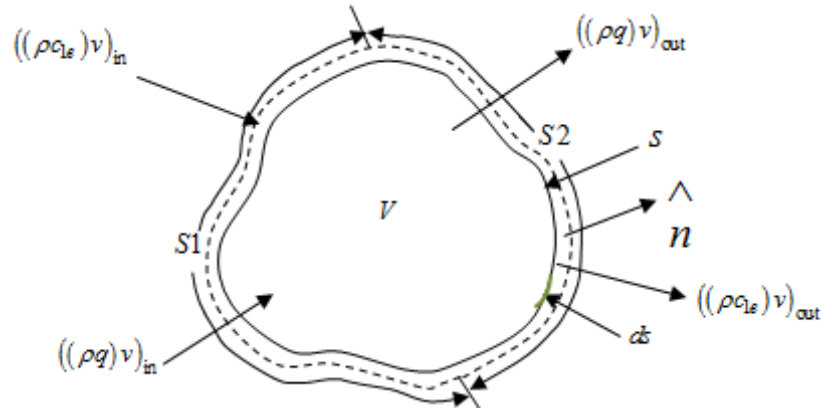
Fig. 6.2 Arbitrary fixed control volume for mass balance in gas and solid phases.

For the model development, the following assumptions are made,

1) The flow of process air is in the axial direction, and the mass transfer in radial and angular directions is neglected.

2) The rate of accumulation of moisture in the desiccant bed is equal to the total mass flux over the pellets and is given by solid phase balance.

3) As moisture is transferred from the bulk air stream to the pellet surface by means of convection, and hence the net mass flux over the desiccant pellet is given by;
    $n_s = K_\omega (c_{1s} - c_{1e})$.

4) Lumped element model or lumped parameter system is adopted, therefore at a given time; the spherical pellet is at constant temperature.

5) The bed water content is a function of fluid concentration at equilibrium with the adsorbed phase and its magnitude is given by the isotherm equation, $q = Kc_{1s}$

6) The heat of adsorption is generated by the condensation of water vapor within the pores of the desiccant pellet. The heat of adsorption is assumed to be totally generated in the composite desiccant pellets (Pesaran and Mills, 1987).

Under the above assumptions and conditions, the governing equations for solid and gas phases of the physical system can be derived as follows

155

6.2.1 Gas-phase mass balance for species water vapor

The expression for moisture content of operating air can be obtained by writing mass balance equations for water vapor. The expression for water vapor species conservation, namely water vapor can be obtained on mass basis in gas phase. Mass balance equations are written for water vapor of process air. The transport of water vapor mass flux $\left((\rho c_{le})v\right)$ across the surfaces $S1$ and $S2$ shown in Fig. 6.3.
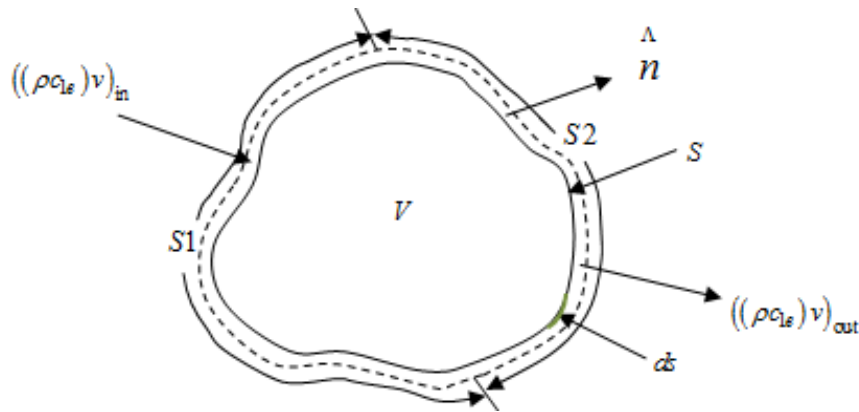
Fig. 6.3 Arbitrary fixed control volume for mass balance of species water vapor in gas phase.

From the law of conservation of mass, the mass balance for water vapor for fixed control volume in gas phase is given by Rate of accumulation of species in V = Net rate of influx of species into V + Rate of generation of species in V

$$\iiint_V \varepsilon_b \frac{\partial}{\partial t}\rho c_{1e}dV + \iiint_V (1-\varepsilon_b)\frac{\partial}{\partial t}\rho c_{1e}dV = \iint_S -(\rho c_{1e}v).\hat{n}ds + \iiint_V Q_g dV \tag{6.1}$$

Where $\rho c_{1e}v$ absolute mass flux of species, ε_b - porosity of bed, $(1-\varepsilon_b)$ - solid fraction of bed, V - the volume of bed, s - closed surface and Q_g - rate of generation of species. Using the divergence theorem

$$\iiint_V \varepsilon_b \frac{\partial}{\partial t}\rho c_{1e}dV + \iiint_V (1-\varepsilon_b)\frac{\partial}{\partial t}\rho c_{1e}dV = \iiint_V \nabla.(\rho c_{1e}v)dV + \iiint_V Q_g dV \tag{6.2}$$

$$\iiint_V \left[\varepsilon_b \frac{\partial \rho c_{1e}}{\partial t} + (1-\varepsilon_b)\frac{\partial \rho c_{1e}}{\partial t} + \nabla.(\rho c_{1e}v) - Q_g\right]dV = 0 \tag{6.3}$$

156

Since the region of integration is arbitrary, the integrand itself must be zero

$$\left[\varepsilon_b \frac{\partial \rho c_{1e}}{\partial t} + (1 - \varepsilon_b) \frac{\partial \rho c_{1e}}{\partial t} + \nabla.(\rho c_{1e} v) - Q_g \right] dV = 0 \tag{6.4}$$

Assuming the rate of generation of species water vapor $Q_g = 0$ and neglecting mass transfer in radial and angular directions, the differential form of the mass conservation of water vapor in the flow direction is given as

$$\varepsilon_b \frac{\partial \rho c_{1e}}{\partial t} Adz + (1 - \varepsilon_b) \frac{\partial \rho c_{1e}}{\partial t} Adz + \frac{\partial \rho c_{1e} v}{\partial z} Adz = 0 \tag{6.5}$$

Eq.(6.5) has two possible sinks, $\varepsilon_b \frac{\partial \rho c_{1e}}{\partial t}$ is the rate accumulation of mass in the gas phase, whereas $(1 - \varepsilon_b) \frac{\partial \rho c_{1e}}{\partial t}$ is the rate of accumulation of mass in the solid bed (moisture transferred to desiccant bed). Since solid phase loses no water vapor and generates none, the rate of accumulation of moisture in the desiccant bed is equal to the total mass flux over the pellets and is given by solid phase balance.

$$(1 - \varepsilon_b) \frac{\partial (\rho c_{1e})}{\partial t} Adz = -(n_s A_{sf}) \tag{6.6}$$

Where n_s is the net water vapor mass flux over the desiccant surface and A_{sf} is the total interfacial area available for heat and mass transfer in the bed and is the product of the average surface area of each desiccant pellet and the number of desiccant pellets in the bed? Substituting Eq. (6.6) in Eq. (6.7) gives,

$$-\frac{\partial ((\rho c_{1e}) v)}{\partial z} Adz = \varepsilon_b \frac{\partial (\rho c_{1e})}{\partial t} Adz - (n_s A_{sf}) \tag{6.7}$$

Dividing Eq. (6.7) by dz on both sides becomes,

$$-\frac{\partial ((\rho c_{1e}) v)}{\partial z} A = \varepsilon_b \frac{\partial (\rho c_{1e})}{\partial t} A - (n_s p) \tag{6.8}$$

Where p is the perimeter of the bed which is the product of the average perimeter of each desiccant and the number of desiccants in the bed? The mass flow rate of air $\dot{m}_a$ is given by

$$\dot{m}_a = \rho_a A v \tag{6.9}$$

Where cross-section of bed is A m^2 and velocity of process air is v m/s. Substituting Eq. (6.9) in Eq. (6.8), gives

$$-\dot{m}_a \frac{\partial c_{1e}}{\partial z} = -(n_s p) \tag{6.10}$$

The net mass flux over the desiccant pellet is given by

$$n_s = K_\omega (c_{1s} - c_{1e}) \tag{6.11}$$

Where K_ω the gas side is the mass transfer coefficient, and rearranging gives

$$\frac{\partial c_{1e}}{\partial z} = \frac{K_\omega p (c_{1s} - c_{1e})}{\dot{m}_a} \tag{6.12}$$

Eq.(6.12) represents the governing equation for water vapor species conservation or moisture conservation in the gas phase.

6.2.2 Solid-phase mass balance for water content

Fig 6.4 representing the rate of flux flowing across the surface $S1$ as $((\rho_s q)v)_{in}$ and out across the surface $S2$ as $((\rho_s q)v)_{out}$. Writing mass balance for the species water vapor for the control volume in the solid phase.

Rate of accumulation of species in V = Net rate of influx of species into V + Rate of the generation of species in V.
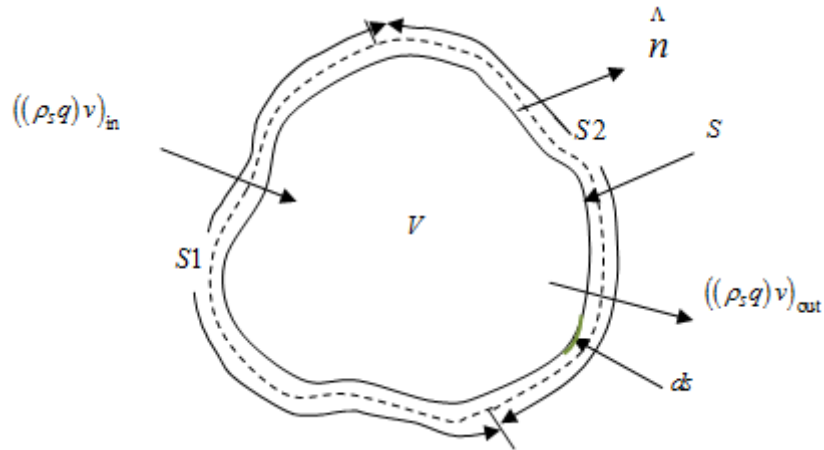
Fig. 6.4 Arbitrary fixed control volume with the flux of water flowing into and out of solid phase.

For a fixed control volume

$$\iiint_V \varepsilon_b \frac{\partial}{\partial t}\rho_s q dV + \iiint_V (1-\varepsilon_b)\frac{\partial}{\partial t}\rho_s q dV = \iint_S -(\rho_s q v).\hat{n}ds + \iiint_V Q_g dV \qquad (6.13)$$

Where $\rho_s q v$ - absolute mass flux of water vapor, ε_b - porosity of bed, $(1-\varepsilon_b)$ the fraction of the mass of bed without porosity, V - volume of bed, s - closed surface and Q_g - rate of generation of species. Using the divergence theorem

$$\iiint_V \varepsilon_b \frac{\partial}{\partial t}\rho_s q dv + \iiint_V (1-\varepsilon_b)\frac{\partial}{\partial t}\rho_s q dV = -\iiint_V \nabla.(\rho_s q v)dV + \iiint_V Q_g dV \qquad (6.14)$$

$$\iiint_V \left[\varepsilon_b \frac{\partial(\rho_s q)}{\partial t} + (1-\varepsilon_b)\frac{\partial(\rho_s q)}{\partial t} + \nabla.(\rho_s q v) - Q_g \right] dV = 0 \qquad (6.15)$$

Since the region of integration is arbitrary, the integrand itself must be zero

$$\left[\varepsilon_b \frac{\partial(\rho_s q)}{\partial t} + (1-\varepsilon_b)\frac{\partial(\rho_s q)}{\partial t} + \nabla.(\rho_s q v) - Q_g \right] dV = 0 \qquad (6.16)$$

Assuming the rate of generation of mass of water vapor $Q_g = 0$ and neglecting mass transfer in radial and angular directions, the differential form of the bed water concentration in the flow direction is given as

$$\varepsilon_b \frac{\partial(\rho_s q)}{\partial t} Adz + (1 - \varepsilon_b) \frac{\partial(\rho_s q)}{\partial t} Adz + \frac{\partial(\rho_s q)v}{\partial z} Adz \qquad (6.17)$$

By considering the system as a lumped capacitance model wherein mass flux is assumed to be uniform throughout the system. Eq. (6.17) is modified by considering

$$\left[(\rho_s q_s)v\right]_{z=0} = \left[(\rho_s q_s)v\right]_{in} = (\rho_s q_s)v$$

$$\left[(\rho_s q_s)v\right]_{z=dz} = \left[(\rho_s q_s)v\right]_{out} = (\rho_s q_s)v + \frac{\partial((\rho_s q_s)v)}{\partial z} Adz = 0 \qquad (6.18)$$

With Eq. (6.18) the Eq. (6.19) changed as follows

$$\varepsilon_b \frac{\partial(\rho_s q)}{\partial t} Adz + (1 - \varepsilon_b) \frac{\partial(\rho_s q)}{\partial t} Adz + (\rho_s q)v \qquad (6.19)$$

Applying product rule of differentiation for Eq. (6.19)

$$-\rho_s qvA = \varepsilon_b \rho_s \frac{\partial q}{\partial t} Adz + \varepsilon_b q \frac{\partial \rho_s}{\partial t} Adz + (1 - \varepsilon_b)\rho_s \frac{\partial q}{\partial t} Adz + (1 - \varepsilon_b)q \frac{\partial \rho_s}{\partial t} Adz \qquad (6.20)$$

$$-\rho_s qvA = \varepsilon_b \rho_s \frac{\partial q}{\partial t} Adz + (1 - \varepsilon_b)\rho_s \frac{\partial q}{\partial t} Adz + q\left(\varepsilon_b \frac{\partial \rho_s}{\partial t} Adz + (1 - \varepsilon_b) \frac{\partial \rho_s}{\partial t}\right) Adz \qquad (6.21)$$

There is no accumulation of desiccant mass in both solid and gas phase, therefore

$$\left(\varepsilon_b \frac{\partial \rho_s}{\partial t} Adz + (1 - \varepsilon_b) \frac{\partial \rho_s}{\partial t}\right) Adz = 0 \qquad (6.22)$$

Eq. (6.22) becomes

$$-\rho_s qvA = \varepsilon_b \rho_s \frac{\partial q}{\partial t} Adz + (1 - \varepsilon_b)\rho_s \frac{\partial q}{\partial t} Adz \qquad (6.23)$$

The term $\rho_s qvA$ - accumulation of moisture in desiccant bed and is equal to vapor mass flux $n_s A_{sf}$ over the desiccant surface.

$$-n_s A_{sf} = \varepsilon_b \rho_s \frac{\partial q}{\partial t} Adz + (1 - \varepsilon_b)\rho_s \frac{\partial q}{\partial t} Adz \qquad (6.24)$$

160

Where n_s the net water vapor is mass flux over the desiccant surface and A_{sf} is the total interfacial area available for mass transfer and is the product of the average surface area of each desiccant and the number of desiccants in the bed. As there is no accumulation of mass in gas phase, hence the term $\varepsilon_b \rho_s \dfrac{\partial q}{\partial t} A dz$ is equal to zero. Eq. (6.24) becomes

$$-n_s A_{sf} = (1 - \varepsilon_b) \rho_s \frac{\partial q}{\partial t} A dz \tag{6.25}$$

Dividing both sides of Eq. (6.25) by dz

$$-n_s p = (1 - \varepsilon_b) \rho_s \frac{\partial q}{\partial t} A \tag{6.26}$$

The density of bed $\rho_b = (1 - \varepsilon_b) \rho_s$ and $n_s = K_\omega (c_{1s} - c_{1e})$, Eq. (6.26) becomes

$$-K_\omega (c_{1s} - c_{1e}) p = \rho_b \frac{\partial q}{\partial t} A \tag{6.27}$$

Where K_ω represents the gas side is the mass transfer coefficient and c_{1s} is the moisture fraction of fluid film around the desiccant pellet. c_{1e} is the moisture fraction of air. On simplifying Eq. (6.27)

$$\frac{\partial q}{\partial t} = \frac{-K_\omega p (c_{1s} - c_{1e})}{A \rho_b} \tag{6.28}$$

The Eq. (6.28) represents the governing equation to find the unsteady water content of the bed at any time. It represents rate of change of moisture content in the bed with accumulation of moisture in the interfacial layer. In the Eq. (6.28) the value q is a function of fluid concentration at equilibrium with the adsorbed phase. (Harmed, 2002)

$$q = K c_{1s} \tag{6.29}$$

Where 'K' is an affinity constant of adsorption equilibrium. Substituting Eq. (6.29) in Eq. (6.28), results in

$$\frac{\partial c_{1s}}{\partial t} = \frac{K_\omega p \left(c_{1e} - c_{1s} \right)}{A \rho_b K} \tag{6.30}$$

Eq. (6.30) represents the governing equation for unsteady equilibrium moisture concentration at any time. The associated boundary and initial conditions are

Boundary condition: $c_{1e}(z = 0, t) = c_{1e0}$ (6.31)

Initial condition: $c_{1s}(z, t = 0) = c_{1s0}$ (6.32)

6.3 FORMULATION OF GOVERNING EQUATION FOR MOISTURE FRACTION OF AIR

The moisture fraction of air and equilibrium moisture content of the interface layer can be known by solving the governing equations. The governing equations are formulated using forward time and forward space (FTFS) scheme of finite difference method (FDM). The moisture content of air c_{1e} and the interface layer moisture content c_{1s} depends on the length of the bed and on the time of operation. The equations are represented as follows

$$\frac{\partial c_{1e}}{\partial z} = \frac{K_\omega p \left(c_{1s} - c_{1e} \right)}{\dot{m}_a} \tag{6.33}$$

$$\frac{\partial c_{1s}}{\partial t} = \frac{K_\omega p \left(c_{1e} - c_{1s} \right)}{A \rho_b K} \tag{6.34}$$

The governing equations are discretized with grids along the length and time. Fig 6.5 shows the physical system of bed divided into layers. The boundary conditions are specified at the bed entrance at any time increment. The initial conditions are specified at bed entrance at any space increments. The discretization of physical system is represented in Fig. 6.6. The value of step length and the time step depends on the number of grid points along the length and time. The bed length is represented in Z-axis, whereas the time of operation is taken along the t-axis.
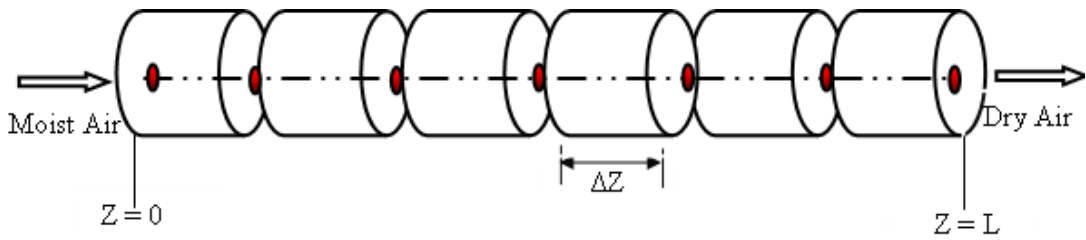
Fig. 6.5 Physical plane illustrating the layers of the desiccant bed.
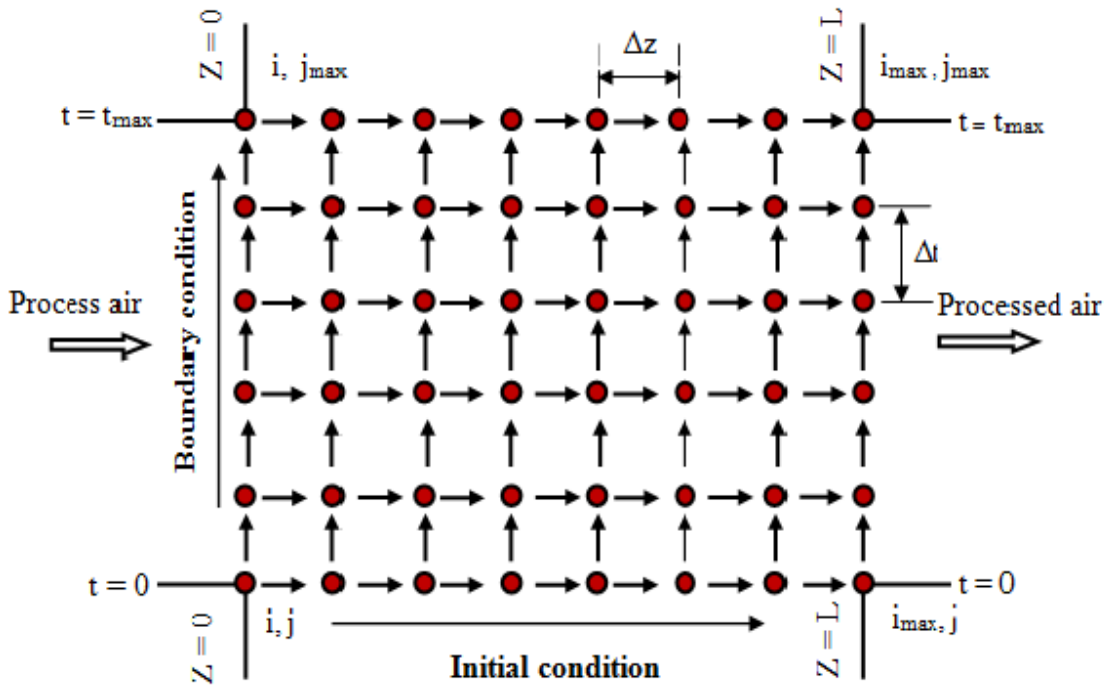
Fig. 6.6 Computational plane for desiccant packed porous bed showing grid structure.

Using the forward time forward space (FTFS) finite difference numerical scheme, the coupled parameters such as process air moisture concentration and equilibrium layer moisture concentration at each node can be obtained by solving the governing differential equations. The governing equations are linear coupled first-order differential equations; a numerical solution is obtained for air moisture reduction at any time step. The velocity and humidity ratio with respect to process air and solution concentration and bed diameter, bed length, bed temperature and bed porosity with respect to desiccant bed is given as input parameters to the mathematical model. By knowing the input conditions at the bottom of the dehumidifier column, outlet

163

conditions at the top are then obtained by carrying out by-stepping in time. Equations (6.35) and (6.36) present the discredited form of governing equations.

$$c_{1e}(i+1,j) = \left((1-dz \times R)c_{1si,j}\right) + \left(dz \times R \times c_{1ei,j}\right) \qquad (6.35)$$

$$c_{1s}(i,j+1) = \left((1-dt \times S)c_{1ei,j}\right) + \left(dt \times S \times c_{1si,j}\right) \qquad (6.36)$$

6.3.1 Auxiliary correlations

The porosity of bed is calculated using the correlation (Pesaran and Mills, 1986)

$$\varepsilon_b = 1 - \frac{\rho_b}{\rho_\phi} \qquad (6.37)$$

The accumulation of moisture in the desiccant pellets is highly dependent upon mass transfer coefficient at air and desiccant interface and specific surface area of the desiccant pellet. The specific surface area is defined as ratio of surface area to volume of desiccant pellet and is given by

$$a = \frac{6(1-\varepsilon_b)}{d_\phi} \qquad (6.38)$$

The amount of area that is total bed surface area available for heat and mass transfer inside the bed for the given volume for moisture transport is evaluated as

$$A_{sf} = a \times 3.142 \times r_b{}^2 \times L \qquad (6.39)$$

The perimeter of the bed is given by

$$P = \frac{A_{sf}}{L} \qquad (6.40)$$

The gas side mass transfer coefficient for intra particle moisture transport is given by (Pesaran and Mills, 1986)

$$K_\omega = 0.704 \times \rho_a \times v \times \mathrm{Re}^{(-0.51)} \qquad (6.41)$$

Based on the vapor pressure, the moisture is transferred from the desiccant surface to the surrounding air or vice versa. The vapor pressure relates the desiccant bed water content and relative humidity of surrounding air with equilibrium humidity ratio. The

164

Antoine equation (Hamed, 2002) is used to obtain isothermal data at different temperatures. The equilibrium vapor pressure p_v for clay-additives- $CaCl_2$ desiccant beds is given by

$$P_v = \exp\left[(a_0 + a_1\tau) - \frac{(b_0 + b_1\tau)}{(T_b + 111.96)}\right]$$

(6.42)

$a_0 = 10.0624, a_1 = 4.4674, b_0 = 739.828, b_1 = 1450.96$ are regression constants. T_b is bed temperature and its range is from 10 to 65°C and τ is concentration and its range is from 0.2 to 0.5. The equilibrium moisture fraction is given by

$$c_{1s} = \frac{0.622 \times P_v}{P_{total} - 0.372 \times P_v}$$

(6.43)

Affinity constant relates equilibrium humidity ratio and water content of desiccant at constant bed temperature. It signifies the ability of desiccant material to attract water vapor to reach a saturation state. The affinity constant as presented by Hamed, 2002 relates solute concentration in solid phase and fluid concentration at equilibrium and is given by

$$K = \left(\frac{q}{c_{1s}}\right)_{T_b=0}$$

(6.44)

The affinity constant relates the desiccant moisture content and the moisture content in the layer surrounding the desiccant pellet. It characterizes the isotherm property of desiccant material. The isotherm correlation, which is required in the theoretical modeling relates the bed water content and equilibrium relative humidity at constant temperature. The moisture ratios in terms of affinity constants are evaluated using Eq. 6.44. Fig.6.7 and 6.8 show the affinity constant for burnt clay- additives - $CaCl_2$ composite desiccants in vertical packed bed and its value varies from 14.09 to 75.34.
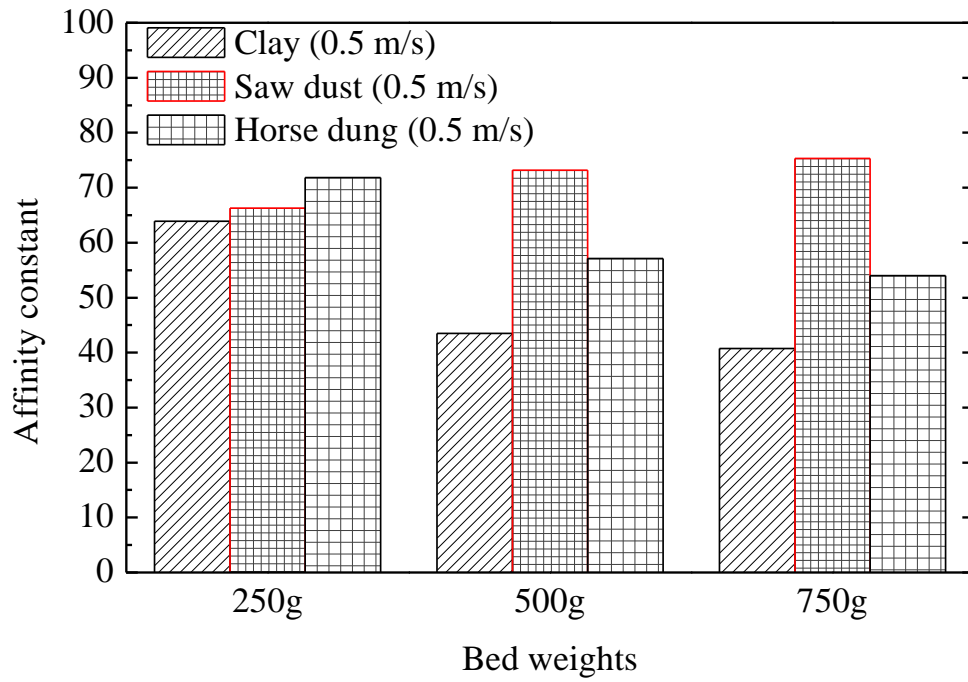
Fig. 6.7 Affinity constant for vertical packed burnt clay - additives - CaCl$_2$ composite desiccant beds at 0.5 m/s.
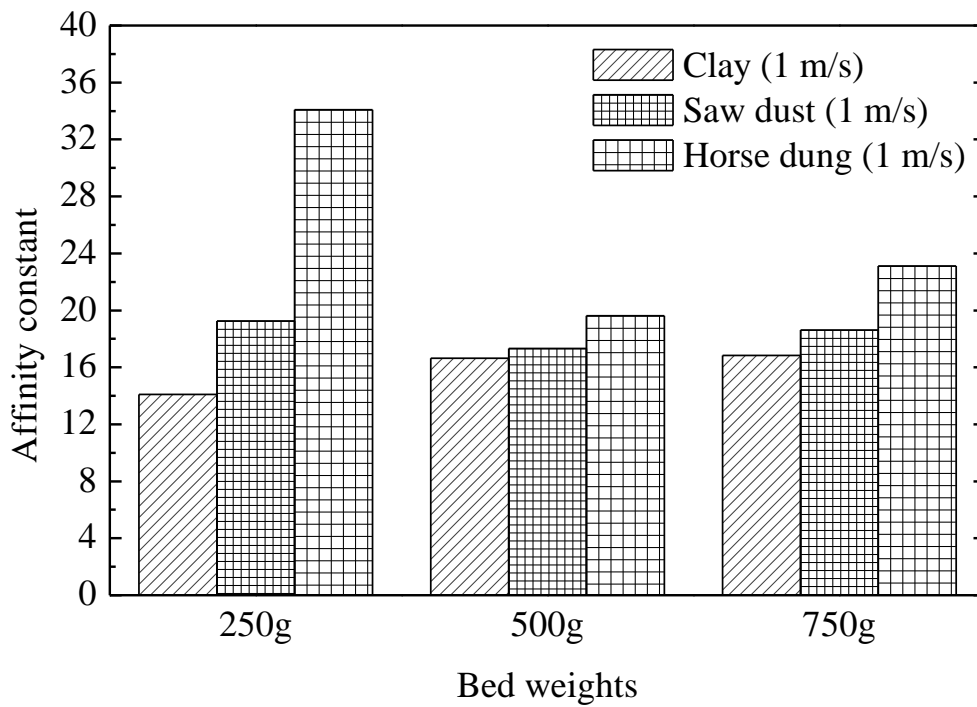
Fig. 6.8 Affinity constant for vertical packed burnt clay - additives - CaCl$_2$ composite desiccant beds at 1 m/s.

The BET analysis reveals higher pore volume for burnt clay- $CaCl_2$ desiccants as compared to burnt clay –additives desiccants. Higher pore volume results in lower values of moisture ratios for burnt clay - $CaCl_2$ desiccant bed. From the experimental results, it is clear that lower moisture ratio for burnt clay - $CaCl_2$ samples bed exhibits higher absorptivity. The affinity constant that is moisture ratios for burnt clay sawdust $CaCl_2$ and burnt clay - horse dung - $CaCl_2$ beds are being higher resulting in lesser absorptivity.

6.4 SOLUTION ALGORITHM AND FLOW CHART

The solution algorithms are illustrated for the governing equations. The sequence of steps required to solve the partial differential equations is given in the form of flow chart and algorithm. The graphical representations of sequence of steps followed to solve the governing equations are shown in Fig.6.9. After defining the input parameters the values of exit air humidity ratio and equilibrium layer moisture content are calculated for each time increment along the length of the bed. Algorithm for evaluating the composite desiccant packed bed performance.

Step 1: Input the values for velocity of air, length, and porosity of bed, mass transfer coefficient, affinity constant, atmospheric pressure and total time of operation.; Step 2: Calculate the time and space increments along time and space axis; Step 3: Define the initial and boundary conditions; Step 4: For each increment in space solve for the properties of bed and condition of air at all the time increments using FTFS numerical scheme.; Step 5: As the time span equals the total time, the properties of air with variation of time can be plotted for the total time specified. The next step in solving the problem is generating the computer code. The code is written in MATLAB using FTFS numerical techniques evaluating the bed and process air heat and mass transfer characteristics.
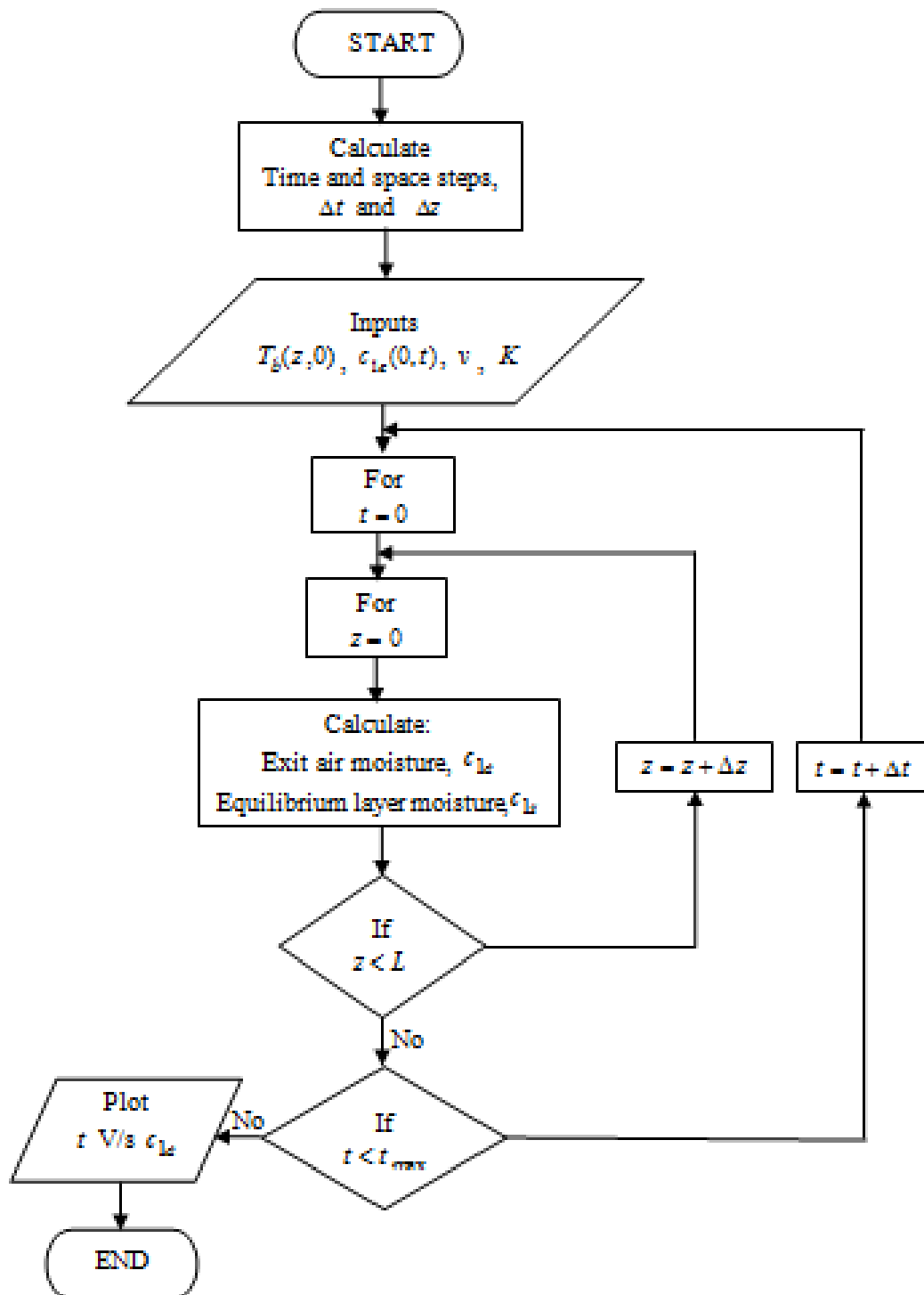
Fig. 6.9 Flow chart to find the performance parameters of the vertical packed desiccant bed.

6.5 COMPARISON OF EXPERIMENTAL AND NUMERICAL RESULTS

The governing equations are solved numerically. The theoretical results are compared with the experimental results of the current study. Table 6.1 lists the experimental parameters for bed and process air as input to the theoretical model.

Table 6. 1 Parameter for bed and process air for the theoretical solution.

Desiccant bed	T_b (°C)	$c_{1e,in}$ (g/kg)	ε_b	K	m_{b_i} (g)	v (m/s)
Burnt clay + CaCl$_2$ [Fig.6.10 (a)]	15.92	3.76	0.40	33.17	500	0.5
Burnt clay + horse dung + CaCl$_2$; [Fig.6.10 (b)]	14.89	3.67	0.32	57.11	500	0.5
Burnt clay + CaCl$_2$; [Fig.6.11(a)]	18.45	3.99	0.35	26.55	250	1
Burnt clay + horse dung + CaCl$_2$; [Fig.6.11(b)]	20.14	3.96	0.33	34.07	250	1
Burnt clay + saw dust + CaCl$_2$; [Fig.6.11 (c)]	11.83	3.67	0.26	66.26	250	0.5
Burnt clay + saw dust + CaCl$_2$; [Fig.6.11 (d)]	16.76	3.66	0.48	42.06	500	0.5

Fig. 6.10 and 6.11 give the comparison between calculated and experimental values for reduction in moisture content of process air. The results are shown with relative error and standard deviation error bars. The RMSE of measured and predicted results of the present theoretical model is in the range of 3.26% to 13.2%. The theoretical results obtained using Eq. (6.35) and (6.36) exhibit reasonably a trend similar to that of the experimental results.
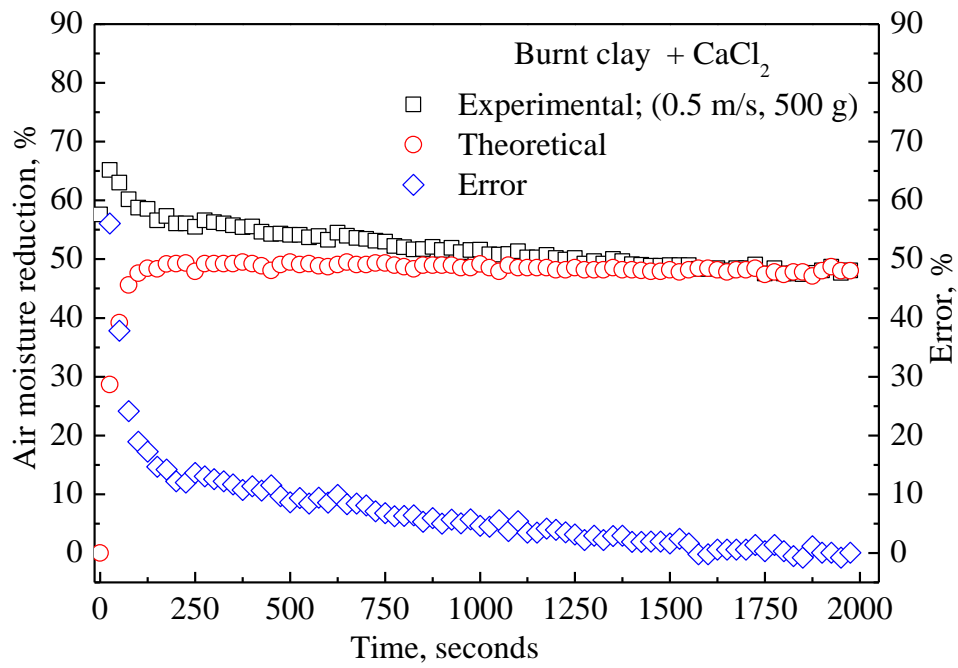
(a)
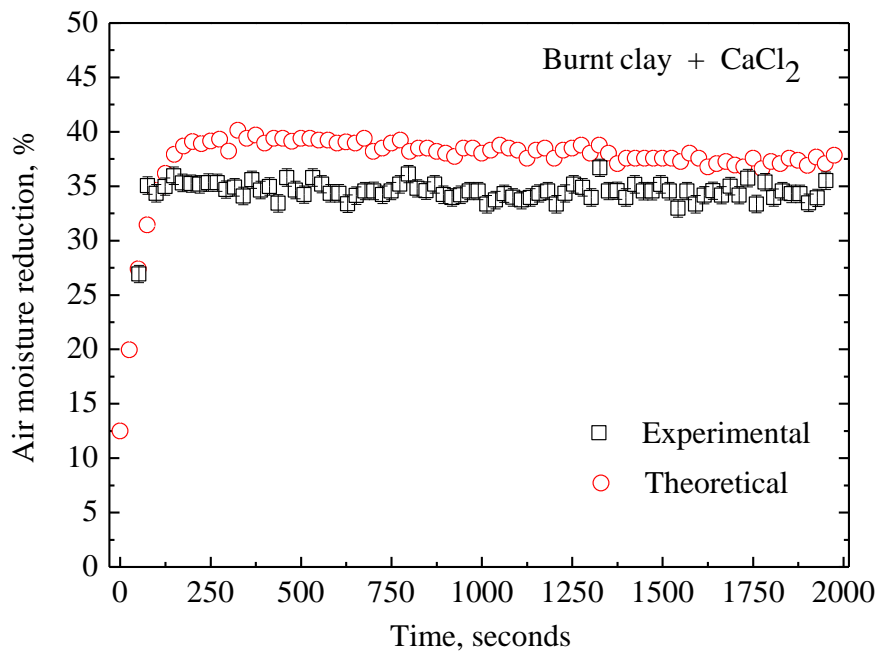
(b)

Fig.6.10 Comparison of measured and predicted results for burnt clay - additives - CaCl$_2$ beds with relative error.
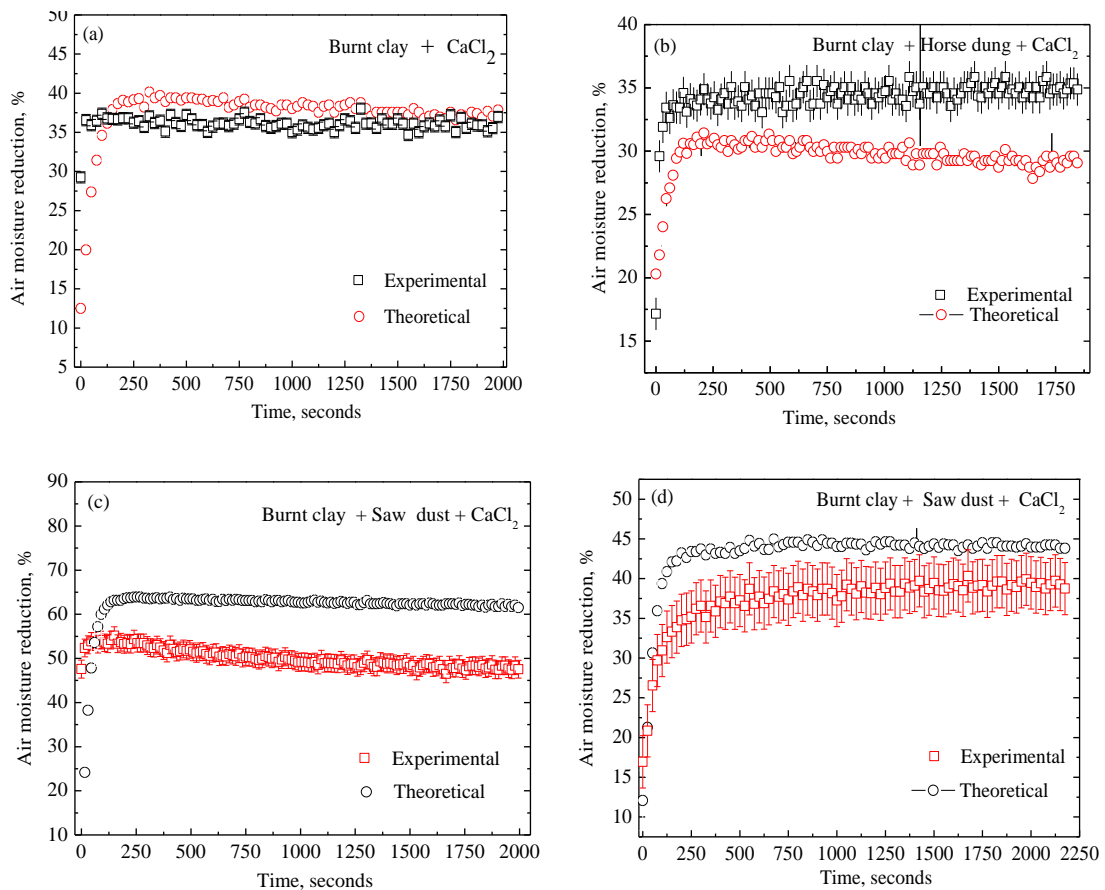
Fig. 6.11 Comparison of measured and predicted results for burnt clay - additives - CaCl$_2$ beds with standard deviation bar**.**

The deviations between experimental and theoretical results may be due to the estimation of affinity constant. It is a function of bed water content and bed temperature. The estimation of bed water content as a function of time is needed. The isotherm property of the desiccant material, which is used in simulation, needs to be developed. In experiments inlet air and exit air relative humidity and temperature are measured by humidity sensor. The theoretical value of reduction in air moisture content is calculated as a function of experimental inlet air humidity ratio and exit air humidity ratio. The data measured by sensors likely to have distortions that reflected in the theoretical results.

6.6 SUMMARY

The heat and mass transfer characteristics of the vertical packed clay-additives-composite desiccant bed are formulated by a set of two governing equations. The derived differential equations are solved numerically using FTFS finite difference method. Isothermal PGC model derived has been employed by including the influencing factors such as interfacial area and mass transfer coefficient. Experimentally estimated bed porosity and affinity constants are used as input parameters in the solution of theoretical gas side resistance model. The results obtained from the theoretical model have been compared with the experimental results. Based on the results obtained the following observations are made,

1. The mass transfer PGC model considers the gas side resistance.

2. The theoretical results for percentage reduction in moisture content show trends similar to that of experimental results of burnt clay additive based $CaCl_2$ composite desiccants. The RMSE errors are higher when the process air velocity is 0.5 m/s.

3. The deviations between experimental and theoretical results are due to the estimation of desiccant material properties such as isotherm and heat of adsorption.

CHAPTER 7

LOW-TEMPERATURE GRAIN DRYER PERFORMANCE COUPLED WITH COMPOSITE DESICCANT BED

7.1 INTRODUCTION

Drying is the process of removal of moisture from the products. Thermal drying is the most commonly used method for drying and preservation of agricultural products, food products, fruits, and vegetables. The most common method employed by farmers in rural areas is sun drying. The absence of control over drying temperature in sun-drying has led to the use of solar dryers. The solar dryers are of passive and active type. Active solar dryers are designed by incorporating external means like fans, blowers for conveying the solar energy in the form of heated air from the collector area to the drying bed. Solar drying, however, can be carried out only during day time. To extend solar drying to off - sunshine hours, thermal storage materials like rocks and phase change materials are employed. However desiccant drying is started off mainly in air conditioning systems to improve air quality for thermal comfort. The focus is to adopt desiccants in drying applications during off-sun shine hours. Desiccant drying enables continuous drying during night times and reduces overall drying time. Solid and liquid desiccants are used in drying systems. In view of this the work presents feasibility of employing low cost fabricated clay additive based composite desiccants for green pea drying in a lab-scale dryer. The experimental analysis of green pea drying with vertical packed burnt clay-50% $CaCl_2$, burnt clay-20% sawdust -50% $CaCl_2$ and burnt clay - 20% horse dung -50% $CaCl_2$ composite desiccant is discussed.

7.2 CONSTRUCTION OF EXPERIMENTAL SETUP

The experimental methodology includes construction and setting the desiccant drying /aeration system for green pea (Pisum sativum). Instrumentation for the measurement

of experimental parameters related to process air, desiccant bed, and grain dryer. The schematic of the experimental set up is shown in Fig. 7.1(a). The experimental set up consists of mainly the reciprocating air compressor (1), vertical acrylic tube as desiccant bed (3), drying chamber (4) consists trays (T1 and T2) and instrumentation.
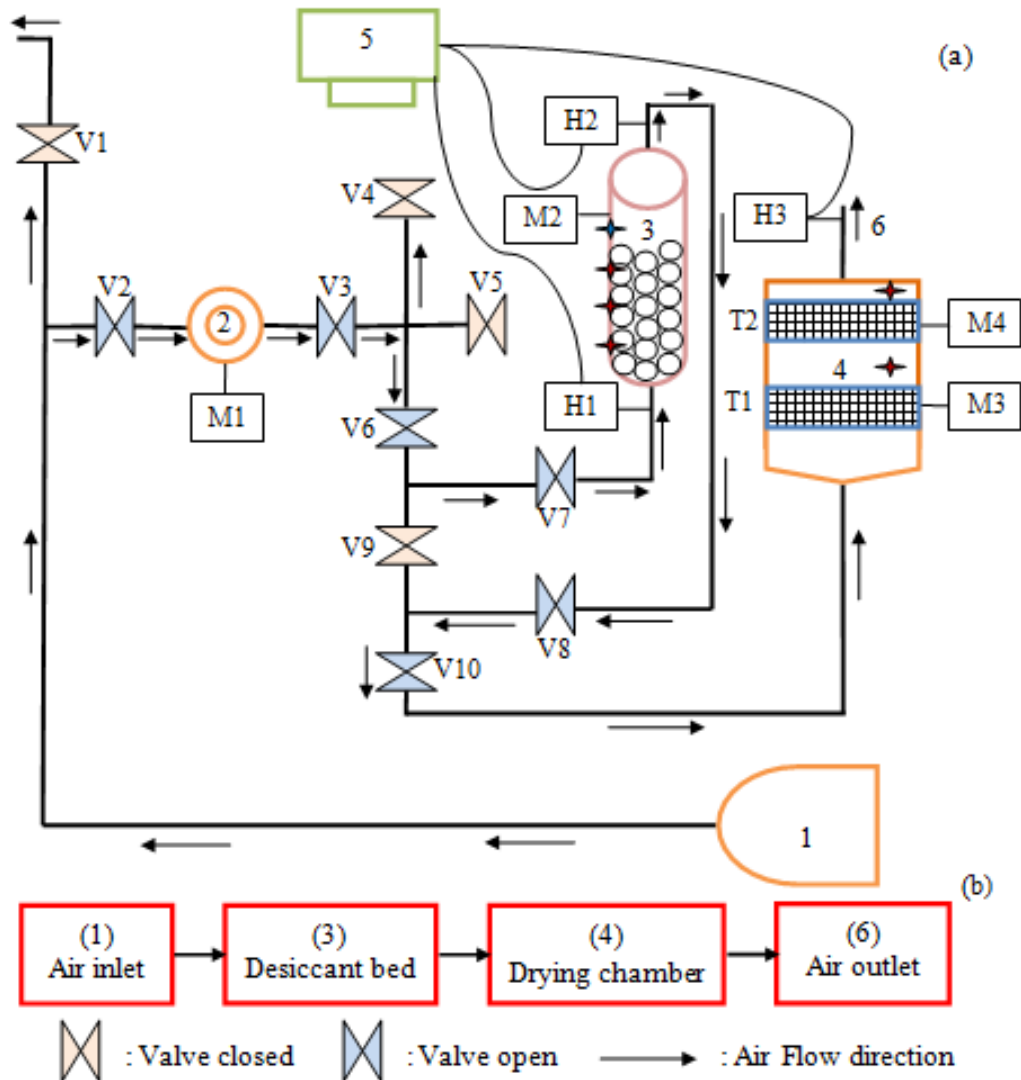
Fig. 7.1 (a) Schematic view of desiccant bed coupled with grain dryer. (b) Airflow diagram.

The reciprocating air compressor has a rating of 2.2 kW with a free air delivery up to 15 m³/h. The vertical acrylic tube has the following dimensions, 0.054 m outside diameter and 0.05 m inside diameter, length of 0.07 m for containing the desiccant

pellets. A perforated sheet is provided at the bottom end of the tube that enables to hold the desiccant pellets.

The pictorial view of the experimental set up is shown in Fig 7.2. Prototype drying cabinet of dimensions 0.43 m × 0.41m × 0.54 m (Length × Width × Height) is fabricated from 19 mm thick mild steel sheets. The drying trays are made using wire mesh placed inside the drying chamber with dimensions of 0.31×0.31 m^2 to hold the wet grains which are subjected to drying. The diameter of perforated holes is of 0.3 mm, and the holes are arranged at a pitch of 7 mm along vertical and horizontal directions. The distance between the two trays is 0.10 m. The bottom tray (T1) is at a distance of 0.45 m from the dryer inlet. The distance between the top tray (T2) and exit of dryer is 0.27 m. The air flows vertically through the grain samples.
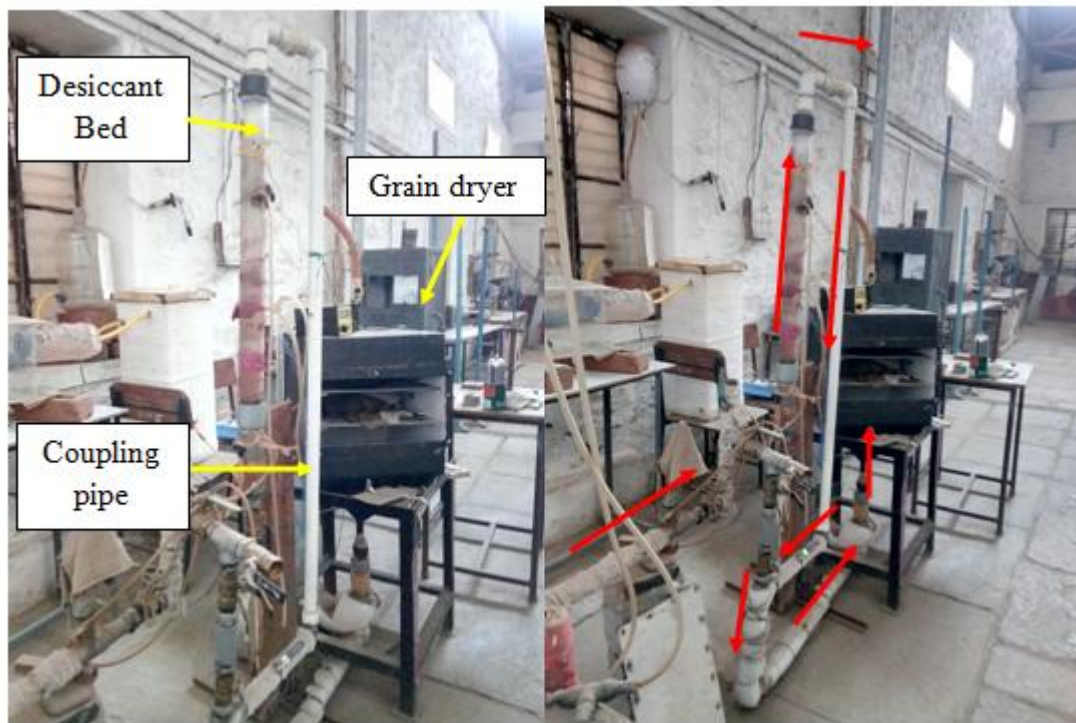
Fig. 7.2 Photograph of experimental arrangement for dry coupled with the desiccant bed.

The drying trays can be easily removed to load and unload the drying products from the door, which is provided on the front side of the drying chamber. At the top of the drying chamber, an air gap of 0.12 m is provided with a GI pipe that exits humid air to

175

the atmosphere. Manually operated gate and ball valves (V1 to V10) are provided to regulate the process airflow. The airflow diagram of the drying system is shown in Fig 7.1 (b) wherein the compressed air is ducted to the drying chamber through the desiccant bed. The warm dehumidified air leaving the desiccant bed transfers its sensible heat to the grains on the trays and finally leaves at the top of drying cabinet to atmosphere under forced circulation mode.

7.2.1 Desiccants, instrumentation details, and theoretical calculations

The materials employed for the experiments are naturally available transported clay, sawdust and horse dung additives and 50% $CaCl_2$ solution. The clay and additives are collected from a local pot maker. The additives are mixed separately with clay in the proportion of 20% by weight. Clay and clay additives are manually molded to spherical shape (10 mm diameter). They are then heated to 500°C. The burnt clay and burnt clay-additives desiccants are now impregnated with $CaCl_2$ liquid desiccant of 50% concentration. Thus the composite desiccants are produced. The fresh green peas for drying experiments are purchased from a local dairy. Drying experiments are carried out to study the green pea dryer performance with three vertical packed composite desiccant beds. (a) dryer coupled with burnt clay - 50% $CaCl_2$ desiccant bed (b) dryer coupled with burnt clay - 20% sawdust - 50% $CaCl_2$ desiccant bed and (c) dryer coupled with burnt clay - 20% horse dung - 50% $CaCl_2$ desiccant bed. The relative humidity and temperature of process air at desiccant bed inlet (H1), exit (H2) and dryer exit (H3) were measured using Rotronic hygroflex humidity sensor. The humidity sensor has 0 to 100% range on relative humidity and -40°C to 85°C range on temperature. The accuracy of the instrument for RH is ±1%, and for temperature it is ±0.2°C. A microcontroller board (Arduino) is employed to interface the humidity sensors to the computer (5). The voltage values corresponding to relative humidity and temperature are written to a text file for every second with the execution of microcontroller code. Chromel - Alumel (K-type) thermocouples (✚) are used to measure the desiccant bed temperature at four positions along the axial direction of the bed. The first thermocouple is located at a distance of 0.06 m from the desiccant bed inlet. The axial distance between the thermocouples is 0.08 m along the vertical

tube. The temperature inside drying chamber is measured using another two Chromel - Alumel thermocouples. Desiccant bed and dryer temperature measurement locations are shown by filled star symbol as shown in Fig 7.1(a). The bed temperatures are measured at an interval of every 5 min. The pressure drop across orifice meter and through the desiccant bed and the dryer are measured by U - tube manometers (M1, M2, M3, and M4). The moisture content of desiccant bed and green pea grains before and after process are measured using an electronic balance with an accuracy of 0.01 g. The mass flow rate of process air measured using calibrated orifice meter (2) is 0.003697 kg/s. Experimental runs were conducted for 500 g of green pea with maximum 750 g of desiccant bed mass.

7.2.2 Process air, desiccant bed, and dryer grain performance indices

The performance parameters are calculated using the following equations. In estimating the performance parameters, the pipe losses are neglected. The moisture reduced from the process air by the desiccant bed and moisture transported to the process air from the moist grains in dryer is calculated on wet basis of process air. The moisture absorbed by the desiccant bed per unit weight of process air on wet basis is expressed as

Moisture transferred to desiccant bed, $M_{db} = \left(\dfrac{S_i - S_e}{S_i} \right) \times 100$ (7.1)

The variation of moisture removed from the green pea grains per unit weight of process air on a wet basis is given as

Moisture removed from grain bed, $M_{gb} = \left(\dfrac{S_e - S_i}{S_e} \right) \times 100$ (7.2)

The enthalpy of humid air can be calculated using the following equation (Hamed et al., 2013)

Enthalpy of humid air, $h = (1005.22 + 0.02615 T_a) T_a + S(2500800 + 1868 T_a)$ (7.3)

The overall drying rate in g/min in drying the product is given by

177

Drying rate, $\dot{d} = \dfrac{\left(m_{gb_i} - m_{gb_f}\right)}{t}$ (7.6)

Where $\left(m_{gb_i} - m_{gb_f}\right)$ is the moisture content removed from the grain product and t is drying time in minutes.

7.3 RESULTS AND DISCISSIONS

Experiments are conducted to determine the effectiveness of heat-treated clay and clay additives composite desiccants in drying of green pea grains. The experimental runs for differing desiccant bed mass (300 g to 700 g) are conducted at a desiccant bed inlet air velocity of 1.5 m/s. The amount of surface area A_{sf} (m^2) available for the given volume of bed for moisture transport/heat transfer is given by:

$A_{sf} = (\text{Number of desiccants}) \times (\text{Surface area of each desiccant})$ (7.7)

$A_{sf} = \left(\dfrac{\text{Mass of desiccant bed}}{\text{Volume of each desiccant}}\right) \times (\text{Surface area of each desiccant})$ (7.8)

$A_{sf} = \left(\left(m_b\right) \Big/ \left(\rho_b \times \frac{4\pi r_\phi^3}{3}\right)\right) \times 4\pi r_\phi^2$ (7.9)

$A_{sf} = \dfrac{\left(6 \times m_b\right)}{\left(\rho_b \times d_\phi\right)}$ (7.10)

The mass of the desiccant bed m_b (kg) is given by

$m_b = \rho_b(1-\varepsilon)V_b$ (7.11)

Substituting Eq. (7.11) in Eq. (7.10), the total surface area of the bed available for mass and heat transfer is given by

$A_{sf} = \dfrac{6\left(1-\varepsilon_b\right)}{\left(d_\phi\right)}V_b$ (7.12)

The Ergun equation is employed to estimate the pressure drop ΔP (Pa) through the desiccant beds and is given by (Sabri., 1952)

178

$$\Delta P = 150 \mu_a \frac{\left(1-\varepsilon_b\right)^2 L}{\varepsilon_b{}^3 d_\phi{}^2} v + 1.75 \frac{\left(1-\varepsilon_b\right) L \rho_a}{d_\phi \varepsilon_b{}^3} v^2 \qquad (7.13)$$

Table 7.1 details the experimental parameters for the dryer with clay-based $CaCl_2$ composite desiccant beds. From the table it is clear that for the same bed masses, the bed surface area available for moisture transport for clay - additives based composite desiccant beds are higher as compared to clay-based composite desiccant beds. The increase in surface is due to higher bed volumes per unit mass of desiccant bed. For the same bed masses higher length of bed that prevails in additive based desiccant beds results in higher surfaces area. For the same bed masses of 500 g, pressure drop through the additive based composite desiccant beds decreases by 56% as compared to clay - $CaCl_2$ bed. For the same diameter to length (D/L) ratio of 0.18, the pressure drop through the vertical packed clay additives beds is 66% lower than vertical packed clay-based desiccant beds. Ergun equation relates the bed pressure drop with bed porosity. For the fixed values of desiccant diameter, bed length, process fluid velocity, density, and viscosity pressure drop inversely proportional to porosity of bed. The porosities estimated for clay - $CaCl_2$, clay - horse dung - $CaCl_2$ and clay - sawdust - $CaCl_2$ composite desiccant beds are 0.70, 0.86 and 0.87. The higher bed porosities prevailing in clay- additives composite desiccant bed results in lower pressure drop.

As humid air comes in contact with the desiccant bed transfers its moisture content to dry desiccant bed. The dehumidification by desiccant releases heat of adsorption. The warm dehumidified air exiting the desiccant bed is conveyed into the dryer containing grains on the bottom and top trays. The higher enthalpy content of air removes more moisture from the grains contained in bottom tray. The difference in amount of moisture removed from top and bottom trays shows nonuniform drying. Table 7.2 lists average values of humidity ratio of process air entering into desiccant bed, entering into the dryer and leaving the dryer. The average decrease in process air humidity ratio on wet basis for 700 g clay - $CaCl_2$, clay - horse dung - $CaCl_2$ and clay - sawdust - $CaCl_2$ composite desiccant beds are 11.91%, 23.78% and 21.76% and the

corresponding average enthalpy (heat content) of air entering into the dryer are 1.46, 2.46 and 2.38 kJ.

Table 7.3 reveals that the average process air temperatures exiting the three clay and clay - additives desiccant beds, entering and exiting the dryer. The average increase in clay and clay-additives desiccant bed ranges from 29 to 34°C. The increase in bed temperatures is due to higher vapor pressure difference from process air to bed surface. Higher vapor pressure difference results in higher mass transfer rates that lead to adsorption heat release. The dehumidified warm air enters the dryer at temperatures ranging from 21 to 25°C that enables low-temperature constant drying process. Comparing the enthalpy content of process air (Table 7.3) and moisture removed from the trays (Table 7.2) shows the effectiveness of clay composite desiccants in drying of green pea grains

Table 7.1 Experimental conditions and calculated results for dryer coupled with clay and clay - additives - CaCl$_2$ composite desiccant bed.

Type of bed	Composite desiccant bed parameters					Grain dryer		Exp Runs
	Bed mass (g)	D/L ratio	Surface area (m^2)	Pressure drop (kPa)	Weight gain (g)	Moisture removed (g)		
						Tray -T1	Tray - T2	
Burnt clay - CaCl$_2$	300	0.40	0.045	20.95	1.31	12.91	10.75	R1
	500	0.19	0.085	42.91	1.85	5.97	4.25	R2
	550	0.19	0.094	44.26	1.19	9.89	3.44	R3
	600	0.18	0.097	45.93	1.71	10.02	6.78	R4
	650	0.16	0.112	52.97	1.66	7.39	5.02	R5
	700	0.15	0.117	55.32	1.28	6.75	8.33	R6
Burnt clay - horse dung - CaCl$_2$	300	0.23	0.061	12.68	4.71	9.79	7.23	R7
	350	0.21	0.067	13.94	3.82	7.21	5.18	R8
	400	0.18	0.076	15.96	3.89	10.05	6.59	R9
	450	0.16	0.083	17.40	4.80	9.89	4.8	R10
	500	0.15	0.091	19.01	1.64	11.71	6.66	R11
	700	0.10	0.135	28.23	1.35	10.63	8.69	R12
Burnt clay - saw dust - CaCl$_2$	300	0.22	0.063	13.04	2.33	4.66	4.54	R13
	350	0.21	0.067	13.77	3.39	10.54	7.26	R14
	400	0.18	0.076	15.76	3.08	9.72	6.35	R15
	450	0.16	0.086	17.68	6.57	8.21	6.27	R16
	500	0.15	0.091	18.70	2.47	12.05	9.44	R17
	700	0.10	0.132	27.21	2..92	7.35	4.92	R18

181

Table 7. 2 Average humidity ratio and heat content of process air for clay - additives - CaCl$_2$ composite desiccant beds.

Type of bed	Mass of bed (g)	Average humidity ratio of process air entering desiccant bed (g of water /kg of dry air)	Average humidity ratio of process air exiting desiccant bed or entering the dryer (g of water /kg of dry air)	The average increase in humidity ratio of process air exiting dryer (g of water /kg of dry air)	Enthalpy (heat content) of air entering dryer (kJ)		
					Maximum	Minimum	Average
Burnt clay - CaCl$_2$	300	4.65	4.59	7.16	3.43	0.030	0.12
	500	3.64	3.26	5.26	3.79	0.084	0.95
	550	4.67	4.28	6.74	3.45	0.23	0.96
	600	4.99	4.66	8.21	2.77	0.081	0.85
	650	3.79	3.43	7.73	4.77	0.019	0.90
	700	4.87	4.29	8.66	6.23	0.61	1.46
Burnt clay - horse dung - CaCl$_2$	300	4.61	3.99	9.28	4.76	0.45	1.57
	350	4.29	3.65	6.76	4.19	0.76	1.64
	400	4.47	3.77	6.65	5.75	0.93	1.76
	450	4.12	3.32	9.48	4.92	0.69	2.01
	500	4.33	3.88	6.81	3.48	0.69	1.11
	700	4.12	3.14	6.10	6.53	1.34	2.46
Burnt clay - saw dust - CaCl$_2$	300	4.21	4.09	6.62	2.69	0.019	0.29
	350	4.37	3.79	6.38	4.76	0.45	1.44
	400	3.68	3.13	6.52	4.12	0.66	1.38
	450	4.36	3.72	6.49	5.05	0.22	1.59
	500	4.09	3.63	6.61	5.01	0.16	1.14
	700	4.32	3.38	7.12	7.64	0.11	2.38

Table 7.3 Average temperatures of process air and bed temperatures for clay - additives - $CaCl_2$ composite desiccant beds.

Type of bed	Mass of bed (g)	The average temperature of process air entering desiccant bed (°C)	The average increase in temperature of air entering dryer (°C)	The average decrease in temperature of air exiting dryer (°C)	Average bed temperature (°C)		
					Maximum	Minimum	Average
Burnt clay - $CaCl_2$	300	23.49	24.72	21.70	31.33	29.88	30.89
	500	17.03	18.16	15.18	32.83	29.48	30.63
	550	23.03	24.75	20.20	32.66	30.10	30.48
	600	23.13	24.73	22.87	32.75	30.43	31.56
	650	19.90	21.89	20.61	30.93	29.40	29.51
	700	21.74	23.37	23.80	31.83	29.93	30.89
Burnt clay - horse dung - $CaCl_2$	300	22.46	24.73	24.07	31.85	29.88	30.67
	350	20.71	22.69	19.36	32.03	29.88	30.66
	400	21.57	24.26	20.00	33.53	30.53	31.65
	450	19.49	22.23	23.89	33.28	30.05	31.27
	500	22.97	25.15	21.66	31.03	29.73	30.26
	700	21.64	25.05	19.99	33.10	30.65	31.63
Burnt clay - saw dust - $CaCl_2$	300	22.58	24.08	20.85	30.88	29.70	30.14
	350	22.49	24.47	19.34	32.03	30.05	30.77
	400	18.95	21.33	18.64	31.28	29.33	29.97
	450	21.82	24.37	19.46	32.05	30.00	30.68
	500	21.89	24.42	20.69	31.63	29.80	30.00
	700	20.33	23.86	19.51	32.80	30.5	31.70

7.3.1 Analysis of moisture reduction and enthalpy of process air for burnt clay additives - CaCl₂ composite desiccant beds.

Figure 7.3 (a) and (b) shows the comparison of transient variation of air moisture reduction and enthalpy of air entering into the dryer.
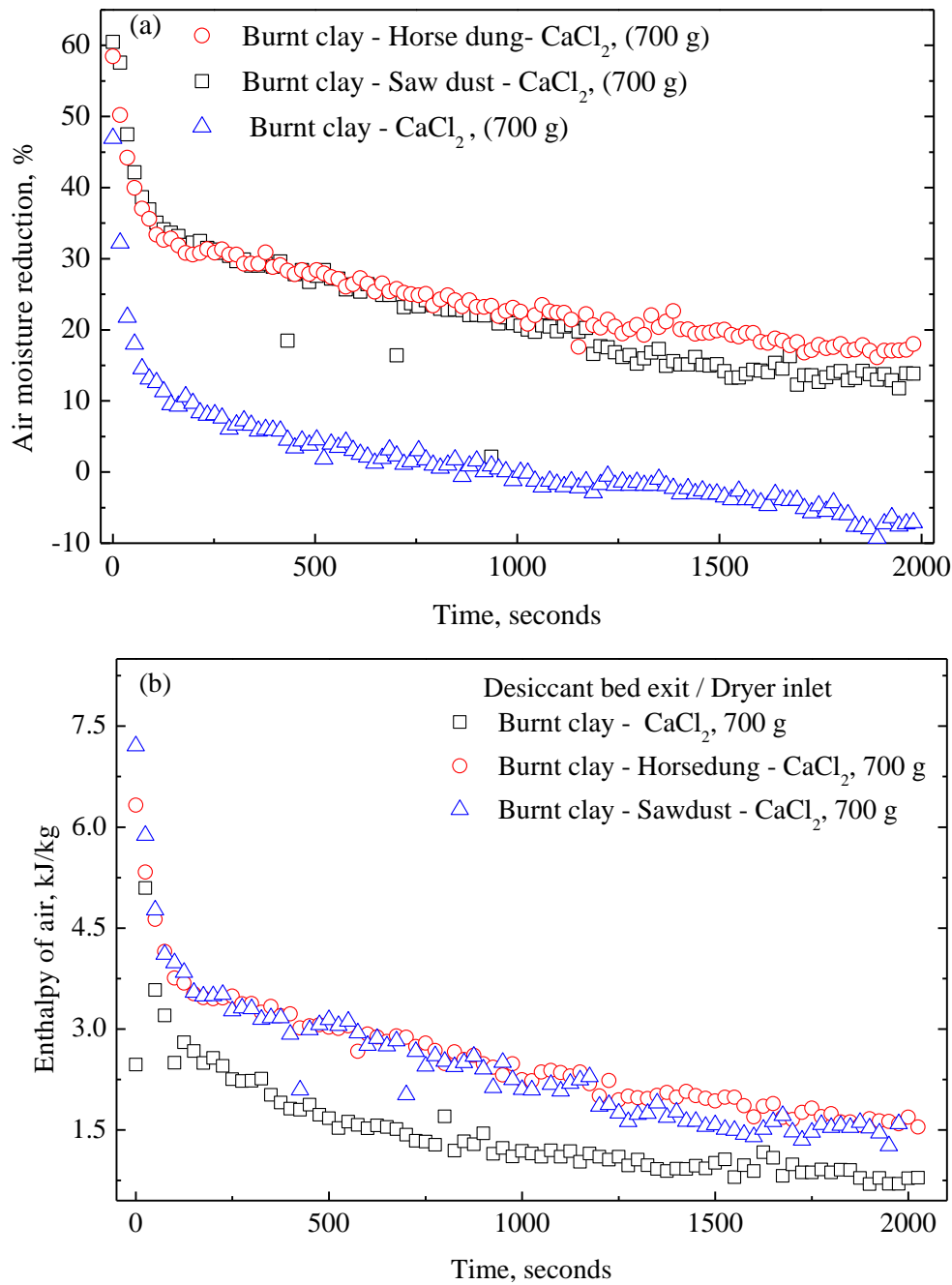
Fig. 7.3 Transient variation of (a) moisture reduction and (b) enthalpy of process air for experimental runs R6, R12 and R18.

Air moisture reduction is estimated using Eq. (7.1) and enthalpy of air exiting the desiccant bed is calculated using Eq. (7.3). For the same bed masses, higher moisture reduction rates are noted for clay - additives - $CaCl_2$ composite desiccant beds. For the identical desiccant bed masses, bed length of 0.33 m and 0.50 m are noted for clay - $CaCl_2$ and clay - additive - $CaCl_2$ desiccant beds respectively. The higher bed length of clay additives desiccant beds enables more bed surface area for process air dehumidification. The higher bed length per unit volume of bed offers higher residence time for the air to pass through the interstitial spaces of bed. As presented in Fig.7.3 (a) for the processing time below 250 s owing to initial dryness of bed moisture reduction increases up to 60% for clay- additives based desiccant beds. With progress in process time the bed water content increases which in turn decrease moisture uptake capacity of bed. The transient variation of enthalpy of air exiting the desiccant bed and entering into dryer is shown in Fig. 7.3 (b). The enthalpy of air is calculated using Eq. (7.3). For the beds having higher surface area, higher will be the moisture absorptivity. Higher absorptivity of additives desiccant beds releases higher heat of adsorption. Due to this the bed temperature increases and subsequently increases temperature of air leaving the desiccant bed.

For the same D/L (bed diameter to bed length) ratios of 0.16 transient variation of moisture reduction and enthalpy of air are graphically presented in Fig.7.4 (a) and (b). As compared to clay-based desiccant bed, additive based desiccant beds show slightly higher absorptivity. The peak values of moisture reduction and heat content are observed within 250 s of process time. From that onwards the increase in bed water content counteracts the adsorption heat and thereby enthalpy of air decreases. From the results of same bed masses (Fig.7.3 (b)) and similar D/L ratios (Fig.7.4 (b)) it is observed that enthalpy levels of process air are higher in clay-additives based composite desiccants. As compared D/L ratios process air moisture reduction and humidity reduction are high when identical desiccant bed masses are considered. For the same bed masses the numbers of desiccants contained in the vertical bed are more in clay-additives composite desiccant beds. The lesser density of additives desiccants enables higher bed length increased by higher numbers. The higher number of pellets for the identical cross-section area of bed yields higher bed absorptivity.

185
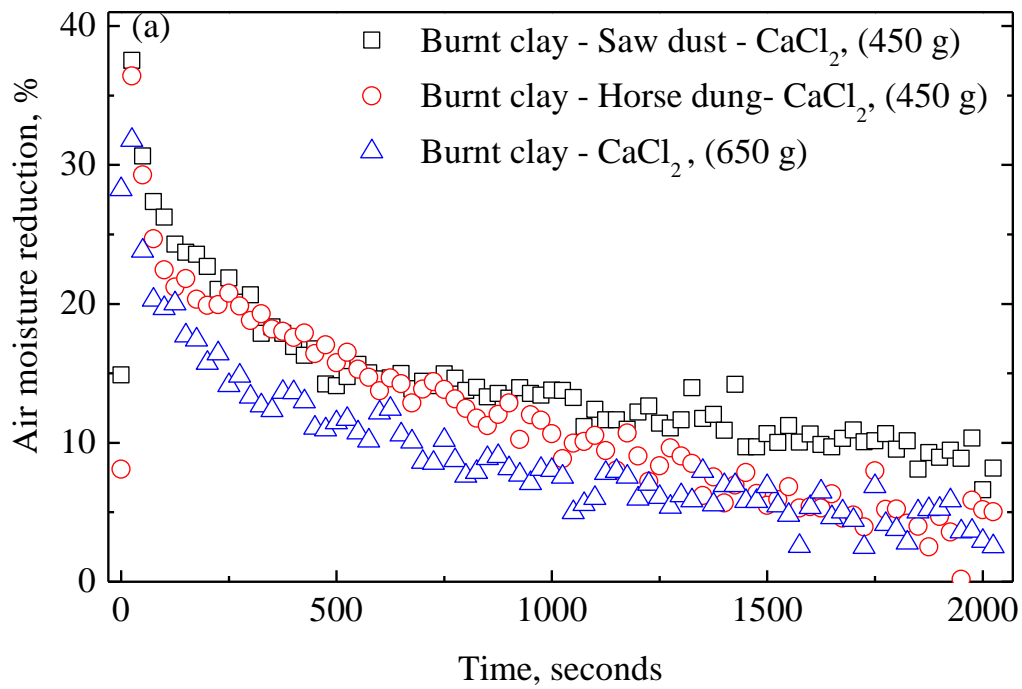
(a)
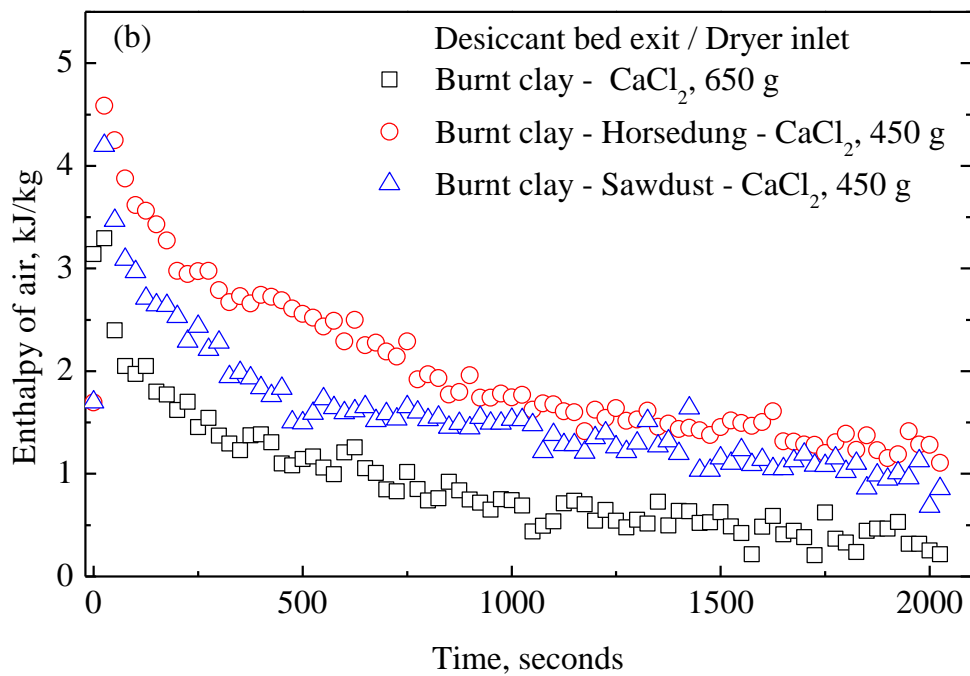
(b)

Fig. 7.4 Transient variation of (a) moisture reduction and (b) enthalpy content of process air for experimental runs R5, R10 and R16.

186

The transient variation net moisture content of air transferred to bed and enthalpy added to the air in adsorption are illustrated in Fig. 7.5(a) and (b).
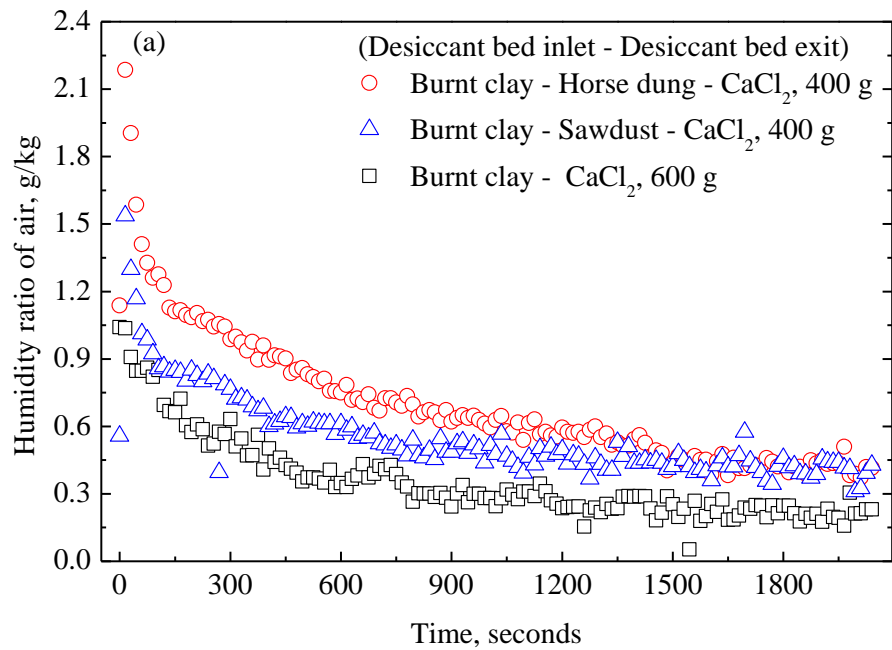
(a)
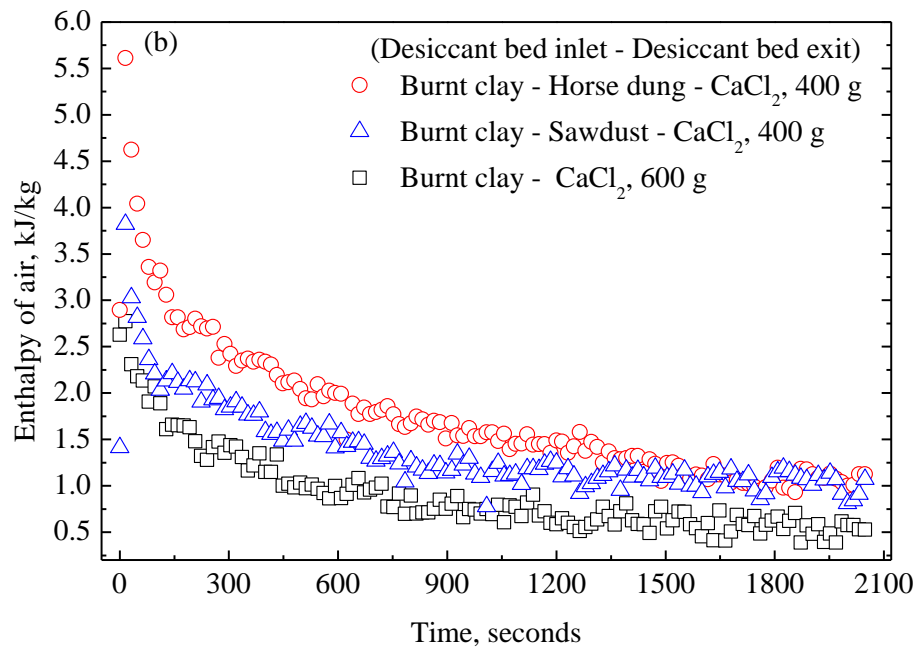
(b)

Fig. 7.5 Transient variation of net (a) humidity ratio and (b) enthalpy of process air for experimental runs: R4, R9, R15.

187

The results are compared for the same D/L ratio of 0.18. The moisture and enthalpy transferred are evaluated by using bed inlet and exit air specific humidity and enthalpy. During the initial period of adsorption, the higher decrease in net air humidity ratio indicated higher potential of clay and clay additives composite desiccant beds towards moisture adsorption. The adsorption heat released during the initial period of operation results in higher enthalpy transferred to process air from the desiccant beds. With advancement in time moisture transferred to the bed and heat transferred to the air decreases.

7.3.2 Analysis humidity ratio and temperature of process air leaving clay and clay - additives based $CaCl_2$ composite desiccant beds and grain dryer

Process time variation of exit air humidity ratio and temperature with respect to desiccant bed inlet air humidity ratio and temperature for desiccant beds and grain dryer are depicted in Figs.7.6 (a) to (f). The process air having average specific humidity of 4.66, 4.4, 4.32 g of water vapor / kg of dry air and temperature of 23.02, 21.57, 20.3°C is introduced into the vertical packed burnt clay - $CaCl_2$, burnt clay-horse dung - $CaCl_2$ and burnt clay - sawdust - $CaCl_2$ composite desiccant bed mass of 550 g, 400 g, and 700 g. The superficial velocity of air is 1.5 m/s. As the feed air comes in contact with the desiccant bed and passes through the bed and transfers its moisture to the dry desiccant bed. Within the process time period of 500 s, the process air experiences maximum reduction in its moisture content. From 500 s onwards the process of adsorption weakens and moisture uptake capacity of bed decreases and subsequently the exit air humidity ratio increases and nears the bed inlet air humidity ratio. As process of adsorption in early stages is high enough to increase the bed temperatures and subsequently increases the exit temperatures of air. The effect of heat of adsorption is significant within 500 s. The heat of adsorption which reflects the enthalpy variation before and after adsorption is calculated using Clausius-Clayperon equation. The average bed temperatures measured for 550 g burnt clay-$CaCl_2$, 400 g burnt clay - horse dung - $CaCl_2$ and 700 g burnt clay - sawdust - $CaCl_2$ are 30.48, 31.65 and 31.07°C. The desiccant bed enthalpy variation in terms of heat

adsorption estimated for the respective composite desiccant bed masses are 28.97, 29.04 and 29.05 kJ/kg.
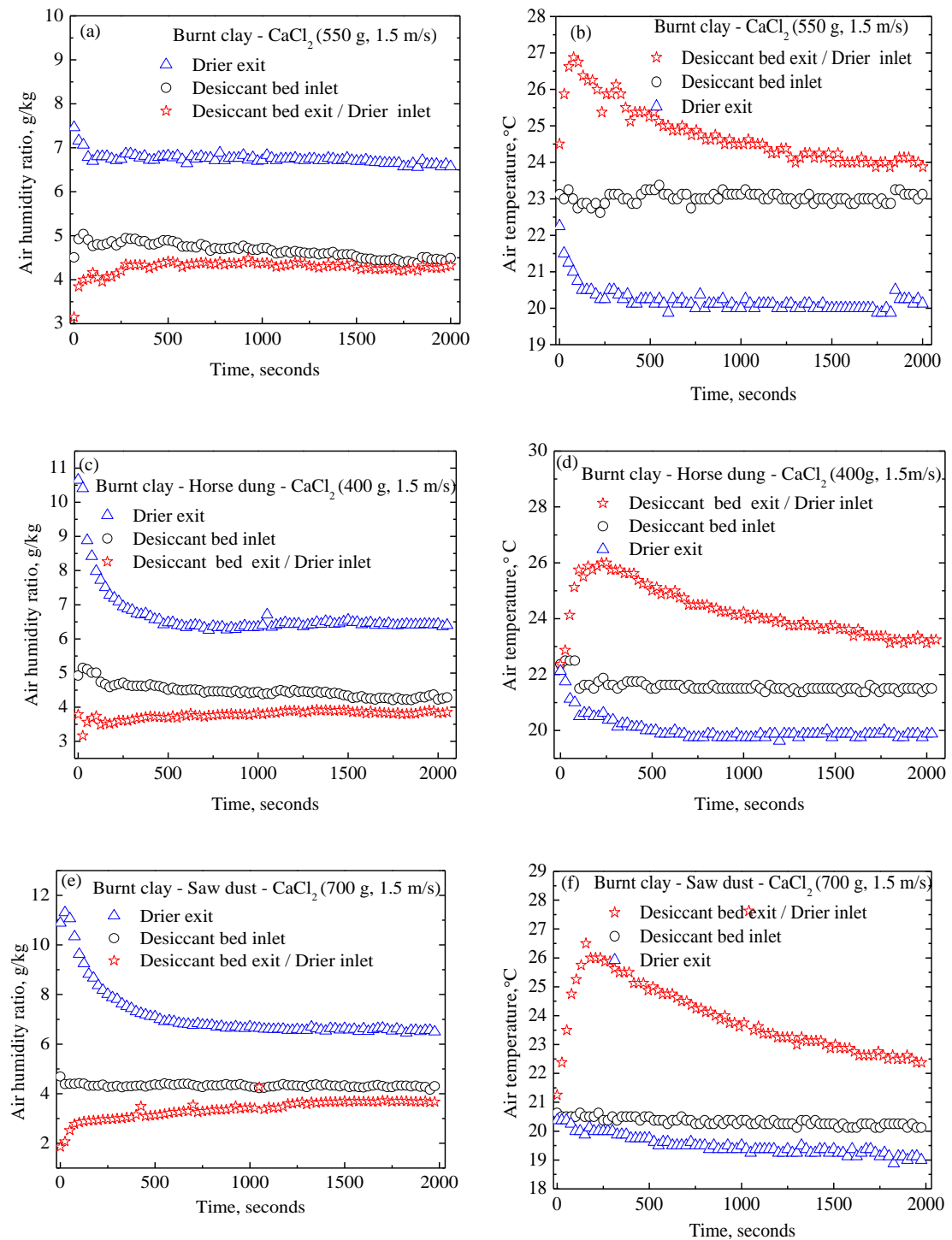
Fig.7.6 Transient variation desiccant bed and dryer exit air humidity ratio and temperature for experimental runs R3 (a, b), R9 (c, d) and R18 (e, f).

The warm dehumidified air exiting the clay composite desiccant beds is conveyed into the grain dryer. The warm dehumidified air comes in contact with the wet grains which are spread on the trays of the dryer. The heat energy transferred to grains extracts moisture and then exits the dryer with higher humidity and lower temperature levels. Owing to heat of adsorption in the early stages of process moisture removal from the grains is more significant in the early stages of drying. The process air after drying leaves the dryer at higher humidity levels than desiccant bed inlet air humidity levels. The temperatures of air leaving the dryer are lower than the desiccant bed inlet air temperatures. The total water content removed from the grains contained on the bottom and top trays are 13.33 g, 16.64 g and 12.27 g for vertical packed 550 g burnt clay - $CaCl_2$, 400 g burnt clay - horse dung - $CaCl_2$ and 700 g burnt clay - sawdust - $CaCl_2$ composite desiccants respectively.

Figure 7.7 (a), (b) and (c) presents the transient variation of net moisture uptake from grain bed by drying air and moisture uptake by desiccant bed from dehumidified process air. The moisture reduction of air is a function of desiccant bed inlet air relative humidity, temperature, bed mass, bed inlet air velocity, and atmospheric conditions. Moisture uptake is a function of dryer inlet air humidity, temperature, mass flow rate, grain initial moisture content. For the 550 g of clay - $CaCl_2$ bed, time variation of moisture content is illustrated in Fig. 7.7 (a). During initial period of adsorption the higher percentage of moisture removal by the desiccant bed results in higher moisture uptake from the grain samples and subsequently increases the dryer exit air moisture content. The whole drying process can be divided into falling rate and constant rate drying periods. The falling rate drying period is of short duration (0 to 500 s) wherein grain bound moisture is likely to be removed. From 500 s onwards constant rate drying process prevails wherein grain surface moisture gets removed. The minimum and maximum moisture content of air leaving the dryer within 500 s are 57.81% and 33.66% for 550 g bed mass. From 500 s onwards the moisture content of process air leaving the desiccant bed and dryer remains steady. The transient variation of moisture content of air exiting the bed mass of 400 g burnt clay - horse dung - $CaCl_2$ desiccant bed and dryer is graphically presented in Fig.7.7 (b).
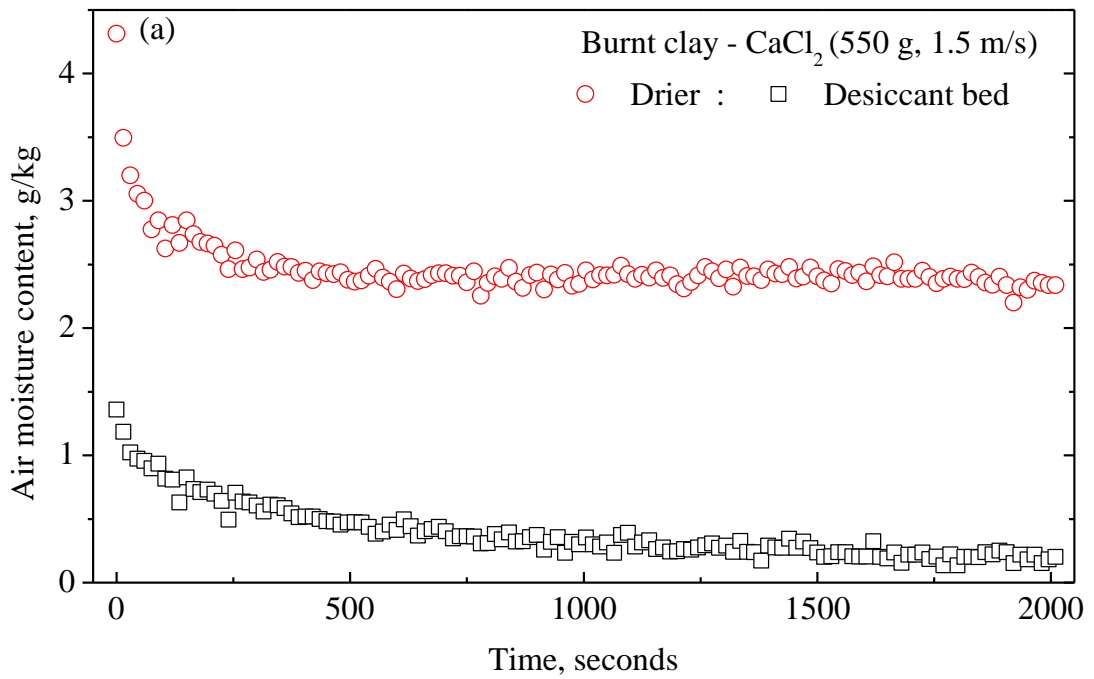
Fig .7.7 (a) Time variation of moisture content of process air exiting the desiccant bed and grain dryer for experimental run R3.
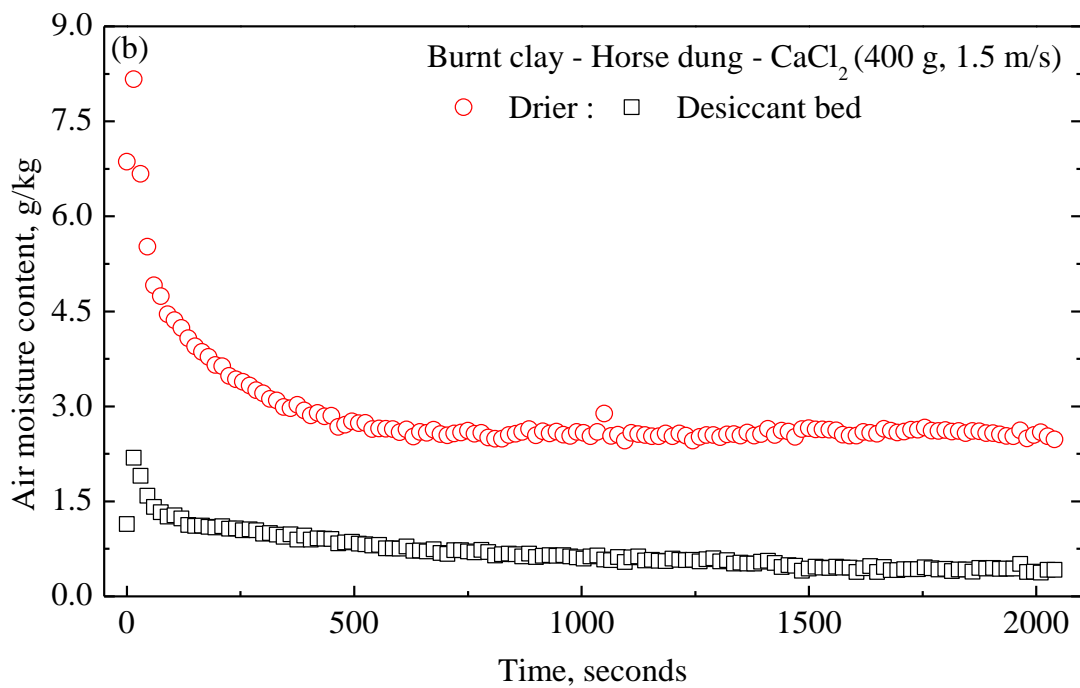
Fig .7.7 (b) Time variation of moisture content of process air exiting the desiccant bed and grain dryer for experimental run R9.
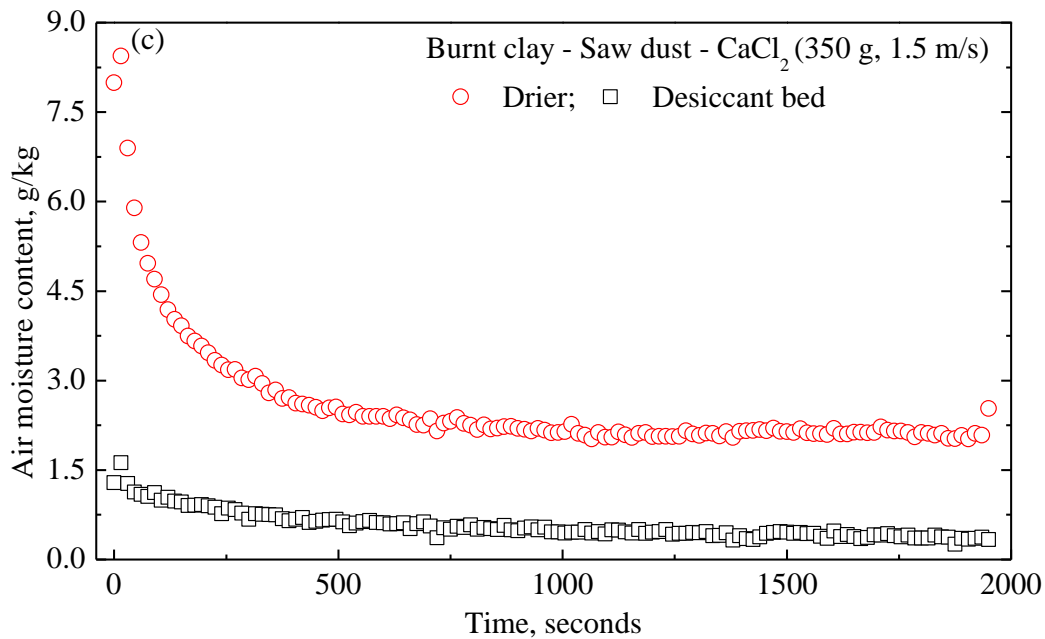
Fig .7.7 (c) Time variation of moisture content of process air exiting the desiccant bed and grain dryer for experimental run R14.

The maximum reduction and gain in moisture by process air due to dry desiccant bed and moist grains during complete process time are 44.23% and 74.58% for 400 g, bed masses. Within the time period of 500 s, the average values of reduction and gain of moisture by process air are 23.88% and 50.34%. The variation of air moisture content with time due to dehumidification and humidification by 350 g bed mass burnt clay - sawdust - $CaCl_2$ desiccant bed and dryer are shown in Fig.7.7 (c). During initial period of 500 s, the average moisture content of process air through the desiccant bed and dryer are 20.15% and 50.24% for 350 g bed mass. At the end of drying process the dryer exit air moisture content decreases to minimum value of 30.91%, for the respective bed masses of 350 g.

7.3.3 Dryer rate with similar D/L ratio for burnt clay - additives - CaCl₂ composite desiccant bed

The initial weight of moist grains before drying and final weight of dried grain after drying is recorded for estimating the moisture removed during the elapsed drying time. Fig.7.8 (a) and (b) illustrates the variation of drying rate with bed diameter to length (D/L) ratio. For the same bed masses of 500 g and 700 g, the bed diameter to

length ratio obtained is 0.21, 0.15 and 0.16, 0.10 for burnt clay - $CaCl_2$ and burnt clay - additives - $CaCl_2$ composite desiccant beds. With D/L ratio of 0.21 (500 g) and 0.16 (700 g) for clay - $CaCl_2$ vertical packed beds the drying rates obtained are 0.44 g/min 0.69 g/min. For D/L ratio of 0.15 (500 g) and 0.10 (700 g) of burnt clay-horse dung - $CaCl_2$ bed the corresponding drying rates are 0.69 g/min and 0.81 g/min. With D/L ratio of 0.15 (500 g) and 0.10 (700 g) for burnt clay - sawdust - $CaCl_2$ vertical packed bed the drying rates estimated are 0.63 g/min and 0.52 g/min.
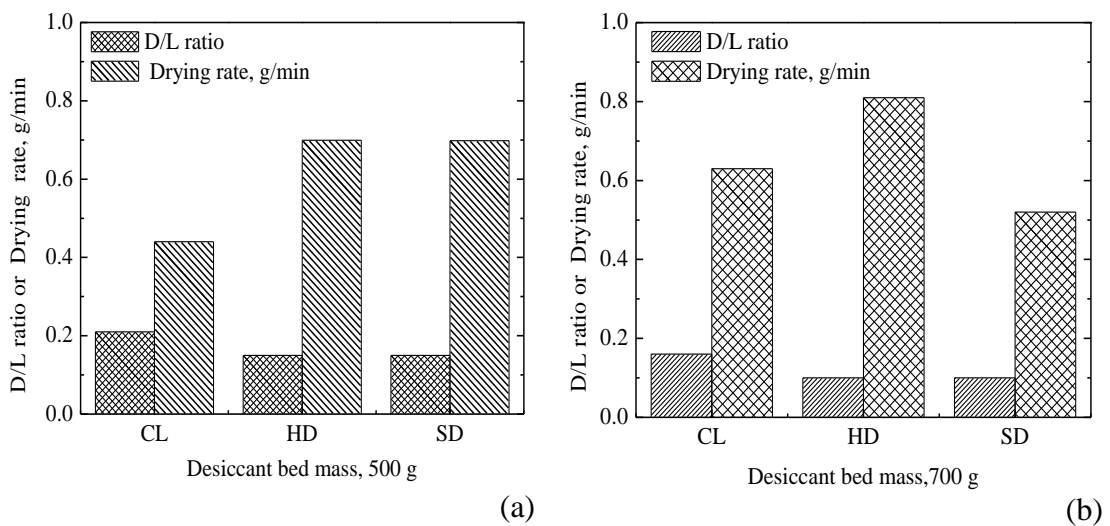
Fig. 7.8 Grain drying speed with respect to D/L ratio for (a) 500 g and (b) 700 g desiccant bed masses.

7.4 CHARACTERISTICS OF DRIED GREEN PEA GRAINS OBTAINED BY IMAGES

The mass of green pea grains considered for drying is 250 g each contained on bottom and top trays of dryer. The photographs of grains before drying and after drying are presented in Fig.7.9 (a) and (b). The mass of water removed from the bottom and top tray grains are tabulated in Table 7.1 From the visual examination of the grains shows the dehydrated surface of the grains after drying. The dehumidified surface indicates the removal of moisture from the grains. Although there is a change in color of grains upon drying but the change is minimal. The smaller change in color indicates the retainment of nutritional content even after drying. Further to quantify the characteristics of the investigation of the image is carried by image processing. A

193

code written in Matlab for the image processing enables estimation of texture features and statistical measures. The parameters are estimated for the images before and after drying are tabulated in Table 7.4.

(a)

(b)
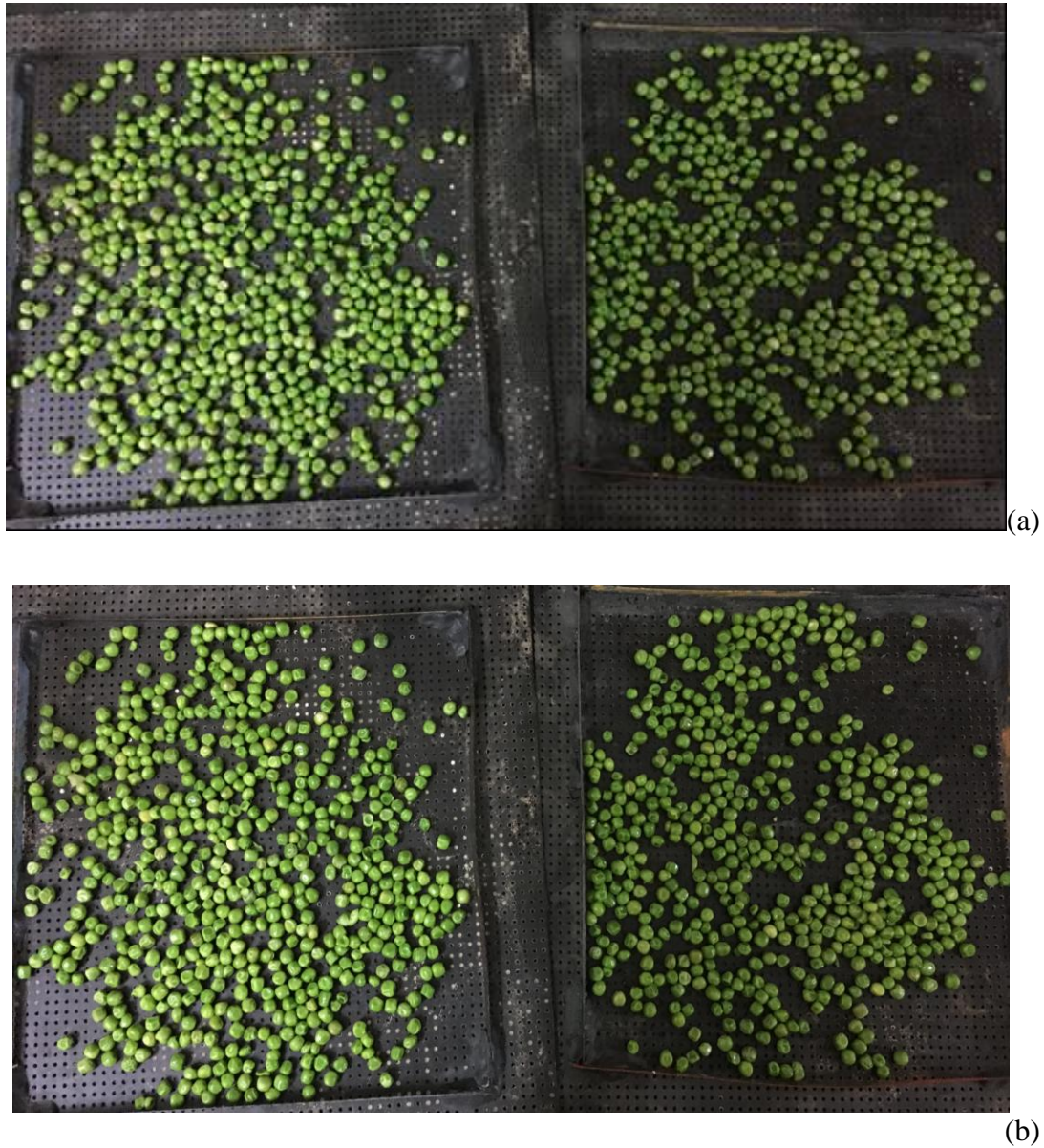
Fig.7.9 Photographs of green pea grains contained in the top and bottom trays of dryer (a) before drying and (b) after drying.

The percentage decrease in entropy which characterizes the randomness of the texture of input image before drying and after drying is 1.30. The energy which measures the uniformity of the texture before drying is 0.1431 and 0.1324 after drying. The

194

intensity of pixels is measured in terms of contrast. The difference in contrast values before drying and after drying is 0.005. The texture analysis of parameters yields a similarity index which is comparative value. Similarity index of 23.51 indicates similarity of processed images as 77%. The image data in terms of statistical and texture parameters reveals minimal change of color, shape, and texture before and after drying. The smaller changes indicate the preservation of dietary and nutritional content of grains even after moisture removal.

Table 7.4 Texture characteristics of green pea grain images before and after drying.

Parameters	Before drying	After drying
Mean	Max:142.16, Min: 76.34	Max:149.59, Min: 89.12
Mode	Max:253, Min: 17	Max:231, Min: 14
Median	Max:145, Min: 62	Max:151, Min: 81
Standard deviation	47.57	52.01
Entropy	7.57	7.67
Energy	0.1431	0.1324
Contrast	0.1374	0.1343
Correlation	0.9697	0.9757
Homogeneity	0.9360	0.9389

7.5 SUMMARY

The detailed experimental set up consisting of desiccant bed coupled with two tray cabinet dryer is illustrated. The desiccants are prepared from locally available transported clay, sawdust, and horse dung additives. The green pea is purchased form a local dairy. The dehumidification potential of burnt clay - additives - $CaCl_2$ composite desiccant bed is illustrated experimentally. Steady-state drying rates are analyzed for the two tray dryer integrated with clay composite desiccant beds. The results are graphically presented, and finally, the following conclusions are summarized.

1. For the bed mass of 700 g and process time within 500 s, the maximum value of average moisture reduction from process air by burnt clay - $CaCl_2$ composite

desiccant bed is 19.67%, and the corresponding maximum value of moisture gain by process air from the grains is 65.34%.

2. For the process air within 500 s of process time, the maximum value of average moisture reduction by burnt clay - sawdust - $CaCl_2$ composite desiccant bed (700 g) is 32.99%, and the corresponding maximum value of moisture gain from the grains is 64.67%.

3. For the process air within 500 s of process time, the maximum value of average moisture reduction by burnt clay - horse dung - $CaCl_2$ composite desiccant bed (700 g) is 32.92%, and the corresponding maximum value of moisture gain from the grains is 54.63%.

4. As compared to burnt clay - $CaCl_2$ vertical packed beds, the dehumidification of process air is enhanced by vertical packed burnt clay - sawdust - $CaCl_2$ and burnt clay - horse dung - $CaCl_2$ composite desiccants beds.

5. The average bed temperatures for burnt clay - additives - $CaCl_2$ composite desiccants ranges from 30 to 31°C.

6. For the bed mass of 700 g, the diameter to bed length ratio of 9.8 and 9.6 for burnt clay - additives - $CaCl_2$ is higher as compared the diameter to bed length of 6.28 for burnt clay - $CaCl_2$ composite desiccant bed. The corresponding drying rates are 0.81 g/min, 0.52 g/min and 0.63 g/min for burnt clay - horse dung - $CaCl_2$, burnt clay- sawdust - $CaCl_2$ and burnt clay - $CaCl_2$ desiccant beds.

7. Drying of green pea grains depends on process air humidity and temperature, desiccant material type and quantity, grain initial moisture content and quantity, and process air mass flow rate.

8. Based on experimental results, the clay composite desiccant bed length required to dry 1 kg of moist green pea is evaluated and presented in appendix-IV.

9. The similarity of images before drying and after death is 77%. Smaller changes in statistical and texture parameters indicate preservation of nutritional content of grains.

10 The experimental study shows the potential application of low-cost clay - additives - $CaCl_2$ composite desiccants in grain drying and aeration during off - sunshine hours in warm and humid climates.

196

CHAPTER 8

CONCLUSIONS

8.1 SUMMARY

The present work focused on the experimental and theoretical investigation on transient dehumidification characteristics of clay and clay-based $CaCl_2$ composite desiccants. Three composite desiccant materials namely heat treated clay - $CaCl_2$, clay - sawdust - $CaCl_2$ and clay - horse dung - $CaCl_2$ composite desiccants have been used in the investigations. In the first phase experimental determination of properties of clay composite desiccants is carried out. In the second phase experimental studies have been carried out to investigate the effect of inlet air velocity, relative humidity, temperature and mass of desiccant bed on transient dehumidification potential of vertical packed and fluidized bed configuration containing clay and clay additives composite desiccants. The gas side resistance theoretical model has been derived and solved for transient variation of exit air humidity ratio. The theoretical results are compared with the experimental results of vertical packed clay and clay additives composite desiccant beds. Further the transient dehumidification potential in terms of process air moisture reduction has been predicted experimentally for green pea aeration or drying. The chapter-wise conclusions were presented at the end of every chapter. Based on the results the following key contributions are drawn.

8.2 OVERALL CONCLUSIONS

1. The gravimetric analysis reveals illite as the principal clay mineral content of the transported soil deposited on banks of the lake at Vijayapur district, Karnataka state, India.

2. The heat treatment of manually molded clay and clay - additives composite desiccants at 500°C yields maximum weight reduction and apparent porosity.

197

3. The initial water contents estimated for burnt clay - $CaCl_2$, burnt clay - sawdust - $CaCl_2$ and burnt clay - horse dung - $CaCl_2$ composite desiccants are in the order of 63.79, 86.04 and 94.44 g water / kg dry desiccant respectively.

4. SEM micrographs indicate the porous surface texture of burnt clay additives pellets and retention of $CaCl_2$ into the pores of burnt clay - additives - $CaCl_2$ composite desiccants.

5. The addition of sawdust and horse dung additives followed by heat treatment of clay increases the porosity, specific heat, thermal diffusivity, and thermal conductivity.

6. The process air is heated to regenerate the composite desiccants attains the steady-state value of temperature after 60 minutes of process time.

7. The dehumidification experimental tests on vertical packed heat treated clay and clay additives $CaCl_2$ composite desiccants bed reveals hyperactivity for moisture adsorption during initial period of adsorption and extends up to 10 minutes. From that onwards the potential for moisture adsorption decreases steadily.

8. The experimental results on vertical packed and fluidized beds comprising clay and clay additives composite desiccants shows higher mass transfer potential in vertical fluidized beds indicated by higher values of mass transfer coefficients.

9. The experimental results on solitary clay and clay additives $CaCl_2$ composite desiccants reveal higher absorptivity and saturation time for heat-treated clay - 20% horse dung - 50% $CaCl_2$ composite desiccants followed by heat-treated clay - 20% sawdust - 50% $CaCl_2$ and clay - 50 % $CaCl_2$ composite desiccant.

10. The experimental study shows the potential of low-cost clay - additives - $CaCl_2$ composite desiccants in grain drying and preservation during off - sunshine hours in warm and humid climates.

11. With the increased use of composite desiccants, the visual observation of desiccants reveals deterioration of surface for clay - $CaCl_2$ composite desiccants.

The surface of clay - sawdust- $CaCl_2$ and clay - horse dung - $CaCl_2$ seems to be powdery.

8.3 KEY CONTRIBUTIONS

➤ Development of low cost clay and clay additives based composite desiccants using naturally available materials like clay, horse dung and saw dust.

➤ The prepared clay composite desiccants have potential application in air conditioning, drying, aeration, water extraction and other dehumidification systems.

➤ The clay composite desiccants have prospect of saving energy and environment.

8.4 FUTURE SCOPE

1. Identifying suitable hygroscopic salts for low humidity conditions. The salts are of interest are $LiCl_2$, LiBr, and glycols.

2. The isotherm is the important property of desiccant material required in mathematical modeling of desiccant beds. Experimental modules for finding the isotherm can be set up.

3. Sieve analysis of soil yields soil of different grain sizes. Investigating the effect of soil grain size on dehumidification performance of clay composite desiccants.

4. The study can be extended to study the humidification and dehumidification performance of nano clay and nano clay - additives composite desiccants.

5. Investigating heat and mass transfer characteristics of clay and clay additives composite desiccants with radial, annular, multilayer, and inclined bed configurations. For continuous operation desiccant wheels comprising clay and clay additives, composite desiccants can be tested.

6. Extending the theoretical study to simulate the transient heat and mass transfer characteristics of desiccants in adsorption and desorption processes. Development of empirical correlations required for numerical simulation of desiccant bed and process air parameters.

7. The heat of adsorption released during the adsorption process is a function of bed water content increases the bed temperature and thereby limits the desiccant bed absorptivity. New experimental procedures can be developed and designed to evaluate the heat of adsorption.

8. To counteract the effect of heat of adsorption, a new family of clay - silica gel composite desiccants can be prepared and tested.

9. The potential of fabricated hygroscopic desiccants is suggested in water production from atmospheric air, drying, and thermal comfort applications.

10. Development and design of solar-based clay composite desiccant drying or aeration systems for agricultural and horticultural products

11. Development and design of solar-based clay composite desiccant air conditioning systems for thermal comfort.

12. Degradation and stability of clay and clay additives based composite desiccants.

13. Study on uptake and heat of adsorption of the composite desiccants using standardized equipments using thermo gravimetric analyzer (TGA).

14. Measurement of adsorption kinetics properties of prepared desiccants.

15. Modeling and simulation of heat and mass transfer characteristics of clay composite desiccants.

16. Exploring the potential application clay based desiccants in drying, aeration and other real time dehumidification applications.

REFERENCES

Adegoke, J. A., Ogunsile, B., and Adetoro, A. O. (2010). "Variation of Thermophysical properties of clay with adsorbtion optimization." *The pacific Journal of science and technology*, 11,639, 648.

Alonso-Santurde, R., Coz, A., Viguri, J. R., and Andrés, A. (2012). "Recycling of foundry by-products in the ceramic industry: Green and core sand in clay bricks." *Construction and Building Materials*, 27(1), 97-106.

Aristov, Y. I., Restuccia, G., Cacciola, G., and Parmon, V. N. (2002). A family of new working materials for solid sorption air conditioning systems. *Appl. Therm. Eng,* 22(2), 191-204.

Baghapour, B., Rouhani, M., Sharafian, A., Kalhori, S. B., and Bahrami, M. (2018). "A pressure drop study for packed bed adsorption thermal energy storage." *Appl. Therm. Eng*, 138, 731-739.

Beery, K. E., and Ladisch, M. R. (2001). "Chemistry and properties of starch based desiccants." *Enzyme Microb. Technol*, 28(7-8), 573-581.

Billiris, M.A., Siebenmorgen, T.J., (2013). "Energy use and efficiency of rice –drying systems II. Commercial, cross- flow dryer measurements." *Appl. Eng. Agric,* 30(2), 217-226

Boukhemkhem, A., and Rida, K. (2017). "Improvement adsorption capacity of methylene blue onto modified Tamazert kaolin." *Adsorpt. Sci. Techno.,* 35(9-10), 753-773.

Bu, X., Wang, L., Li, H., and Lu, Z. (2012). "Preparation of composite adsorbent of sawdust and $CaCl_2$ by carbonization method for creating pore." *Science China Technological Sciences*, 55(9), 2404-2408.

Caturla, F., Molina-Sabio, M., and Rodriguez-Reinoso, F. (1999). "Adsorption–desorption of water vapor by natural and heat-treated sepiolite in ambient air." *Appl. Clay Sci,* 15(3-4), 367-380.

Chan, K. C., Chao, C. Y., Sze-To, G. N., and Hui, K. S. (2012). "Performance predictions for a new zeolite 13X/$CaCl_2$ composite adsorbent for adsorption cooling systems." *Int. J. Heat Mass Transfer*, 55(11-12), 3214-3224.

Chua, K. J. (2015). "Heat and mass transfer of composite desiccants for energy efficient air dehumidification: modelling and experiment." *Appl. Therm. Eng,* 89, 703 -716.

Chemkhi, S., Zagrouba, F., and Bellagi, A. (2004). "Thermodynamics of water sorption in clay." *Desalination*, 166, 393-399.

Chen, H. J., Cui, Q., Tang, Y., Chen, X. J., and Yao, H. Q. (2008). "Attapulgite based LiCl composite adsorbents for cooling and air conditioning applications." *Appl. Therm. Eng*, 28(17-18), 2187-2193.

Chen, C. H., Hsu, C. Y., Chen, C. C., Chiang, Y. C., and Chen, S. L. (2016). "Silica gel/polymer composite desiccant wheel combined with heat pump for air-conditioning systems." *Energy*, 94, 87-99.

Chen, C. H., Hsu, C. Y., Chen, C. C., and Chen, S. L. (2015). "Silica gel polymer composite desiccants for air conditioning systems." *Energy Build*, 101, 122-132.

Chen, C. H., Ma, S. S., Wu, P. H., Chiang, Y. C. and Chen, S. L. (2015). "Adsorption and desorption of silica gel circulating fluidized beds for air conditioning systems." *Appl. Energy,* 155, 708-718.

Chen, C. H., Schmid, G., Chan, C. T., Chiang, Y. C., and Chen, S. L. (2015). "Application of silica gel fluidised bed for air-conditioning systems." *Appl. Therm. Eng*, 89, 229-238.

Chiang, Y. C., Chen, C. H., Chiang, Y. C., and Chen, S. L. (2016). "Circulating inclined fluidized beds with application for desiccant dehumidification systems." *Appl. Energy*, 175, 199-211.

Chua, K. J., Chou, S. K., and Islam, M. R. (2018). "On the experimental study of a hybrid dehumidifier comprising membrane and composite desiccants." *Appl. Energy*, *220*, 934-943.

Close, D.J., and Dunkle, R.V., (1977). "Use of adsorbent beds for energy storage in drying of heating systems." *Sol. Energy*, 19(3), 233-238.

Çmar, M., Ersever, G., Şahbaz, O., and Çelik, M. S. (2011). "Sepiolite/calcium interactions in desiccant clay production." *Appl. Clay Sci, 53*(3), 386-394.

Daou, K., Wang, R. Z., Xia, Z. Z., and Yang, G. Z. (2007). "Experimental comparison of the sorption and refrigerating performances of a $CaCl_2$ impregnated composite adsorbent and those of the host silica gel." *Int. J. Refrig*, 30(1), 68-75.

Doymaz, I., and Kocayigit, F. (2011). "Drying and rehydration behaviors of convection drying of green peas." *Drying Technol*, 29(11), 1273-1282.

Dupont, M., Celestine, B., and Beghin, B. (1994). "Desiccant solar air conditioning in tropical climates: II-field testing in Guadeloupe." *Sol. Energy*, 52(6), 519-524.

Dupont, M., Celestine, B., Nguyen, P. H., Merigoux, J., and Brandon, B. (1994). "Desiccant solar air conditioning in tropical climates: I-Dynamic experimental and numerical studies of silica gel and activated alumina. *Sol. Energy,* 52(6), 509-517.

Fasunwon, O. O., Olowofela, J. A., Ocan, O. O. and Akinyemi, O. D. (2008). "Determination of thermal conductivity of rocks samples using fabricated equipment." *J. Therm. Sci*, 12(2), 119-128.

Fazilati, M. A., Sedaghat, A., and Alemrajabi, A. A. (2017). "Transient performance and temperature field of a natural convection air dehumidifier loop." *Heat Mass Transfer*, 53(7), 2287-2296.

Fungtammasan, B. (2001). "Prediction of minimum fluidisation velocity from correlations: an observation." *Asian J. Energy Environ*. Vol, 2(2), 145-154.

Gad, H. E., Hamed, A. M., and El-Sharkawy, I. I. (2001). "Application of a solar desiccant/collector system for water recovery from atmospheric air." *Renewable Energy*, 22(4), 541-556.

Ghosh, D., and Bhattacharyya, K. G. (2002). "Adsorption of methylene blue on kaolinite." *Appl. Clay Sci,* 20(6), 295-300.

Hamed, A. M. (2000), "Absorption-regeneration cycle for production of water from air-theoretical approach." *Renewable energy*, 19, 625-635.

Hamed, A. M. (2002). "Theoretical and experimental study on the transient adsorption characteristics of a vertical packed porous bed." *Renewable Energy*, 27(4), 525-541.

Hamed, A. M. (2003). "Experimental investigation on the natural absorption on the surface of sandy layer impregnated with liquid desiccant." *Renewable energy*, 28(10), 1587-1596.

Hamed, A. M. (2003). "Desorption characteristics of desiccant bed for solar dehumidification/humidification air conditioning systems." *Renewable Energy*, 28(13), 2099-2111.

Hamed, A. M., El Rahman, W. R. A., and El-Emam, S. H. (2010). "Experimental study of the transient adsorption/desorption characteristics of silica gel particles in fluidized bed." *Energy*, 35(6), 2468-2483.

Hiremath, C. R., and Kadoli, R. (2013). "Experimental studies on heat and mass transfer in a packed bed of burnt clay impregnated with $CaCl_2$ liquid desiccant and exploring the use of gas side resistance model." *Appl. Therm. Eng*, 50(1), 1299-1310.

Hodali, R., and Bougard, J. (2001). "Integration of a desiccant unit in crops solar drying installation: optimization by numerical simulation." *Energy Convers. Manage*, 42(13), 1543-1558.

Hung B. N., Nuntaphan, A., Kiatsiriroat, T., (2009). "Integration of desiccant tray unit with internal cooling for aeration of paddy silo in humid tropical climate." *Biosyst. Eng,* 102, 75-82.

Jani, D.B., Manish, M., and Sahoo, P.K., (2016). "Performance analysis of hybrid solid desiccant vapor compression air conditioning system in hot and humid weather of India." *Journal of Building Services Engineering Research and Technology*, 0, 1-16.

Jain, S., Dhar, P. L., and Kaushik, S. C. (1995). "Evaluation of solid-desiccant-based evaporative cooling cycles for typical hot and humid climates." *Int. J. Refrig*. 1995; 18: 287 - 96.

Jain, S., Dhar, P. L., and Kaushik, S. C. (2000). "Experimental studies on the dehumidifier and regenerator of a liquid desiccant cooling system." *Appl. Therm. Eng,* 20(3), 253-267.

Ji, J. G., Wang, R. Z., and Li, L. X. (2007). "New composite adsorbent for solar-driven fresh water production from the atmosphere." *Desalination*, 212(1-3), 176-182.

Joshua Folaranmi. (2009). "Effect of additives on the thermal conductivity of clay." *Leonardo Journal of sciences*, 14, 74 -77.

Kabeel, A. E., (2010). "Dehumidification and humidification process of desiccant solution by air injection." *Energy*, 35, 5193-5201.

Khedari, J., Nankongnab, N., Hirunlabh, J., and Teekasap, S. (2004). "New low-cost insulation pelletboards from mixture of durian peel and coconut coir." *Build. Environ,* 39(1), 59-65.

Kinsara, A. A., Elsayed, M. M., and Al-Rabghi, O. M. (1996). "Proposed energy-efficient air-conditioning system using liquid desiccant." *Appl. Therm. Eng*, 16(10), 791-806.

Kline, S. J. (1953). "Describing uncertainty in single sample experiments." *Mech. Engineering*, 75, 3-8.

Konta, J., I. (1995). "Clay and man: clay raw materials in the service of man." *Applied Clay Science*, 10(4), 275-335.

Kulkarni, N. G., Bhandarkar, U. V., Puranik, B. P., and Rao, A. B. (2016). "Experimental determination of thermal properties of alluvial soil." *Heat Mass Transfer*, *52*(12), 2661-2669

Kumar, R., and Asati, A. K. (2016). "Experimental study on performance of celdek packed liquid desiccant dehumidifier." *Heat Mass Transfer*, 52(9), 1821-1832.

Kumar, D., and Kalita, P. (2017). "Reducing postharvest losses during storage of grain crops to strengthen food security in developing countries." *Foods*, 6(1), 8.

Kumar, R., and Asati, A. K. (2018). "Experimental Study on Effectiveness of Celdek Packed Liquid Desiccant Cooling System." *Heat Transfer Eng*, 39(10), 914-922.

Kumar, M., and Yadav, A.(2017). "Composite desiccant material "$CaCl_2$ /Vermiculite/Saw wood": a new material for fresh water production from atmospheric air." *Appl. Water Sci*, 7(5), 2103-2111.

La, D., Dai, Y. J., Li, Y., Wang, R. Z., and Ge, T. S. (2010). "Technical development of rotary desiccant dehumidification and air conditioning: A review." *Renewable Sustainable Energy Rev,* 14(1), 130-147.

Lee, J., and Lee, D. Y. (2012). "Sorption characteristics of a novel polymeric desiccant." *Int. J. Refrig*, 35(7), 1940-1949.

Li, A., Zhang, J., and Wang, A. (2007). "Utilization of starch and clay for the preparation of superabsorbent composite." *Bioresour. Technol.,* 98(2), 327-332.

Li, H., Bu, X., Wang, L., Lu, Z., and Ma, W. (2012). "Composite adsorbents of $CaCl_2$ and sawdust prepared by carbonization for ammonia adsorption refrigeration." *Frontiers in Energy*, 6(4), 356-360.

Melda Ozdinc Carpinlioglu., emrah Ozahi., (2008), "A simplified correlation for fixed bed pressure drop." *Powder Technol*, 187, 94-101.

Middleton, M. F. (1993). "A transient method of measuring the thermal properties of rocks." *Geophysics,* 58(3), 357-365.

Moffat, R. J. (1988). "Describing the uncertainties in experimental results." *Exp. Therm Fluid Sci,* 1(1), 3-17.

Murray, H. H. (1999). "Applied clay mineralogy today and tomorrow." *Clay Miner,* 34(1), 39-49.

Muthukumar, P., Maiya, M. P., and Murthy, S. S. (2002). "Parametric studies on a metal hydride based single stage hydrogen compressor." *Int. J. Hydrogen Energy*, 27(10), 1083-1092.

Nagaya, K., Li, Y., Jin, Z., Fukumuro, M., Ando, Y., and Akaishi, A. (2006). "Low-temperature desiccant-based food drying system with airflow and temperature control." *J. Food Eng*, 75(1), 71-77.

Nciri, R., Rabhi, K., Nasri, F., Ali, C. and Bacha, H. B. (2018). "Original methodology and nomography tool for dimensioning multi-packed-bed dehumidifiers." *Heat Mass Transfer*, 1-13.

Ntsoukpoe, K. E., Rammelberg, H. U., Lele, A. F., Korhammer, K., Watts, B. A., Schmidt, T., and Ruck, W. K. (2015). "A review on the use of calcium chloride in Applied Thermal Engineering." *Appl. Therm. Eng*, 75, 513-531.

Oliveira, L. C., Rios, R. V., Fabris, J. D., Sapag, K., Garg, V. K., and Lago, R. M. (2003). "Clay-iron oxide magnetic composites for the adsorption of contaminants in water." *Appl. Clay Sci*, 22(4), 169-177.

Phate, A. K., Maiya, M. P., and Murthy, S. S. (2007). "Simulation of transient heat and mass transfer during hydrogen sorption in cylindrical metal hydride beds." *Int. J. Hydrogen Energy*, 32(12), 1969-1981.

Pranav, C. P., Pramod, V., Walke and Kriplani., (2015). "A review on indirect solar dryers." *ARPN Journal of Engineering and Applied Sciences*, 10(8), 3360-3370.

Rady, M. A., Huzayyin, A. S., Arquis, E., Monneyron, P., Lebot, C. and Palomo, E. (2009). Study of heat and mass transfer in a dehumidifying desiccant bed with macro-encapsulated phase change materials. *Renewable Energy*, 34(3), 718-726.

Rambhad, K. S., Walke, P. V., and Tidke, D. J. (2016). Solid desiccant dehumidification and regeneration methods-A review. *Renewable Sustainable Energy Rev.*, 59, 73-83.

Ramzy, A., Elawady, W. M., and AbdelMeguid, H. (2014). Modelling of heat and moisture transfer in desiccant packed bed utilizing spherical pellets of clay impregnated with $CaCl_2$. *Appl. Therm. Eng*, 66(1-2), 499-506.

Rawangkula, R., Khedaria, J., Hirunlabhb, J., and Zeghmatic, B. (2010). "Characteristics and performance analysis of a natural desiccant prepared from coconut coir." *Chemical Analysis*, 1269(01), 11.

Riangvilaikul, B., and Kumar, S. (2010). "An experimental study of a novel dew point evaporative cooling system." *Energy Build*, 42(5), 637-644.

Riangvilaikul, B., and Kumar, S. (2010). "Numerical study of a novel dew point evaporative cooling system." *Energy Build*, 42(11), 2241-2250.

Ristic, A., Maucec, D., Henninger, S. K., and Kaucic, V. (2012). "New two-component water sorbent $CaCl_2$-FeKIL2 for solar thermal energy storage." *Microporous Mesoporous Mater*, 164, 266-272.

Robert. J. M. (1988) "Describing the Uncertainties in Experimental Results." J. *Exp.Therm Fluid Sci*. 1, 3 – 17.

Sabri Ergun. (1952). "Fluid flow through packed columns." *Chem. Eng. Prog,* 48(2), 89-94.

Saha, B. B., Chakraborty, A., Koyama, S., and Aristov, Y. I. (2009). "A new generation cooling device employing $CaCl_2$-in-silica gel–water system." *Int. J. Heat Mass Transfer,* 52(1-2), 516-524.

Shanmugam, V., and Natarajan, E. (2006). "Experimental investigation of forced convection and desiccant integrated solar dryer." *Renewable Energy*, 31(8), 1239-1251.

Srivastava, N.C., and Eames, I.W., (1998). "A review of adsorbents and adsorbates in solid-vapor adsorption heat pump systems." *Appl. Therm. Eng*, 18 (1998), 707–714.

Stamenic , M, S.(2016), "Experimental investigation of pressure drop in packed beds of monosized spheres." *J. Therm. Sci.*, 2(6), 1 - 8.

Sturton , S,L., Bilanski, W,K., Menzies, D,R., (1981). "Drying of cereal grains with the desiccant bentonite." *Can. Agric. Eng*, 23, 101-103.

Thoruwa, T. F. N., Grant, A. D., Smith, J. E., and Johnstone, C. M. (1998). A solar-regenerated desiccant dehumidifier for the aeration of stored grain in the humid tropics. *J. Agric. Eng. Res*, 71(3), 257-262.

Thoruwa, T.F.N., Johnstone, C.M., Grant, A.D., Smith, J.E. (2000), "Novel, low cost $CaCl_2$ based desiccants for solar crop drying applications." *Renewable energy*, 19, 513-520.

Tokarev, M., Gordeeva, L., Romannikov, V., Glaznev, I. and Aristov, Y. (2002). "New composite sorbent $CaCl_2$ in mesopores for sorption cooling/heating." *Int. J. Therm. Sci*, 41(5), 470-474.

Tretiak, C. S., and Abdallah, N. B. (2009)." Sorption and desorption characteristics of a packed bed of clay-$CaCl_2$ desiccant pellets." *Sol. Energy*, 83(10), 1861-1870.

Tsilingiris, P. T. (2008). "Thermophysical and transport properties of humid air at temperature range between 0 and 100°C." *Energy Convers. Manage*. 49(5), 1098-1110.

Walid Aissa., Mostafa El-Sallak., and Ahmed Elhakem., (2014). "Performance of solar dryer chamber used for convective drying of sponge-cotton." *Thermal Science,* 18(2), 5451 - 5462.

Wang, L. W., Tamainot-Telto, Z., Metcalf, S. J., Critoph, R. E. and Wang, R. Z. (2010). "Anisotropic thermal conductivity and permeability of compacted expanded natural graphite." *Appl. Therm. Eng*, 30(13), 1805-1811.

Wang, L. W., Wang, R. Z. and Oliveira, R. G. (2009). "A review on adsorption working pairs for refrigeration." *Renewable Sustainable Energy Rev*, 13(3), 518-534.

Watts, K.C., Bilanski, K., and Menzies, D.R., (1985)."Comparison of drying corn using sodium and calcium bentonite." *Can. Agric. Eng*, 28, 35-41.

Yao, Y. (2010). "Using power ultrasound for the regeneration of dehumidizers in desiccant air-conditioning systems: A review of prospective studies and unexplored issues." *Renewable Sustainable Energy Rev*, 14(7), 1860-1873.

Yeboah, S. K., and Darkwa, J. (2016). "A critical review of thermal enhancement of packed beds for water vapour adsorption." *Renewable Sustainable Energy Rev,* 58, 1500-1520.

Zhang, J., and Wang, A. (2007). "Study on superabsorbent composites. IX: synthesis, characterization and swelling behaviors of polyacrylamide/clay composites based on various clays." *React. Funct. Polym*, 67(8), 737-745.

Yu, Q., Tang, X., Yi, H., Ning, P., Yang, L., Yang, L., and Li, H. (2009). "Equilibrium and heat of adsorption of phosphine on $CaCl_2$ modified molecular sieve." *Asia Pacific Journal of Chemical Engineering,* 4(5), 612-617.

Zheng, X., Ge, T. S., and Wang, R. Z. (2014). "Recent progress on desiccant materials for solid desiccant cooling systems." *Energy*, 74, 280-294.

Zhu, D., Wu, H., and Wang, S. (2006). "Experimental study on composite silica gel supported $CaCl_2$ sorbent for low grade heat storage." *Int. J. Therm. Sci*, 45(8), 804-813.

Conference Proceedings and Symposiums

Hiremath, C. R, and Kadoli Ravikiran A. (2011). Burnt clay impregnated with calcium chloride liquid desiccant-an experimental study. *Proceedings of 56th Congress of ISTAM*, SVNIT, Surat, Gujarat.

Walaa, Abd-Elrahman; Ahmad, Hamed; Salah, El-Emam and Mahmoud, Awad. (2010).Theoretical and experimental investigation on the performance of hybrid desiccant air conditioning system using activated alumina in a radial flow packed bed. *Thermal Issues in Emerging Technologies, Theta 3*, Cairo, Egypt, Dec 19 - 22.

Books and Thesis

Biswas, T.D , Mukharji, S.K., (1994) "Textbook of soil science. Tata McGraw-Hill publishing company limited." ISBN 0-07-462043-6.

Calcium Chloride data hand book A Guide to Properties. Available at: http://www.scribd.com/doc/49373766/Calcium-Chloride-Handbook

Carslaw, H, S.,Jaeger,J,C., (1959) "Conduction of heat in solids." Oxford University press Inc, pp.281-304.

Gupta, R.C. (2010). "Theory and laboratory experiments in Ferous Metallurgy." PHI learning private limited , Publication

Cullity, B. D., (1978). "Elements of X-ray diffraction." Addison- Wesley publishing company Inc, second edition, ISBN 0-201-01174-3.

Kothandaraman C.P and Subramanyan. S., (2007). "Heat and mass transfer data book." New Age international publishers, Delhi, sixth edition.

Ralph, E. G., (1962) "Applied Clay Mineralogy." Mcgraw-Hill book company, Inc, New York.

Thomas, W., J. Barry Crittenden. (1998). "Adsorption Technology and Design." Elsevier Science and Technology Books, ISBN: 0750619597.

Xiaodong, Nie (2010). "Heat and Moisture Migration within a Porous Urea Pellet Bed." A thesis in Mechanical engineering Submitted to the University of Saskatchewan, Saskatoon.

Zorbas, F. (1987). "Low temperature drying using liquid desiccants" A thesis in Mechanical engineering Submitted to the Graduate Faculty of Texas Tech University.

EXPERIMENTAL ESTIMATION OF THERMAL PROPERTIES OF CLAY AND CLAY ADDITIVES CACL$_2$ COMPOSITE DESICCANTS

The estimation of thermal diffusivity, thermal conductivity, density, and thermal conductivity for the clay, clay additives and impregnated with CaCl$_2$ samples is illustrated with sample calculation. The transient measurement technique is used to estimate thermal diffusivity. Specific heat is determined by making energy balance between samples and hot water.

I.1 THERMAL DIFFUSIVITY:

The thermal diffusivity is estimated according to the theory of transient measurement technique (Middleton, 1993). Table I.1 shows the temperatures recorded at the bottom surface of the clay sample disk of diameter 45 mm and thickness 20 mm. The temperatures are noted in terms of voltage for 150 s at an interval of 10 s. The mili voltmeter having a range of 0 to 200 mV DC is used to record the voltage values. The voltage readings (E) are converted to temperature values by the following equation.

$$T = (24.52 \times E) + 3.986 \tag{I.1}$$

The measured temperatures at every interval of time are subtracted from the initial time temperature, thus effectively making the temperature equal to zero at initial time. Fig I.1 shows the graphical presentation of experimentally measured temperature at the bottom of cylindrical clay disk with time. Fig.I.2 illustrates transient variation of temperature as predicted by the theory. A linear fit to experimental data yields the value of intercept t_i at $T = 0$. From the linear fit to experimental data the value of t_i is obtained. Thermal diffusivity is calculated using the following equation

$$\text{Thermal diffusivity}(\alpha) = \frac{\xi^2}{(6 \times t_i)} = \frac{(0.02 \times 0.02)}{(6 \times 20)} = 3.33 \times 10^{-6} \ \text{m}^2 / s \tag{I.2}$$

Table I.1 Temperature values recorded for the estimation of thermal diffusivity.

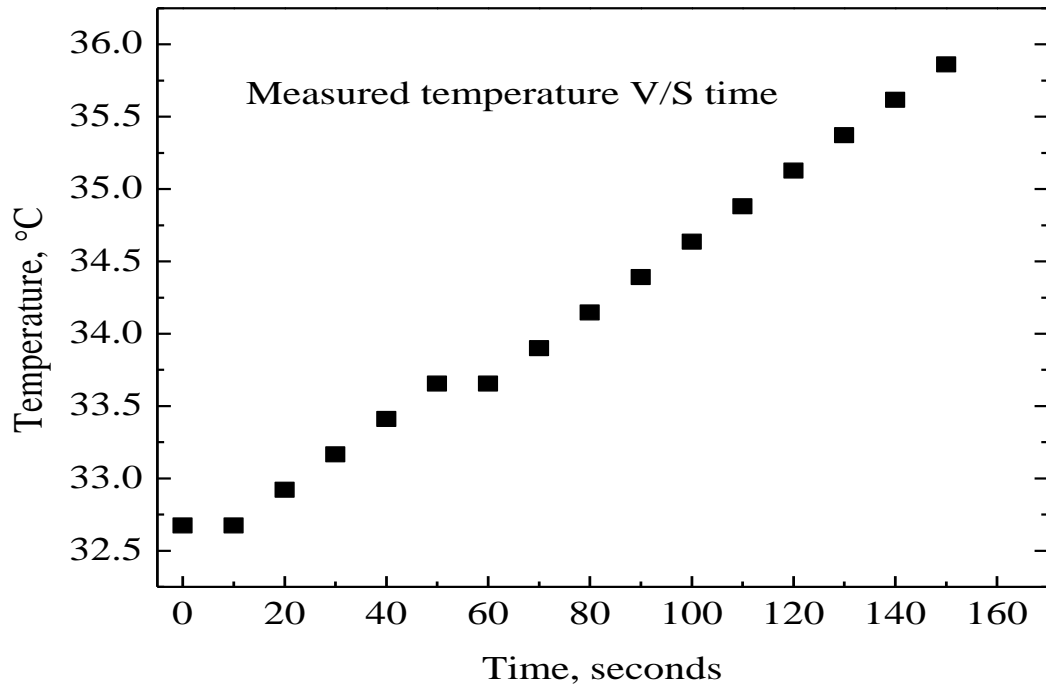| Time	Mili voltmeter reading (E) mV	Measured temperature (T)°C	Temperature predicted by theory (($T - T_0$))°C	Experimental parameters
0	1.17	32.6744	0	
10	1.17	32.6744	0	
20	1.18	32.9196	0.2452	Room temperature = 30.2°C
30	1.19	33.1648	0.4904	Sample type = Clay
40	1.20	33.4100	0.7356	Weight of sample = 75.920 g Diameter of sample = 45 mm
50	1.21	33.6552	0.9808	Thickness of sample = 20 mm
60	1.21	33.6552	0.9808	Voltage input = 50 V
70	1.22	33.9004	1.226	Current input = 0.45 A
80	1.23	34.1456	1.4712	Heating coil surface temperature = 92°C
90	1.24	34.3908	1.7164	
100	1.25	34.636	1.9616	y = 0.0245×E - 0.4904
110	1.26	34.8812	2.2068	R^2 = 1
120	1.27	35.1264	2.452	
130	1.28	35.3716	2.6972	
140	1.29	35.6168	2.9424	
150	1.30	35.8620000	3.1876	

Fig.I.1 Graphs of temperature versus time measured at the base of the clay sample block.
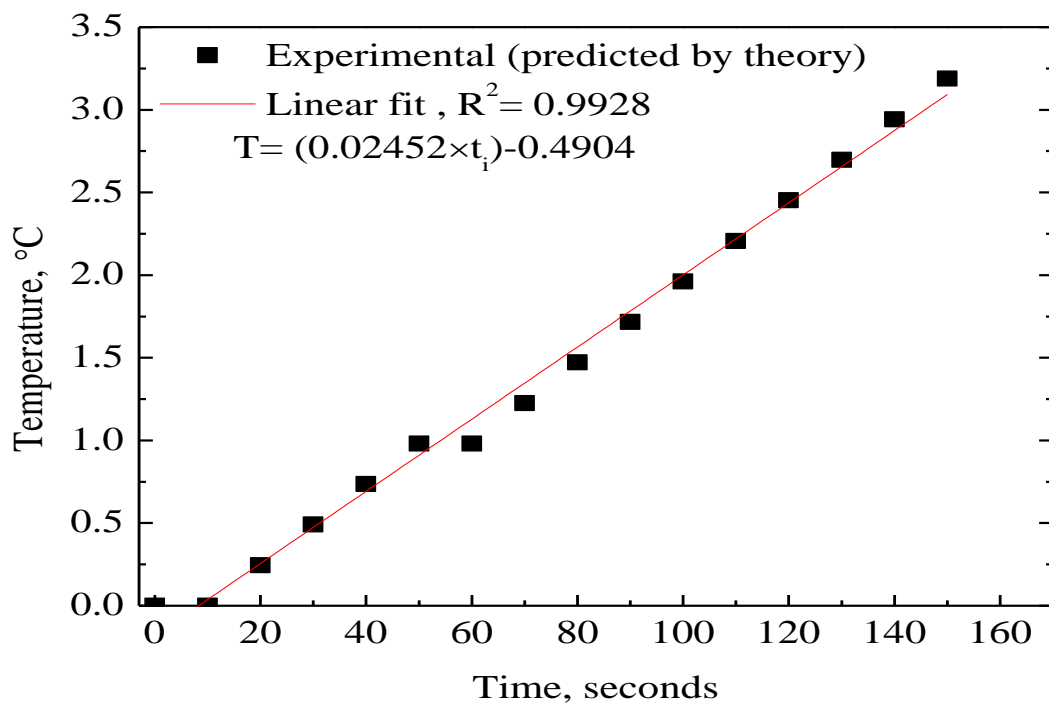

Fig I.2 Graph of temperature versus time for clay sample predicted by theory.

I.2 SPECIFIC HEAT:

The specific heat is calculated by energy balance. The heated water is collected and stored in the thermos flask. The cylindrical pellet is placed into the thermos flask containing hot water. The temperature change is noted by the thermometer. The heat lost by the water is equal to heat gained by the sample. The energy balance is written as

$$m_\phi C_{p_\phi} \left(T_{\phi_f} - T_{\phi_i} \right) = m_w C_{p_w} \left(T_{w_i} - T_{w_f} \right) \tag{I.3}$$

During heating the density of water changes. The mass of water is calculated by reading the density of water at 75.7°C. The density of water at 75.7°C is 976.37 kg/m^3 (Kothandaraman, 2014). By knowing the height of the water column in the thermos flask, the volume of water is calculated. The mass of water (m_w) is calculated as

$$\text{Mass of water } (m_w) = \text{Density of water } (\rho_w) \times \text{Volume of water in the flask} \tag{I.3a}$$

$$\text{Mass of water}(m_w) = 976.365 \times \left(\left(3.14 \times (27 \times 10^{-3})^2 \right) / 4 \right) \times \left(240 \times 10^{-3} \right)$$
$$\text{Mass of water}(m_w) = 0.134153 \text{ kg} \tag{I.3b}$$

By knowing the specific heat and mass of water and substring in Eq. (I.2) specific heat (C_{p_ϕ}) of clay sample is calculated as follows

$$(75.92 \times 10^{-3}) \times C_{p_\phi} \times (71.8 - 36) = (0.134152 \times 4.178 \times (75.7 - 71.8))$$
$$C_{p_\phi} = 804.22 \text{ J/kg K} \tag{I.4}$$

I.3 DENSITY:

The density of the sample is calculated based on mass and volume of the spherical geometry sample.

$$\text{Density of pellet } (\rho_\phi) = \frac{\text{Mass of pellet}}{\text{Volume of pellet}}$$

$$\text{Density of pellet } (\rho_\phi) = \frac{\left(75.92 \times 10^{-3}\right)}{\left(\dfrac{\left(3.14 \times (45 \times 10^{-3})^2 \times 0.02\right)}{(4)}\right)} = 2386.77 \text{ kg/m}^3 \qquad (I.5)$$

I.4 THERMAL CONDUCTIVITY:

The thermal diffusivity, specific heat, density, and thermal conductivity are related by the Eq. (I.6). The thermal conductivity of the sample is determined using

$$\text{Thermal conductivity } (k) = \alpha \times \rho_\phi \times C_{p_\phi}$$

$$\text{Thermal conductivity } (k) = 3.33 \times 10^{-6} \times 2386.77 \times 804.22 = 6.3976 \text{ W/m K} \qquad (I.6)$$

The above theory and calculation procedure is adopted for the estimation of other clay, and clay-saw dust and clay-horse dung samples and $CaCl_2$ impregnated composite desiccants. Table I.2 lists the properties estimated for heat-treated clay, and heat treated clay additives samples and heat-treated clay and clay additives samples impregnated with 30%, 40%, and 50% $CaCl_2$ desiccant concentration. The methodology adopted for the determination properties of clay samples is employed to estimate the properties for the samples listed in Table I.2.

Table I.2 Properties for heat-treated clay and heat-treated clay with additives impregnated with $CaCl_2$ composite desiccants.

Properties / Sample type	Thermal diffusivity α (m^2/s)	Specific heat C_{p_s} (kJ/kg)	Density ρ (kg/m^3)	Thermal conductivity k. (W/m K)
Clay	2.67×10^{-6}	27.23	1746.370	0.127
Clay +30% CaCl$_2$	2.64×10^{-5}	23.74	2031.075	1.273
Clay + 40% CaCl$_2$	4.99×10^{-5}	22.23	2192.053	2.432
Clay + 50% CaCl$_2$	6.54×10^{-5}	20.64	2430.973	3.281
Clay + 20% Horse dung	1.93×10^{-7}	26.20	1734.080	0.0088
Clay + 20% Horse dung + 30% CaCl$_2$	3.35×10^{-7}	22.18	2145.695	0.0159
Clay + 20% Horse dung + 40% CaCl$_2$	1.23×10^{-4}	22.86	2065.715	5.808
Clay + 20% Horse dung + 50% CaCl$_2$	4.54×10^{-5}	23.39	1928.680	2.048
Clay + 20% Sawdust	2.67×10^{-7}	33.53	1192.080	0.0107
Clay + 20% Sawdust + 30% CaCl$_2$	2.00×10^{-5}	21.41	1923.586	0.8237
Clay + 20% Sawdust + 40% CaCl$_2$	2.90×10^{-5}	22.06	1805.400	1.155
Clay + 20% Sawdust + 50% CaCl$_2$	3.30×10^{-5}	22.86	1731.040	1.306

APPENDIX-II

EXPERIMENTAL DETERMINATION OF PRESSURE DROP THROUGH VERTICAL PACKED CLAY AND CLAY - ADDITIVES DESICCANTS BED

Experiments are conducted to determine pressure drop through vertical packed heat treated clay and clay - additives desiccant carrier pellets. The fabricated spherical shaped 10 mm diameter clay and clay additives desiccant pellets are heated to a temperature of 500°C for 60 min. After heat treatment, the respective reduction in weight of pellets or samples is 6%, 10% and 14% for clay, clay + horse dung, and clay + sawdust pellets. The variation of pressure drop with Reynolds number through bed of clay, clay + sawdust, and clay + horse dung had been recorded. Two trials of experiments have been conducted for each type of porous bed of 50 mm diameter. In this appendix the pressure drop results are presented through the vertical packed bed comprising clay composite desiccants without impregnation of $CaCl_2$.

II.1 VARIATION OF BED POROSITY WITH BED HEIGHTS COMPRISING BURNT CLAY - ADDITIVES DESICCANTS

Figure II.1 (a) and (b) shows the variation of packed bed porosity with a variation of bed depths. The total bed porosity comprises of internal and external bed porosities. The bed porosity remains constant for all the bed heights. The internal bed porosity ε_{b_i} is calculated by gravimetric method (Xiaodong, 2010).

$$\varepsilon_b = \left[1 - \frac{m_\phi - m_e}{\rho_\phi} \times \frac{\rho_w}{m_w - m_e} \right] \tag{II.1}$$

Where ρ_ϕ is the density of samples; ρ_w is the density of distilled water; m_e is mass of the dry and empty container; m_ϕ is the total mass of the container filled with pellets; m_w is the total mass of the container full of distilled water. Fig. II.4 (a) and (b) shows the variation of internal and external bed porosities with bed depth.
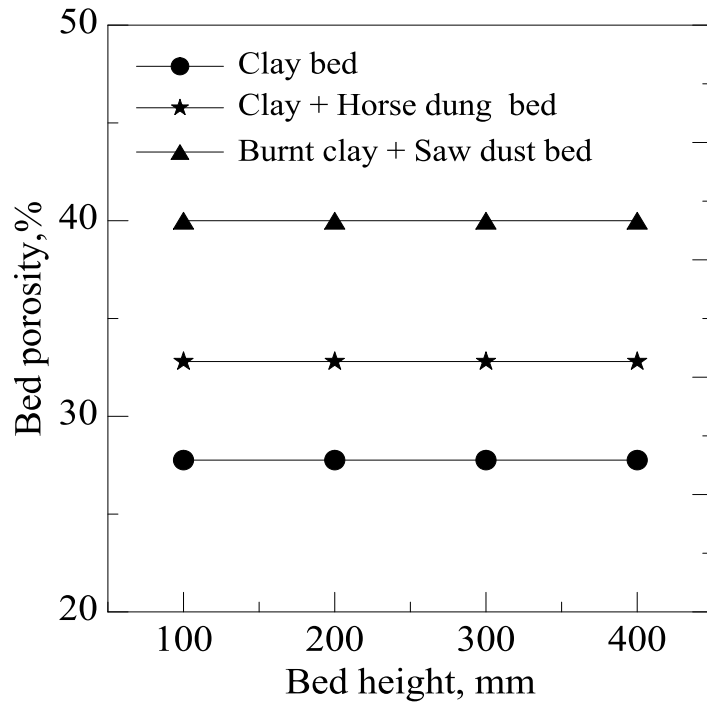
(a)
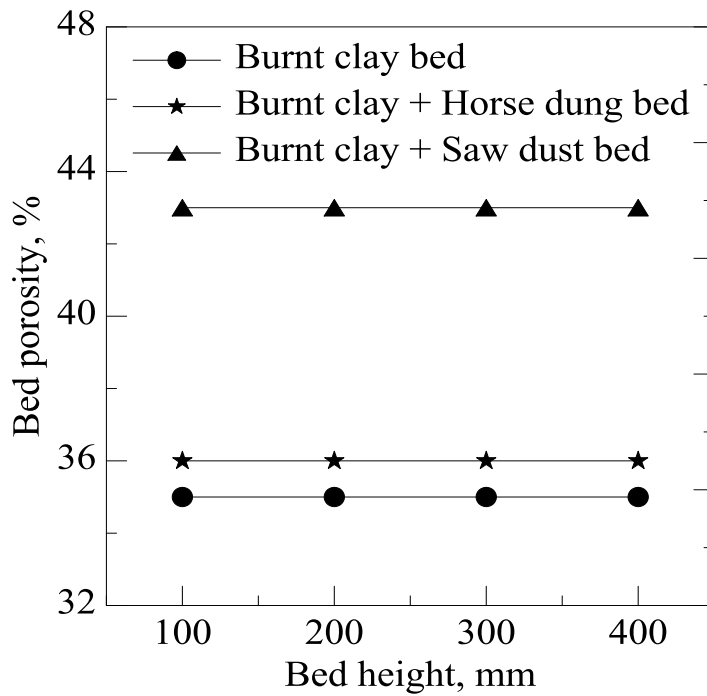
(b)

Fig.II. 1 Variation of experimental bed porosity with bed heights (a) internal porosity and (b) external porosity.

The external bed porosities (voids volume in the bed) function of bed mass and volume are estimated by knowing the density of desiccant pellets and desiccant bed. Eq. (4.8) presented in chapter 4 is used to calculate the external porosity. The higher value of bed porosity of 43 to 44 % is estimated for burnt clay - additives desiccant pellets bed.

II.2 VARIATION OF PRESSURE DROP WITH BED HEIGHT THROUGH VERTICAL PACKED BED OF BURNT CLAY ADDITIVES DESICCANTS

Figure II.2 (a) and (b) shows the variation of pressure drop for different bed lengths with Reynolds number for vertical packed bed comprising heat-treated clay and clay + horse dung additives pellets. The measured values of desiccant pellet porosities are 0.37 and 0.40 for burnt clay and burnt clay + horse dung pellets. The estimated value of bed porosities is 0.35 and 0.36 for clay desiccant pellets and clay + horse dung desiccant pellets bed. For the 100 mm bed length of burnt clay pellets, the pressure drop varies from 18 to 55 mm of water column with variation of Reynolds number from 3089.23 to 6114.89. The higher value of pressure drop of 184 mm of water column for the Reynolds number of 6114.89 is measured for the 400 mm burnt clay pellets bed. Similarly for the 100 mm bed length of burnt clay + horse dung pellets, the pressure drop varies from 15 to 55 mm of water column with variation of Reynolds number from 3089.23 to 6114.89. The higher value of pressure drop of 181 mm of water column for the Reynolds number of 6114.89 is measured for the 400 mm burnt clay + horse dung pellets bed. At a particular value of Reynolds number the pressure drop increases with increase in bed height. With increase in bed height the pressure drop increases with increase in Reynolds number. With higher bed lengths the residence time for the process air through the bed increases. The higher bed length increases resistance to the airflow. Higher bed resistance and residence time for the process air leads to increase in pressure drop.

Fig. II.3 shows the variation of pressure drop for different bed lengths with Reynolds number for burnt clay + sawdust additives desiccant pellets bed. The measured values of pellet porosity are 0.44 and bed porosity is 0.43. The bed porosity remains constant

for all the bed heights. For the 100 mm bed length, the pressure drop varies from 15 to 46 mm of water column with variation of Reynolds number from 3089.23 to 6114.89. The higher value of pressure drop of 163 mm of water column for the Reynolds number of 6114.89 is measured for the 400 mm bed height.

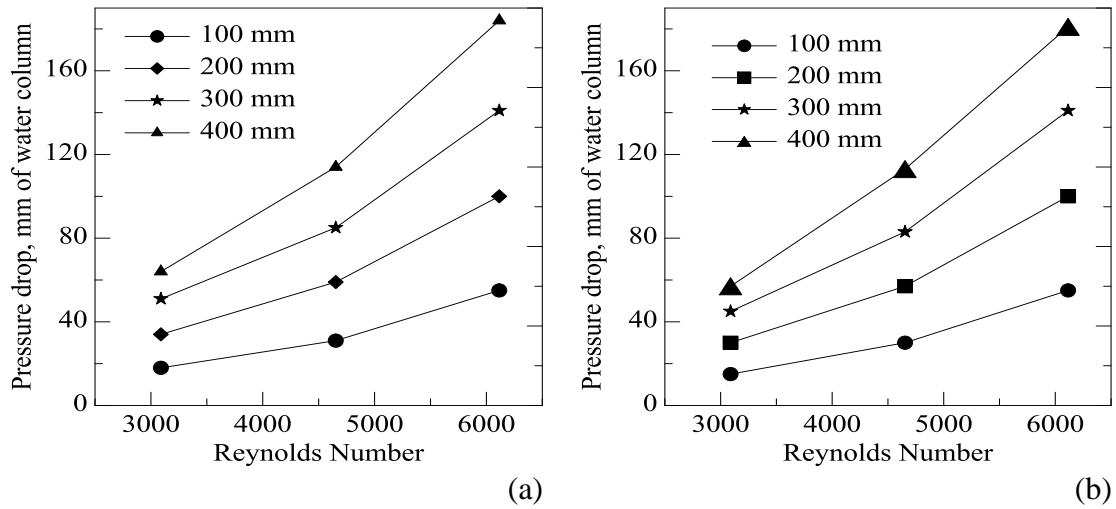(a)   (b)

Fig.II. 2 Variation of pressure drop with Reynolds numbers (a) burnt clay desiccant pellets, (b) burnt clay - horse dung pellets.
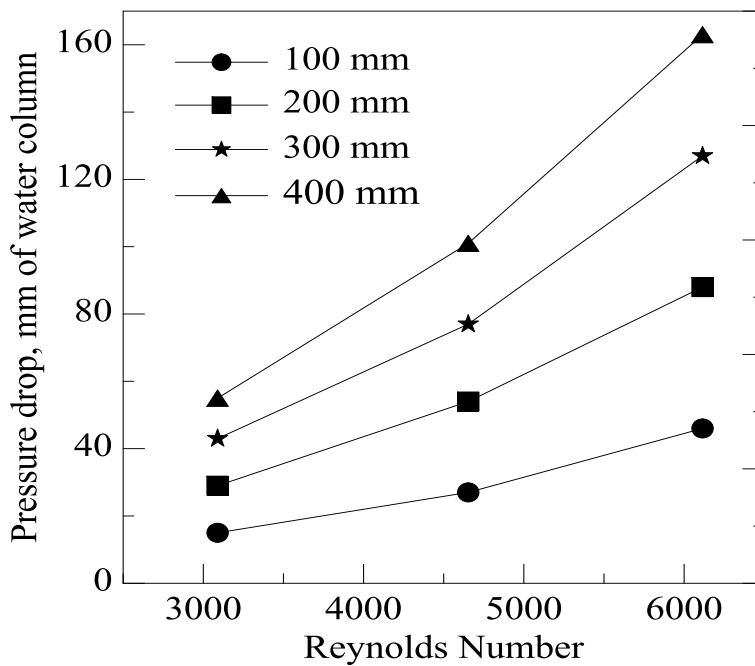

Fig.II. 3 Variation of pressure drop with Reynolds number for burnt clay - sawdust desiccant pellets bed.

II.3 COMPARISON OF VARIATION OF PRESSURE DROP THROUGH VERTICAL PACKED BED OF BURNT CLAY - ADDITIVES DESICCANTS

Figure II.4 (a) and (b) shows the comparison of variation of pressure drop for different bed lengths comprising burnt clay + additives desiccant pellets bed. The bed porosities estimated are 0.35, 0.36, and 0.43 for burnt clay, burnt clay + horse dung and burnt clay + sawdust desiccant pellets bed. For the bed inlet velocity of 1.46 m/s and bed length of 400 mm (Fig.II.4 (a)), the bed porosity is higher for burnt clay + sawdust pellets bed. The pressure drop decreases by about 11.40 % as compared to burnt clay pellets bed and by about 10.62 % as compared to burnt clay + horse dung pellets bed.

Fig.II. 4 (a) Comparison of pressure drop with different bed heights at a bed inlet velocity of 1.46 m/s.

For the bed inlet velocity of 1.93 m/s and bed length of 400 mm (Fig.II.4 (b)), the bed porosity is higher for burnt clay + sawdust desiccant pellets bed. The pressure drop

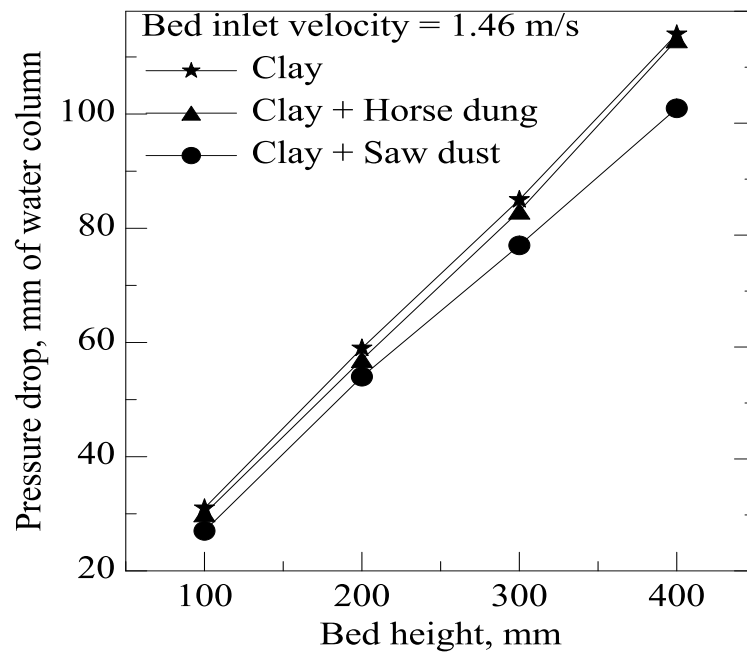decreases by about 11.41 % as compared to burnt clay pellets bed and by about 9.94 % as compared to burnt clay + horse dung desiccant pellets bed.
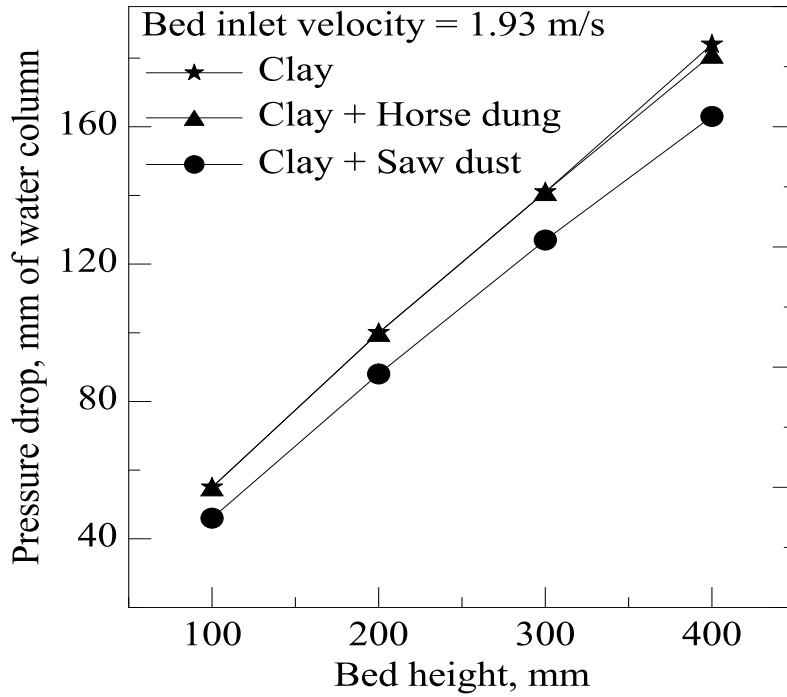

Fig.II. 4 (b) Comparison of pressure drop with different bed heights at bed inlet of 1.93 m/s.

APPENDIX-III

CLAY AND CLAY ADDITIVES COMPOSITE DESICCANTS

The materials employed for the preparation of composite desiccants are transported soil, horse dung, and sawdust additives and $CaCl_2$ hygroscopic salt. The proportion of additives mixed with clay is 20% by weight. Manually fabricated nearly spherical shaped 10 mm diameter desiccants without impregnation of $CaCl_2$ are heat-treated to a temperature of 500°C. The three composite desiccants prepared with 50% concentration of $CaCl_2$ impregnation are clay - $CaCl_2$, clay - sawdust - $CaCl_2$ and clay - horse dung - $CaCl_2$. The vertical packed bed experiments show the nonuniform hygroscopic behavior of composite desiccants. The exposure of single sample of desiccants to humid conditions reveals highest adsorptive power and higher water uptake by clay - horse dung -$CaCl_2$ desiccants followed by clay - sawdust - $CaCl_2$ and clay - $CaCl_2$.

III.1 MATERIALS FOR THE PREPARATION OF CLAY AND CLAY COMPOSITE DESICCANTS
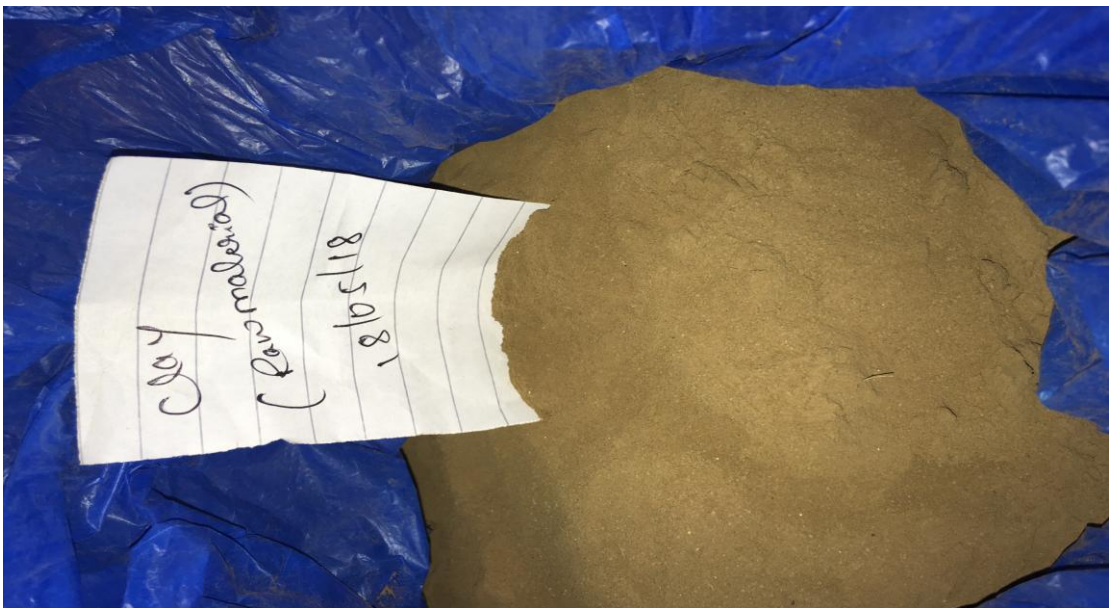
Fig. III. 1 Photograph of transported soil containing illite as major clay mineral.

223
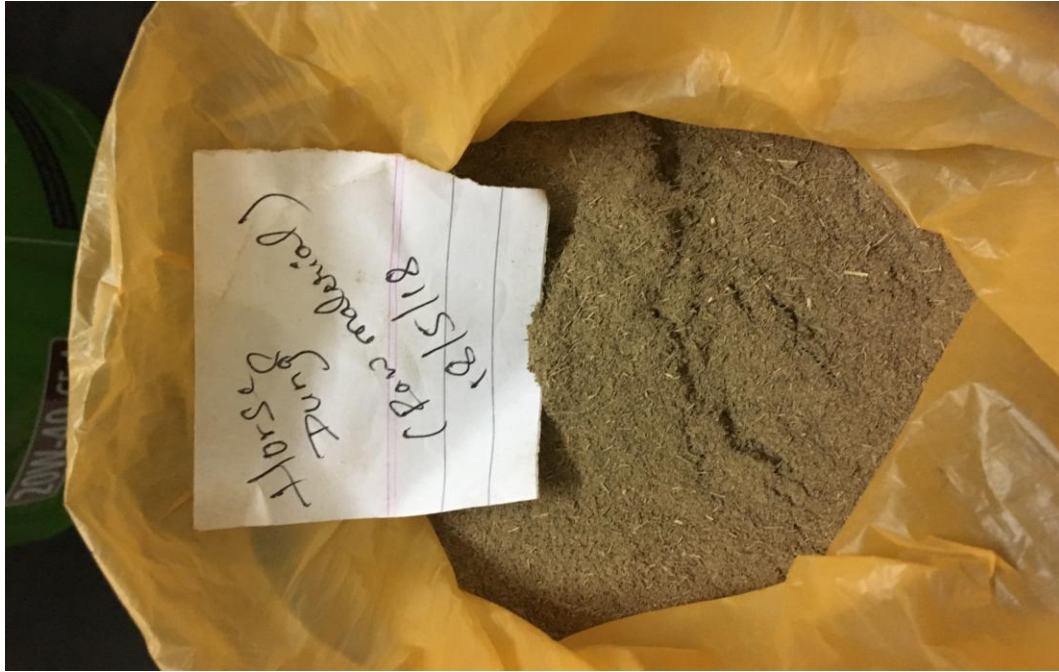
Fig. III.2 Photograph of horse dung additive collected from local pot maker.
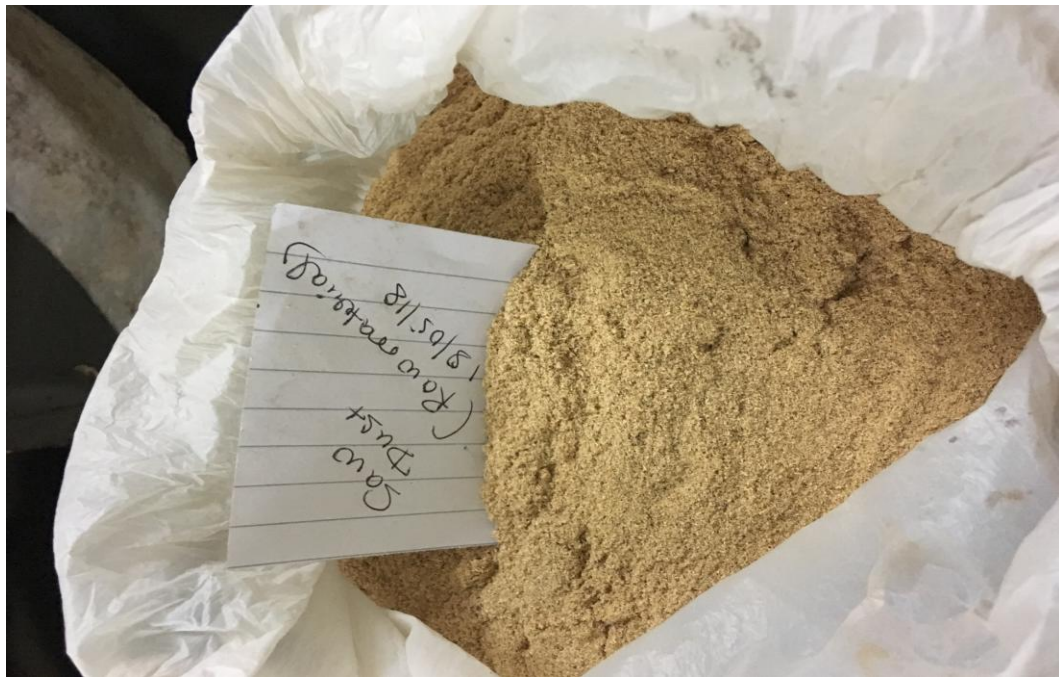
Fig.III.3 Photograph of saw dust additive a residue of saw mill.

III.2 HEAT TREATED CLAY - CaCl₂ COMPOSITE DESICCANTS

Fig. III. 4 Photographs are showing moisture uptake by heat-treated clay -50% CaCl₂ composite desiccants.

III.3   HEAT   TREATED   CLAY   -   SAWDUST   -   CaCl₂   COMPOSITE DESICCANTS
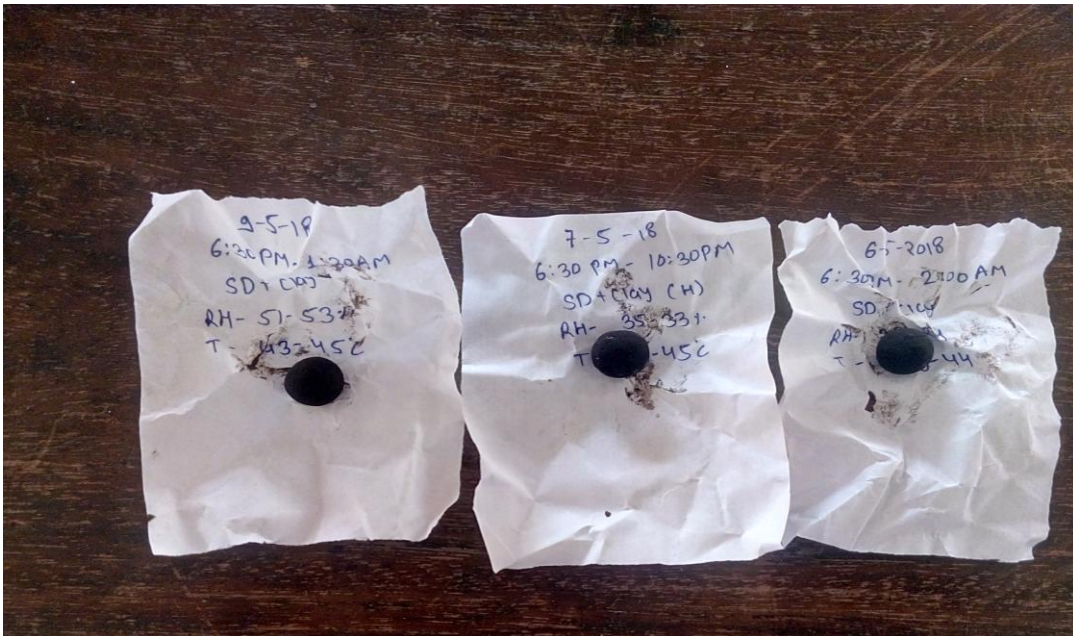
Fig. III. 5 Photographs showing moisture uptake by heat-treated clay - 20% saw dust-50% CaCl₂ composite desiccants.

III.4 HEAT TREATED CLAY - HORSE DUNG - CaCl$_2$ COMPOSITE DESICCANTS

Fig. III. 6 Photographs are showing moisture uptake by heat-treated clay - 20% horse dung - 50% CaCl$_2$ composite desiccant.

III.5 HEAT TREATED CLAY - ADDITIVES - CaCl₂ COMPOSITE DESICCANTS

Heat treated clay - 50% CaCl₂

Heat treated clay – 20% saw dust-
50% CaCl₂

Heat treated clay – 20% horse dung-
50% CaCl₂
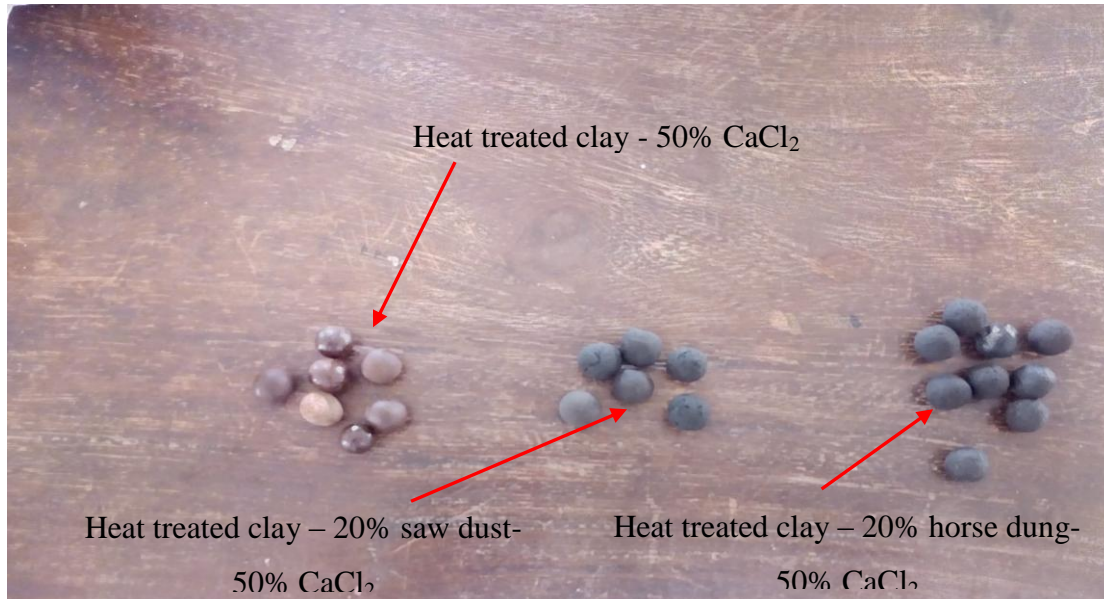
Fig. III. 7 Photographs are showing moisture uptake by heat-treated clay - additives - CaCl₂ composite desiccants.

APPENDIX – IV

CLAY AND CLAY ADDITIVES CaCl$_2$ COMPOSITE DESICCANT BED LENGTH FOR GREEN PEA DRYING

Based on experimental results of clay and clay additives CaCl$_2$ composite desiccant based green pea drying system the bed length is evaluated and designed. The length of bed required for drying of 1 kg of grains is presented in Table IV.1. The desiccant bed diameter and desiccant diameters considered for bed length design are 50 mm and 10 mm. On desiccant bedside a factor of safety of 1.5 is considered to account the desiccant bed porosity and heat loss from the bed. The bed length estimated for drying of 1 kg of moist grains is 2.28 m.

Table IV.1 Design of clay-based composite desiccant bed length for drying of grains.

Weight of grains to be dried ; kg (I)	Initial moisture content of grains; % (II)	Final moisture content; % (III)	Drying time ; hr (IV)	Moisture to be removed from grains ; kg (V)	Moisture removal rate ; kg/hr (VI)	Latent heat of vaporization of water ; kJ/kg (VII)	Average heat release in desiccant bed; kW (VIII)
				(I) × (II-III)	(V) / (IV)		(VI × VII) / 3600
1	80	05	01	0.75	0.75	2400	0.5

Maximum heat release in desiccant bed using a factor of safety of 1.5; kW (IX)	Enthalpy for 750 g bed mass; kW (Experimental) (X)	Bed mass for 0.75 kW ; kg (XI)	Density of bed ; kg/m³ (XI)	The volume of bed; m³ (XIII)	The volume of bed with the factor of safety of 1.2; m³ (XIV)	Bed cross-section area; m² (XV)	Bed length ; m (XVI)
(VIII × 1.5)		(750 × XI) / (X)		(XI) / (XII)	(XIII) × 1.2		(XIV) / (XV)
0.75	0.004945	106.17	2372	0.045	0.054	0.01963	2.28

230

APPENDIX – V

COST ESTIMATION OF CLAY AND CLAY ADDITIVES CaCl$_2$ COMPOSITE DESICCANT

The composite desiccants are prepared of natural materials like clay, sawdust and horse dung. The cost estimation of clay composite desiccant is as follows

Material	Cost (per kg)
Transported soil (clay)	Rs 50
CaCl$_2$ hygroscopic salt	Rs 600
Additives (Horse dung, Sawdust)	Rs 50
Miscellaneous (Transportation, packing, distilled water)	Rs 200
Total cost	Rs 950
Total cost by @ loss of 5% = Rs 997.50	

The cost of clay and clay additives composite desiccant material is considerably low as compared to the commercially available composite desiccants. The cost silica gel-CaCl$_2$ composite desiccant is Rs 1700 per kg.

APPENDIX-VI

HUMIDITY AND TEMPERATURE TRANSMITTER
CALIBRATION CERTIFICATE

ITER INTEGRATED SENSOR SYSTEMS PVT. Ltd.

TEST CERTIFICATE

CLIENT: BLDEAET, VIJAYPUR

CERTIFICATE NO: JI/DK/16-17/00340

DETAILS OF UNIT UNDER CALIBRATION (UUC)

INSTRUMENT :	Humidity & Temperature Transmitter	MODEL:	HF435-DBAXX1XX+ DUAL CH. INDICATOR
MAKE:	Rotronic	CAL DATE:	13/04/2016
RANGE :	Humidity 0 to 100%r.h. (4 to 20mA) Temperature: -40 to 85°C (4 to 20mA)	DUE DATE:	12/04/2017
Sr. No:	60876299 + AK-1108-01	ACCURACY:	±1.0%rh & ±0.2 °C

DETAILS OF STANDARDS USED

INSTRUMENT/EQUIPMENT & MAKE	SERIAL NO.	CERTIFICATE NO.	DUE DATE
HP23 & HC2-S3 MAKE: ROTRONIC	60453701 & 60257233	15164690/P/TH/01	06/03/2017

Result of Calibration at const temp

AMBIENT CONDITION: 23 °C ±2 °C / 50% RH ±5%

Reference Temperature Ts (°C)	Reference Humidity Hs (%r.h.)	UNIT UNDER CALIBRATION			
		Indicated Temp. Ti (°C)	Correction Ti-Ts (°C)	Indicated %Rh	Correction Hi-Hs (%r.h.)
23.0	25.0	22.8	-0.2	24.9	-0.1
23.0	50.0	22.8	-0.2	49.9	-0.1
23.0	80.0	22.8	-0.2	75.2	0.2

Procedure: Sensor is calibrated by comparison against standard sensor by using hygrogen as temperature & humidity source.

FOR JUPITER INTEGRATED SENSOR SYSTEMS PVT LTD
Checked By:

G-414-416, Kailash Complex, Near Dynalog, Behind Godrej Colony, Parksite, Vikhroli (W), Mumbai - 400 079.
Tel. : +91 22 6755 1606, 2518 5474, 2517 0795 Fax : +91 22 2517 0867
Email : sales@jupiterelectronics.co.in Website : www.jupiterelectronics.com
Godown : 7C, Shree Sai Gopalkrishnababa Indl. Complex, Atgaon, Tal. Shahpur, Dist. Thane.

BIO-DATA

Name: HIREMATH. CHANDRASHEKHARAYYA. RACHAYYA

Date of Birth: 25th JANUARY 1975

Gender: Male

Nationality: Indian

Office Address: Hiremath C R, Assistant Professor, Department of Mechanical Engg, BLDEA's V.P Dr. P.G.H CET, Ashram road, Vijayapur-586103.

Permanent Address: Hiremath C R, Veerabhadreshwar Nilaya, Talikoti Road, Mahantesh Nagar, Muddebihal-586212, Dist:Vijayapur.

Contact Numbers: 8310180013, 9986337190

Email: chandra.hiremath@yahoo.com

Educational Qualification:

Qualification	Year of passing	College/University	Class obtained
M.Tech.Thermal Engineering	2011	NITK Surathkal	6.75 (CGPA)
BE in Mechanical Engineering	1996	Karnataka University Dharawad	First class with distinction
Intermediate	1992	Basaveshwar Science College Bagalkot	First class
SSLC	1990	Govt High School Narayanapur	First class with distinction

Details of previous experience:

1. Industrial:

Name of the Industry	Duration of working
HMT Watch Factory Unit I and II, Bangalore	10-11-1997 to 09-11-1998
ARR Precision works Pvt Limited Bangalore	Jan-1997 to Jan-2001

2. Teaching:

Name of the Institute	Duration of working
S T S K K Polytechnic Gadag	Aug-2002 to June-2007
R. N. Shetty Rural polytechnic Murudeshwar	July-2007 to July-2008
BLDEA'S V.P Dr P.G. Halakatti College of Engineering & Technology	August-2008 to Till date

Publications from the M.Tech research work:

International Journals:

C. R. Hiremath, Ravikiran Kadoli., "Experimental studies on heat and mass transfer in a packed bed of burnt clay impregnated with $CaCl_2$ liquid desiccant and exploring the use of gas side resistance model" *Applied Thermal Engineering*, 50(2013) 1299-1310.

International Conference:

Hiremath C. R, Kadoli Ravikiran., "Burnt clay impregnated with calcium chloride liquid desiccant- an experimental study" *Proceedings of 56th Congress of ISTAM* (http://istam.iitkgp.ac.in) Held at : SVNIT Surat, , Gujarat, India, Dec. 19-21, 2011

Declaration:

I hereby declare that the details given above are true to the best of my knowledge and belief.

HIREMATH C. R.

LIST OF PUBLICATIONS BASED ON PH.D. RESEARCH WORK

Sl. No	Title of the paper	Authors	Name of the Journal / Conference / Symposium, Vol., No., Pages	Month and year of publication	Category *
01	Experimental and theoretical study on dehumidification potential of clay-additives based CaCl$_2$ composite desiccants	C.R. Hiremath., Ravikiran Kadoli., V.V. Katti	Applied Thermal Engineering (Elsevier), 129 (2018), 70 - 83	January 2018	1
02	Experimental determination of specific heat and thermal conductivity of clay + additives + CaCl$_2$ composite desiccant	C. R. Hiremath., V.V. Katti ., Kadoli Ravikiran	Procedia Materials Science (Elsevier), 5 (2014) 188 – 197,	July 2014	3
03	Burnt Clay + Additives + Calcium Chloride Composite desiccant – An experimental study.	Hiremath, C. R., Kadoli Ravikiran and Katti, V.V	Proceedings of 59th Congress of ISTAM (http://istam.iitkgp.ac.in), Dec. 17-20, 2014. Alliance university (www.alliance.edu.in), Bangalore, India.	December 2014	3
04	Experimental study on adsorption-desorption of burnt Clay composite desiccant packed dehumidification bed impregnated with calcium chloride	Hiremath, C. R., Kadoli Ravikiran and Katti, V.V,	*ICEE-2014*, JNTUH, ISBN: 978-93-81212-96-7, JNTUH, Hyderabad, India.	December 2014	3
05	Adsorption and desorption through packed and fluidized clay based composite desiccant beds: A comparison study.	Hiremath, C. R., Kadoli Ravikiran	Heat and Mass Transfer (Springer)	Under review	1

*Category: 1: Journal paper, full paper reviewed   2: Journal paper, Abstract reviews   3: Conference /Symposium paper, full paper reviewed 4: Conference /Symposium paper, abstract reviewed   5: Others (including papers in Workshops, NITK Research Bulletins, Short notes etc.)